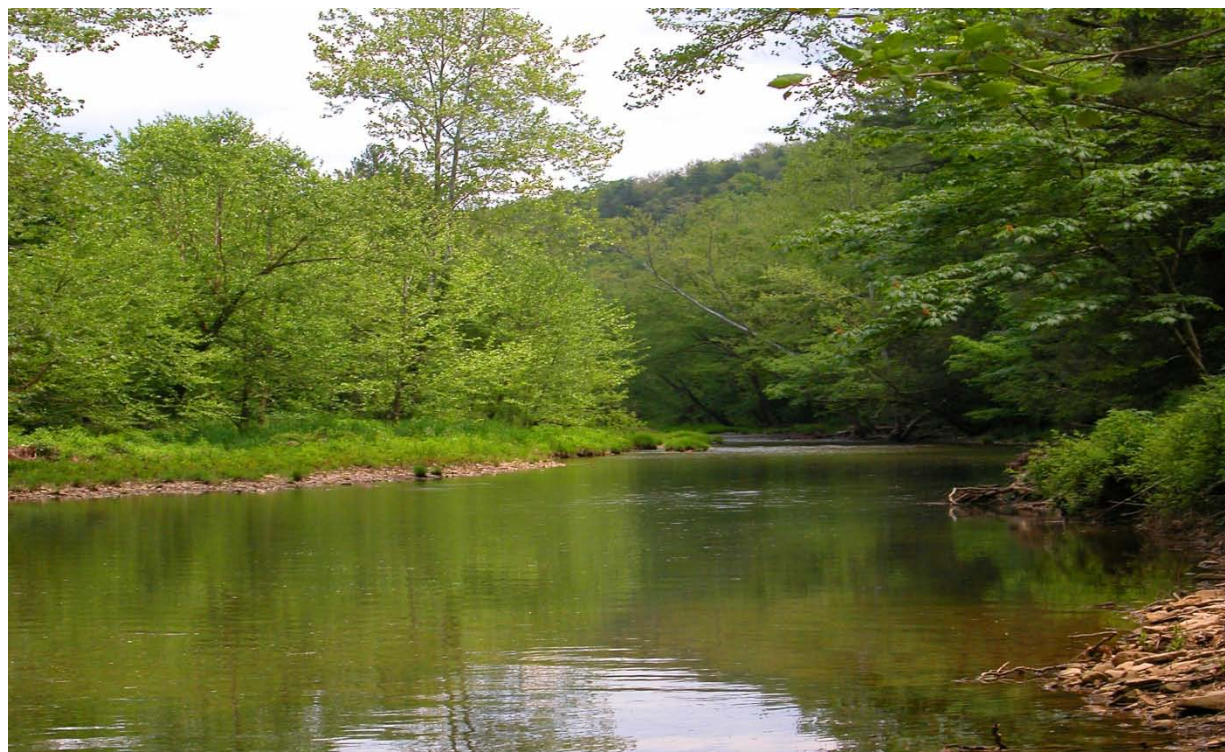




Policy Assessment for the Review of the Secondary National Ambient Air Quality Standards for Oxides of Nitrogen and Oxides of Sulfur

Appendices



EPA-452/R-11-005b
February 2011

Policy Assessment for the Review of the Secondary National Ambient Air Quality Standards for Oxides of Nitrogen and Oxides of Sulfur

Appendices

**U.S. Environmental Protection Agency
Office of Air Quality Planning and Standards
Health and Environmental Impacts Division
Research Triangle Park, North Carolina**

DISCLAIMER

This document has been reviewed by the Office of Air Quality Planning and Standards, U.S. Environmental Protection Agency, and approved for publication. This final document has been prepared by staff from the Office of Air Quality Planning and Standards, U.S. Environmental Protection Agency. Any opinions, findings, conclusions, or recommendations are those of the authors and do not necessarily reflect the views of the U.S. Environmental Protection Agency. Mention of trade names or commercial products is not intended to constitute endorsement or recommendation for use. Any questions or comments concerning this document should be addressed to Richard Scheffe, U.S. Environmental Protection Agency, Office of Air Quality Planning and Standards, C304-02, Research Triangle Park, North Carolina 27711 (email: scheffe.richard@epa.gov).

APPENDICES

Appendix A: Analysis of Critical Loads, Comparing Aquatic and Terrestrial Acidification

Appendix B: Methodologies and Assumptions Used In Steady State Ecosystem Modeling

Appendix C: Ecoregions, Level III: Description And Summary of Environmental Conditions

Appendix D: Maps and Calculation Procedures for Alternative Standards

Appendix E: Derivation to Use Measured Total Nitrate as a Surrogate for NO_y

Appendix F: Evaluation of Variability, Sensitivity and Uncertainty in the Acidification Index

Appendix G: Cumulative Uncertainty Analysis

Appendix A

Analysis of Critical Loads, Comparing Aquatic and Terrestrial Acidification

Background

Critical load is defined as, “a quantitative estimate of ecosystem exposure to one or more pollutants below which significant harmful effects on specified sensitive elements of the environment do not occur, according to present knowledge” (McNulty et al., 2007), and critical loads can be estimated for aquatic and terrestrial ecosystems. Within the *Risk and Exposure Assessment for Review of the Secondary National Ambient Air Quality Standards for Oxides of Nitrogen and Sulfur* (hereafter referred to as REA Report) (US EPA, 2009), critical loads of acidification for aquatic systems were determined by relating specific amounts of acidifying nitrogen and sulfur deposition to selected Acid Neutralizing Capacities (ANC) within freshwater lakes or streams. The presence and abundance of fish species served as the biological indicator of the impacts of the exceedance of critical acid loads by nitrogen and sulfur deposition. Estimation of critical acid loads for terrestrial systems within the REA Report (US EPA, 2009) related acidifying nitrogen and sulfur deposition to the base cation to aluminum (Bc/Al) ratio in the soil solution, and the health of sugar maple and red spruce in forest ecosystems served as the biological indicator of the impacts of critical acid load exceedance. A main distinction between these two critical loads is that aquatic critical loads are largely an integrated function of the chemistry of run-off waters that feed the lake or stream within a watershed, while terrestrial critical acid loads are determined by the rooting zone section of the soil profile in a forest ecosystem. Therefore, it is possible to have different critical load values for aquatic and terrestrial ecosystems within the same watershed.

The goal of this Task was to determine the relative degree of protection offered by aquatic versus terrestrial critical acid loads within a landscape. Critical acid loads for lakes and streams within watersheds of the Adirondacks and Shenandoah Valley were compared against terrestrial critical loads calculated for same watersheds to determine which estimate had the lowest, most protective critical load for acidifying nitrogen and sulfur deposition.

Methods

For the REA Report (US EPA, 2009), critical acid loads were determined for 169 lakes and 60 streams in the Adirondacks and Shenandoah Case Study Areas, respectively. These critical loads were calculated using four different ANCs, 0, 20, 50 and 100 $\mu\text{eq/L}$, that ranged in the level of protection offered to fish species abundance and diversity, and the resulting critical acid loads were classified into four “current condition of acidity and sensitivity to acidification” categories. “Highly Sensitive” water bodies had critical loads less than or equal to 50 $\text{meq/m}^2/\text{yr}$, “Moderately Sensitive” systems had critical loads ranging from 51 to 100 $\text{meq/m}^2/\text{yr}$, “Low Sensitivity” lakes and streams had critical loads that ranged from 101 to 200 $\text{meq/m}^2/\text{yr}$, and “Not Sensitive” systems had critical acid loads greater than 201 $\text{meq/m}^2/\text{yr}$.

For the purposes of this Task, aquatic critical acid loads corresponding to an ANC of 50 $\text{meq/m}^2/\text{yr}$ were selected, and the locations of the lakes and streams in the Adirondacks and Shenandoah Case Study Areas were mapped by HUC12 watersheds. Availability of data for terrestrial acidification estimates was determined for each HUC, and only HUCs that had sufficient data were mapped. Data from the U.S. Department of Agriculture- Natural Resources Conservation Service (USDA-NRCS) SSURGO soils database (USDA-NRCS, 2008) had the poorest coverage. This data restriction limited the number of water bodies that could be included in the analysis to 62 and 35 for the Adirondacks and Shenandoah Case Study Areas, respectively.

To examine a representative selection of water bodies in each Case Study Area, four watersheds containing lakes or streams from each of the four “current condition of acidity and sensitivity to acidification” categories were randomly selected. Therefore, a total of 16 watersheds were chosen for each Case Study Area. All four “current condition of acidity and sensitivity to acidification” categories were evenly represented for the Adirondacks Case Study Area (four watersheds for each of the four categories). However, due to the limited number of watersheds in the Shenandoah Area and a lower proportion of lakes with low sensitivities to acidifying nitrogen and sulfur deposition (“Low Sensitivity” and “Not Sensitive”), it was not possible to have equal representation of all “current condition of acidity and sensitivity to acidification” categories. Therefore, there was a larger representation of streams that were more sensitive to acidification (“Highly Sensitive” and “Moderately Sensitive”). All water bodies that were located in each of the selected HUCs were included in the analyses. In many cases, these

water bodies ranged in sensitivity to acidification. In total, 29 lakes and 20 streams were analyzed in the Adirondacks and Shenandoah Case Study Areas, respectively (Table A-1 and A-2).

Table A-1. Watersheds (HUC 12) and fresh water lakes in the Adirondacks Case Study Area that were used in the comparison of aquatic and terrestrial critical acid loads. Lake IDs and associated aquatic critical acid loads (CL) in meq/m²/yr, based on an ANC of 50 µeq/L, are indicated in each cell and are from the REA REPORT (US EPA, 2009).

| HUC | CURRENT CONDITION OF ACIDITY AND SENSITIVITY TO ACIDIFICATION CATEGORY | | | |
|--------------|--|---|---|---|
| | Highly Sensitive (CL ≤ 50 meq/m ² /yr) | Moderately Sensitive (CL = 51-100 meq/m ² /yr) | Low Sensitivity (CL = 101-200 meq/m ² /yr) | Not Sensitive (CL > 201 meq/m ² /yr) |
| 020100010103 | | | | NY534L (CL = 1043) |
| 020100040203 | | | 1A2-028O (CL = 106) NY310L (CL = 147) | NY308L (CL = 485) |
| 020100080304 | | | | NY312L (CL = 588) NY313L (CL = 598) |
| 020100081602 | | | | NY500L (CL = 610) |
| 020200020101 | | NY013L (CL = 64) | | |
| 020200020704 | | NY536L (CL = 69) | | |
| 020200040805 | 1A2-078O (CL = 33) | | NY292L (CL = 117) | |
| 041501011001 | NY029L (CL = 39) | | | |
| 041503020801 | | | | NY783L (CL = 455) |
| 041503040102 | NY284L (CL = 23) NY285L (CL = 42) | | | |
| 041503040204 | | NY278L (CL = 57) | | |
| 041503050103 | 1A1-089O (CL = 43) | 050215AO (CL = 74) NY793L (CL = 97) | | |
| 041503050104 | NY290L (CL = 30) NY289L (CL = 50) | | | |
| 041503050302 | | | NY008L (CL = 146) NY007L (CL = 165) | |

| HUC | CURRENT CONDITION OF ACIDITY AND SENSITIVITY TO ACIDIFICATION CATEGORY | | | |
|--------------|--|---|---|---|
| | Highly Sensitive (CL ≤ 50 meq/m ² /yr) | Moderately Sensitive (CL = 51-100 meq/m ² /yr) | Low Sensitivity (CL = 101-200 meq/m ² /yr) | Not Sensitive (CL > 201 meq/m ² /yr) |
| 041503050407 | | NY767L (CL = 51) NY529L (CL = 73) NY528L (CL = 82) NY769L (CL = 99) | NY768L (CL = 114) | |
| 041503050601 | | | NY004L (CL = 168) | |

Table A-2. Watersheds (HUC 12) and streams in the Shenandoah Case Study Area that were used in the comparison of aquatic and terrestrial critical acid loads. Stream IDs and associated aquatic critical acid loads (CL) in meq/m²/yr, based on an ANC of 50 µeq/L, are indicated in each cell and are from the REA REPORT (US EPA, 2009).

| HUC | CURRENT CONDITION OF ACIDITY AND SENSITIVITY TO ACIDIFICATION CATEGORY | | | |
|--------------|--|---|---|---|
| | Highly Sensitive (CL ≤ 50 meq/m ² /yr) | Moderately Sensitive (CL = 51-100 meq/m ² /yr) | Low Sensitivity (CL = 101-200 meq/m ² /yr) | Not Sensitive (CL > 201 meq/m ² /yr) |
| 020700050401 | VT37 (CL = 26) | | | |
| 020700050502 | VT57 (CL = 39) | | | |
| 020700050703 | VT40 (CL = 13) | | | |
| 020700050705 | VT35 (CL = 37) VT36 (CL = 24) | | | |
| 020700050801 | DR01 (CL = 33) WOR1 (CL = 43) | | | |
| 020700050803 | VT53 (CL = 40) | | | |
| 020700060101 | | VT54 (CL = 69) | | |
| 020801030301 | | | VT60 (CL = 198) | VT61 (CL = 231) |
| 020801030402 | | VT62 (CL = 68) | | |
| 020802010702 | VT10 (CL = 15) | | | |
| 020802010703 | VT11 (CL = 14) | VT12 (C = 75) | | |
| 020802010801 | VT14 (CL = 14) VT15 (CL = 13) | | | |
| 020802010803 | VT16 (CL = 20) | | | |
| 020802020102 | | VT38 (CL = 66) | | |
| 020802020401 | VT41 (CL = 15) | | | |
| 020802030601 | | VT46 (CL = 52) | | |

Terrestrial critical acid loads were calculated for each of the 16 watersheds using the simple mass balance method (UNECE, 2004) and data sources outlined in the REA Report (US EPA, 2009), and Bc/Al soil solution indicator values of 1.2 and 10.0. Briefly, average values for base cation deposition (calcium, potassium, magnesium and sodium), chloride deposition, and annual runoff ($\text{m}^3/\text{ha}/\text{yr}$) were determined for each watershed (Table A-3). The Kgibb constant (m^6eq^2) was determined by the average percent organic matter in the soil (Table A-4), and N immobilization in the soil was set to the constant value of 42.86 eq/ha/yr (McNulty et al., 2007). It was assumed that active harvesting did not occur in each of the watersheds. Therefore base cation (calcium, magnesium and potassium) and nitrogen uptake were 0 eq/ha/yr (UNECE, 2004). Similarly, it was assumed that the majority of each watershed consisted of upland sites. Therefore, denitrification losses were assumed to be 0 eq/ha/yr (McNulty et al., 2007). Base cation weathering was estimated using the clay substrate model (equations 1-3) (McNulty et al., 2007).

$$\text{Acid Substrate: } \text{BC}_e = (56.7 \times \% \text{clay}) - (0.32 \times (\% \text{clay})^2) \quad (1)$$

$$\text{Intermediate Substrate: } \text{BC}_e = 500 + (53.6 \times \% \text{clay}) - (0.18 \times (\% \text{clay})^2) \quad (2)$$

$$\text{Basic Substrate: } \text{BC}_e = 500 + (59.2 \times \% \text{clay}) \quad (3)$$

where

BC_e = empirical soil base cation ($\text{Ca}^{2+} + \text{K}^+ + \text{Mg}^{2+} + \text{Na}^+$) weathering rate (eq/ha/yr)

% clay = the percentage of clay within the top 50cm of the soil.

The U.S. Department of Agriculture- Natural Resources Conservation Service (USDA-NRCS) SSURGO soils database (USDA-NRCS, 2008)) and state-level geology (U.S. Geological Survey (USGS) state-level integrated map database for the United States (USGS, 2009)) were used to determine parent material acidity classification. Parent material acidity was determined for each SSURGO polygon within each watershed using the criteria outlined in the REA Report (US EPA, 2009), and the contributions of base cations from the weathering of acid, intermediate and basic substrates (eq/ha/yr) were determined by a weighted average based on the proportion of area occupied by each parent material acidity class. Rooting depth was assumed to be 50 cm and masses of calcium, magnesium, potassium, sodium and nitrogen were converted to eq/ha/yr units based on molar charge equivalents. Unless indicated otherwise, the units used in the calculation

of critical acid loads were eq/ha/yr. The estimated terrestrial critical loads for the 16 watersheds in the Adirondacks and Shenandoah Case Study Areas are presented in Table A-5.

Table A-3. Name, type and source of data used in the simple mass balance estimates of terrestrial critical acid loads for the watersheds in the Adirondacks and Shenandoah Case Study Areas.

| DATA | NAME | TYPE | SOURCE |
|---|---|-------------------|--|
| Base cation (Ca ²⁺ , Mg ²⁺ , Na ⁺ , K ⁺) deposition— wet | CMAQ/ NADP | GIS datalayers | Provided by U.S. Environmental Protection Agency (EPA)/NADP, 2003a,c, d, e |
| Chloride (Cl ⁻) deposition— wet | NADP | GIS datalayer | NADP, 2003b |
| Runoff | Annual run-off (1: 7,500,000 scale) | GIS datalayer | Gebert et al., 1987 |
| Soil horizon depth | SSURGO | GIS datalayer | USDA-NRCS, 2008 |
| Percentage of clay by soil horizon | SSURGO | GIS datalayer | USDA-NRCS, 2008 |
| Percentage of organic matter by soil horizon | SSURGO | GIS datalayer | USDA-NRCS, 2008 |
| Soil parent material | SSURGO | GIS datalayer | USDA-NRCS, 2008 |
| State-level bedrock geology | State Geological Map Compilation | GIS datalayer | USGS, 2009 |

Note: CMAQ = Community Multiscale Air Quality Model; NADP = National Atmospheric Deposition Program; GIS = Geographic Information System; SSURGO = Soil Survey Geographic Database

Table A-4. Gibbsite equilibrium (K_{gibb}) constant determined by percentage of soil organic matter (modified from McNulty et al. 2007).

| Soil Type Layer | Organic Matter % | K_{gibb} (m^6/eq^2) |
|--|------------------|---------------------------|
| Mineral soils: C layer | <5 | 950 |
| Soils with low organic matter: B/C layers | 5 to 15 | 300 |
| Soils with some organic material: A/E layers | 15 to 70 | 100 |
| Peaty and organic soils: organic layers | >70 | 9.5 |

Table A-5. Terrestrial critical acid loads (in eq/ha/yr) for the watersheds in the Adirondacks and Shenandoah Case Study Areas.

| Case Study Area | HUC12 | Terrestrial Critical Acid Load (eq/ha/yr) | |
|-----------------|--------------|---|--------------|
| | | Bc/Al = 1.2 | Bc/Al = 10.0 |
| Adirondacks | 020100010103 | 2045 | 1134 |
| Adirondacks | 020100040203 | 1316 | 712 |
| Adirondacks | 020100080304 | 1329 | 731 |
| Adirondacks | 020100081602 | 1670 | 922 |
| Adirondacks | 020200020101 | 1484 | 819 |
| Adirondacks | 020200020704 | 1707 | 935 |
| Adirondacks | 020200040805 | 1770 | 951 |
| Adirondacks | 041501011001 | 1770 | 955 |
| Adirondacks | 041503020801 | 1664 | 912 |
| Adirondacks | 041503040102 | 1627 | 880 |
| Adirondacks | 041503040204 | 1436 | 786 |
| Adirondacks | 041503050103 | 1774 | 957 |
| Adirondacks | 041503050104 | 1794 | 968 |
| Adirondacks | 041503050302 | 1754 | 947 |
| Adirondacks | 041503050407 | 1447 | 789 |
| Adirondacks | 041503050601 | 1203 | 656 |
| Shenandoah | 020700050401 | 1440 | 802 |
| Shenandoah | 020700050502 | 1560 | 871 |
| Shenandoah | 020700050703 | 1762 | 979 |
| Shenandoah | 020700050705 | 1852 | 1032 |
| Shenandoah | 020700050801 | 1799 | 1003 |
| Shenandoah | 020700050803 | 1975 | 1102 |
| Shenandoah | 020700060101 | 1638 | 914 |
| Shenandoah | 020801030301 | 1511 | 843 |
| Shenandoah | 020801030402 | 1393 | 776 |
| Shenandoah | 020802010702 | 1603 | 890 |
| Shenandoah | 020802010703 | 1642 | 912 |
| Shenandoah | 020802010801 | 1635 | 909 |
| Shenandoah | 020802010803 | 1573 | 876 |
| Shenandoah | 020802020102 | 1519 | 845 |
| Shenandoah | 020802020401 | 1264 | 703 |
| Shenandoah | 020802030601 | 1660 | 918 |

Maps were generated to compare the aquatic and terrestrial critical acid loads in each watershed to determine which estimate provided the greatest protection against acidifying nitrogen and sulfur deposition. In each watershed, the terrestrial critical load estimate was compared against each aquatic critical load, and the load with the lowest value was set to represent the most sensitive component in the watershed. All critical load estimates were converted to eq/ha/yr for the comparisons.

Results

Maps indicating and comparing the sensitivities of the terrestrial and aquatic critical loads to nitrogen and sulfur deposition in each watershed of the Adirondacks and Shenandoah Case Study Areas are presented in Figures A-1 to A-4 and Tables A-6 to A-9.

In the Adirondacks Case Study Area, 7 of the 16 watersheds had terrestrial critical acid loads (based on a Bc/Al of 10.0) that were lower and therefore more sensitive to acidification than all the lakes in the watershed. However, when the terrestrial critical loads were calculated with a Bc/Al soil solution ratio of 1.2, only 5 of the 16 watersheds were protected by a terrestrial critical load that was lower than the aquatic critical loads of the lakes. Three watersheds in the Adirondacks Case Study Area had terrestrial critical loads (based on a Bc/Al of 10.0) that were lower and higher than the critical loads for the lakes in the watershed, and one watershed had a similar mixture of aquatic versus terrestrial acid load protections for terrestrial critical loads estimated with a Bc/Al of 1.2. In general, a main trend in the Adirondacks Case Study Area was that watersheds with “Highly Sensitive” and “Moderately Sensitive” lakes were more protected by aquatic than terrestrial critical acid loads, while the watersheds with “Low Sensitivity” and “Not Sensitive” lakes were more protected by terrestrial critical acid loads.

Similar trends were found in the Shenandoah Case Study Area. However, there was little distinction between terrestrial acid loads that were calculated with a Bc/Al of 10.0 versus 1.2. Terrestrial critical acid loads offered a higher level of protection than did the stream aquatic critical loads in only one watershed. The two streams in this watershed had “Low Sensitivity” or were “Not Sensitive” to acidifying nitrogen and sulfur deposition. The 15 watersheds that had streams with aquatic critical loads lower and more protective than the terrestrial critical loads were all “Highly Sensitive” or “Moderately Sensitive” to acidifying nitrogen and sulfur deposition.

In summary, a comparison of the terrestrial and aquatic critical acid loads for watersheds in the Adirondacks and Shenandoah Case Study Areas indicated that, in general, the aquatic critical acid loads offered greater protection to the watersheds than did the terrestrial critical loads. In situations where the terrestrial loads were more protective, the lakes or streams in the watershed were rated as having “Low Sensitivity” or “Not Sensitive” to acidifying nitrogen and sulfur deposition. Conversely, when the water bodies were more sensitive to deposition (“Highly Sensitive” or “Moderately Sensitive”), the aquatic critical acid loads consistently provided a greater level of protection against acidifying nitrogen and sulfur deposition in the watershed.

Figure A-1. Comparison of aquatic and terrestrial critical loads of acidification (in eq/ha/yr) in the 16 watersheds of the Adirondacks Case Study Area, based on an ANC of 50 eq/L for the aquatic loads and a Bc/AI of 10.0 for the terrestrial loads. Colored circles indicate the locations of the waters bodies within each watershed. Green circles indicate lakes with critical load values less than the terrestrial critical load for the same watershed. Red circles indicate a condition where the terrestrial critical load is lower than the lake critical load.

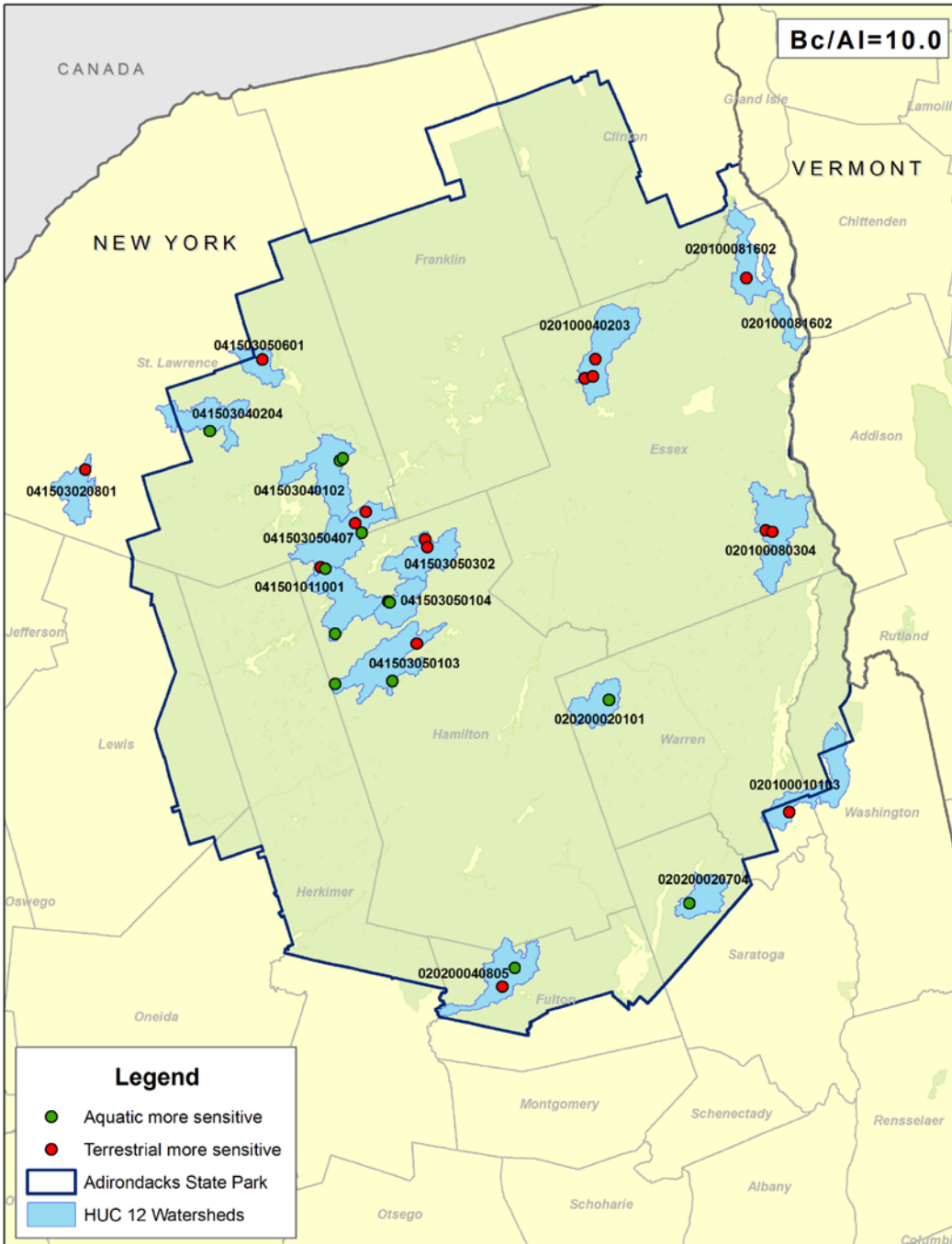


Figure A-2. Comparison of aquatic and terrestrial critical loads of acidification (in eq/ha/yr) in the 16 watersheds of the Adirondacks Case Study Area, based on an ANC of 50 eq/L for the aquatic loads and a Bc/AI of 1.2 for the terrestrial loads. Colored circles indicate the locations of the waters bodies within each watershed. Green circles indicate lakes with critical load values less than the terrestrial critical load for the same watershed. Red circles indicate a condition where the terrestrial critical load is lower than the lake critical load.

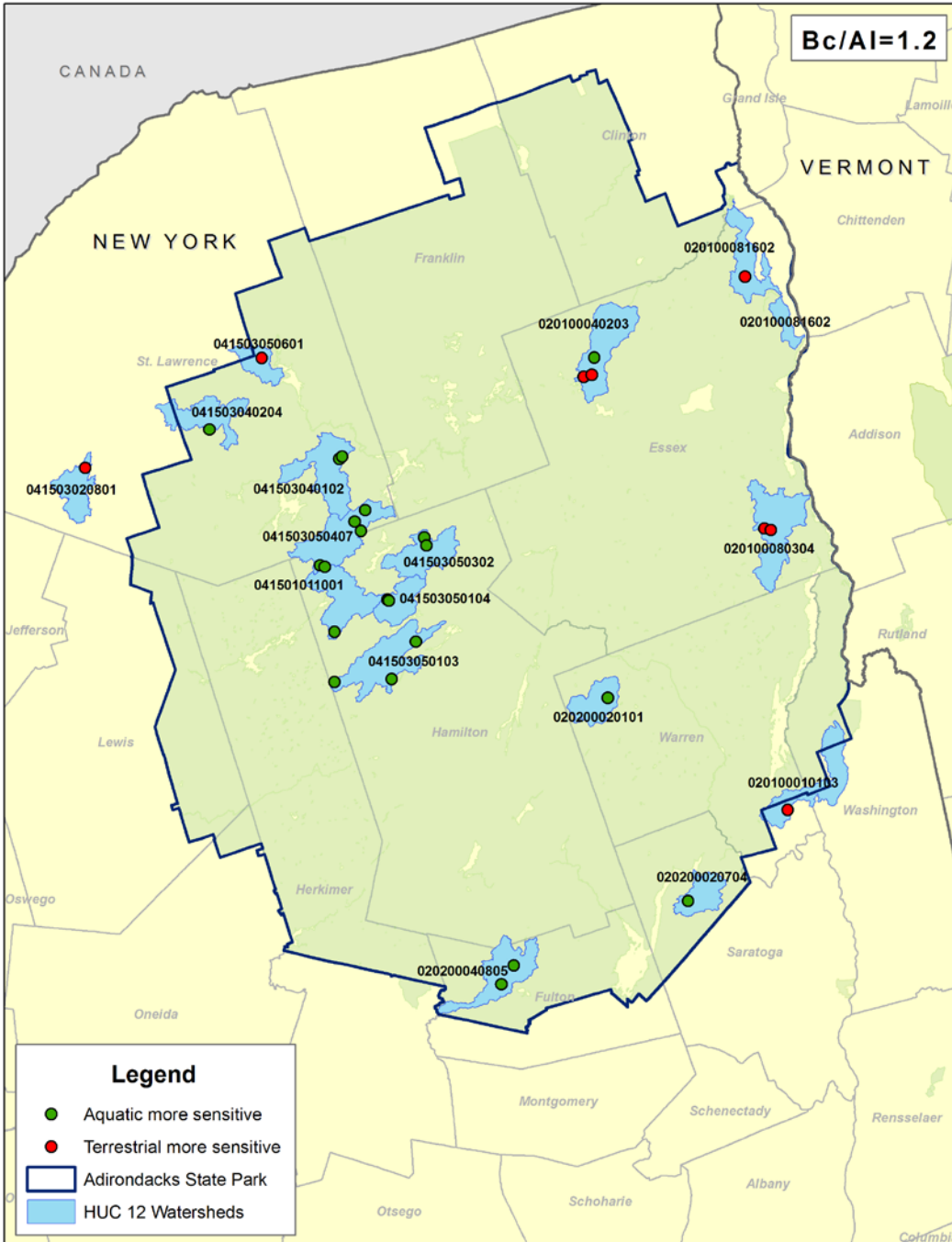


Figure A-3. Comparison of aquatic and terrestrial critical loads of acidification (in eq/ha/yr) in the 16 watersheds of the Shenandoah Case Study Area, based on an ANC of 50 eq/L for the aquatic loads and a Bc/AI of 10.0 for the terrestrial loads. Colored circles indicate the locations of the water bodies within each watershed. Green circles indicate streams with critical load values less than the terrestrial critical load for the same watershed. Red circles indicate a condition where the terrestrial critical load is lower than the stream critical load.

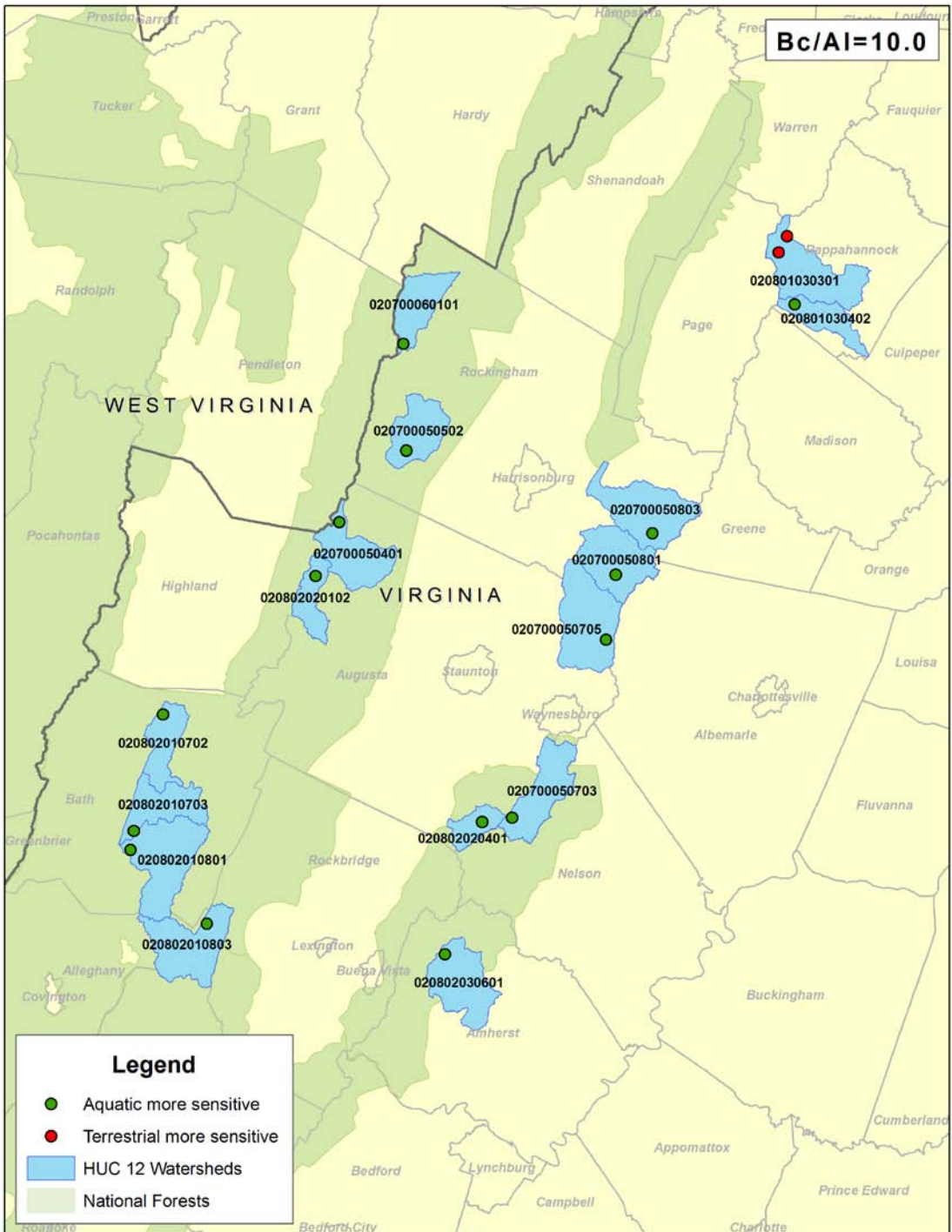


Figure A-4. Comparison of aquatic and terrestrial critical loads of acidification (in eq/ha/yr) in the 16 watersheds of the Shenandoah Case Study Area, based on an ANC of 50 eq/L for the aquatic loads and a Bc/AI of 1.2 for the terrestrial loads. Colored circles indicate the locations of the waters bodies within each watershed. Green circles indicate streams with critical load values less than the terrestrial critical load for the same watershed. Red circles indicate a condition where the terrestrial critical load is lower than the stream critical load.

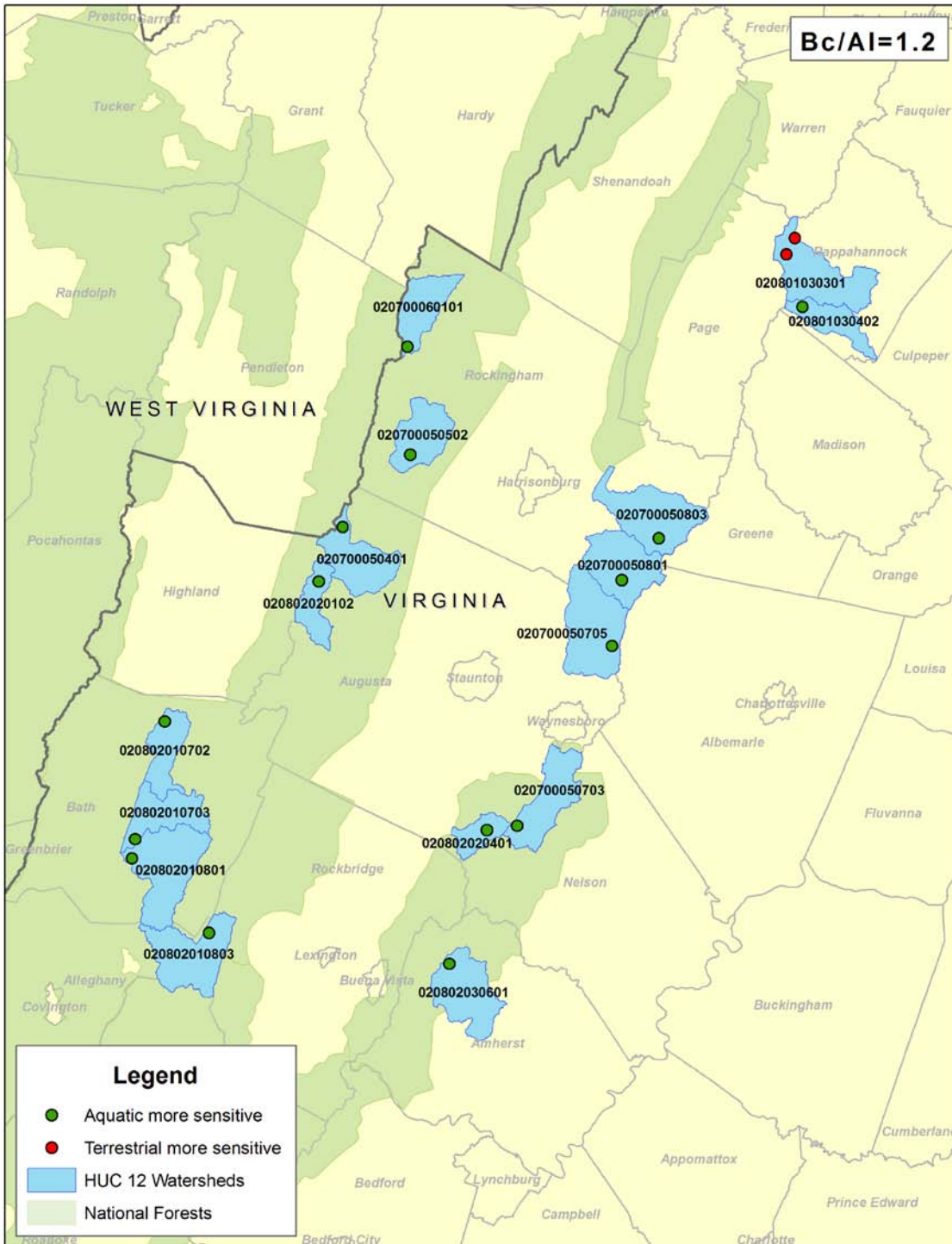


Table A-6. Relative sensitivities of aquatic versus terrestrial critical loads in the 29 lakes and 16 watersheds of the Adirondack Case Study Area (based on an ANC of 50 µeq/L for the aquatic loads and a Bc/Al of 10.0 for the terrestrial critical loads and common unit of eq/ha/yr) to acidifying nitrogen and sulfur deposition. Lake IDs are indicated in each cell and are from the REA REPORT (US EPA, 2009). Green text indicates lakes where the aquatic critical load was less than the terrestrial critical load value for the watershed. Red text indicates a condition where the terrestrial critical load for the watershed was lower than the aquatic critical load for the lake within the same watershed.

| HUC | CURRENT CONDITION OF ACIDITY AND SENSITIVITY TO ACIDIFICATION CATEGORY | | | |
|--------------|--|---|---|---|
| | Highly Sensitive (CL ≤ 50 meq/m ² /yr) | Moderately Sensitive (CL = 51-100 meq/m ² /yr) | Low Sensitivity (CL = 101-200 meq/m ² /yr) | Not Sensitive (CL > 201 meq/m ² /yr) |
| 020100010103 | | | | NY534L |
| 020100040203 | | | 1A2-028O NY310L | NY308L |
| 020100080304 | | | | NY312L NY313L |
| 020100081602 | | | | NY500L |
| 020200020101 | | NY013L | | |
| 020200020704 | | NY536L | | |
| 020200040805 | 1A2-078O | | NY292L | |
| 041501011001 | NY029L | | | |
| 041503020801 | | | | NY783L |
| 041503040102 | NY284L NY285L | | | |
| 041503040204 | | NY278L | | |
| 041503050103 | 1A1-089O | 050215AO NY793L | | |
| 041503050104 | NY290L | | | |

| HUC | CURRENT CONDITION OF ACIDITY AND SENSITIVITY TO ACIDIFICATION CATEGORY | | | |
|--------------|--|---|---|---|
| | Highly Sensitive (CL ≤ 50 meq/m ² /yr) | Moderately Sensitive (CL = 51-100 meq/m ² /yr) | Low Sensitivity (CL = 101-200 meq/m ² /yr) | Not Sensitive (CL > 201 meq/m ² /yr) |
| | NY289L | | | |
| 041503050302 | | | NY008L NY007L | |
| 041503050407 | | NY767L NY529L NY528L NY769L | NY768L | |
| 041503050601 | | | NY004L | |

Table A-7. Relative sensitivities of aquatic versus terrestrial critical loads in the 29 lakes and 16 watersheds of the Adirondack Case Study Area (based on an ANC of 50 µeq/L for the aquatic loads and a Bc/Al of 1.2 for the terrestrial critical loads and common unit of eq/ha/yr) to acidifying nitrogen and sulfur deposition. Lake IDs are indicated in each cell and are from the REA REPORT (US EPA, 2009). Green text indicates lakes where the aquatic critical load was less than the terrestrial critical load value for the watershed. Red text indicates a condition where the terrestrial critical load for the watershed was lower than the aquatic critical load for the lake within the same watershed.

| HUC | CURRENT CONDITION OF ACIDITY AND SENSITIVITY TO ACIDIFICATION CATEGORY | | | |
|--------------|--|---|---|---|
| | Highly Sensitive (CL ≤ 50 meq/m ² /yr) | Moderately Sensitive (CL = 51-100 meq/m ² /yr) | Low Sensitivity (CL = 101-200 meq/m ² /yr) | Not Sensitive (CL > 201 meq/m ² /yr) |
| 020100010103 | | | | NY534L |
| 020100040203 | | | 1A2-028O NY310L | NY308L |
| 020100080304 | | | | NY312L NY313L |
| 020100081602 | | | | NY500L |
| 020200020101 | | NY013L | | |
| 020200020704 | | NY536L | | |
| 020200040805 | 1A2-078O | | NY292L | |
| 041501011001 | NY029L | | | |
| 041503020801 | | | | NY783L |
| 041503040102 | NY284L NY285L | | | |
| 041503040204 | | NY278L | | |
| 041503050103 | 1A1-089O | 050215AO NY793L | | |

| HUC | CURRENT CONDITION OF ACIDITY AND SENSITIVITY TO ACIDIFICATION CATEGORY | | | |
|--------------|--|---|---|---|
| | Highly Sensitive (CL ≤ 50 meq/m ² /yr) | Moderately Sensitive (CL = 51-100 meq/m ² /yr) | Low Sensitivity (CL = 101-200 meq/m ² /yr) | Not Sensitive (CL > 201 meq/m ² /yr) |
| 041503050104 | NY290L NY289L | | | |
| 041503050302 | | | NY008L NY007L | |
| 041503050407 | | NY767L NY529L NY528L NY769L | NY768L | |
| 041503050601 | | | NY004L | |

Table A-8. Relative sensitivities of aquatic versus terrestrial critical loads in the 20 streams and 16 watersheds of the Shenandoah Case Study Area (based on an ANC of 50 µeq/L for the aquatic loads and a Bc/Al of 10.0 for the terrestrial critical loads and common unit of eq/ha/yr) to acidifying nitrogen and sulfur deposition. Stream IDs are indicated in each cell and are from the REA REPORT (US EPA, 2009). Green text indicates streams where the aquatic critical load was less than the terrestrial critical load value for the watershed. Red text indicates a condition where the terrestrial critical load for the watershed was lower than the aquatic critical load for the stream within the same watershed.

| HUC | CURRENT CONDITION OF ACIDITY AND SENSITIVITY TO ACIDIFICATION CATEGORY | | | |
|--------------|--|---|---|---|
| | Highly Sensitive (CL ≤ 50 meq/m ² /yr) | Moderately Sensitive (CL = 51-100 meq/m ² /yr) | Low Sensitivity (CL = 101-200 meq/m ² /yr) | Not Sensitive (CL > 201 meq/m ² /yr) |
| 020700050401 | VT37 | | | |
| 020700050502 | VT57 | | | |
| 020700050703 | VT40 | | | |
| 020700050705 | VT35 VT36 | | | |
| 020700050801 | DR01 WOR1 | | | |
| 020700050803 | VT53 | | | |
| 020700060101 | | VT54 | | |
| 020801030301 | | | VT60 | VT61 |
| 020801030402 | | VT62 | | |
| 020802010702 | VT10 | | | |
| 020802010703 | VT11 | VT12 | | |
| 020802010801 | VT14 VT15 | | | |

| HUC | CURRENT CONDITION OF ACIDITY AND SENSITIVITY TO ACIDIFICATION CATEGORY | | | |
|--------------|--|---|---|---|
| | Highly Sensitive (CL ≤ 50 meq/m ² /yr) | Moderately Sensitive (CL = 51-100 meq/m ² /yr) | Low Sensitivity (CL = 101-200 meq/m ² /yr) | Not Sensitive (CL > 201 meq/m ² /yr) |
| 020802010803 | VT16 | | | |
| 020802020102 | | VT38 | | |
| 020802020401 | VT41 | | | |
| 020802030601 | | VT46 | | |

Table A-9. Relative sensitivities of aquatic versus terrestrial critical loads in the 20 streams and 16 watersheds of the Shenandoah Case Study Area (based on an ANC of 50 µeq/L for the aquatic loads and a Bc/Al of 1.2 for the terrestrial critical loads and common unit of eq/ha/yr) to acidifying nitrogen and sulfur deposition. Stream IDs are indicated in each cell and are from the REA REPORT (US EPA, 2009). Green text indicates streams where aquatic critical loads were less than the terrestrial critical load value for the watershed. Red text indicates a condition where the terrestrial critical load for the watershed was lower than the aquatic critical load for the stream within the same watershed.

| HUC | CURRENT CONDITION OF ACIDITY AND SENSITIVITY TO ACIDIFICATION CATEGORY | | | |
|--------------|--|---|---|---|
| | Highly Sensitive (CL ≤ 50 meq/m ² /yr) | Moderately Sensitive (CL = 51-100 meq/m ² /yr) | Low Sensitivity (CL = 101-200 meq/m ² /yr) | Not Sensitive (CL > 201 meq/m ² /yr) |
| 020700050401 | VT37 | | | |
| 020700050502 | VT57 | | | |
| 020700050703 | VT40 | | | |
| 020700050705 | VT35 VT36 | | | |
| 020700050801 | DR01 WOR1 | | | |
| 020700050803 | VT53 | | | |
| 020700060101 | | VT54 | | |
| 020801030301 | | | VT60 | VT61 |
| 020801030402 | | VT62 | | |
| 020802010702 | VT10 | | | |
| 020802010703 | VT11 | VT12 | | |
| 020802010801 | VT14 VT15 | | | |

| HUC | CURRENT CONDITION OF ACIDITY AND SENSITIVITY TO ACIDIFICATION CATEGORY | | | |
|--------------|--|---|---|---|
| | Highly Sensitive (CL ≤ 50 meq/m ² /yr) | Moderately Sensitive (CL = 51-100 meq/m ² /yr) | Low Sensitivity (CL = 101-200 meq/m ² /yr) | Not Sensitive (CL > 201 meq/m ² /yr) |
| 020802010803 | VT16 | | | |
| 020802020102 | | VT38 | | |
| 020802020401 | VT41 | | | |
| 020802030601 | | VT46 | | |

REFERENCES

- Gebert, W.A., D.J. Graczyk, and W.R. Krug, 1987. *Average Annual Runoff in the United States, 1951-80: U.S. Geological Survey Hydrologic Investigations Atlas HA-710, Scale 1:7,500,000*. GIS datalayer. U.S. Department of Interior, U.S. Geological Survey, Madison, WI. Available at: <http://water.usgs.gov/GIS/dsdl/runoff.e00.gz> (accessed September 9, 2009).
- McNulty, S.G., E.C. Cohen, H. Li, and J.A. Moore-Myers. 2007. Estimates of critical acid loads and exceedences for forest soils across the conterminous United States. *Environmental Pollution* 149:281–292.
- NADP (National Atmospheric Deposition Program). 2003a. *Annual Calcium Wet Deposition, 2002*. GIS datalayer. National Atmospheric Deposition Program, Illinois State Water Survey, Champaign, IL. Available at <http://nadp.sws.uiuc.edu/maps/2002>.
- NADP (National Atmospheric Deposition Program). 2003b. *Annual Chloride Wet Deposition, 2002*. GIS datalayer. National Atmospheric Deposition Program, Illinois State Water Survey, Champaign, IL. Available at <http://nadp.sws.uiuc.edu/maps/2002>.
- NADP (National Atmospheric Deposition Program). 2003c. *Annual Magnesium Wet Deposition, 2002*. GIS datalayer. National Atmospheric Deposition Program, Illinois State Water Survey, Champaign, IL. Available at <http://nadp.sws.uiuc.edu/maps/2002>.
- NADP (National Atmospheric Deposition Program). 2003d. *Annual Potassium Wet Deposition, 2002*. GIS datalayer. National Atmospheric Deposition Program, Illinois State Water Survey, Champaign, IL. Available at <http://nadp.sws.uiuc.edu/maps/2002>.
- NADP (National Atmospheric Deposition Program). 2003e. *Annual Sodium Wet Deposition, 2002*. GIS datalayer. National Atmospheric Deposition Program, Illinois State Water Survey, Champaign, IL. Available at <http://nadp.sws.uiuc.edu/maps/2002>.
- UNECE (United Nations Economic Commission for Europe). 2004. *Manual on Methodologies and Criteria for Modeling and Mapping Critical Loads and Levels and Air Pollution Effects, Risks, and Trends*. Convention on Long-Range Transboundary Air Pollution, Geneva Switzerland. Available at <http://www.icpmapping.org> (accessed August 16, 2006).
- USDA-NRCS (United States Department of Agriculture-Natural Resources Conservation Service). 2008. *Soil Survey Geographic (SSURGO) Database*. GIS datalayer. U.S. Department of Agriculture, Natural Resources Conservation Service, Washington, DC. Available at <http://datagateway.nrcs.usda.gov>.
- US EPA (United States Environmental Protection Agency). 2009. *Risk and Exposure Assessment for Review of the Secondary National Ambient Air Quality Standards for Oxides of Nitrogen and Sulfur*. Final. U.S. Environmental Protection Agency, Office of Research and Development, National Center for Environmental Assessment, Research Triangle Park, NC. September.
- USGS (U.S. Geological Survey). 2009. *State Geological Map Compilation*. U.S. Department of the Interior, U.S. Geological Survey, Reston, VA. Available at: <http://tin.er.usgs.gov/geology/state> (accessed January 28, 2009).

Appendix B

Methodologies and assumptions used in steady state ecosystem modeling

Technical summary of critical loads modeling in the REA

The critical load of acidity for lakes or streams was derived from present-day water chemistry using a combination of steady-state models. Both the Steady-State Water Chemistry (SSWC) model and First-order Acidity Balance model (FAB) are based on the principle that excess base-cation production within a catchment area should be equal to or greater than the acid anion input, thereby maintaining the ANC above a preselected level (Reynolds and Norris, 2001; Posch et al. 1997). These models assume steady-state conditions and assume that all SO_4^{2-} in runoff originates from sea salt spray and anthropogenic deposition. Given a critical ANC protection level, the critical load of acidity is simply the input flux of acid anions from atmospheric deposition (i.e., natural and anthropogenic) subtracted from the natural (i.e., preindustrial) inputs of base cations in the surface water (REA 2009 Appendix 4).

Atmospheric deposition of NO_x and SO_x contributes to acidification in aquatic ecosystems through the input of acid anions, such as NO_3^- and SO_4^{2-} . The acid balance of headwater lakes and streams is controlled by the level of this acidifying deposition of NO_3^- and SO_4^{2-} and a series of biogeochemical processes that produce and consume acidity in watersheds. The biotic integrity of freshwater ecosystems is then a function of the acid-base balance, and the resulting acidity-related stress on the biota that occupy the water. The calculated ANC of the surface waters is a measure of the acid-base balance:

$$\text{ANC} = [\text{BC}]^* - [\text{AN}]^* \quad (1)$$

where $[\text{BC}]^*$ and $[\text{AN}]^*$ are the sum of base cations and acid anions (NO_3^- and SO_4^{2-}), respectively. Equation (1) forms the basis of the linkage between deposition and surface water acidic condition and the modeling approach used. Given some “target” ANC concentration $[\text{ANClimit}]$ that protects biological integrity, the amount of deposition of acid anions $[\text{AN}]$ or depositional load of acidity $\text{CL}(\text{A})$ is simply the input flux of acid anions from atmospheric deposition that result in a surface water ANC concentration equal to the $[\text{ANClimit}]$ when balanced by the sustainable flux of base cations input and the sinks of nitrogen and sulfur in the lake and watershed catchment.

Critical loads for nitrogen and sulfur (CL(N) + CL(S)) or critical load of acidity CL(A) were calculated for each waterbody from the principle that the acid load should not exceed the nonmarine, nonanthropogenic base cation input and sources and sinks in the catchment minus a target ANC (ANClim) to protect selected biota from being damaged:

$$CL(N) + CL(S) \text{ or } CL(A) = BC^*_{dep} + BC_w - B_{cu} - AN - ANClimit \quad (2)$$

Where,

$BC^*_{dep} = (BC^* = Ca^* + Mg^* + K^* + Na^*)$, nonanthropogenic deposition flux of base cations,

BC_w = the average weathering flux producing base cations,

B_{cu} ($B_c = Ca^* + Mg^* + K^*$) = the net long-term average uptake flux of base cations in the biomass (i.e., the annual average removal of base cations due to harvesting),

AN = the net long-term average uptake, denitrification, and immobilization of nitrogen anions (e.g. NO_3^-) and uptake of SO_4^{2-} , and

$ANClimit$ = the lowest ANC-flux that protects the biological communities.

Since the average flux of base cations weathered in a catchment and reaching the lake or streams is difficult to measure or compute from available information, the average flux of base cations and the resulting critical load estimation were derived from water quality data (Henriksen and Posch, 2001; Henriksen et al., 1992; Sverdrup et al., 1990). Weighted annual mean water chemistry values were used to estimate average base cation fluxes, which were calculated from water chemistry data collected from the Temporally Integrated Monitoring of Ecosystems (TIME)/Long-Term Monitoring (LTM) monitoring networks, that include Adirondack Longterm Monitoring (ALTM), Virginia Trout Stream Sensitivity Study (VTSSS), and the Shenandoah Watershed Study (SWAS), and Environmental Monitoring and Assessment Program (EMAP) (see REA Section 4.1.2.1 of Chapter 4).

The preacidification nonmarine flux of base cations for each lake or stream, BC^*_0 , is

$$BC^*_0 = BC^*_{dep} + BC_w - B_{cu} \quad (3)$$

Thus, critical load for acidity can be rewritten as

$$CL(N) + CL(S) = BC^*0 - AN - ANClimit = Q([BC^*]0 - [AN] - [ANC]limit), \quad (4)$$

where the second identity expresses the critical load for acidity in terms of catchment runoff (Q) m/yr and concentration ($[x] = X/Q$). The sink of nitrogen in the watershed is equal to the uptake (Nupt), immobilization (Nimm), and denitrification (Nden) of nitrogen in the catchment. Thus, critical load for acidity can be rewritten as

$$CL(N) + CL(S) = \{fNupt + (1 - r)(Nimm + Nden)\} + ([BC]0^* - [ANClimit])Q \quad (5)$$

where f and r are dimensionless parameters that define the fraction of forest cover in the catchment and the lake/catchment ratio, respectively. The in-lake retention of nitrogen and sulfur was assumed to be negligible.

Equation (5) described the FAB model that was applied in the REA when sufficient data was available to estimate the uptake, immobilization, and denitrification of nitrogen and the neutralization of acid anions (e.g. NO₃⁻) in the catchment. In the case where data were not available, the contribution of nitrogen anions to acidification was assumed to be equal to the nitrogen leaching rate (Nleach) into the surface water. The flux of acid anions in the surface water is assumed to represent the amount of nitrogen that is not retained by the catchment, which is determined from the sum of measured concentration of NO₃⁻ and ammonia in the stream chemistry. This case describes the SSWC model and the critical load for acidity is

$$CL(A) = Q([BC^*]0 - [ANC]limit) \quad (6)$$

where the contribution of acid anions is considered as part of the exceedances calculation (see REA App 4 Section 1.2.5). For the assessment of current condition in both case study areas in the REA, the critical load calculation described in Equation (6) was used for most lakes and streams. The lack of sufficient data for quantifying nitrogen denitrification and immobilization prohibited the wide use of the FAB model. In addition, given the uncertainty in quantifying

nitrogen denitrification and immobilization, the flux of nitrogen anions in the surface water was assumed to more accurately reflect the contribution of NO₃⁻ to acidification. Several major assumptions are made: (1) steady-state conditions exist, (2) the effect of nutrient cycling between plants and soil is negligible, (3) there are no significant nitrogen inputs from sources other than atmospheric deposition, (4) ammonium leaching is negligible because any inputs are either taken up by biota or adsorbed onto soils or nitrate compounds, and (5) longterm sinks of sulfate in the catchment soils are negligible.

Pre-industrial Base Cation Concentration

The pre-industrial concentration of base cations [BC]₀^{*} effectively set the long term capacity of the catchment to neutralize acidic deposition, because it represents the only source of base cation input that is sustainable over the long-term. Input of cations from weathering is assumed to be a relatively constant process driven largely by the reaction of CO₂ with primary minerals in the soils and bedrock. Base cations are removed by leaching from the soil solution through surface water runoff. At a steady-state, the leaching rate of base cation occurs at lesser or greater rates than the weathering supply. However, base cation leaching is not at steady-state today because anthropogenic acid deposition actually increases the leaching of base cations through ion-exchange within catchment soils. Soils contain a store of adsorbed base cations, as measured as base saturation, which are derived from weathering, but have accumulated in the soil over millennia, until eventually a steady-state is achieved, whereby the supply of base cations from weathering was in approximate equilibrium with the removal of base cations by rainwater, itself in equilibrium with the atmosphere. For this reason, [BC]₀^{*} cannot be derived from measured data in runoff, but derived from a empirical relationships (i.e., pre-industrial base cation concentration).

The pre-industrial base cation concentration is the sum of weathering ([BC]_w^{*}) supply plus base cation deposition ([BC]_{dep}^{*}), if it is assumed that base cation deposition has not significantly changed since pre-industrial times, minus long-term average uptake of base cations in the biomass (i.e., the annual average removal of base cations due to harvesting):

$$[BC]_0^* = [BC_w] + [BC_{dep}^*] - [BC_u] \quad (7)$$

F-factor

An F-factor was used to correct the concentrations and estimate preindustrial base concentrations for lakes in the Adirondack Case Study Area (REA 2009). In the case of streams in the Shenandoah Case Study Area, the preindustrial base concentrations were derived from the MAGIC model as the base cation supply in 1860 (hindcast) because the F-factor approach is untested in this region. An F-factor is a ratio of the change in nonmarine base cation concentration due to changes in strong acid anion concentrations (Henriksen, 1984; Brakke et al., 1990):

$$F = ([BC^*]_t - [BC^*]_0) / ([SO_4^*]_t - [SO_4^*]_0 + [NO_3^*]_t - [NO_3^*]_0), \quad (8)$$

where the subscripts t and 0 refer to present and preacidification conditions, respectively. If F=1, all incoming protons are neutralized in the catchment (only soil acidification); at F=0, none of the incoming protons are neutralized in the catchment (only water acidification). The F-factor was estimated empirically to be in the range 0.2 to 0.4, based on the analysis of historical data from Norway, Sweden, the United States, and Canada (Henriksen, 1984). Brakke et al. (1990) later suggested that the F-factor should be a function of the base cation concentration:

$$F = \sin(\pi/2 Q[BC^*]_t/[S]) \quad (9)$$

Where

Q = the annual runoff (m/yr),

[S] = the base cation concentration at which F=1; and

for $[BC^*]_t > [S]$ F is set to 1.

For Norway [S] has been set to 400 milliequivalents per cubic meter (meq/m³) (circa 8 mg Ca/L) (Brakke et al., 1990). We assumed the steady-state concentration of nitrate ($[AA]_0$) was zero ($[AA]_0^* = 0$). The preacidification SO₄²⁻ concentration in lakes, $[SO_4^*]_0$, is assumed to consist of a constant atmospheric contribution and a geologic contribution proportional to the concentration of base cations (Brakke et al., 1989; Harriman and Christie, 1995). The preacidification SO₄²⁻ concentration in lakes, $[SO_4^*]_0$ was estimated from the relationship between $[SO_4^{2-}]_0^*$ and $[BC]_t^*$ based on work completed by Henriksen et al., 2002 as described by the following equation:

$$[\text{SO}_4^{2-}]_0^* = 15 + 0.16 * [\text{BC}]_t^* \quad (10)$$

This F value is then used to calculate the pre-industrial base cation concentration according to the following equation:

$$[\text{BC}^*]_0^* = [\text{BC}^*]_t - F([\text{AA}]_t^* - [\text{AA}]_0^*) \quad (11)$$

Tables B-1 and B-2 list the factors used in the SSWC and FAB approaches.

| Table B-1 Illustrates SSWC Approach – Environmental Variables | | | |
|--|---------------|---|------------------------------------|
| $CL(A) = BC_{dep}^* + BC_w - Bc_u - ANC_{limit}$ $CL(A) = Q([BC^*]_0 - [ANC]_{limit})$ | | | |
| | Variable Code | Description | Source |
| 1 | BC_{dep}^* | Sum ($Ca^*+Mg^*+K^*+Na^*$), nonanthropogenic deposition flux of base cations | Wet NADP and Dry CASTNET |
| 2 | BC_w | Average weathering flux of base cations | Calculated (5-17) |
| 3 | Bc_u | Sum ($Ca+Mg+K$), the net long-term average uptake flux of base cations in the biomass | USFS-FIA data |
| 4 | ANC_{limit} | Lowest ANC-flux that protects the biological communities | Set |
| 5 | Ca^* | Sea Salt corrected Surface water concentration ($\mu eq/L$) growing season average. ($Ca - (CL \times 0.0213)$) | Water quality data |
| 6 | Mg^* | Sea Salt corrected Surface water concentration ($\mu eq/L$) growing season average. ($Mg - (CL \times 0.0669)$) | Water quality data |
| 7 | Na^* | Sea Salt corrected Surface water concentration ($\mu eq/L$) growing season average. ($Na - (CL \times 0.557)$) | Water quality data |
| 8 | K^* | Sea Salt corrected Surface water concentration ($\mu eq/L$) growing season average. ($K - (CL \times 0.0206)$) | Water quality data |
| 9 | SO_4^* | Sea Salt corrected Surface water concentration ($\mu eq/L$) growing season average. ($SO_4 - (CL \times 0.14)$) | Water quality data |
| 10 | CL | Surface water concentration ($\mu eq/L$) growing season average. | Water quality data |
| 11 | SO_4^* | Surface water concentration ($\mu eq/L$) growing season average. | Water quality data |
| 12 | NO_3^* | Surface water concentration ($\mu eq/L$) growing season average. | Water quality data |
| 13 | Q | The annual runoff (m/yr) | USGS |
| 14 | $[BC^*]_0$ | Preindustrial flux of base cations in surface water, corrected for sea salts | Calculated from water quality data |
| 15 | $[SO_4^*]_0$ | Preindustrial flux of sulfate in surface water, corrected for sea salts | Estimated |
| 16 | $[NO_3^*]_0$ | Preindustrial flux of nitrate, corrected for sea salts | Equal to 0 |
| 17 | F | Calculated factor | Fix values |

| Table B-2 FAB Approach – Environmental Variables | | | |
|---|----------------------|---|------------------------------------|
| $DL(N) + DL(S) = \{fN_{upt} + (1 - r)(N_{imm} + N_{den}) + (N_{ret} + S_{ret})\} + ([BC]_0^* - [ANC_{limit}])Q$ | | | |
| | Variable Code | Description | Source |
| 1 | Ndepo | Total N deposition | NADP/CMAQ |
| 2 | ANCLimit | Lowest ANC-flux that protects the biological communities | Set |
| 3 | $[BC^*]_0$ | Preindustrial flux of base cations in surface water, corrected for sea salt | Calculated from water quality data |
| 4 | Ca^* | Sea Salt corrected Surface water concentration ($\mu\text{eq/L}$) growing season average. ($Ca - (CL \times 0.0213)$) | Water quality data |
| 5 | Mg^* | Sea Salt corrected Surface water concentration ($\mu\text{eq/L}$) growing season average. ($Mg - (CL \times 0.0669)$) | Water quality data |
| 6 | Na^* | Sea Salt corrected Surface water concentration ($\mu\text{eq/L}$) growing season average. ($Na - (CL \times 0.557)$) | Water quality data |
| 7 | K^* | Sea Salt corrected Surface water concentration ($\mu\text{eq/L}$) growing season average. ($K - (CL \times 0.0206)$) | Water quality data |
| 8 | SO_4^* | Sea Salt corrected Surface water concentration ($\mu\text{eq/L}$) growing season average. ($SO_4 - (CL \times 0.14)$) | Water quality data |
| 9 | CL | Surface water concentration ($\mu\text{eq/L}$) growing season average. | Water quality data |
| 10 | SO_4^* | Surface water concentration ($\mu\text{eq/L}$) growing season average. | Water quality data |
| 11 | NO_3^* | Surface water concentration ($\mu\text{eq/L}$) growing season average. | Water quality data |
| 12 | Q | The annual runoff (m/yr) | USGS |
| 13 | f | f is a dimensionless parameter that define the fraction of forest cover in the catchment | |
| 14 | r | r is a dimensionless parameter that define the lake/catchment ratio | |
| 14 | N_{ret} | The in-lake retention of nitrogen | Estimated |
| 15 | S_{ret} | The in-lake retention of sulfur | Estimated |
| 16 | N_{upt} | The net long-term average uptake flux of N in the biomass | USFS-FIA data |
| 17 | N_{imm} | Immobilization of N in the soils | Estimated fix value |
| 18 | N_{den} | Denitrification | Estimated fix value |
| 19 | Lake Size | Lake size (ha) | DLMs |
| 20 | WSH | Watershed area (ha) | Calculated |

Data requirements for MAGIC

The MAGIC model (Cosby et al., 1985a; 1985b; 1985c) is a mathematical model (a lumped-parameter model) of soil and surface water acidification in response to atmospheric deposition based on process-level information about acidification. A process model, such as MAGIC, characterizes acidification into (1) a section in which the concentrations of major ions are assumed to be governed by simultaneous reactions involving SO_4^{2-} adsorption, cation exchange, dissolution-precipitation- speciation of aluminum, and dissolution-speciation of inorganic carbon; and (2) a mass balance section in which the flux of major ions to and from the soil is assumed to be controlled by atmospheric inputs, chemical weathering, net uptake and loss in biomass and losses to runoff. At the heart of MAGIC is the size of the pool of exchangeable base cations in the soil. As the fluxes to and from this pool change over time owing to changes in atmospheric deposition, the chemical equilibria between soil and soil solution shift to give changes in surface water chemistry. The degree and rate of change of surface water acidity thus depend both on flux factors and the inherent characteristics of the affected soils.

There are numerous input data required to run MAGIC making it rather data intensive. Atmospheric deposition fluxes for the base cations and strong acid anions are required as inputs to the model. These inputs are generally assumed to be uniform over the catchment. The volume discharge for the catchment must also be provided to the model. In general, the model is implemented using average hydrologic conditions and meteorological conditions in annual simulations, i.e., mean annual deposition, precipitation and lake discharge are used to drive the model. Values for soil and surface water temperature, partial pressure of carbon dioxide and organic acid concentrations must also be provided at the appropriate temporal resolution.

The aggregated nature of the model requires that it be calibrated to observed data from a system before it can be used to examine potential system response. Calibrations are based on volume weighted mean annual or seasonal fluxes for a given period of observation. The length of the period of observation used for calibration is not arbitrary. Model output will be more reliable if the annual flux estimates used in calibration are based on a number of years rather than just one year. There is a lot of year-to-year variability in atmospheric deposition and catchment runoff. Averaging over a number of years reduces the likelihood that an “outlier” year (very dry, etc.) is used to specify the primary data on which model forecasts are based. On the other hand,

averaging over too long a period may remove important trends in the data that need to be simulated by the model.

The calibration procedure requires that stream water quality, soil chemical and physical characteristics, and atmospheric deposition data be available for each catchment. The water quality data needed for calibration are the concentrations of the individual base cations (Ca, Mg, Na, and K) and acid anions (Cl, SO₄²⁻, and NO₃⁻) and the pH. The soil data used in the model include soil depth and bulk density, soil pH, soil cation-exchange capacity, and exchangeable bases in the soil (Ca, Mg, Na, and K). The atmospheric deposition inputs to the model must be estimates of total deposition, not just wet deposition. In some instances, direct measurements of either atmospheric deposition or soil properties may not be available for a given site with stream water data. In these cases, the required data can often be estimated by: (a) assigning soil properties based on some landscape classification of the catchment; and (b) assigning deposition using model extrapolations from some national or regional atmospheric deposition monitoring network. Soil data for model calibration are usually derived as aerially averaged values of soil parameters within a catchment. If soils data for a given location are vertically stratified, the soils data for the individual soil horizons at that sampling site can be aggregated based on horizon, depth, and bulk density to obtain single vertically aggregated values for the site, or the stratified data can be used directly in the model.

Example of the two ways to calculate N_{ECO}

The steady-state critical load model suggested for use in the NAAQS by the PA could be constrained by a quantity of N which would be taken up, immobilized or denitrified by ecosystems and used to adjust the quantity of deposition required to meet a specified critical load. This term is abbreviated by N_{eco}, and could be derived multiple ways. The first is by taking the mean value calculated to represent the long-term amount of N an ecosystem can immobilize and denitrify before leaching (i.e., N saturation) that is derived from the FAB model. This approach requires the input of multiple ecosystem parameters. Its components are expressed by equation (13).

$$N_{eco} = fN_{upt} + N_{ret} + (1 - r)(N_{imm} + N_{den}) \quad (13)$$

Where,

N_{upt}= nitrogen uptake by the catchment,

N_{imm} = nitrogen immobilization by the catchment soil,
 N_{den} = denitrification of nitrogen in the catchment,
 N_{ret} = in-lake retention of nitrogen,
 f = forest cover in the catchment (dimensionless parameter),
 r = fraction lake/catchment ratio (dimensionless parameter),

The second approach for estimating N_{eco} is to take the difference between N deposition and measured N leaching in a catchment as expressed by equation (14).

$$N_{eco} = DL(N) - N_{leach} \quad (14)$$

The site specific values of critical loads can be used to derive such a deposition loading, here called the deposition metric, which represents a group or percentage of water bodies that reach a specified ANC (or higher) in a given spatial area. For example, if it is desired that all water bodies reach a specified ANC, the allowable amount of deposition for all water bodies is equal to the lowest critical load of the population of water bodies. Because the deposition metric represents a percentage of individual catchments from a population of water bodies, and not an individual catchment, the deposition metric is noted by the follow abbreviation $DL_{\%ECO}$.

Two methods to calculate pre-industrial base cation weathering: F factor and MAGIC

The preindustrial concentration of base cations ($[BC]_0^*$) is calculated to represent conditions prior to industrialization (~about 1860). It incorporates the main source of base cations to an ecosystem including preindustrial weathering from soil and pre-industrial base cation deposition. It is therefore considered one of the governing factors of critical loads. $[BC]_0^*$ is commonly calculated using one of two approaches: dynamic modeling (i.e. MAGIC) and calculation by the F-factor approach (Henriksen and Posch 2001).

In this section, critical load estimates obtained from two steady-state approaches were compared. The exercise is not intended to provide an assessment of the accuracy of the two models, but rather to provide a means for evaluating the relative performance of the two different models. The EPA conducted analysis compared steady-state CL values based on Henriksen and Posch (2001) F-factor approach and output from the MAGIC model. The primary purpose of the F-factor is to obtain estimates of preindustrial surface water base cation concentrations ($[BC]_0^*$) for equation (3). The MAGIC (Cosby et al., 1985) model can also be used to derive preindustrial

surface water base cation concentrations. MAGIC is a process-based model designed to mimic the geochemical effects of mineral weathering, soil cation exchange, and other watershed processes. Once the model has been calibrated for a watershed, it can be run to simulate how surface water chemistry changes with time and to predict preindustrial cation concentrations ($[BC]_0^*$) to be used in the steady-state SSWC CL model in equation (6).

The comparison of CLs between the F-factor and MAGIC approached was done for two regions, streams in Southern Appalachia and lakes in the Adirondack Mountains. For 67 streams and 99 lakes, $[BC]_0^*$ were determined for both approaches and CLs were calculated using the same value of Q. The results are show in Figure B-1. For this analysis, the steady-state MAGIC model yielded critical load values that show the same trend for both regions, but were on average 16 meq S /m²-yr for the Adirondack Lakes and 5 meq S/m²-yr for Southern Appalachia streams higher than those from the SSWC F-factor approach. The two models converge at low critical loads, but diverge as the buffering potential for watersheds increase. This is particularly the case for CL values above 80 meq/m²-yr for lakes in the Adirondack Mountains. These results are consistent with similar comparison of critical loads done by Holdren et al. 1992. Holdren et al 1992 found that the MAGIC model yielded CL values that were on average 29 meq S /m²-yr higher than those from the SSWC model. Holdren et al 1992 also found that as the buffering potential for watersheds increased, as indicated by increasing CLs, the results from the two models gradually diverge.

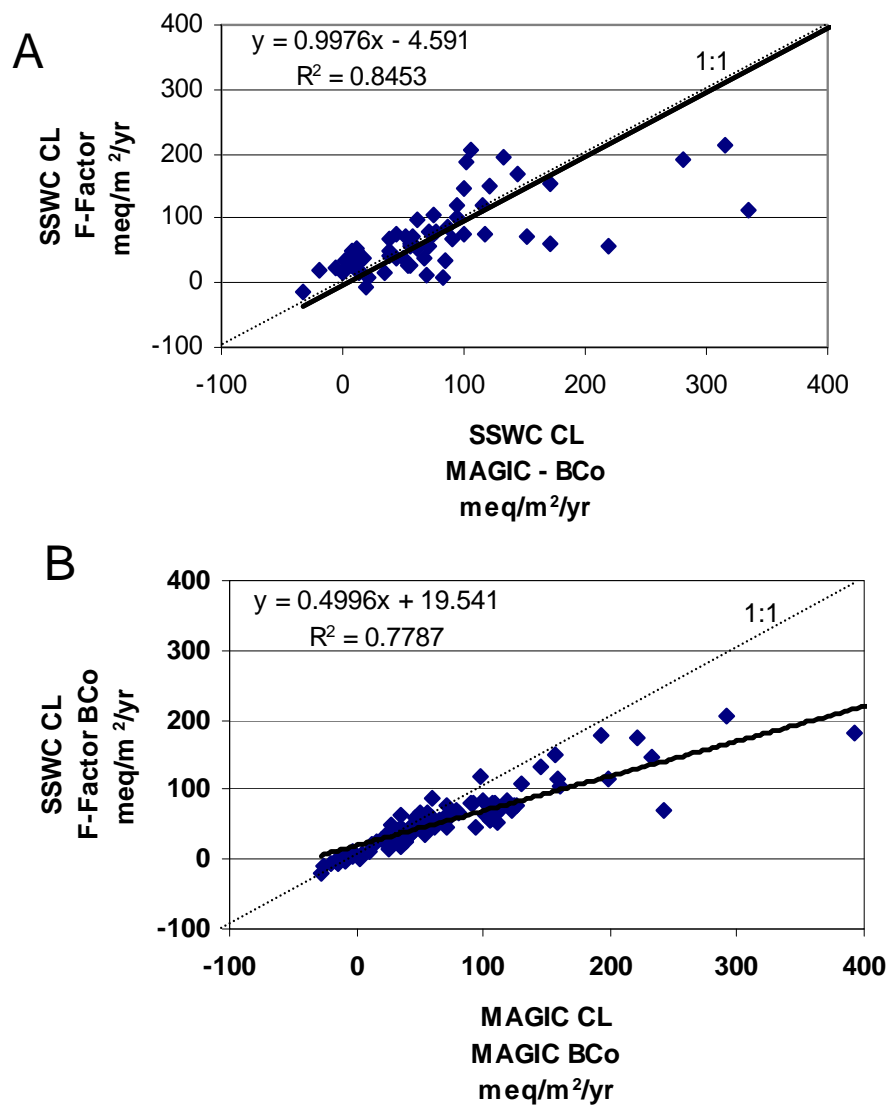


Figure B-1 Relationship between CLs using pre-industrial base cation weathering ($[BC]_0^* = BCo$) calculated by MAGIC versus the F-factor methods: **A)** 67 streams in the Southern Appalachian and **B)** 99 lakes in the Adirondacks Mountains.

References

- Brakke, D.F., A. Henriksen, and S.A. Norton. 1989. Estimated background concentrations of sulfate in dilute lakes. *Water Resources Bulletin* 25(2):247–253.
- Brakke, D.F., A. Henriksen, and S.A. Norton. 1990. A variable F-factor to explain changes in base cation concentrations as a function of strong acid deposition. *International Association of Theoretical and Applied Limnology, Proceedings* 24:146–149.
- Cosby, B.J., R.F. Wright, G.M. Hornberger, and J.N. Galloway. 1985a. Modelling the effects of acid deposition: Assessment of a lumped parameter model of soil water and streamwater chemistry. *Water Resources Research* 21:51–63.
- Cosby, B.J., R.F. Wright, G.M. Hornberger, and J.N. Galloway. 1985b. Modelling the effects of acid deposition: Estimation of long-term water quality responses in a small forested catchment. *Water Resources Research* 21:1591–1601.
- Cosby B.J., G.M. Hornberger, J.N. Galloway, and R.F. Wright. 1985c. Time scales of catchment acidification: a quantitative model for estimating freshwater acidification. *Environ Sci Technol*, 19, 1144-1149.
- Harriman, R. and Christie, A. E. G.: 1995, ‘Estimating Critical Loads for Biota: the Steady-state Water Chemistry (Henriksen) Model’, in *Critical Loads of Acid Deposition for United Kingdom Freshwaters*, Critical Loads Advisory Group, Sub-group on Freshwaters, Institute of Terrestrial Ecology: Edinburgh, pp. 7–8.
- Henriksen, A. 1984. Changes in base cation concentrations due to freshwater acidification. *International Association of Theoretical and Applied Limnology, Proceedings* 22:692–698.
- Henriksen A., P.J. Dillon, and J. Aherne. 2002. Critical loads of acidity to surface waters in south-central Ontario, Canada: Regional application of the steady-state water chemistry model. *Can J Fish Aquat Sci*, 59, 1287-1295.
- Henriksen, A., and M. Posch. 2001. Steady-state models for calculating critical loads of acidity for surface waters. *Water, Air, and Soil Pollution: Focus* 1:375–398.
- Henriksen, A., J. Kämäri, M. Posch, and A. Wilander. 1992. Critical loads of acidity: Nordic surface waters. *Ambio* 21:356–363.
- Holdren, G., T. Strickland, P. Shaffer, P. Ryan, P. Ringold, and R. Turner. 1992. Sensitivity of Critical Load Estimates for Surface Waters to Model Selection and Regionalization Schemes. *Journal of Environmental Quality*, 22: 279-289.
- Posch, M., J. Kämäri, M. Forsius, A. Henriksen, and A. Wilander. 1997. Exceedance of critical loads for lakes in Finland, Norway and Sweden: Reduction requirements for acidifying nitrogen and sulfur deposition. *Environmental Management* 21: 291–304.
- Reynolds, B., and D.A. Norris. 2001. Freshwater critical loads in Wales. *Water, Air, and Soil Pollution: Focus* 1:495–505.
- Sverdrup, H., W. de Vries, and A. Henriksen. 1990. Mapping Critical Loads. *Miljörapport 14*. Nordic Council of Ministers, Copenhagen, Denmark.
- US EPA. 2009. Risk and Exposure Assessment for Review of the Secondary National Ambient Air Quality Standards for Oxides of Nitrogen and Oxides of Sulfur-Main Content - Final Report. U.S. Environmental Protection Agency, Washington, D.C., EPA-452/R-09-008a.

Appendix C

Ecoregions, Level III: Description and Summary of Environmental Conditions

Introduction

This appendix provides descriptions of each of the level III ecoregions as described by Omernik (U.S. EPA 2010) and used in this Policy Assessment. The level III ecoregions are presented grouped by the level II ecoregion in which they are located. Figure C-1 illustrates the location of the level II ecoregions across the U.S. The subsequent figures illustrate the level III ecoregions within each level II ecoregion and present a summary of the raw water quality data. Figure C-2 is a summary of the water quality data at the national level for comparison with the level III ecoregion data. These maps also indicate the extent of ANC and critical load values available for each ecoregion. The general regional descriptions are taken from Omernik (U.S. EPA 2010).

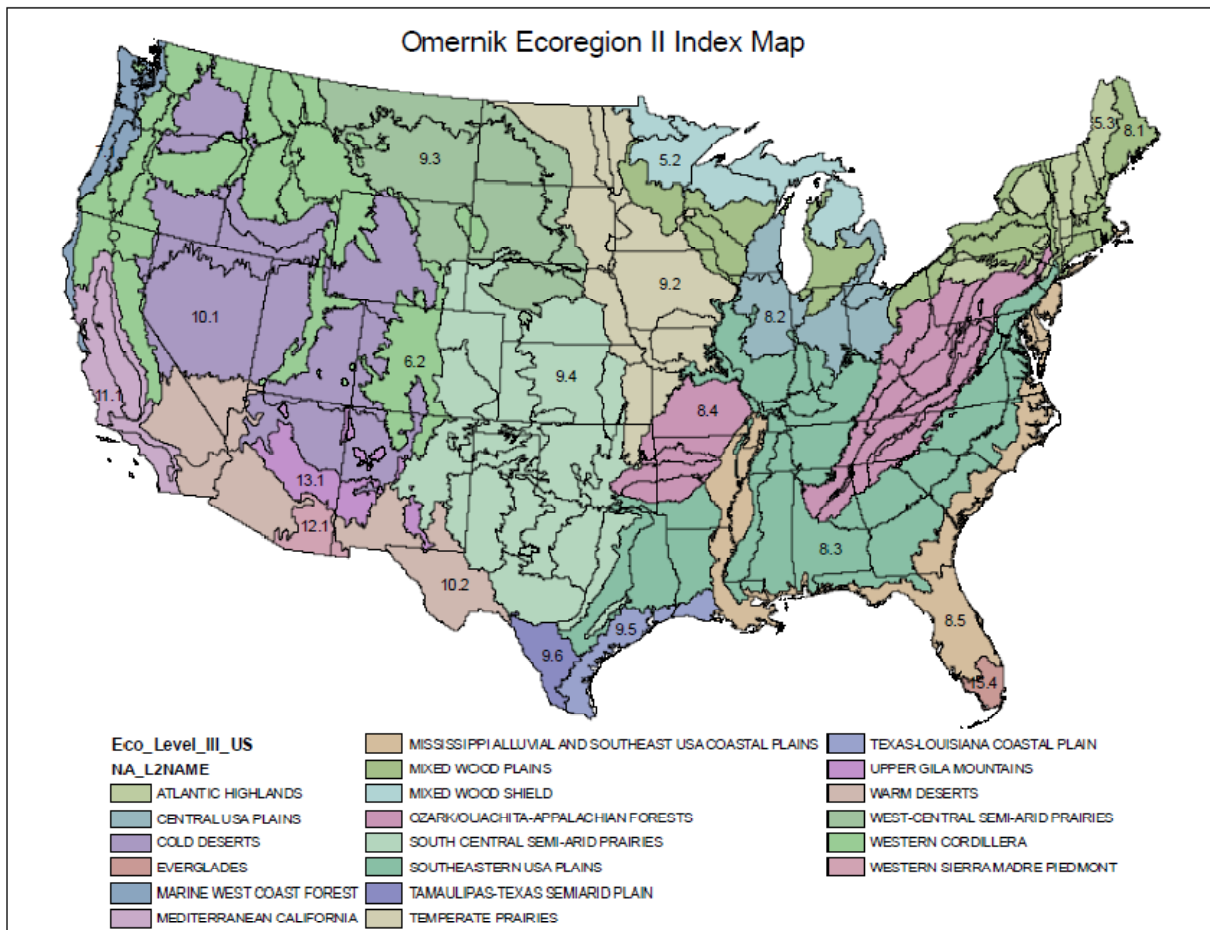


Figure C-1. Omernik Ecoregions, Levels II and III

All Regions

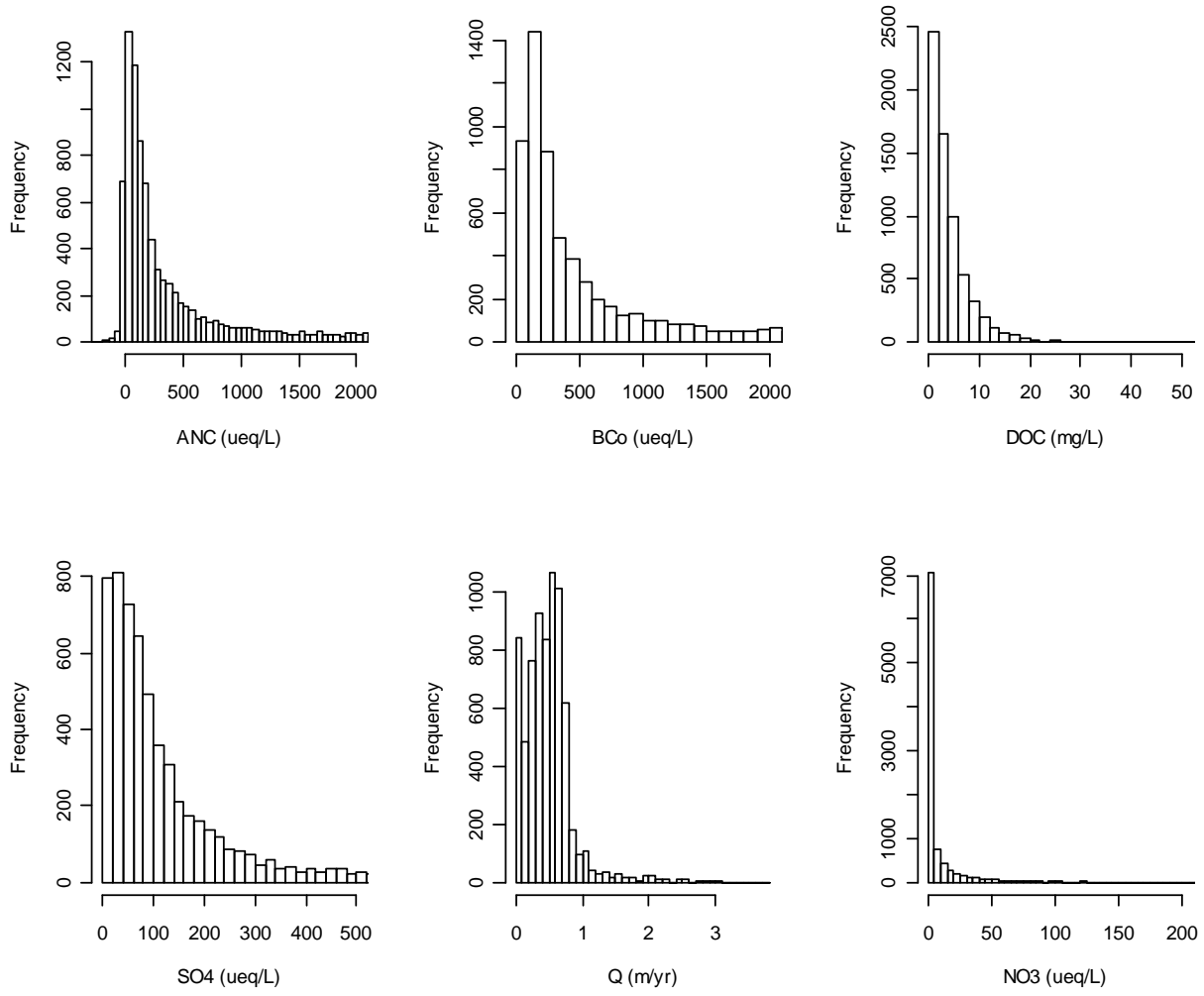


Figure C-2. National Water Quality Data Summary

Region 5.2 Mixed Wood Shield

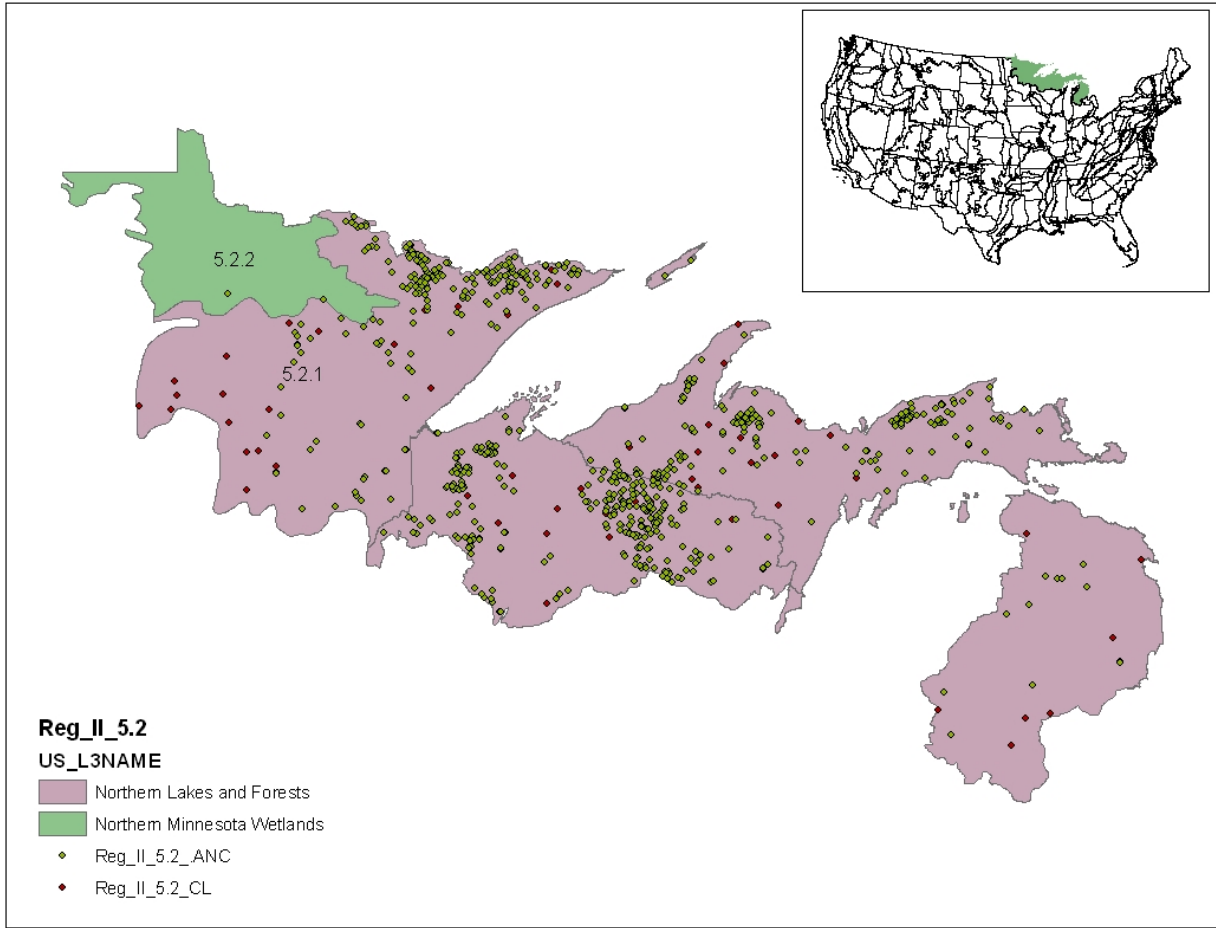


Figure C-3. Region 5.2

Region 5.2.1 Northern Lakes and Forests

The Northern Lakes and Forests is a region of relatively nutrient-poor glacial soils, coniferous and northern hardwood forests, undulating till plains, morainal hills, broad lacustrine basins, and extensive sandy outwash plains. Soils in this ecoregion are thicker than in those to the north and generally lack the arability of soils in adjacent ecoregions to the south. The numerous lakes that dot the landscape are clearer and less productive than those in ecoregions to the south.

Region 5.2.1

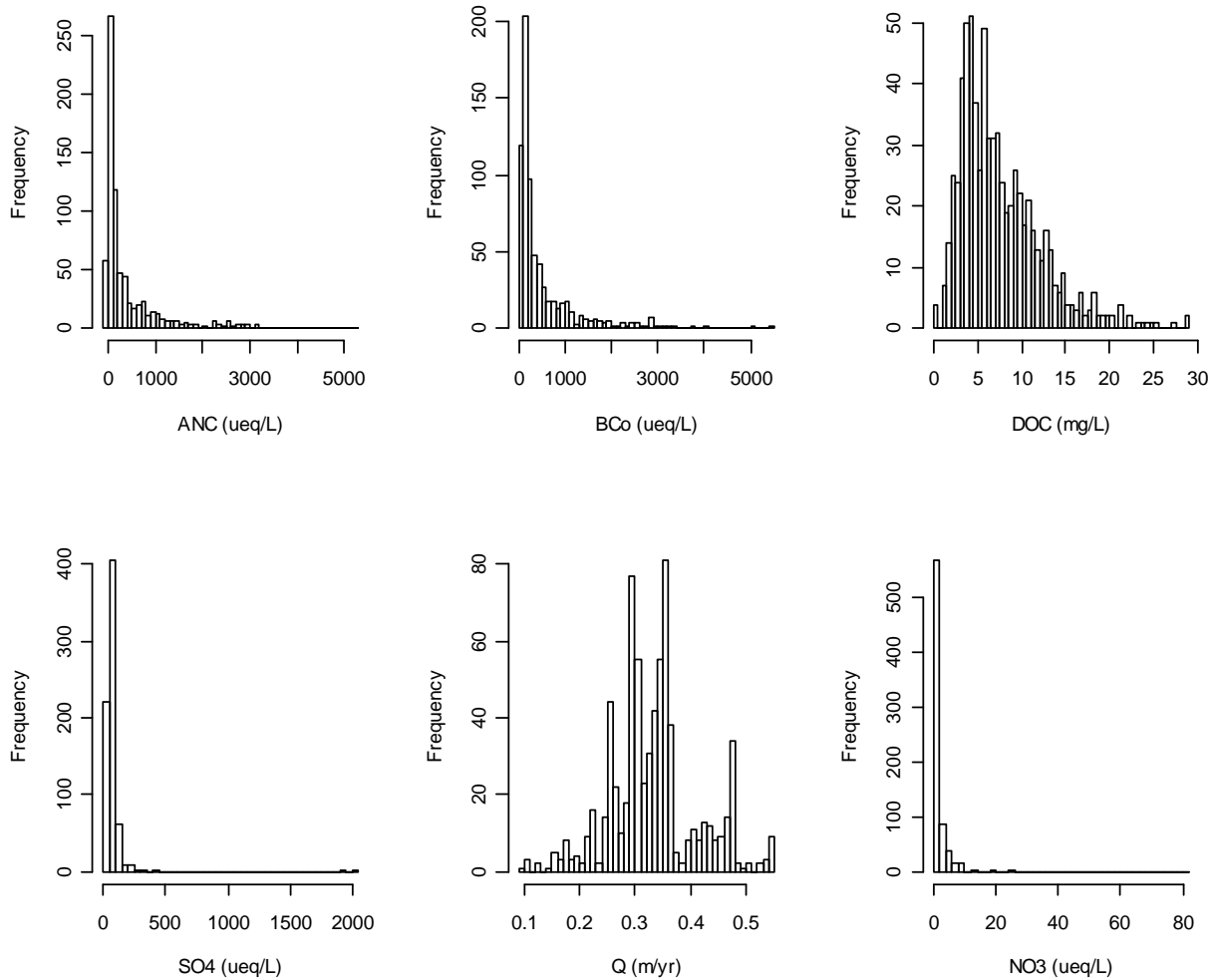


Figure C-4. Region 5.2.1 Water Quality Data Summary

Region 5.2.2 Northern Minnesota Wetlands

Much of the Northern Minnesota Wetlands is a vast and nearly level marsh that is sparsely inhabited by humans and covered by swamp and boreal forest vegetation. Formerly occupied by broad glacial lakes, most of the flat terrain in this ecoregion is still covered by standing water.

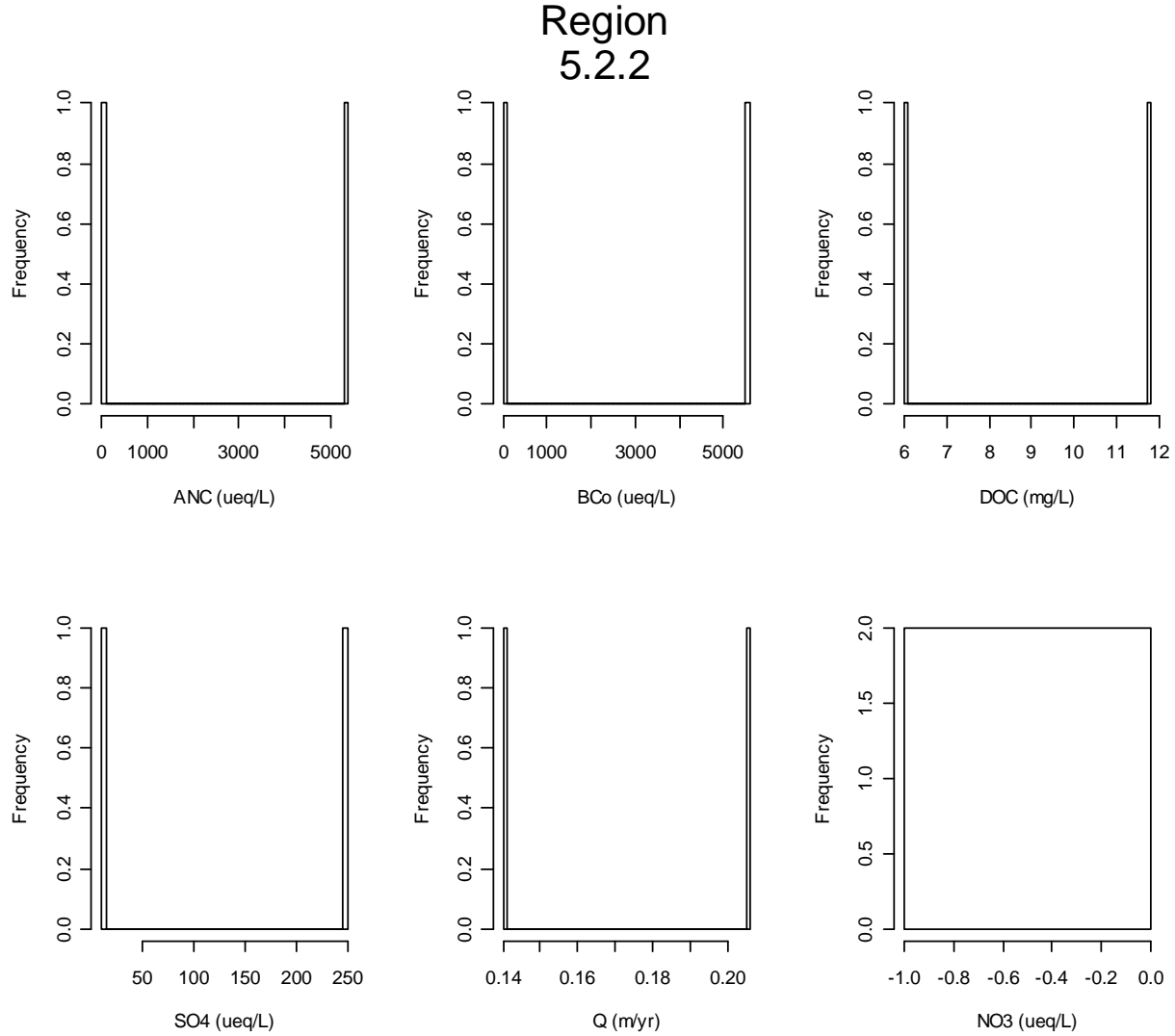


Figure C-5. Region 5.2.2 Water Quality Data Summary

Note: This region had only 1 data point

Region 5.3 Atlantic Highlands

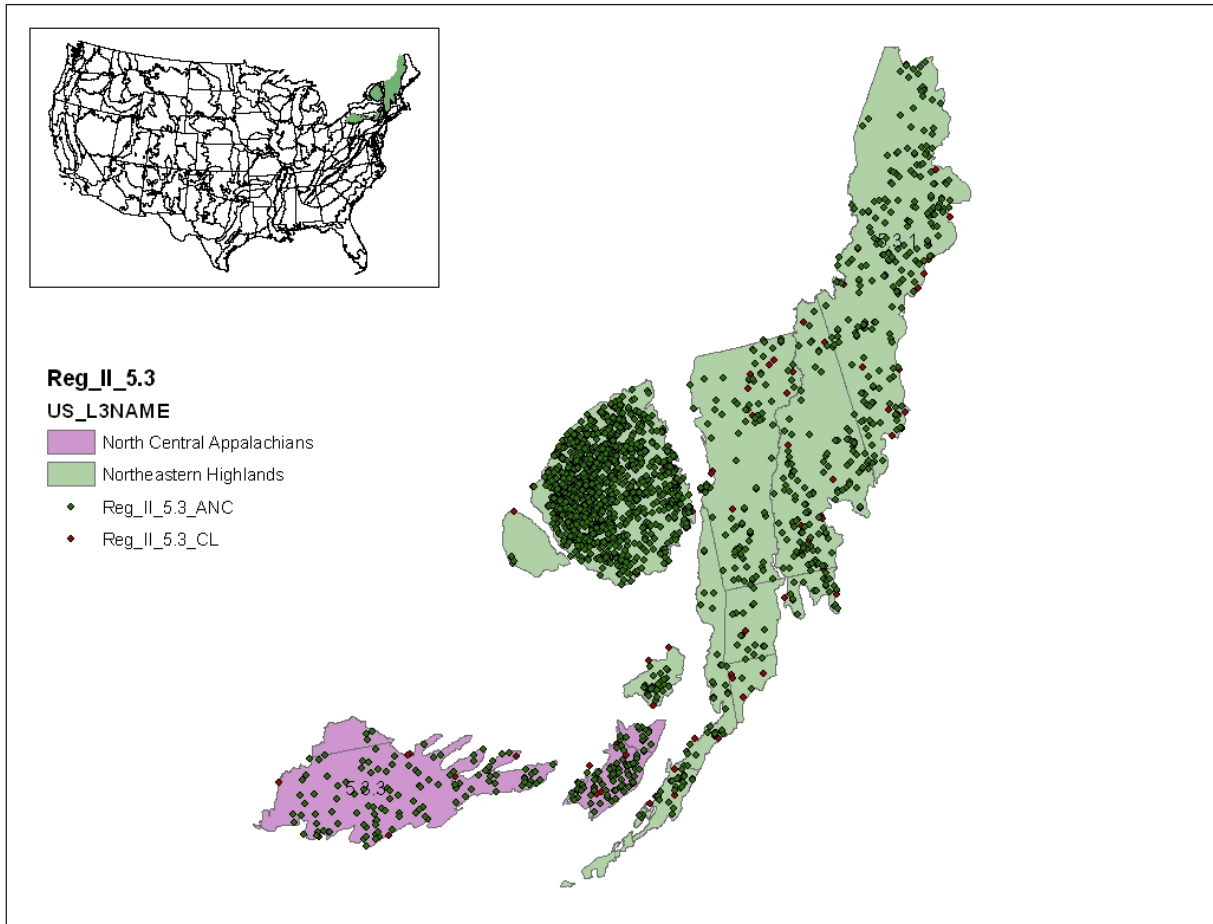


Figure C-6. Region 5.3

Region 5.3.1 Northeastern Highlands

The Northeastern Highlands cover most of the northern and mountainous parts of New England as well as the Adirondacks and higher Catskills in New York. It is a relatively sparsely populated region characterized by hills and mountains, a mostly forested land cover, nutrient-poor soils, and numerous high-gradient streams and glacial lakes. Forest vegetation is somewhat transitional between the boreal regions to the north in Canada and the broadleaf deciduous forests to the south. Typical forest types include northern hardwoods (maple-beech-birch), northern hardwoods/spruce, and northeastern spruce-fir forests. Recreation, tourism, and forestry are primary land uses. Farm-to-forest conversion began in the 19th century and continues today. In spite of this trend, alluvial valleys, glacial lake basins, and areas of limestone-derived soils are still farmed for dairy products, forage crops, apples, and potatoes. Many of the lakes and streams in this region have been acidified by sulfur depositions originating in industrialized areas upwind from the ecoregion to the west.

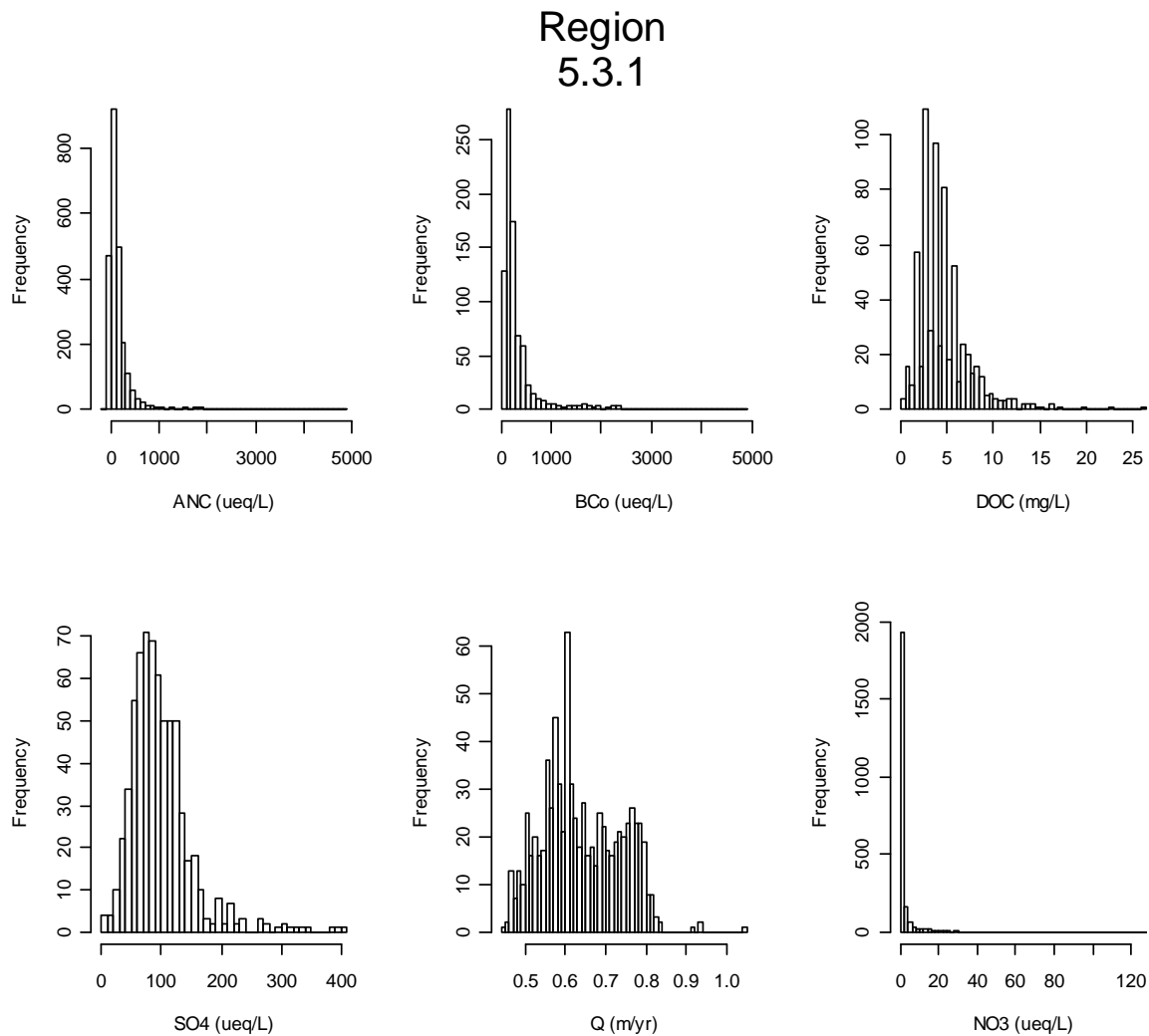


Figure C-7. Region 5.3.1 Water Quality Data Summary

Region 5.3.3 North Central Appalachians

More forest-covered than most adjacent ecoregions, the North Central Appalachians ecoregion is part of a vast, elevated plateau composed of horizontally bedded sandstone, shale, siltstone, conglomerate, and coal. It is made up of plateau surfaces, high hills, and low mountains, which, unlike the ecoregions to the north and west, were largely unaffected by continental glaciation. Only a portion of the Poconos section in the east has been glaciated. Land use activities are generally tied to forestry and recreation, but some coal and natural gas extraction occurs in the west.

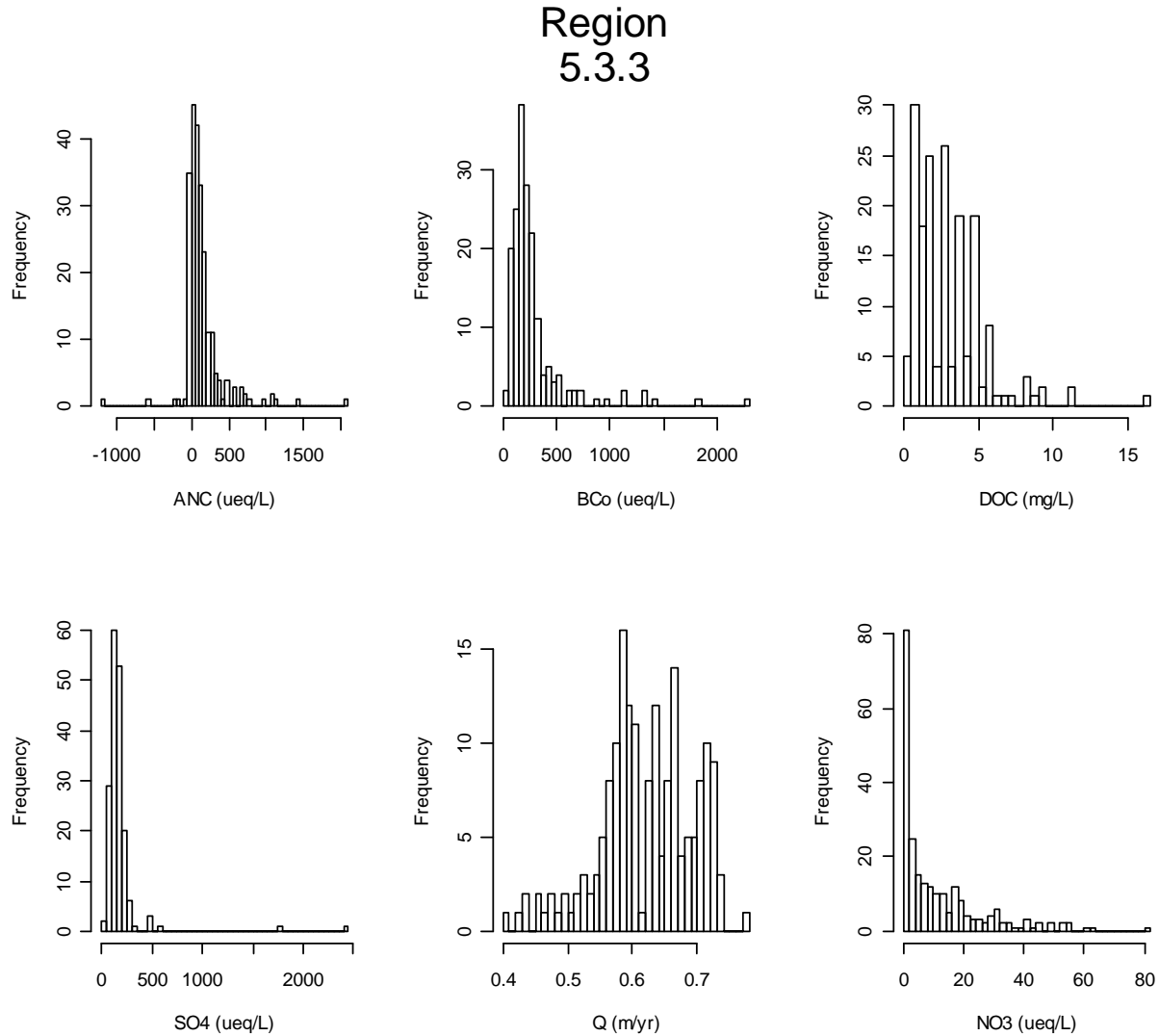


Figure C-8. Region 5.3.3 Water Quality Data Summary

Region 6.2 Western Cordillera

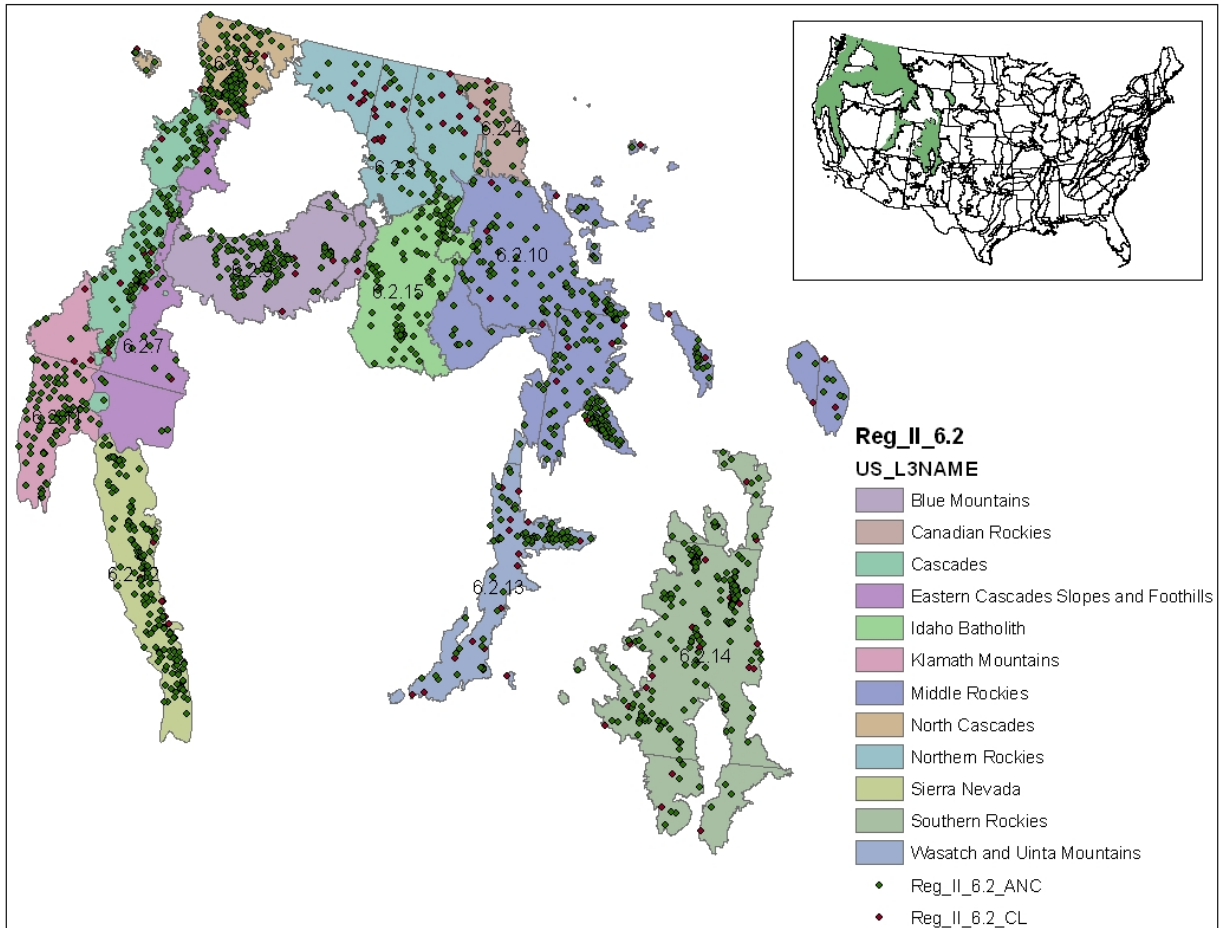


Figure C-9. Region 6.2

Region 6.2.3 Northern Rockies

The Northern Rockies ecoregion is mountainous and rugged. Despite its inland position, climate and vegetation are, typically, marine-influenced. Douglas-fir, subalpine fir, Englemann spruce, and ponderosa pine and Pacific indicators such as western red cedar, western hemlock, and grand fir are found in the ecoregion. The vegetation mosaic is different from that of the Idaho Batholith (6.2.15) and Middle Rockies (6.2.10) which are not dominated by maritime species. The Northern Rockies ecoregion is not as high nor as snow- and ice-covered as the Canadian Rockies (6.2.4) although alpine characteristics occur at highest elevations and include numerous glacial lakes. Granitics and associated management problems are less extensive than in the Idaho Batholith.

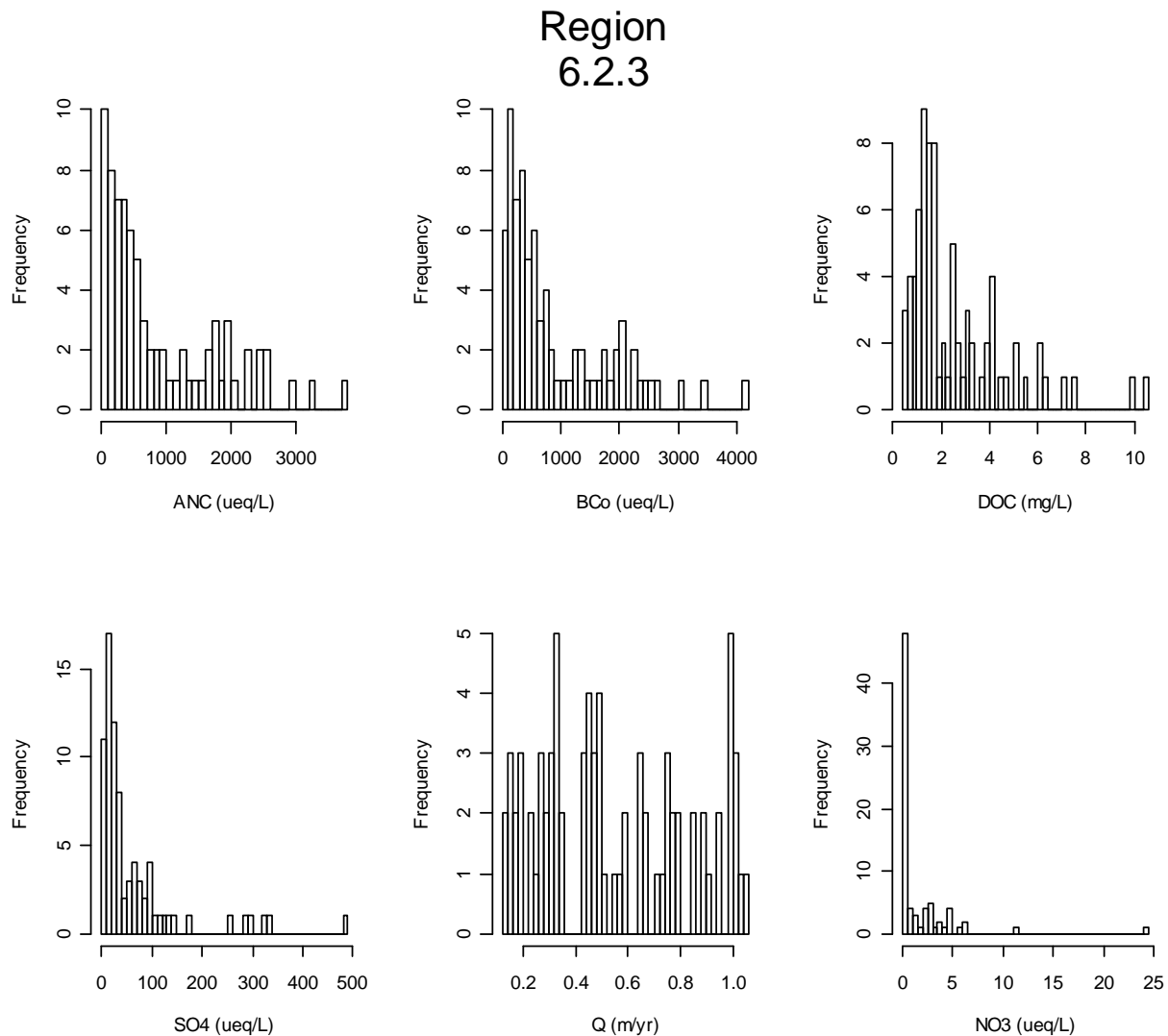


Figure C-10. Region 6.2.3 Water Quality Data Summary

Region 6.2.4 Canadian Rockies

As its name indicates, most of this region is located in Canada. It straddles the border between Alberta and British Columbia in Canada and extends southeastward into northwestern Montana. The region is generally higher and more ice-covered than the Northern Rockies, and portions are strongly influenced by moist maritime air masses. Vegetation is mostly Douglas-fir, Engelmann spruce, subalpine fir, and lodgepole pine in the forested elevations, with treeless alpine conditions at higher elevations. A large part of the region is in national parks where tourism is the major land use. Forestry and mining occur on the non-park lands.

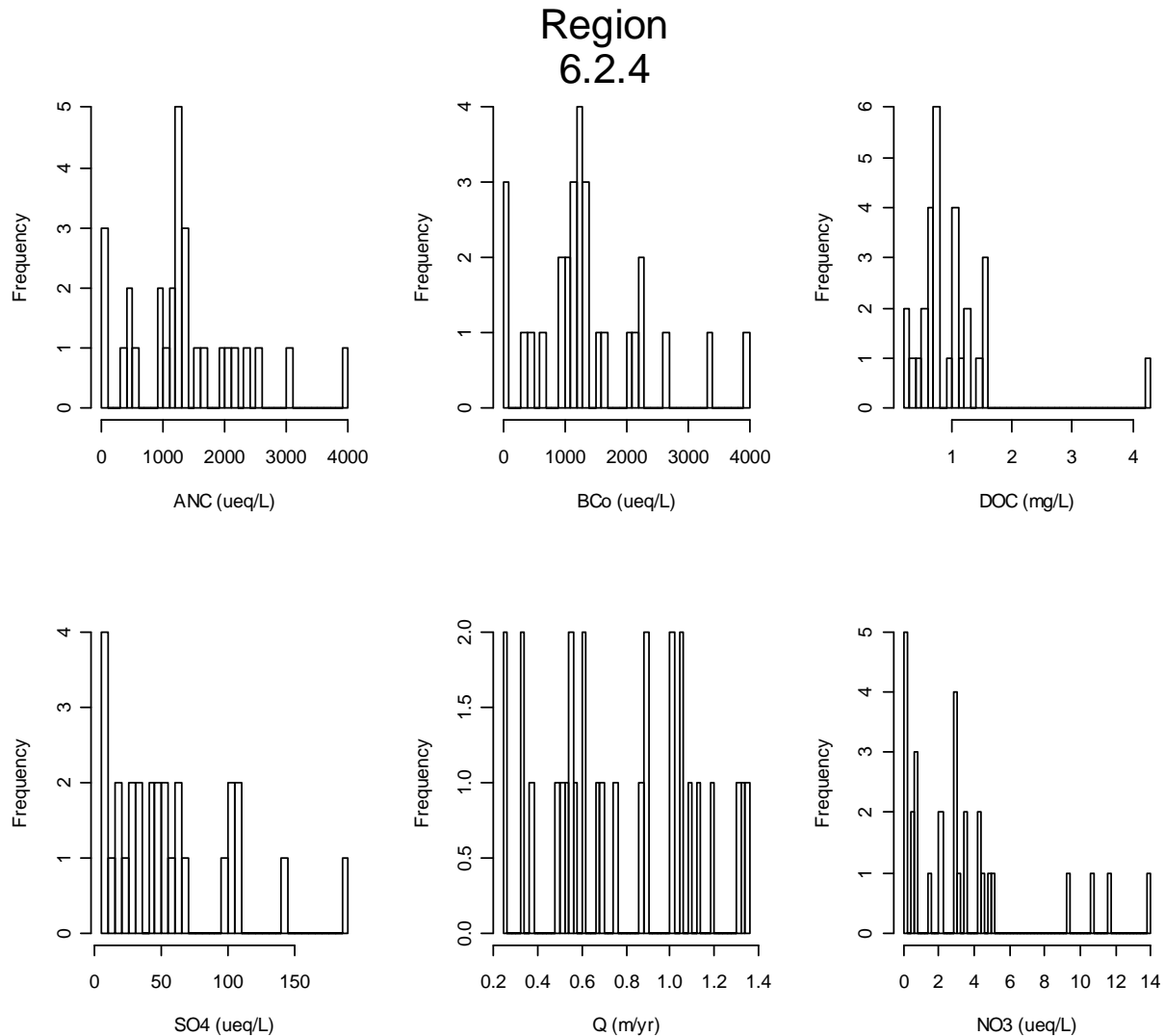


Figure C-11. Region 6.2.4 Water Quality Data Summary

Region 6.2.5 North Cascades

The terrain of the North Cascades is composed of high, rugged mountains. It contains the greatest concentration of active alpine glaciers in the conterminous United States and has a variety of climatic zones. A dry continental climate occurs in the east and mild, maritime, rainforest conditions are found in the west. It is underlain by sedimentary and metamorphic rock in contrast to the adjoining Cascades (6.2.7) which are composed of volcanics.

Region 6.2.5

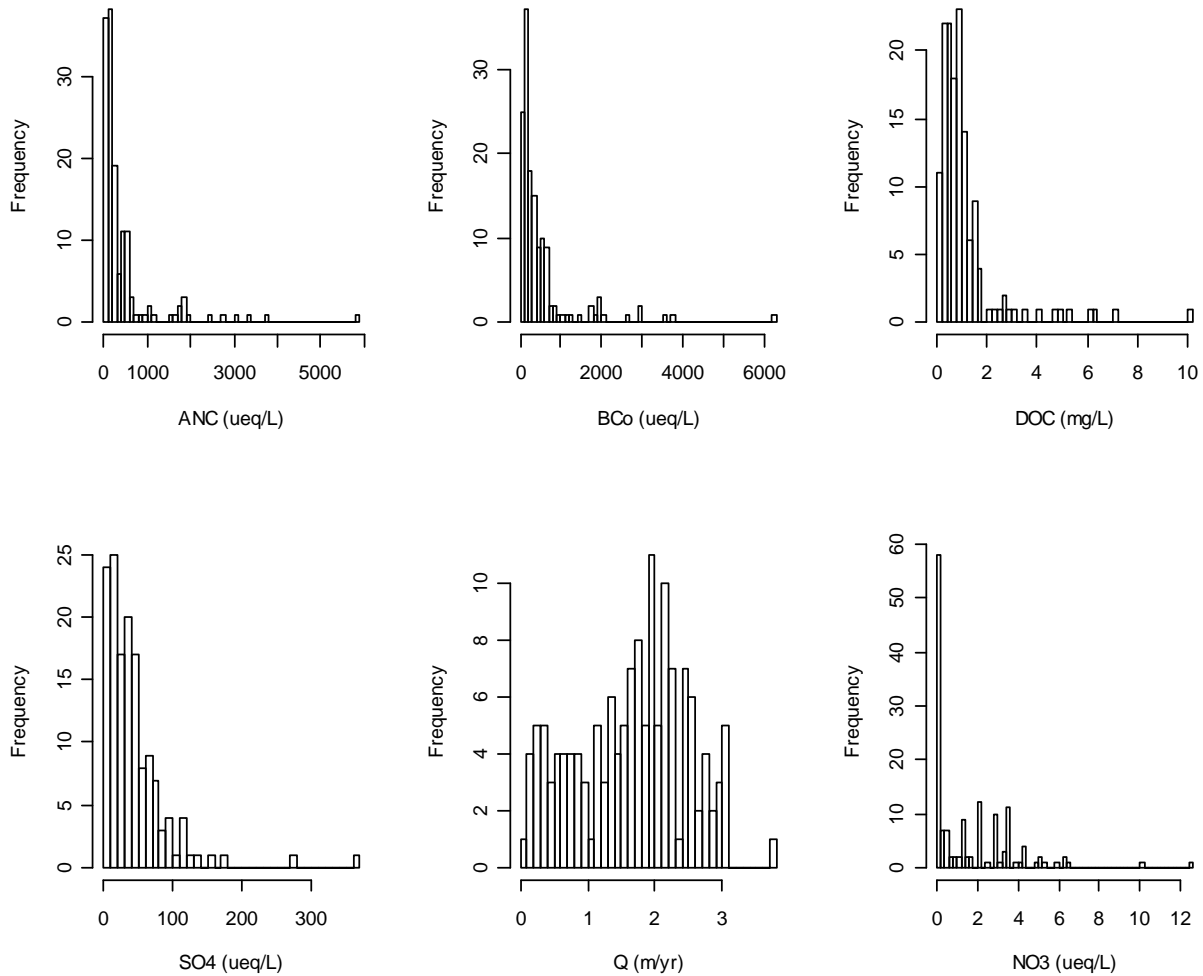


Figure C-12. Region 6.2.5 Water Quality Data Summary

Region 6.2.7 Cascades

This mountainous ecoregion is underlain by Cenozoic volcanics and much of the region has been affected by alpine glaciation. It is characterized by steep ridges and river valleys in the west, a high plateau in the east, and both active and dormant volcanoes. Elevations range upwards to 14,411 feet. Its moist, temperate climate supports an extensive and highly productive coniferous forest that is intensively managed for logging. Subalpine meadows and rocky alpine zones occur at high elevations.

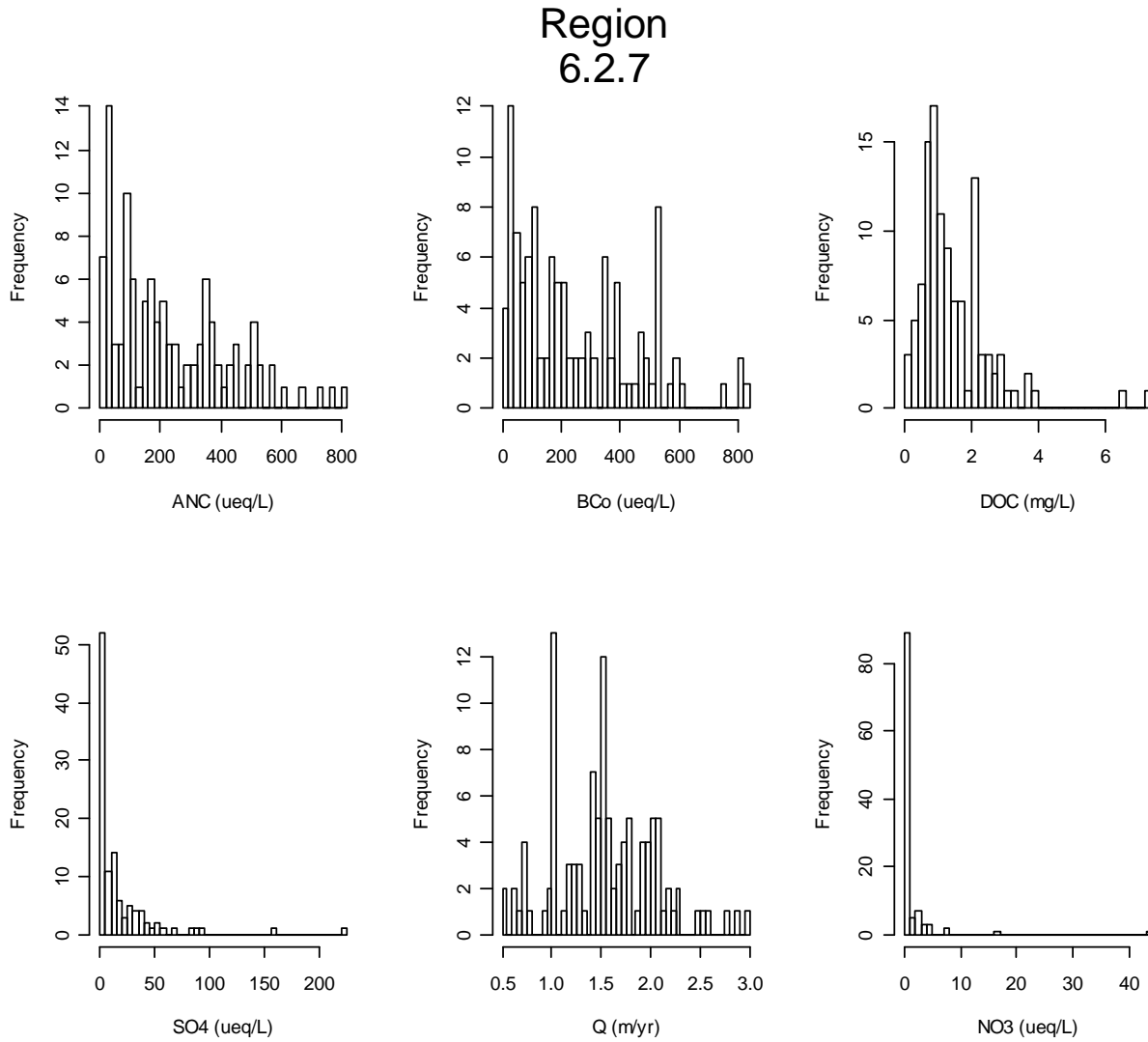


Figure C-13. Region 6.2.7 Water Quality Data Summary

Region 6.2.8 Eastern Cascades Slopes and Foothills

The Eastern Cascade Slopes and Foothills ecoregion is in the rainshadow of the Cascade Range. It experiences greater temperature extremes and receives less precipitation than ecoregions to the west. Open forests of ponderosa pine and some lodgepole pine distinguish this region from the higher ecoregions to the west where fir and hemlock forests are common, and the lower dryer ecoregions to the east where shrubs and grasslands are predominant. The vegetation is adapted to the prevailing dry continental climate and is highly susceptible to wildfire. Historically, creeping ground fires consumed accumulated fuel, and devastating crown fires were less common in dry forests. Volcanic cones and buttes are common in much of the region.

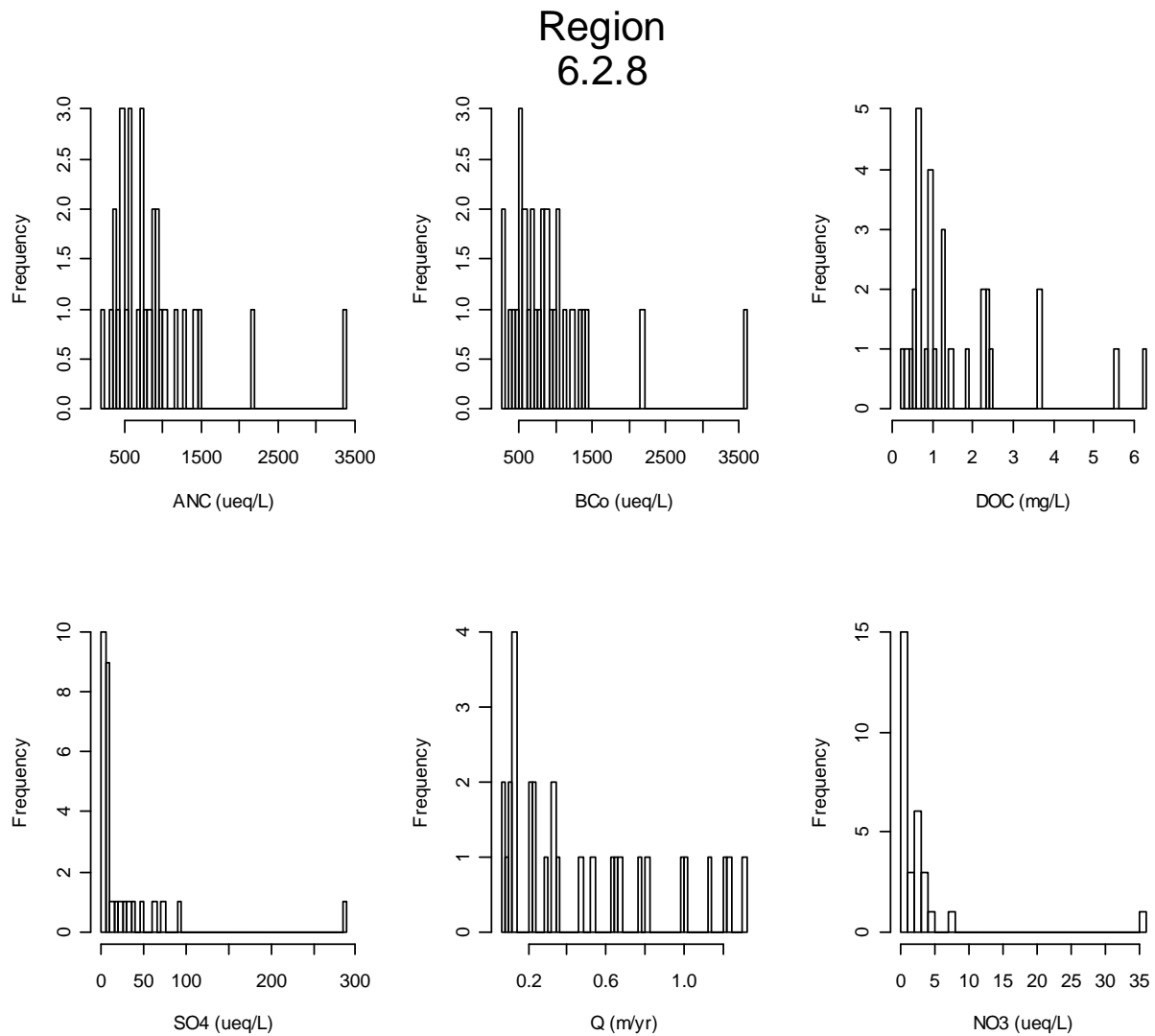


Figure C-14. Region 6.2.8 Water Quality Data Summary

Region 6.2.9 Blue Mountains

The Blue Mountains ecoregion is a complex of mountain ranges that are generally lower and more open than the neighboring Cascades (6.2.7), Northern Rockies (6.2.3), and the Idaho Batholith (6.2.15) ecoregions. Like the Cascades, but unlike the Northern Rockies, the region is mostly volcanic in origin. Only the few higher ranges, particularly the Wallowa and Elkhorn Mountains, consist of granitic intrusive and metamorphic rocks that rise above the dissected lava surface of the region. Unlike the bulk of the Cascades, Idaho Batholith, and Northern Rockies, much of this ecoregion is grazed by cattle.

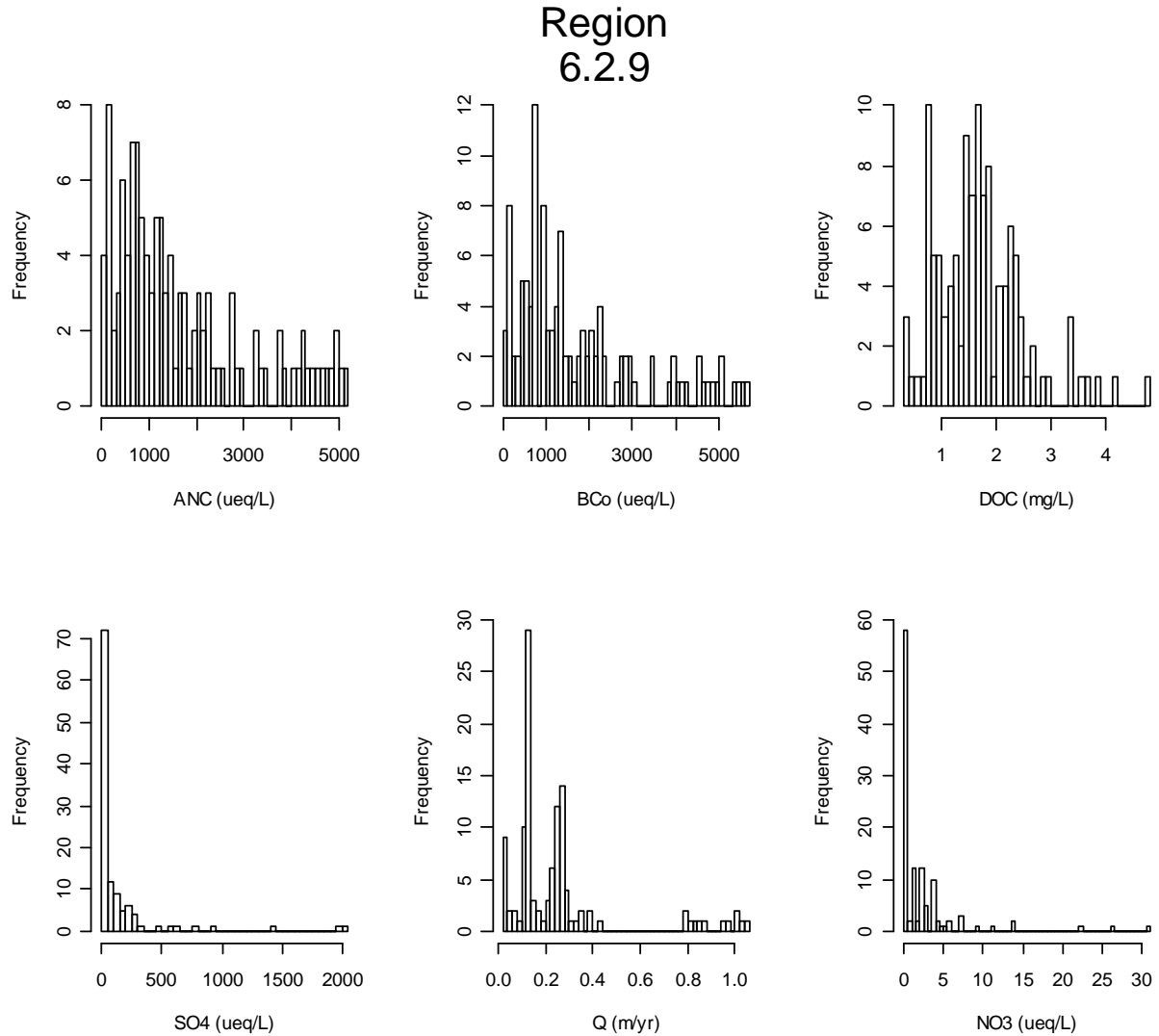


Figure C-15. Region 6.2.9 Water Quality Data Summary

Region 6.2.10 Middle Rockies

The climate of the Middle Rockies lacks the strong maritime influence of the Northern Rockies (6.2.3). Mountains have Douglas-fir, subalpine fir, and Engelmann spruce forests, as well as some large alpine areas. Pacific tree species are never dominant and forests can have open canopies. Foothills are partly wooded or shrub- and grass-covered. Intermontane valleys are grass- and/or shrub-covered and contain a mosaic of terrestrial and aquatic fauna that is distinct from the nearby mountains. Many mountain-fed, perennial streams occur and differentiate the intermontane valleys from the Northwestern Great Plains (9.3.3). Granitics and associated management problems are less extensive than in the Idaho Batholith (6.2.15). Recreation, logging, mining, and summer livestock grazing are common land uses.

Region 6.2.10

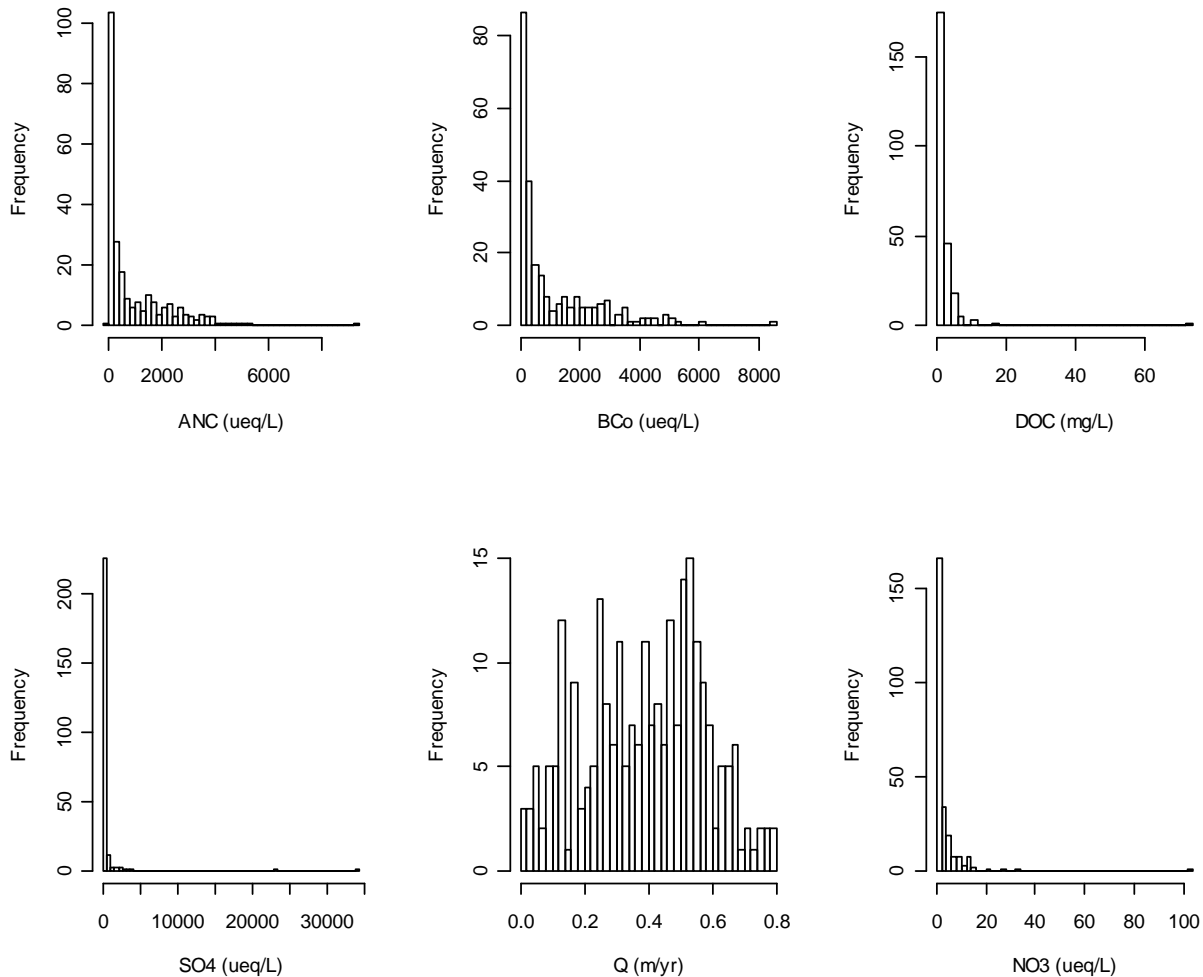


Figure C-16. Region 6.2.10 Water Quality Data Summary

Region 6.2.11 Klamath Mountains

This physically and biologically diverse ecoregion covers the highly dissected ridges, foothills, and valleys of the Klamath and Siskiyou mountains. It also extends south in California to include the mixed conifer and montane hardwood forests that occur in the North Coast Range mountains. The region's mix of granitic, sedimentary, metamorphic, and extrusive rocks contrasts with the predominantly volcanic rocks of the Cascades (6.2.7) to the east. It was unglaciated during the Pleistocene epoch, when it served as a refuge for northern plant species. The region's diverse flora, a mosaic of both northern Californian and Pacific Northwestern conifers and hardwoods, is rich in endemic and relic species. The mild, subhumid climate of the Klamath Mountains is characterized by a lengthy summer drought.

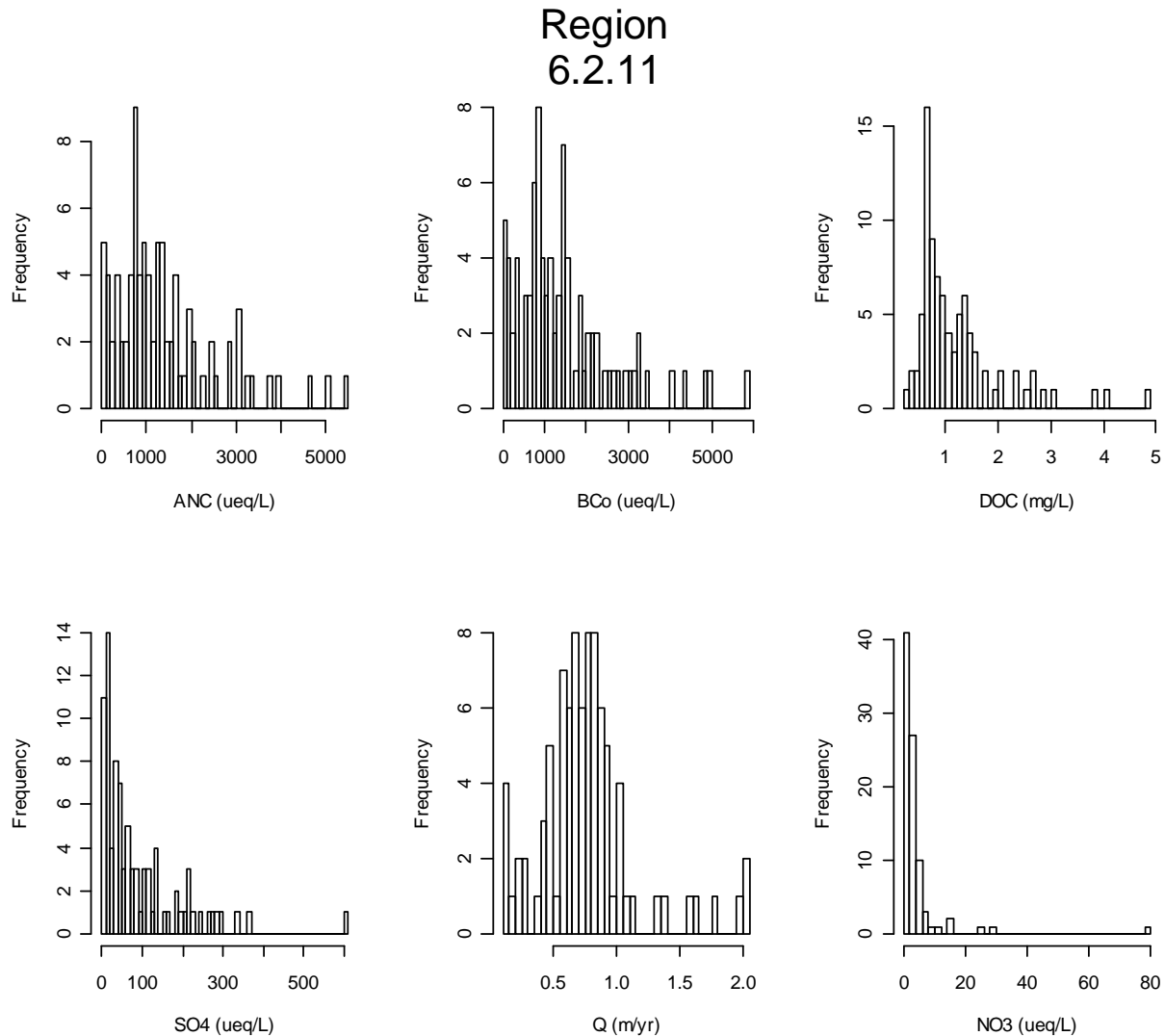


Figure C-17. Region 6.2.11 Water Quality Data Summary

Region 6.2.12 Sierra Nevada

The Sierra Nevada is a deeply dissected fault-block mountain range that rises sharply from the arid basin and range ecoregions on the east and slopes gently toward the Central California Valley to the west. The eastern portion has been strongly glaciated and generally contains higher mountains than are found in the Klamath Mountains (6.2.11) to the northwest. Much of the central and southern parts of the region is underlain by granite as compared to the mostly sedimentary and metamorphic formations of the Klamath Mountains and the volcanic rocks of the Cascades (6.2.7). The higher elevations of this region are largely federally owned and include several national parks. The vegetation grades from mostly ponderosa pine and Douglas-fir at the lower elevations on the west side, pines and Sierra juniper on the east side, to fir and other conifers at the higher elevations. Alpine conditions exist at the highest elevations.

Region 6.2.12

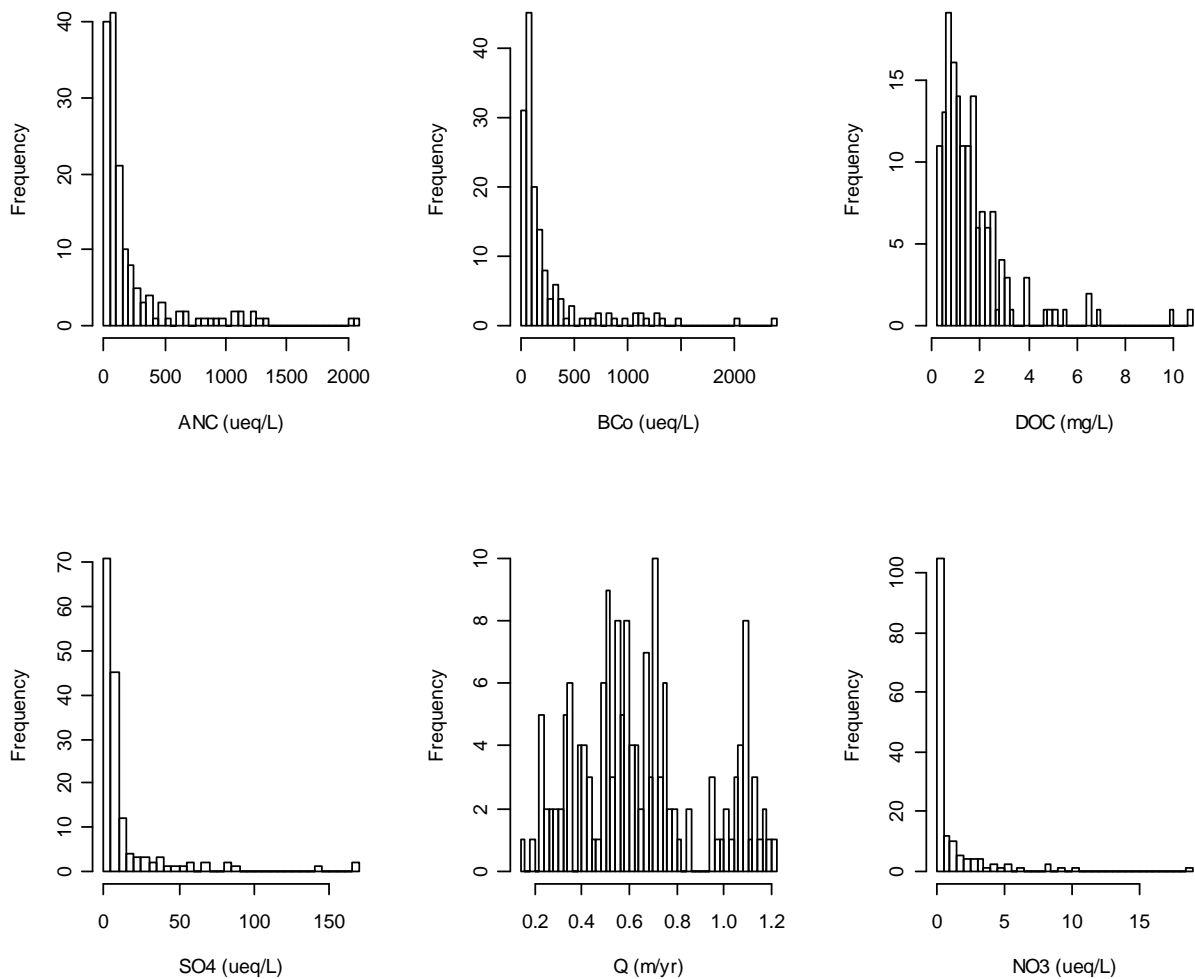


Figure C-18. Region 6.2.12 Water Quality Data Summary

Region 6.2.13 Wasatch and Uinta Mountains

This ecoregion is composed of a core area of high, precipitous mountains with narrow crests and valleys flanked in some areas by dissected plateaus and open high mountains. The elevational banding pattern of vegetation is similar to that of the Southern Rockies (6.2.14) except that areas of aspen, interior chaparral, and juniper-pinyon and scrub oak are more common at middle elevations. This characteristic, along with a far lesser extent of lodgepole pine and greater use of the region for grazing livestock in the summer months, distinguish the Wasatch and Uinta Mountains ecoregion from the more northerly Middle Rockies (6.2.10).

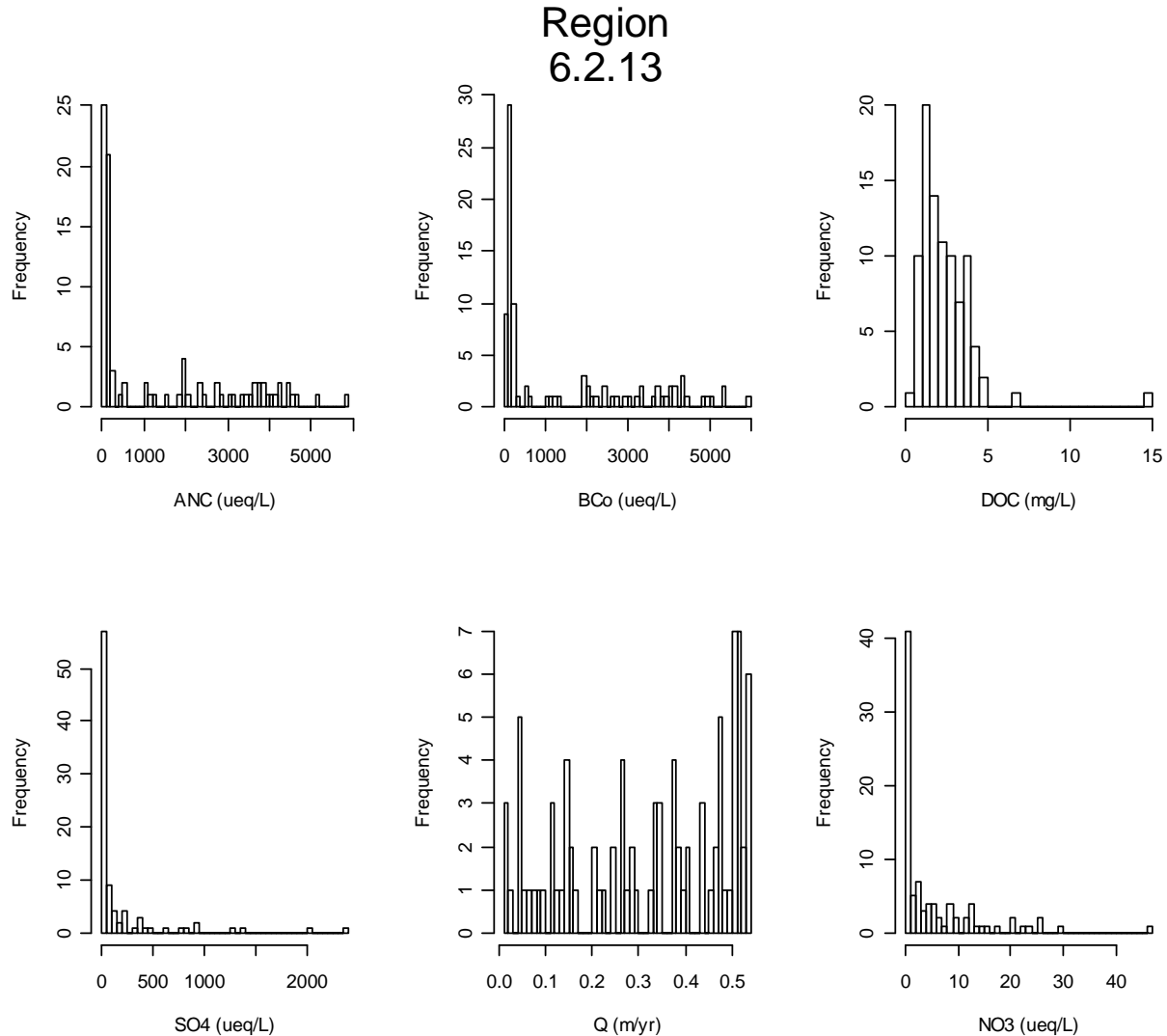


Figure C-19. Region 6.2.13 Water Quality Data Summary

Region 6.2.14 Southern Rockies

The Southern Rockies are composed of steep, rugged mountains with high elevations. Although coniferous forests cover much of the region, as in most of the mountainous regions in the western United States, vegetation, as well as soil and land use, follows a pattern of elevational banding. The lowest elevations are generally grass or shrub covered and heavily grazed. Low to middle elevations are also grazed and covered by a variety of vegetation types including Douglas-fir, ponderosa pine, aspen, and juniper-oak woodlands. Middle to high elevations are largely covered by coniferous forests and have little grazing activity. The highest elevations have alpine characteristics.

Region 6.2.14

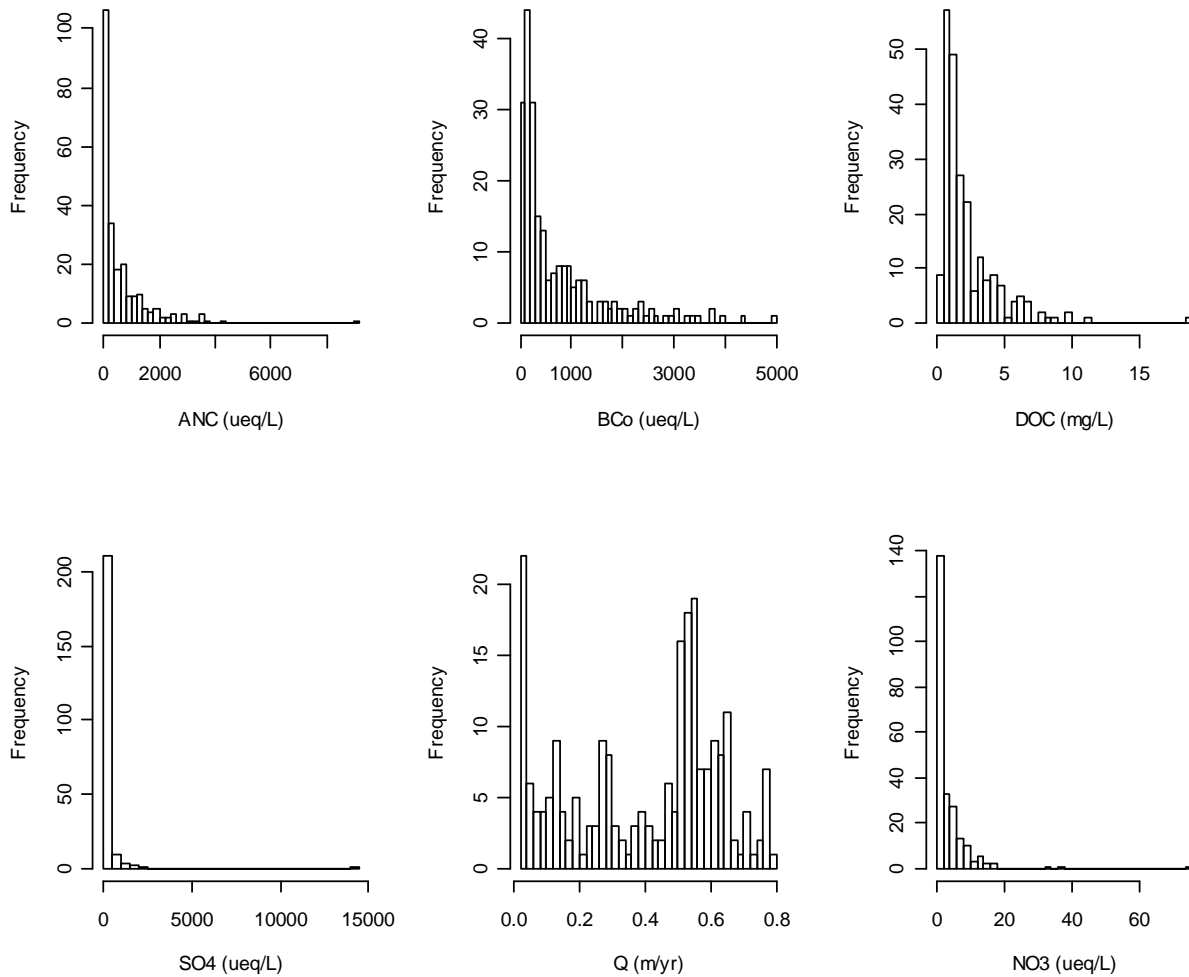


Figure C-20. Region 6.2.14 Water Quality Data Summary

Region 6.2.15 Idaho Batholith

This ecoregion is a dissected, partially glaciated, mountainous plateau. Many perennial streams originate here and water quality can be high if basins are undisturbed. Deeply weathered, acidic, intrusive igneous rock is common and is far more extensive than in the Northern Rockies (6.2.3) or the Middle Rockies (6.2.10). Soils are sensitive to disturbance especially when stabilizing vegetation is removed. Land uses include logging, grazing, and recreation. Mining and related damage to aquatic habitat was widespread. Grand fir, Douglas-fir, and, at higher elevations, Engelmann spruce and subalpine fir occur. Ponderosa pine, shrubs, and grasses grow in very deep canyons. Maritime influence lessens toward the south and is never as strong as in the Northern Rockies.

Region 6.2.15

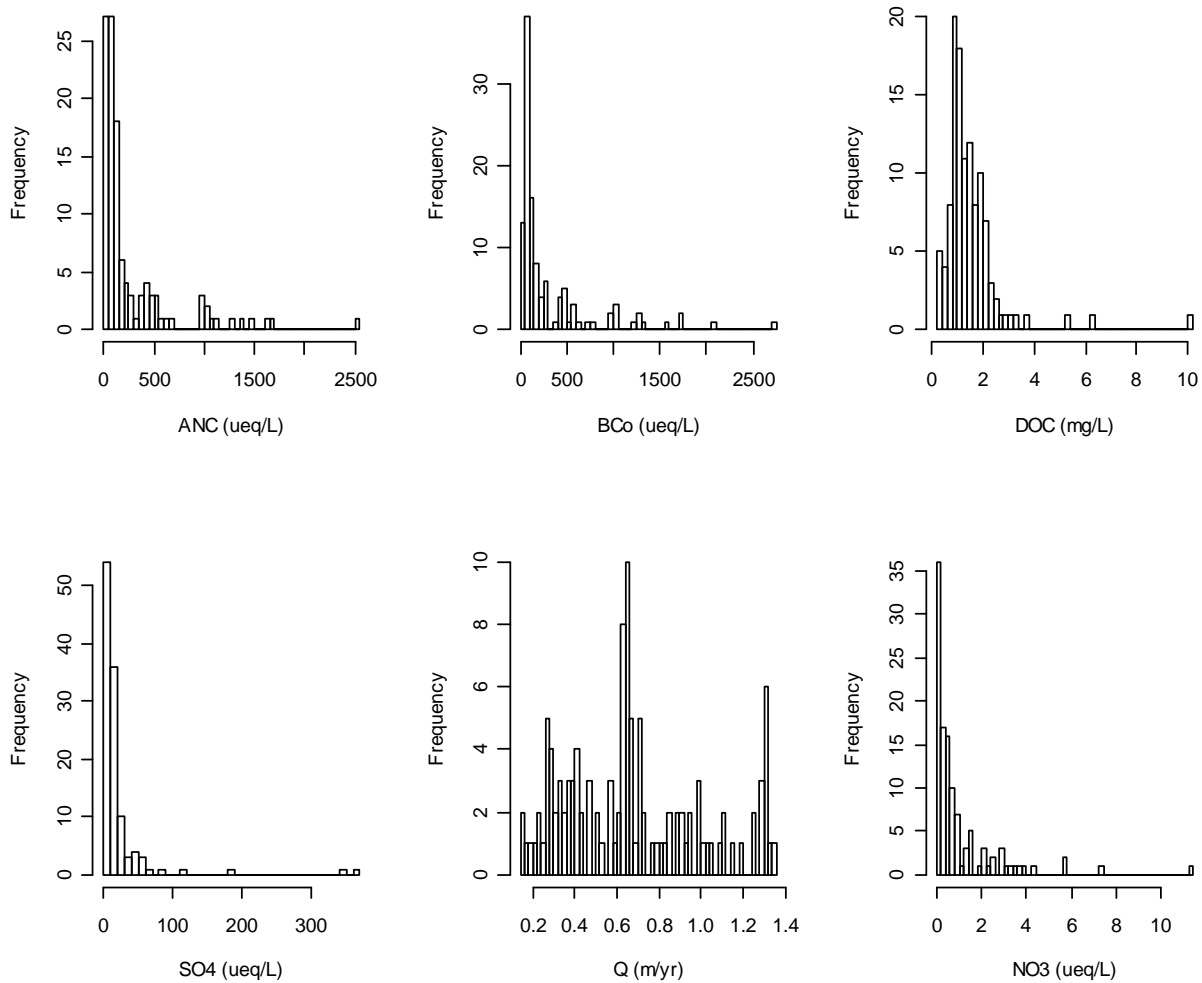


Figure C-21. Region 6.2.15 Water Quality Data Summary

Region 7.1 Marine West Coast Forest

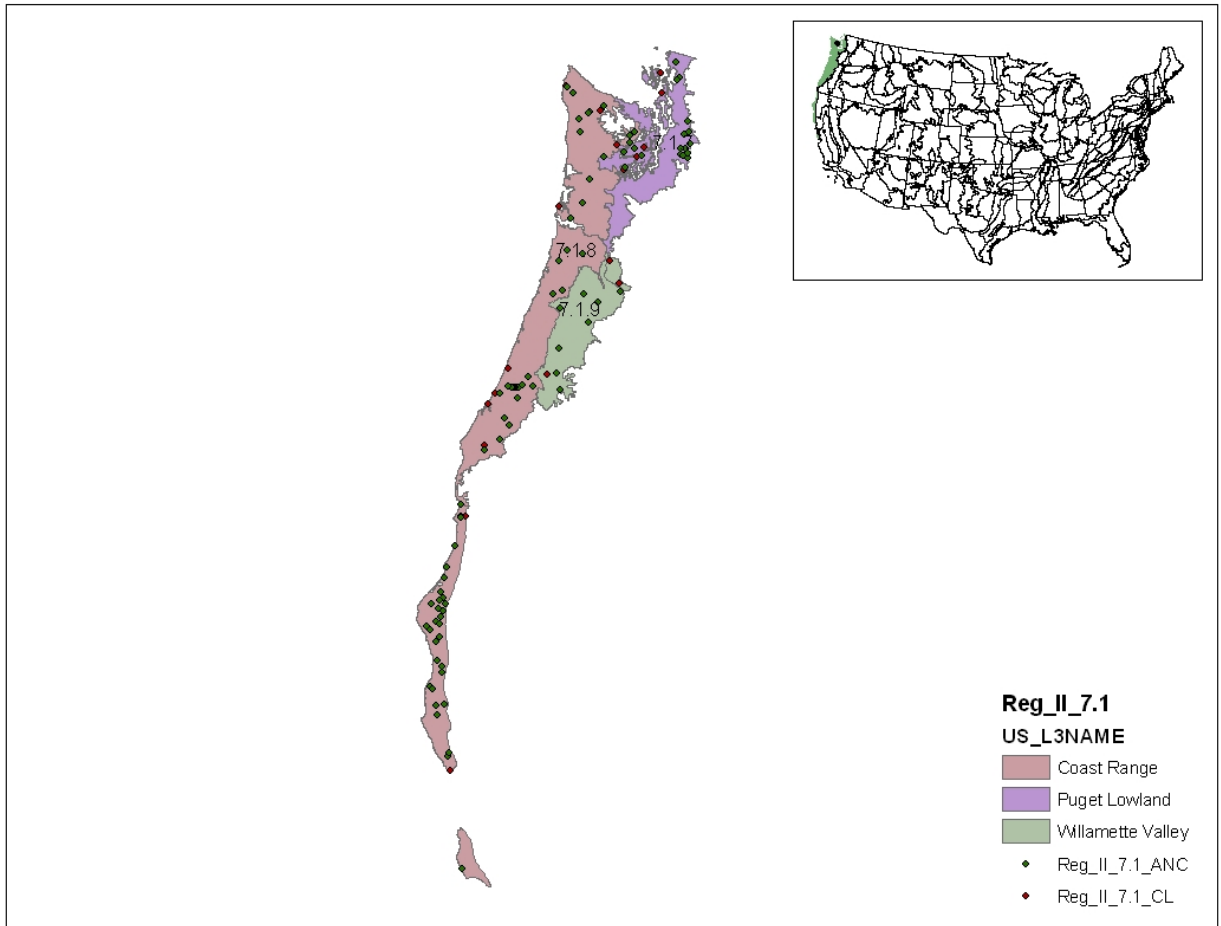


Figure C-22. Region 7.1

Region 7.1.7 Puget Lowland

This broad rolling lowland is characterized by a mild maritime climate. It occupies a continental glacial trough and is composed of many islands, peninsulas, and bays in the Puget Sound area. Coniferous forests originally grew on the ecoregion's ground moraines, outwash plains, floodplains, and terraces. The distribution of forest species is affected by the rainshadow from the Olympic Mountains.

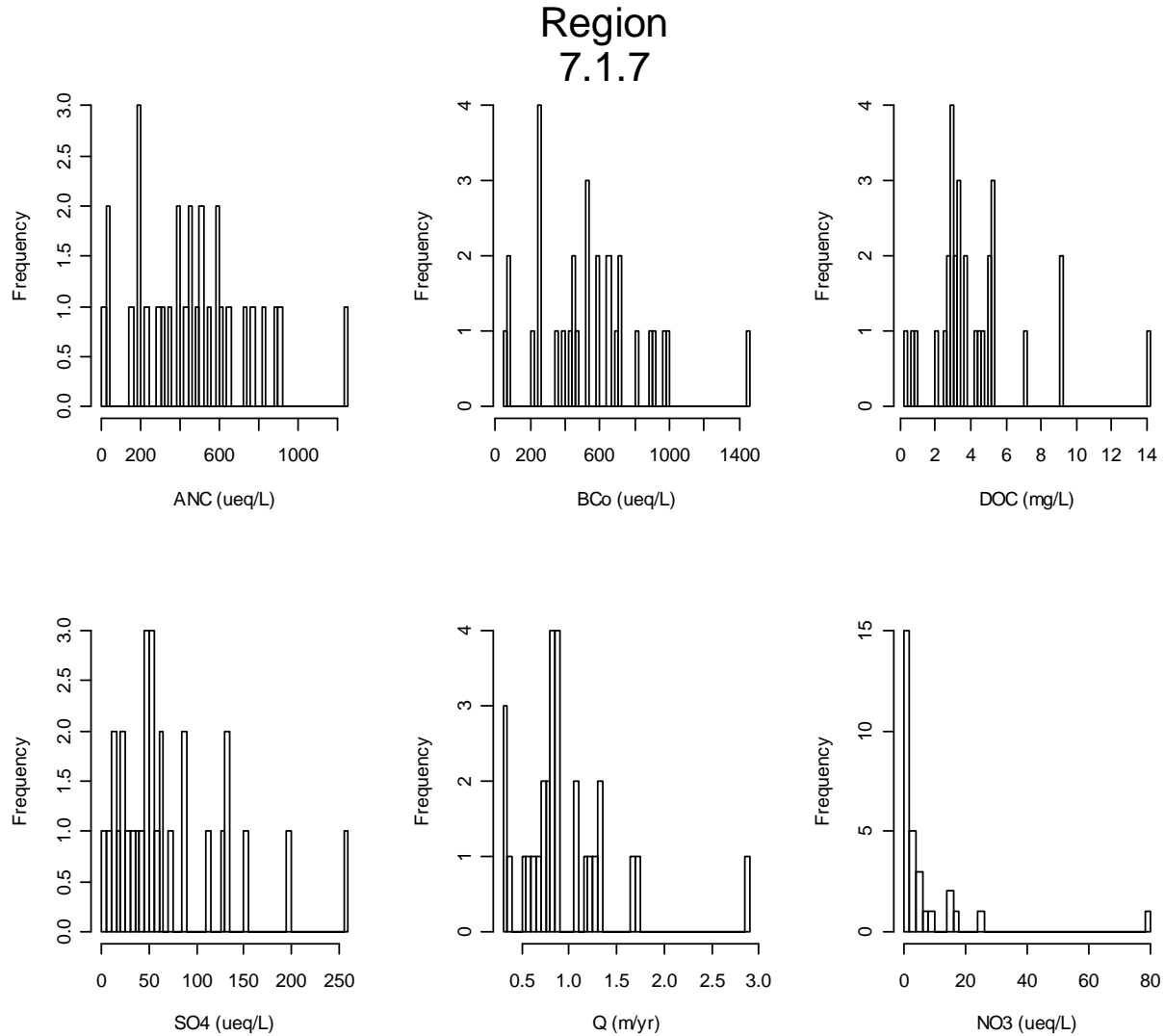


Figure C-23. Region 7.1.7 Water Quality Data Summary

Region 7.1.8 Coast Range

The low mountains of the Coast Range are covered by highly productive, rain-drenched coniferous forests. Sitka spruce forests originally dominated the fog-shrouded coast, while a mosaic of western redcedar, western hemlock, and seral Douglas-fir blanketed inland areas. Today, Douglas-fir plantations are prevalent on the intensively logged and managed landscape. In California, redwood forests are a dominant component in much of the region.

Region 7.1.8

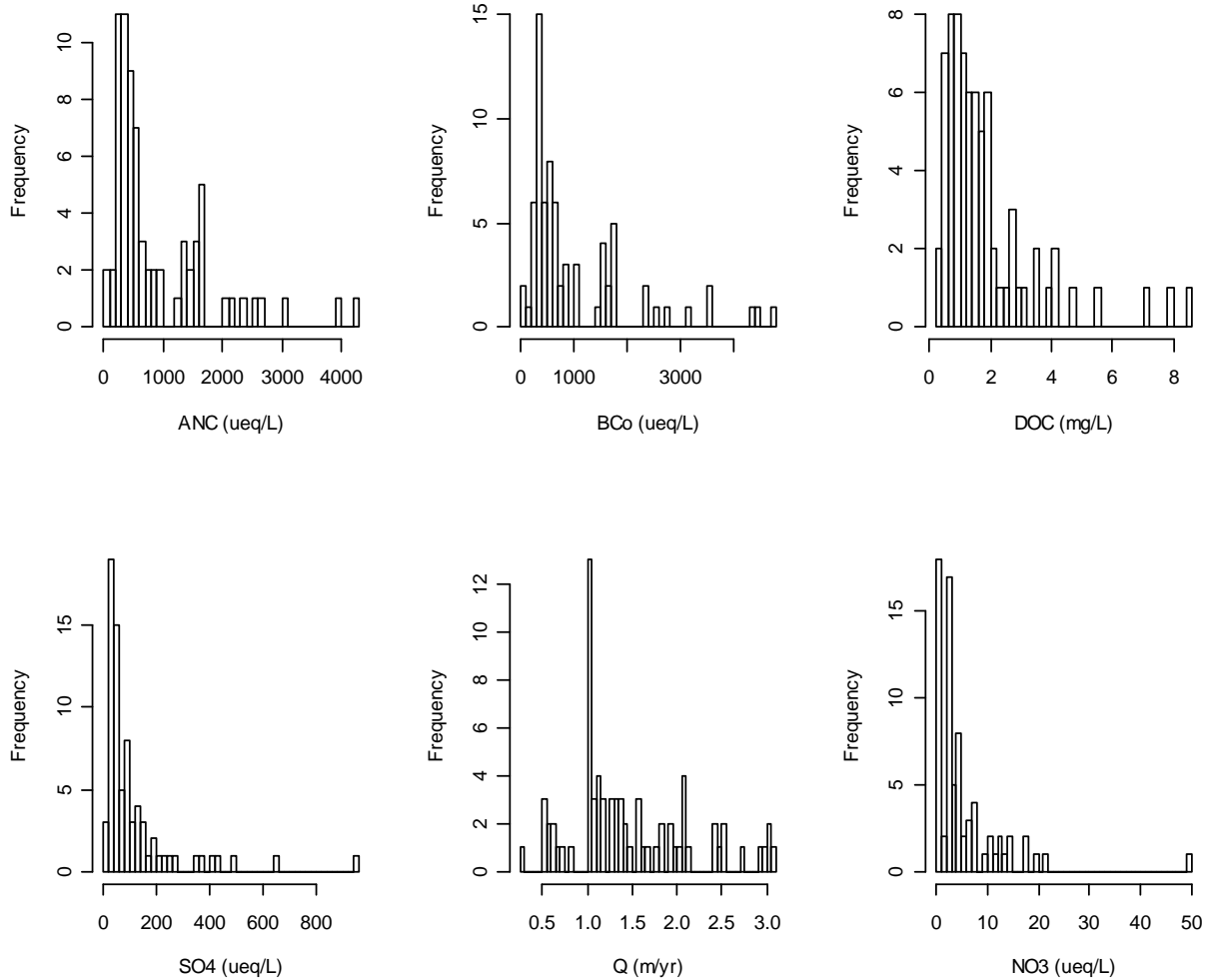


Figure C-24. Region 7.1.8 Water Quality Data Summary

Region 7.1.9 Willamette Valley

This ecoregion contains terraces and floodplains of the Willamette River system, along with scattered hills, buttes, and adjacent foothills. Originally, it was covered by prairies, oak savannas, coniferous forests, extensive wetlands, and deciduous riparian forests. Elevation and relief are lower and the vegetation mosaic differs from the coniferous forests of the surrounding Coast Range (7.1.8), Cascades (6.2.7), and Klamath Mountains (6.2.11). Mean annual rainfall is 37 to 60 inches and summers are generally dry; overall, precipitation is lower than in the surrounding mountains. Today, the Willamette Valley contains the bulk of Oregon's population, industry, commerce, and cropland. Productive soils and a temperate climate make it one of the most important agricultural areas in Oregon.

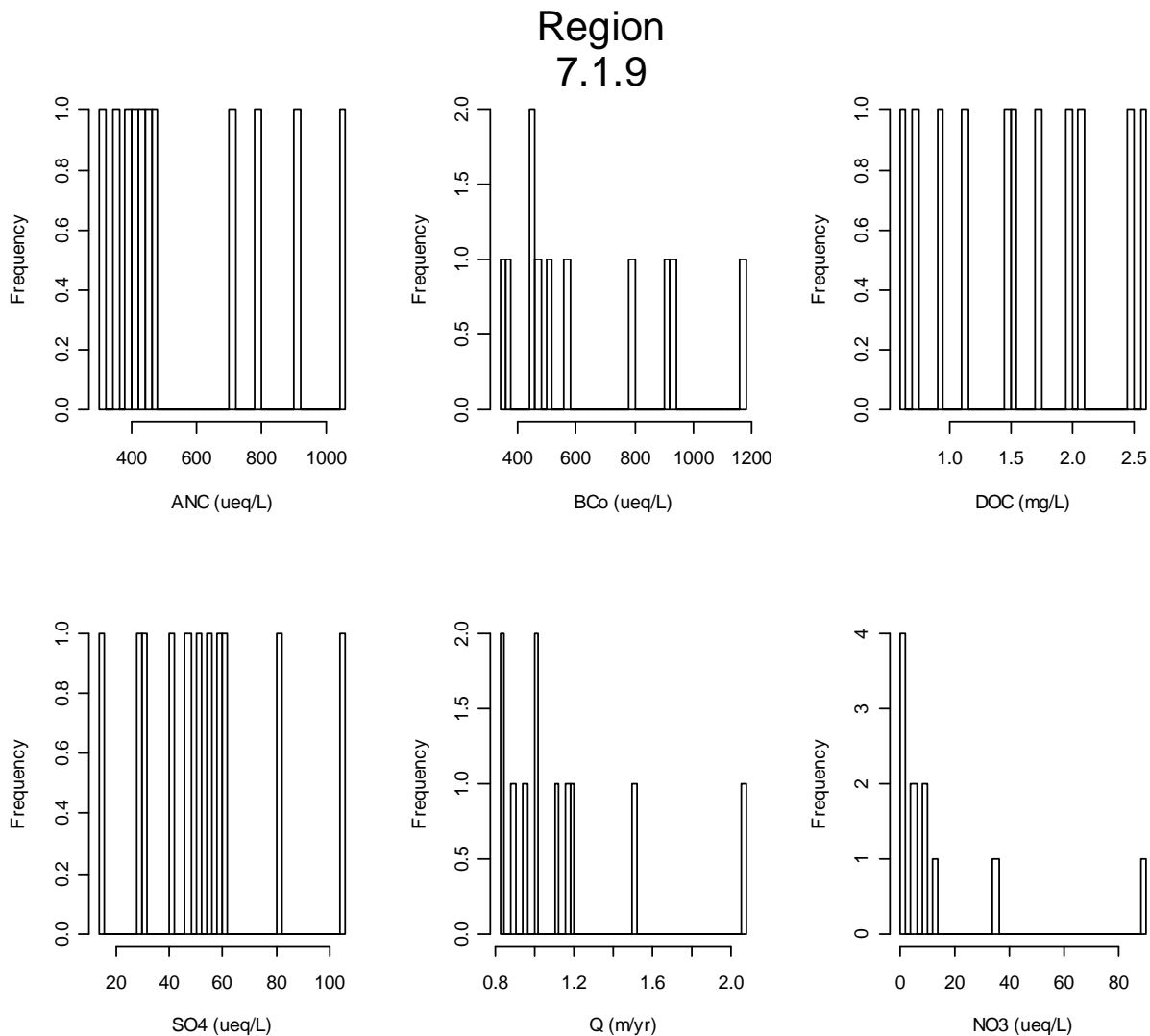


Figure C-25. Region 7.1.9 Water Quality Data Summary

Region 8.1 Mixed Wood Plains



Figure C-26. Region 8.1

Region 8.1.1 Eastern Great Lakes Lowlands

This glaciated region of irregular plains bordered by hills generally contains less surface irregularity and more agricultural activity and population density than the adjacent Northeastern Highlands (5.3.1) and Northern Allegheny Plateau (8.1.3). Although orchards, vineyards, and vegetable farming are important locally, a large percentage of the agriculture is associated with dairy operations. The portion of this ecoregion that is in close proximity to the Great Lakes experiences an increased growing season, more winter cloudiness, and greater snowfall.

Region 8.1.1

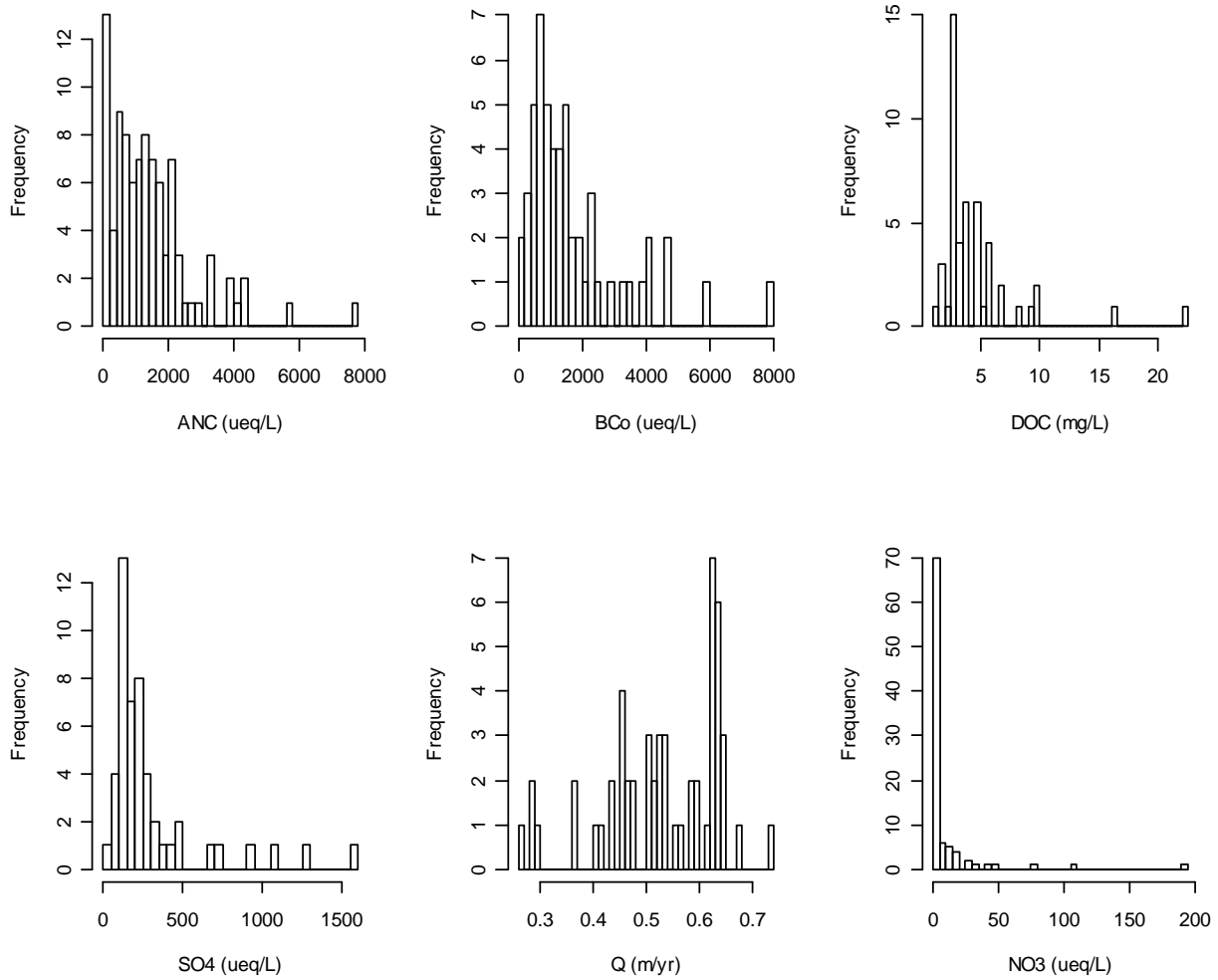


Figure C-27. Region 8.1.1 Water Quality Data Summary

Region 8.1.3 Northern Allegheny Plateau

The Northern Allegheny Plateau is made up of horizontally bedded, erodible shales and siltstones, and moderately resistant sandstones of Devonian age. It is generally lower and less forested than the adjacent unglaciated North Central Appalachians (5.3.3). Its rolling hills, open valleys, and low mountains are covered by till from Wisconsin Age glaciation and the landscape is a mosaic of cropland, pastureland, and woodland. Historically, the natural vegetation was primarily Appalachian oak forest dominated by white oak and red oak, with some northern hardwood forest at higher elevations. The Northern Allegheny Plateau has more level topography and more fertile, arable land than the more rugged and forested North Central Appalachians (5.3.3).

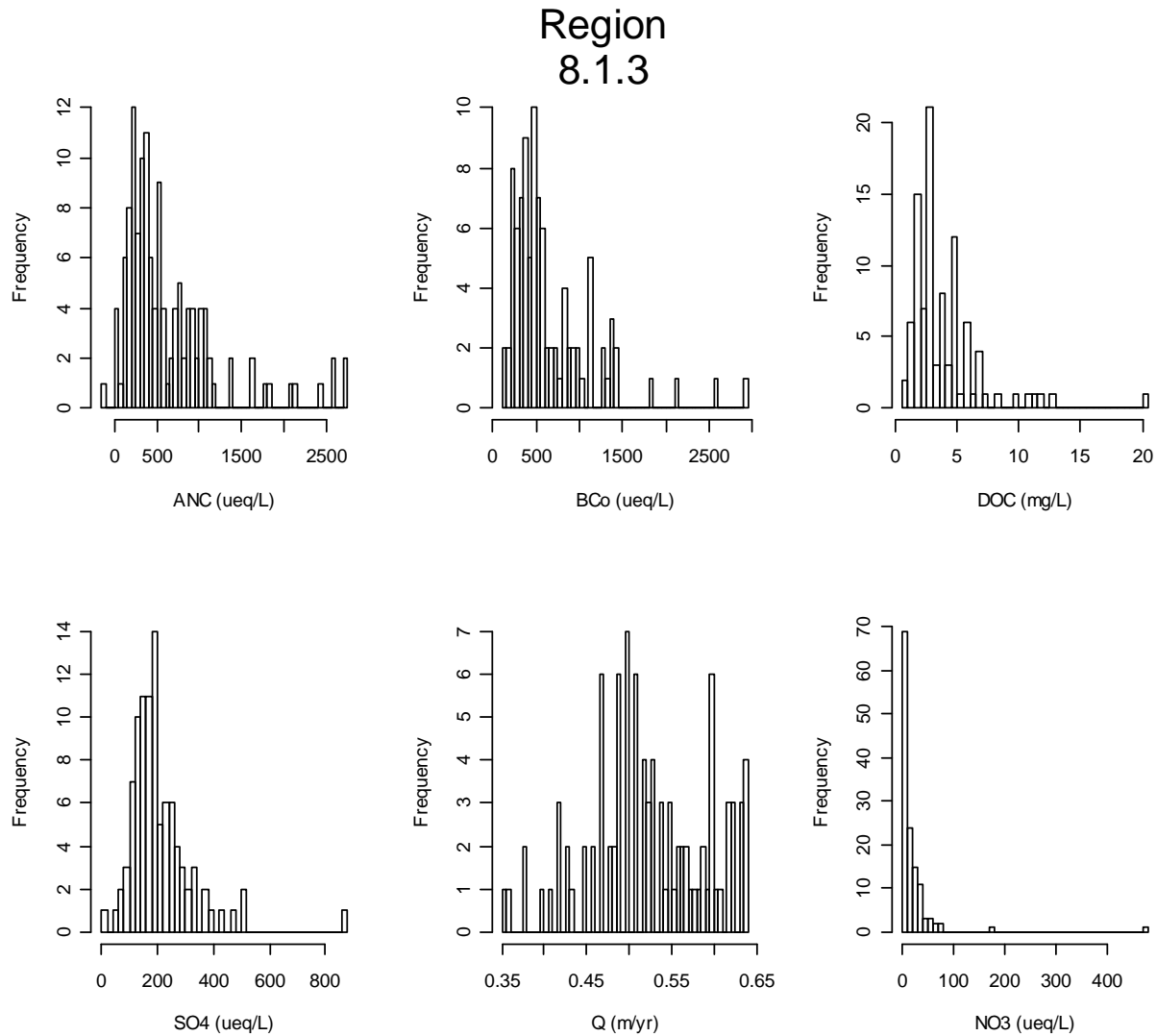


Figure C-28. Region 8.1.3 Water Quality Data Summary

Region 8.1.4 North Central Hardwood Forests

The North Central Hardwood Forests ecoregion is transitional between the predominantly forested Northern Lakes and Forests (5.2.1) to the north and the agricultural ecoregions to the south. Land use/land cover in this ecoregion consists of a mosaic forests, wetlands and lakes, cropland agriculture, pasture, and dairy operations. The growing season is generally longer and warmer than that of the Northern Lakes and Forest and the soils are more arable and fertile, contributing to the greater agricultural component of land use. Lake trophic states tend to be higher here than in the Northern Lakes and Forests, with higher percentages in eutrophic and hypereutrophic classes.

Region 8.1.4

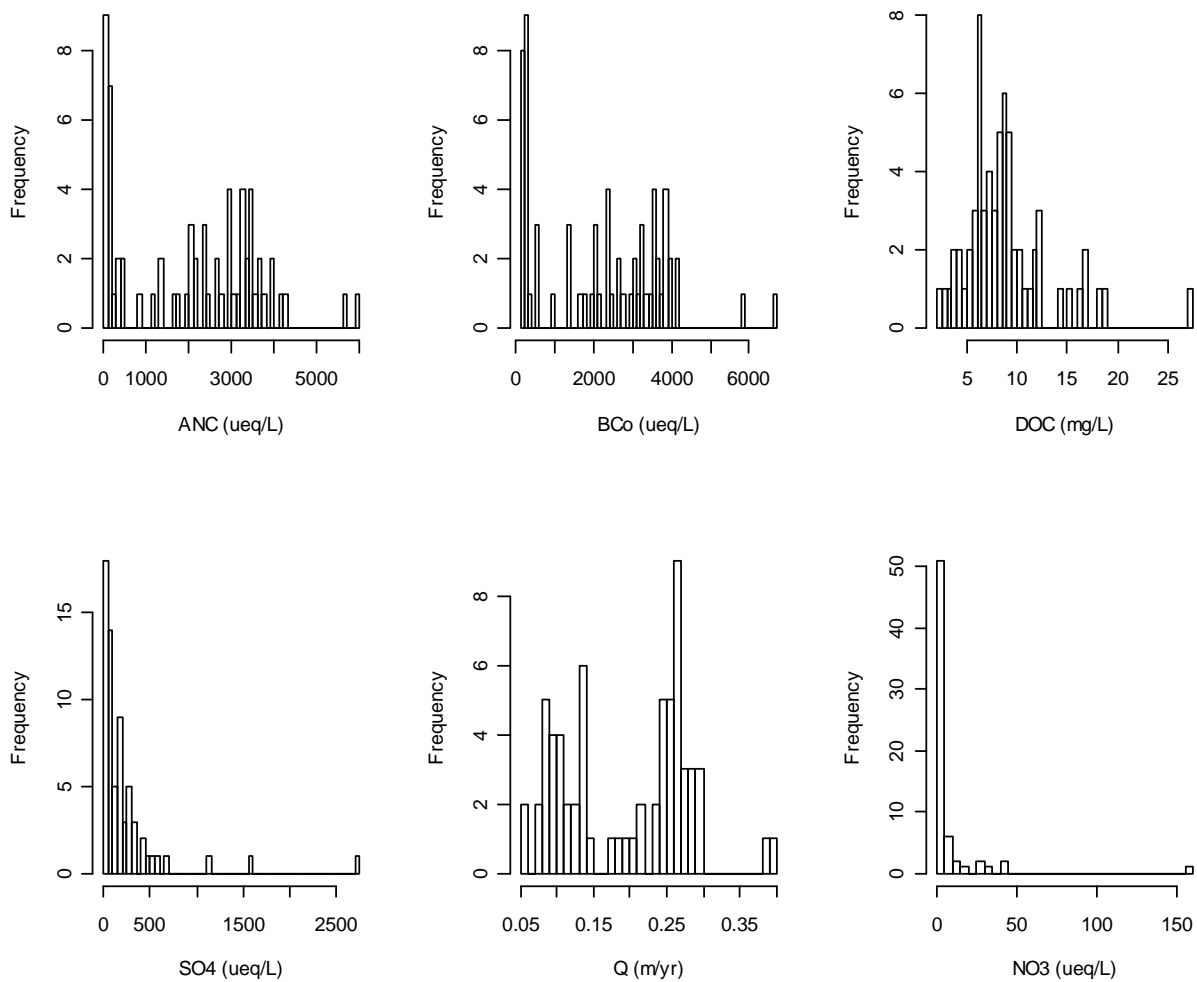


Figure C-29. Region 8.1.4 Water Quality Data Summary

Region 8.1.5 Driftless Area

The hilly uplands of the Driftless Area easily distinguish it from surrounding ecoregions. Much of the area consists of a deeply dissected, loess-capped, bedrock dominated plateau. The region is also called the Paleozoic Plateau because the landscape's appearance is a result of erosion through rock strata of Paleozoic age. Although there is evidence of glacial drift in the region, its influence on the landscape has been minor compared to adjacent ecoregions. In contrast to adjacent ecoregions, the Driftless Area has few lakes, most of which are reservoirs with generally high trophic states. Livestock and dairy farming are major land uses and have had a major impact on stream quality.

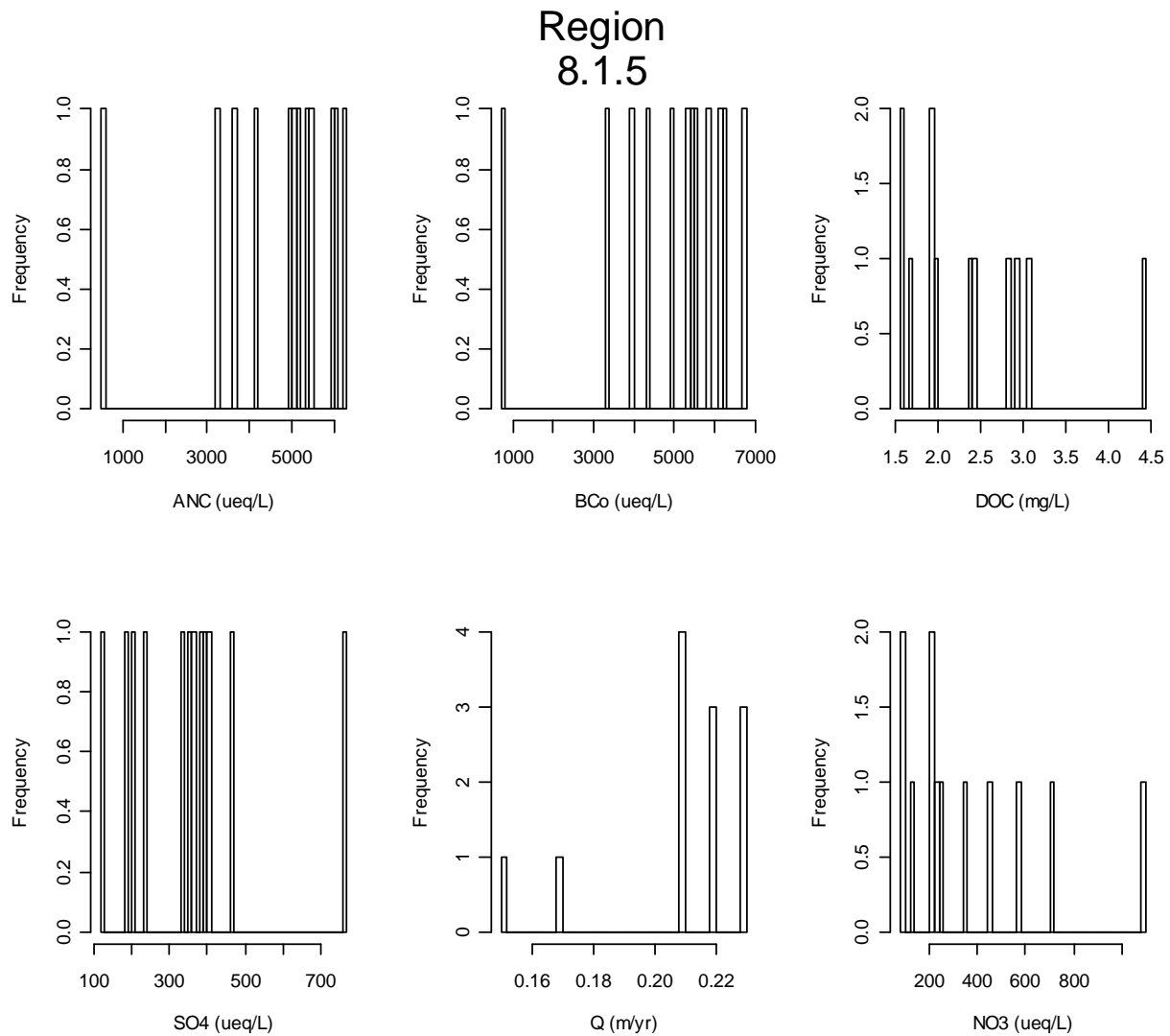


Figure C-30. Region 8.1.5 Water Quality Data Summary

Region 8.1.6 Southern Michigan/Northern Indiana

Bordered by Lake Michigan on the west, this ecoregion is less agricultural than the Central Corn Belt (8.2.3) and Eastern Corn Belt (8.2.4) to the south, it is better drained and contains more lakes than the flat agricultural Huron/Erie Lake Plains (8.2.2) to the east, and its soils are not as nutrient poor as Northern Lakes and Forests (5.2.1) to the north. The region is characterized by many lakes and marshes as well as an assortment of landforms, soil types, soil textures, and land uses. Broad till plains with thick and complex deposits of drift, paleobeach ridges, relict dunes, morainal hills, kames, drumlins, meltwater channels, and kettles occur. Oak-hickory forests, northern swamp forests, and beech forests were typical. Feed grain, soybean, and livestock farming as well as woodlots, quarries, recreational development, and urban-industrial areas are now common.

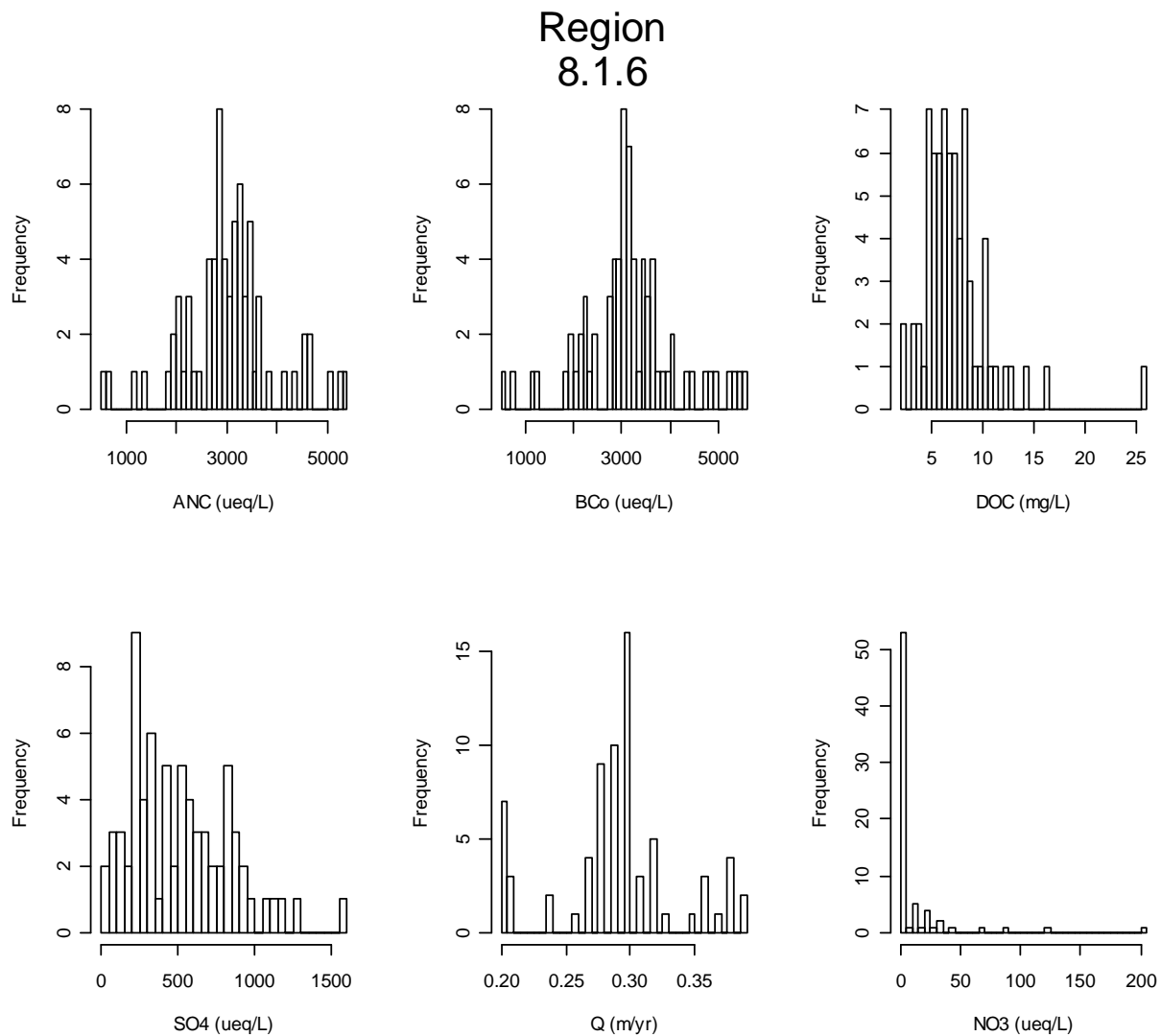


Figure C-31. Region 8.1.6 Water Quality Data Summary

Region 8.1.7 Northeastern Coastal Zone

Similar to the Northeastern Highlands (5.3.1), the Northeastern Coastal Zone contains relatively nutrient poor soils and concentrations of continental glacial lakes, some of which are sensitive to acidification; however, this ecoregion contains considerably less surface irregularity and much greater concentrations of human population. Landforms in the region include irregular plains, and plains with high hills. Appalachian oak forests and northeastern oak-pine forests are the natural vegetation types. Although attempts were made to farm much of the Northeastern Coastal Zone after the region was settled by Europeans, land use now mainly consists of forests, woodlands, and urban and suburban development, with only some minor areas of pasture and cropland.

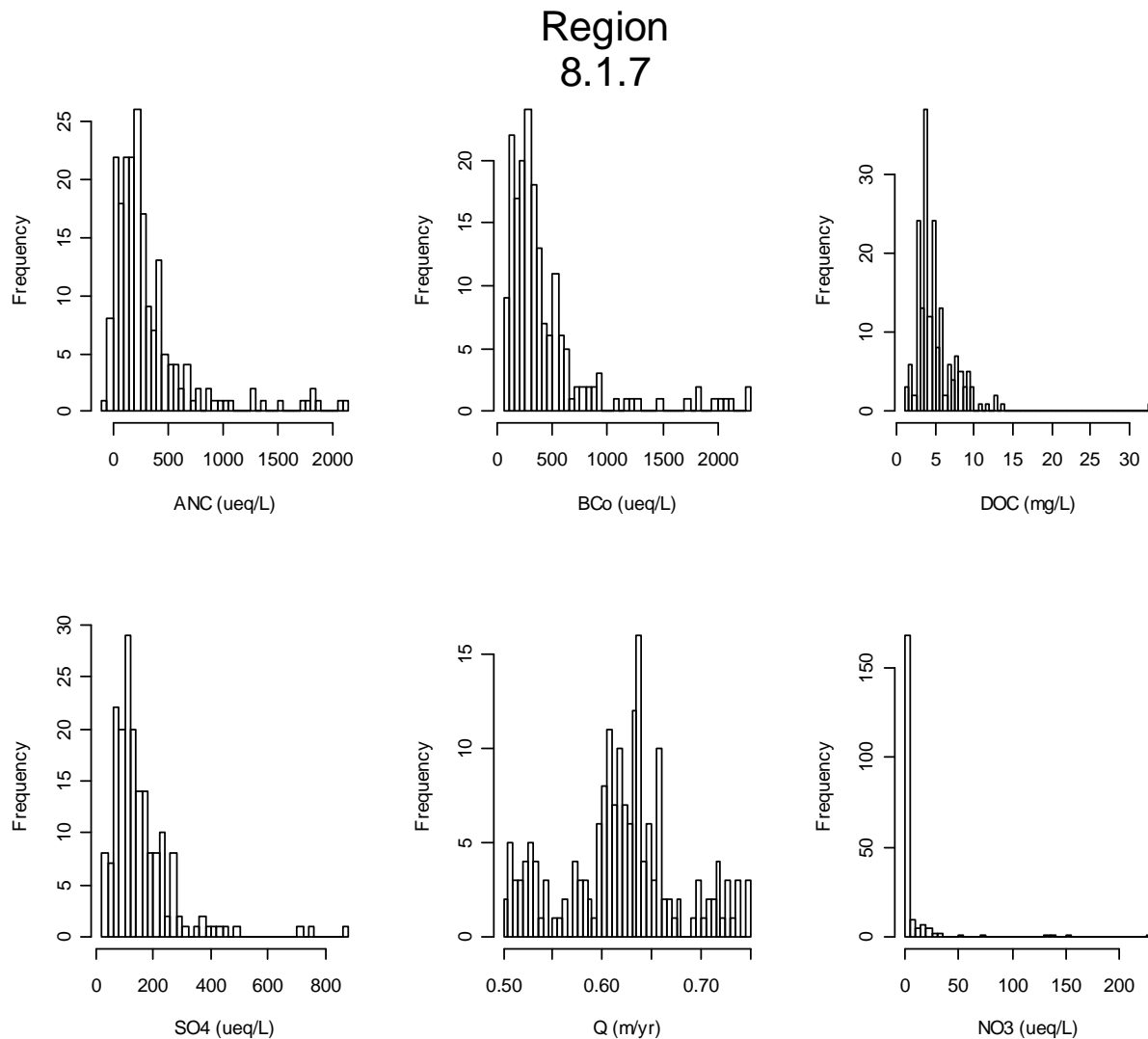


Figure C-32. Region 8.1.7 Water Quality Data Summary

Region 8.1.8 Acadian Plains and Hills

This mostly forested region, with dense concentrations of continental glacial lakes, is less rugged than the Northeastern Highlands (5.3.1) to the west and considerably less populated than Northeastern Coastal Zone (8.1.7) to the south. Vegetation here is mostly spruce-fir on the lowlands with some patches of maple, beech, and birch on the hills. Soils are predominantly frigid Spodosols. By contrast, the forests in the Northeastern Coastal Zone (8.1.7) to the south are mostly Appalachian oak or northeastern oak-pine and the soils are generally mesic Inceptisols and Entisols.

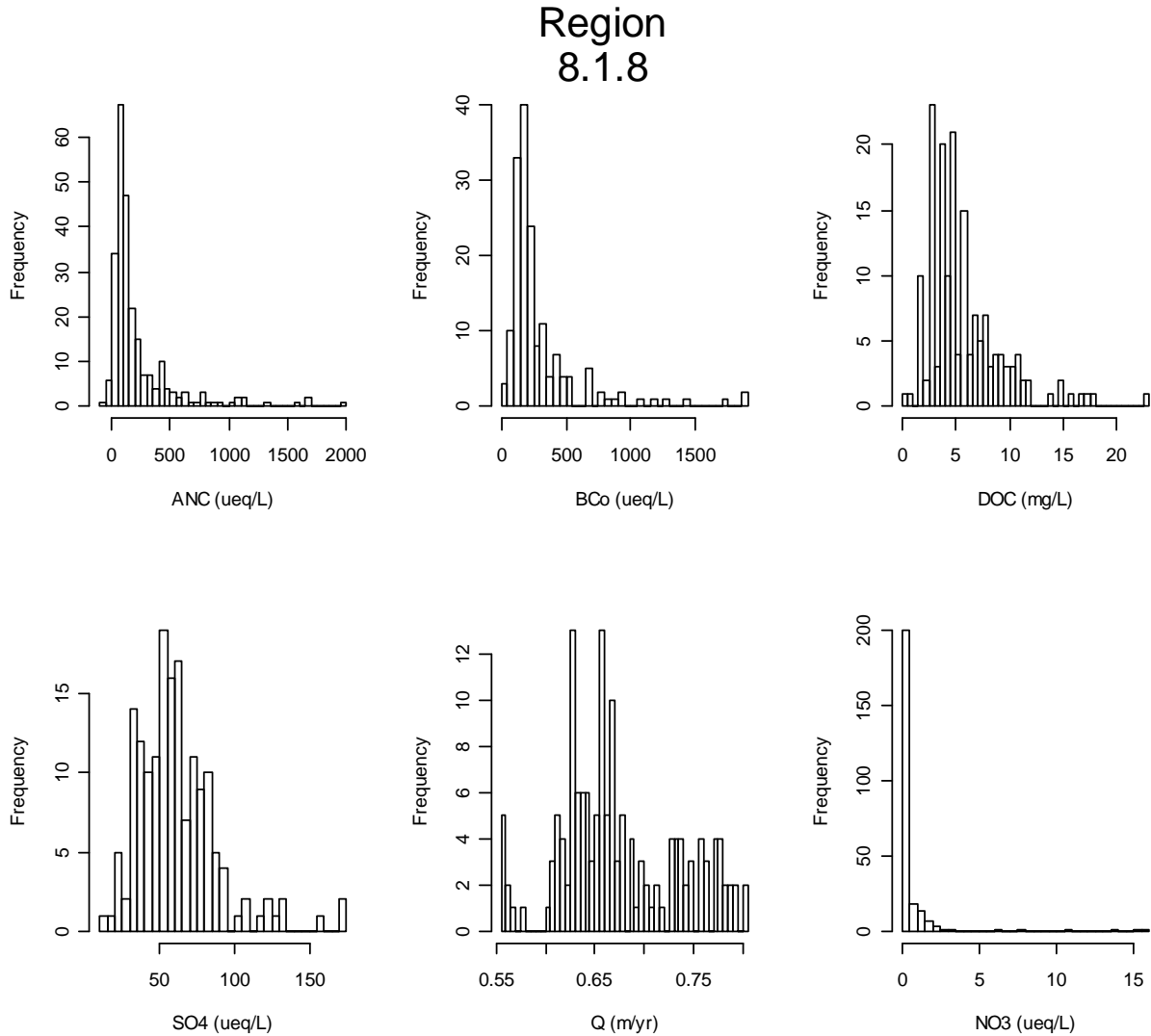


Figure C-33. Region 8.1.8 Water Quality Data Summary

Region 8.1.10 Erie Drift Plain

Once largely covered by a maple-beech-birch forest in the west and northern hardwoods in the east, much of the Erie Drift Plain is now in farms, many associated with dairy operations. The Eastern Corn Belt Plains (8.2.4), which border the region on the west, are flatter, more fertile, and therefore more agricultural. The glaciated Erie Drift Plain is characterized by low rounded hills, scattered end moraines, kettles, and areas of wetlands, in contrast to the adjacent unglaciated ecoregions (5.3.3, 8.4.3) to the south and east that are more hilly and less agricultural. Areas of urban development and industrial activity occur locally. Lake Erie's influence substantially increases the growing season, winter cloudiness, and snowfall in the northernmost areas bordering the strip of the Eastern Great Lakes Lowland (8.1.1) which fringes the lake.

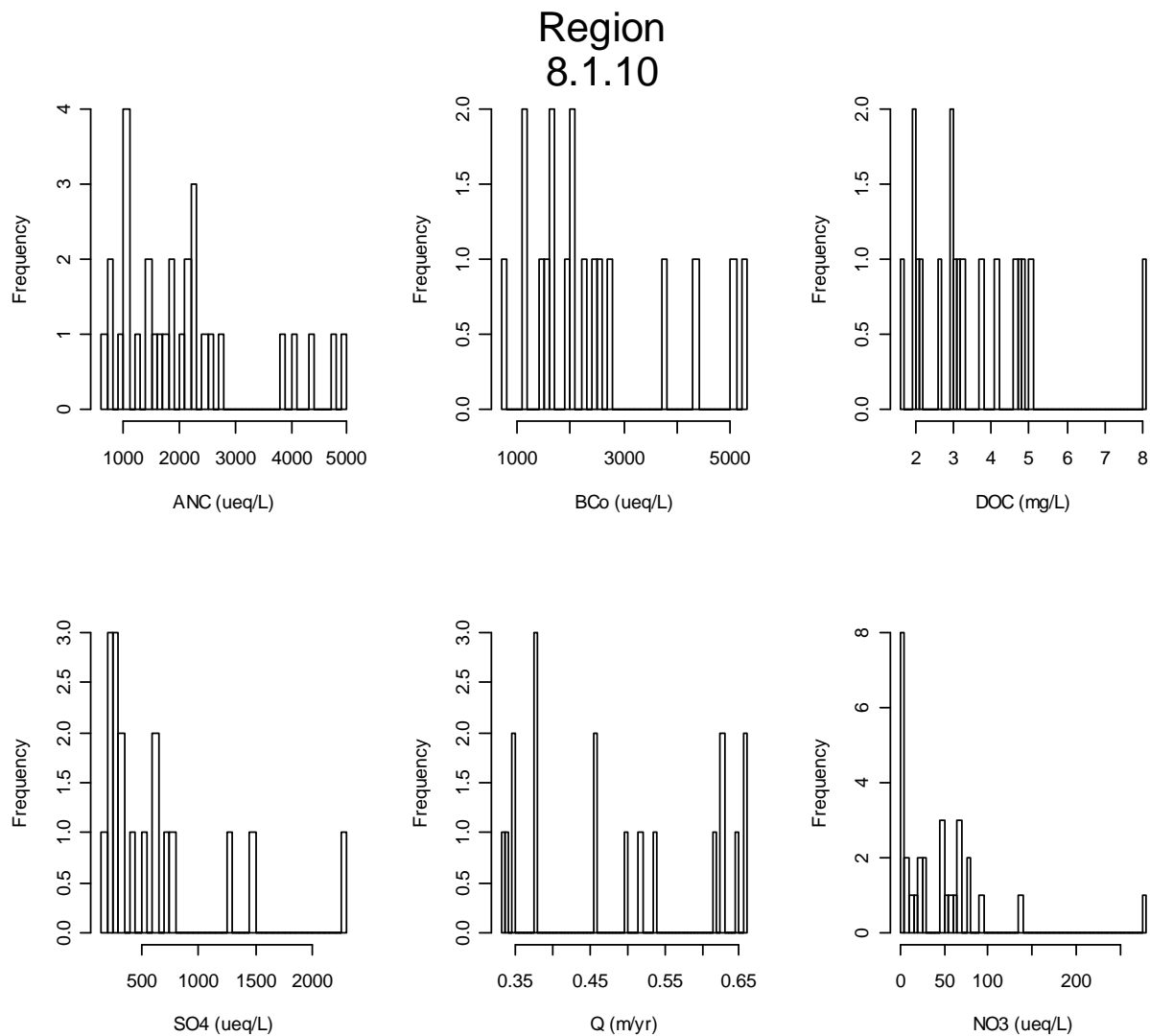


Figure C-34. Region 8.1.10 Water Quality Data Summary

Region 8.2 Central USA Plains

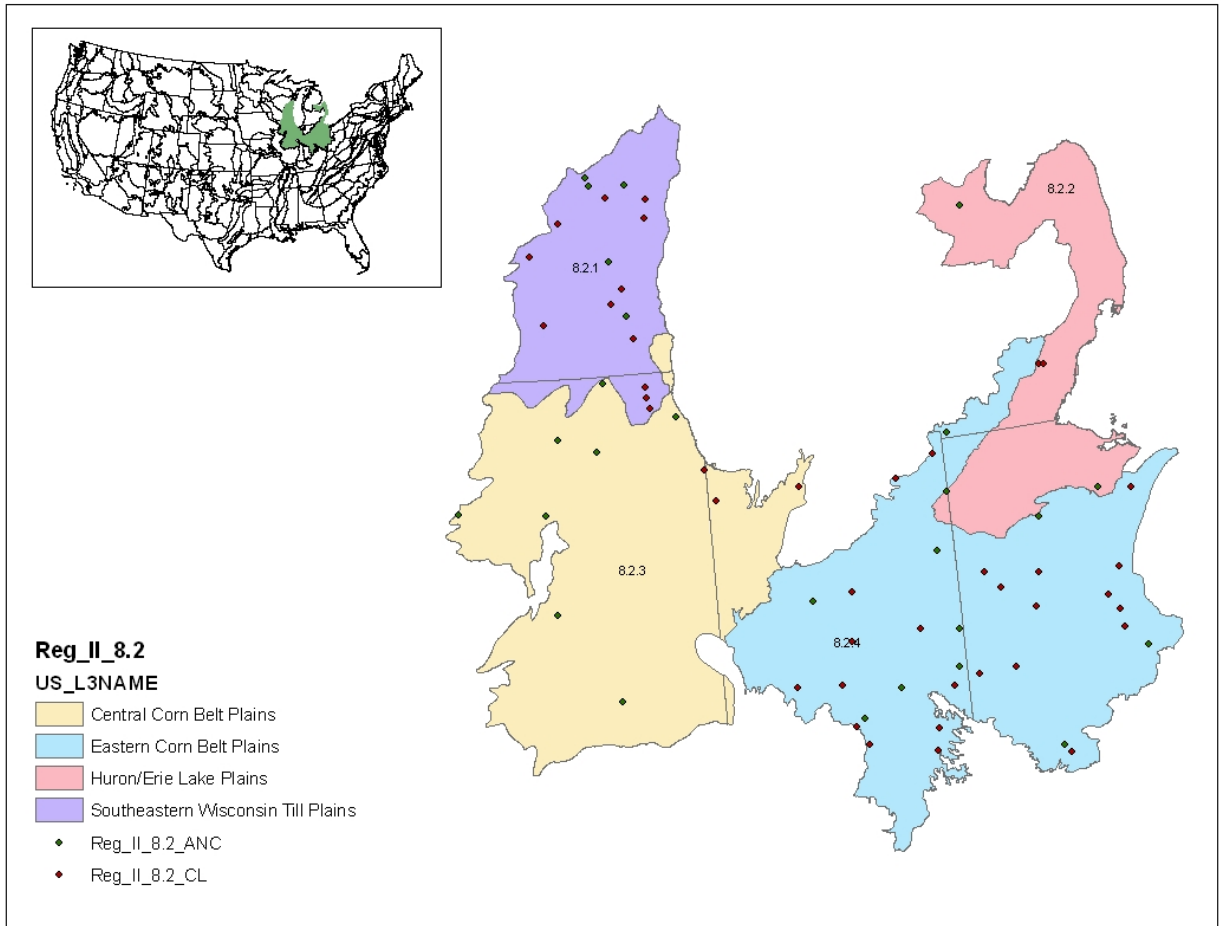


Figure C-35. Region 8.2

Region 8.2.1 Southeastern Wisconsin Till Plains

The Southeastern Wisconsin Till Plains support a mosaic of vegetation types, representing a transition between the hardwood forests and oak savannas of the ecoregions to the west and the tallgrass prairies of the Central Corn Belt Plains (8.2.3) to the south. Like Ecoregion 54, land use in the Southeastern Wisconsin Till Plains is mostly cropland, but the crops are largely forage and feed grains to support dairy operations, rather than corn and soybeans for cash crops. The ecoregion has a higher plant hardiness value and a different mosaic of soils than ecoregions to the north and west.

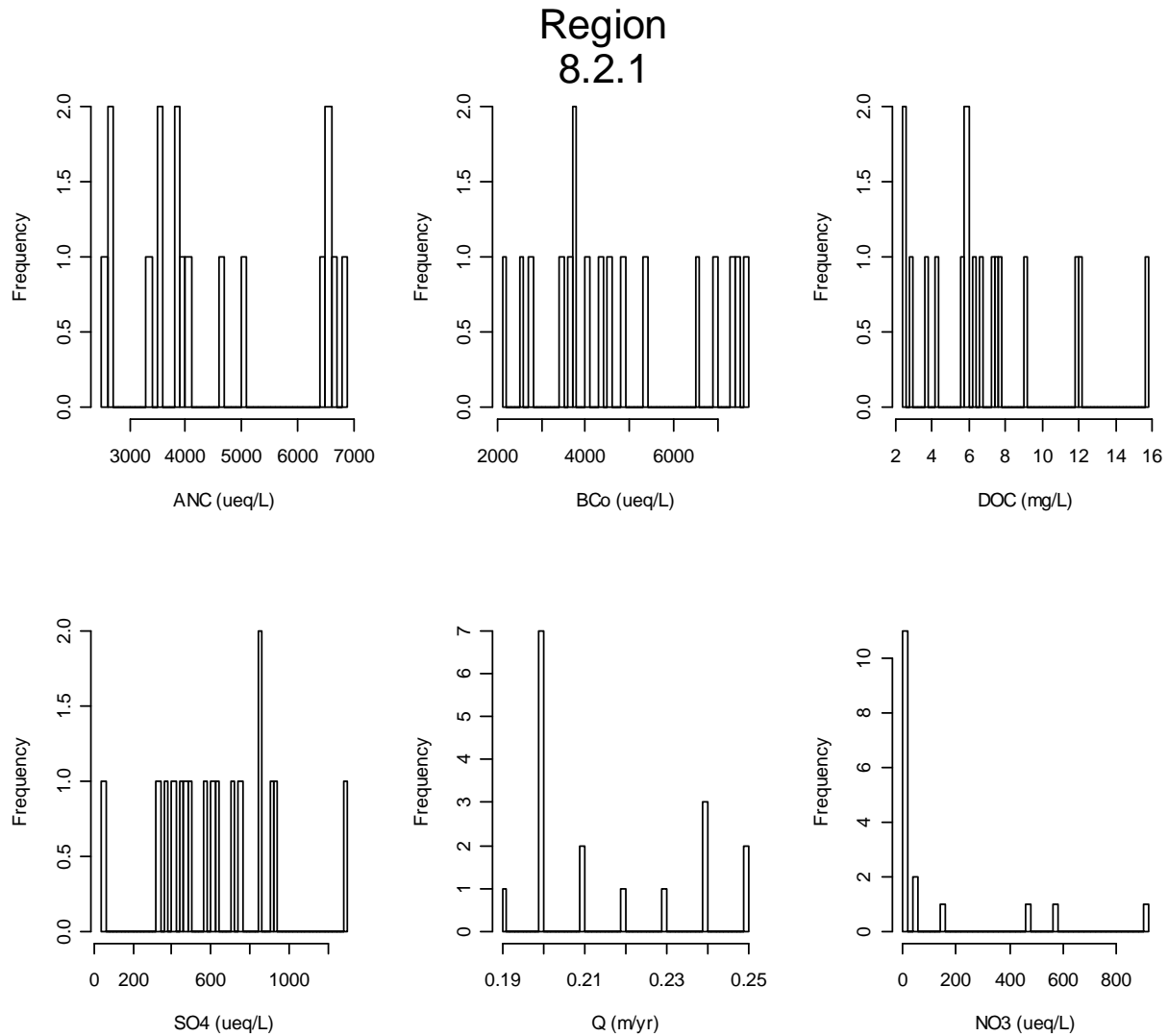


Figure C-36. Region 8.2.1 Water Quality Data Summary

Region 8.2.2 Huron/Erie Lake Plains

The Huron/Erie Lake Plains ecoregion is a broad, fertile, nearly flat plain punctuated by relic sand dunes, beach ridges, and end moraines. Originally, soil drainage was typically poorer than in the adjacent Eastern Corn Belt Plains (8.2.4), and elm-ash swamp and beech forests were dominant. Oak savanna was typically restricted to sandy, well-drained dunes and beach ridges. Today, most of the area has been cleared and artificially drained and contains highly productive farms producing corn, soybeans, livestock, and vegetables; urban and industrial areas are also extensive. Stream habitat and quality have been degraded by channelization, ditching, and agricultural activities.

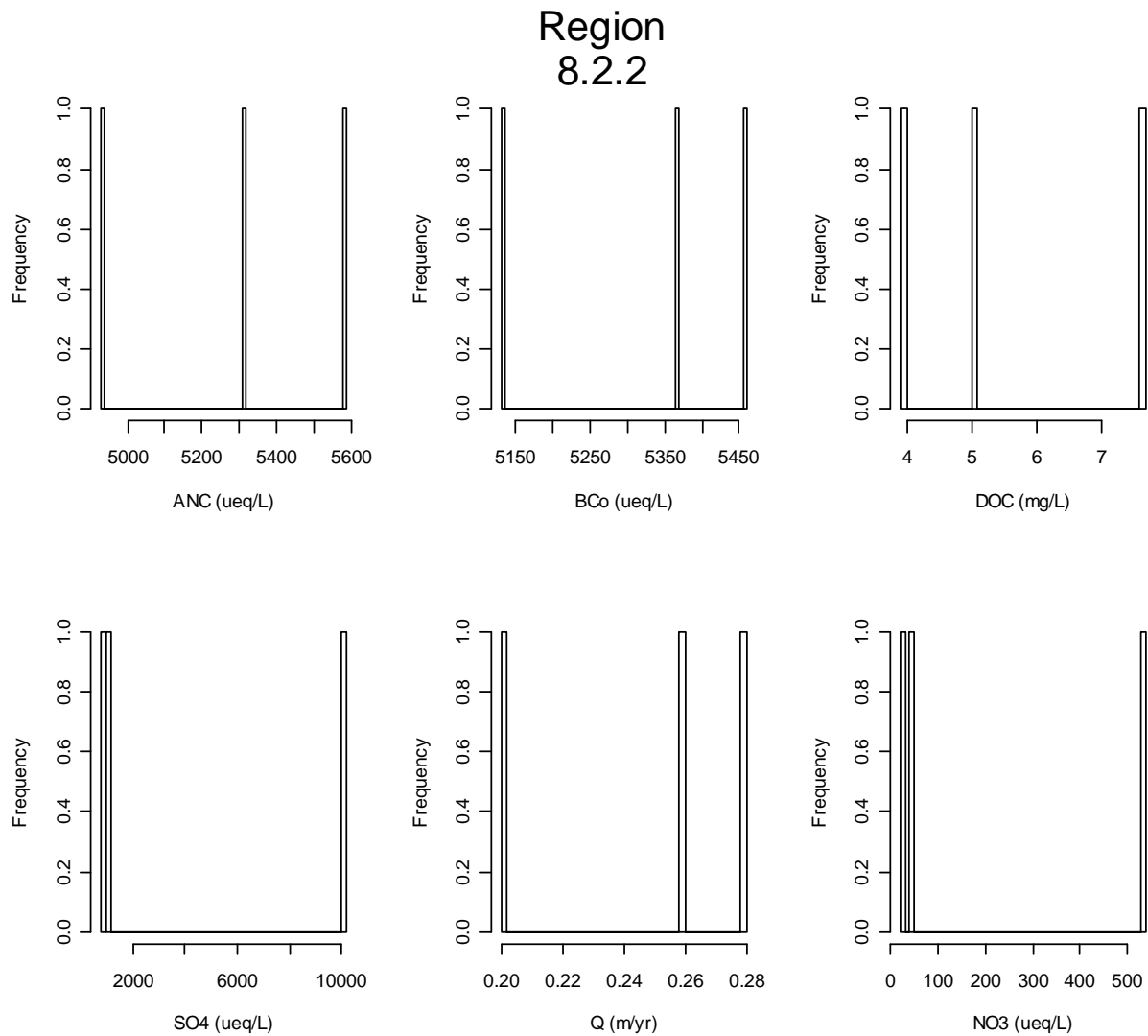


Figure C-37. Region 8.2.2 Water Quality Data Summary

Region 8.2.3 Central Corn Belt Plains

Extensive prairie communities intermixed with oak-hickory forests were native to the glaciated plains of the Central Corn Belt Plains; they were a stark contrast to the hardwood forests that grew on the drift plains of Ecoregions 8.2.4 and 8.1.6 to the east. Ecoregions 9.2.4 and 9.2.3 to the west were mostly treeless except along larger streams. Beginning in the nineteenth century, the natural vegetation was gradually replaced by agriculture. Farms are now extensive on the dark, fertile soils of the Central Corn Belt Plains and mainly produce corn and soybeans; cattle, sheep, poultry, and, especially hogs, are also raised, but they are not as dominant as in the drier Western Corn Belt Plains (9.2.3) to the west. Agriculture has affected stream chemistry, turbidity, and habitat.

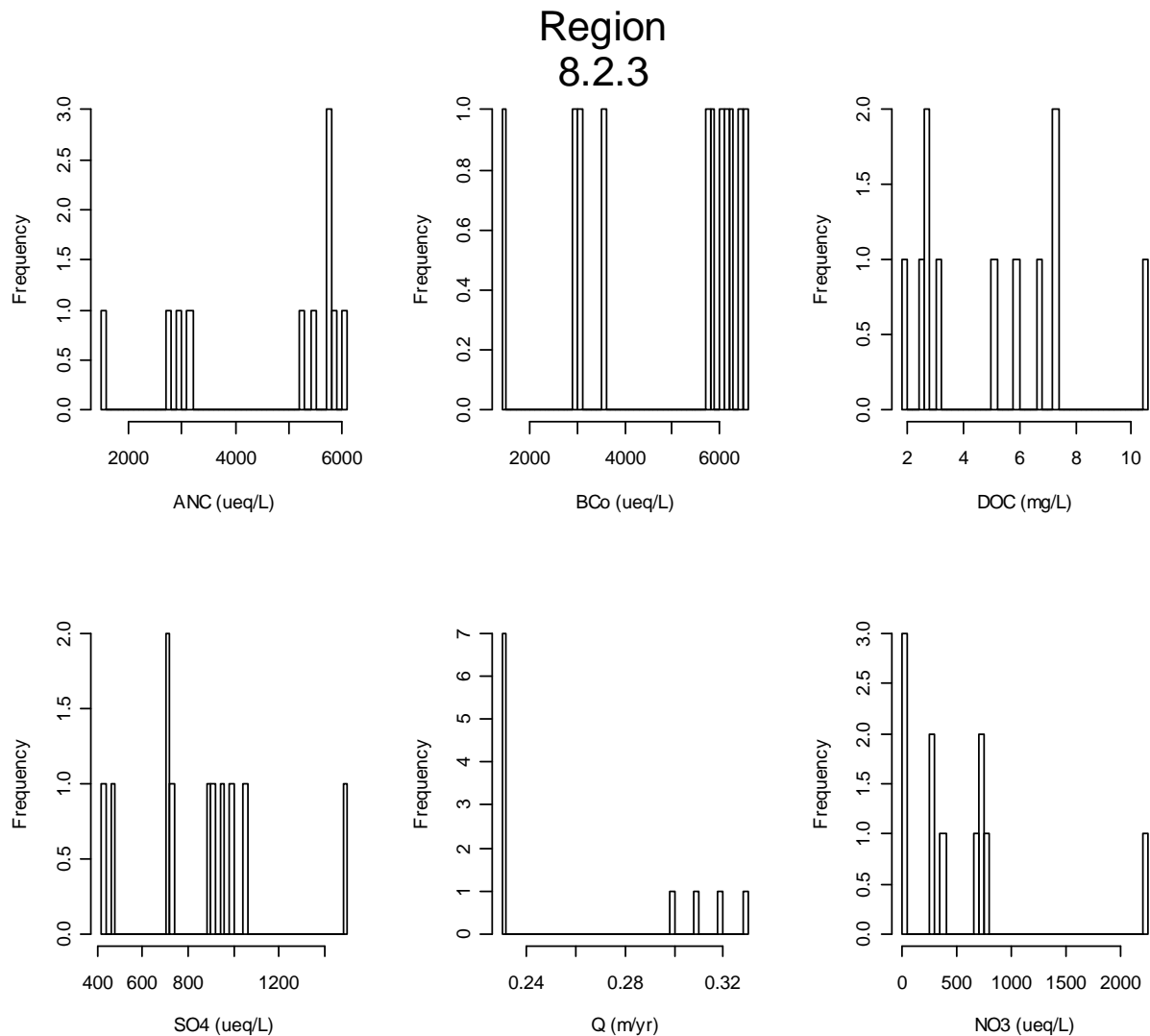


Figure C-38. Region 8.2.3 Water Quality Data Summary

Region 8.2.4 Eastern Corn Belt Plains

The Eastern Corn Belt Plains ecoregion is primarily a rolling till plain with local end moraines; it had more natural tree cover and has lighter colored soils than the Central Corn Belt Plains (8.2.3). The region has loamier and better drained soils than the Huron/Erie Lake Plain (8.2.2), and richer soils than the Erie Drift Plain (8.1.10). Glacial deposits of Wisconsin age are extensive. They are not as dissected nor as leached as the pre-Wisconsinan till which is restricted to the southern part of the region. Originally, beech forests were common on Wisconsin soils while beech forests and elm-ash swamp forests dominated the wetter pre-Wisconsinan soils. Today, extensive corn, soybean, and livestock production occurs and has affected stream chemistry and turbidity.

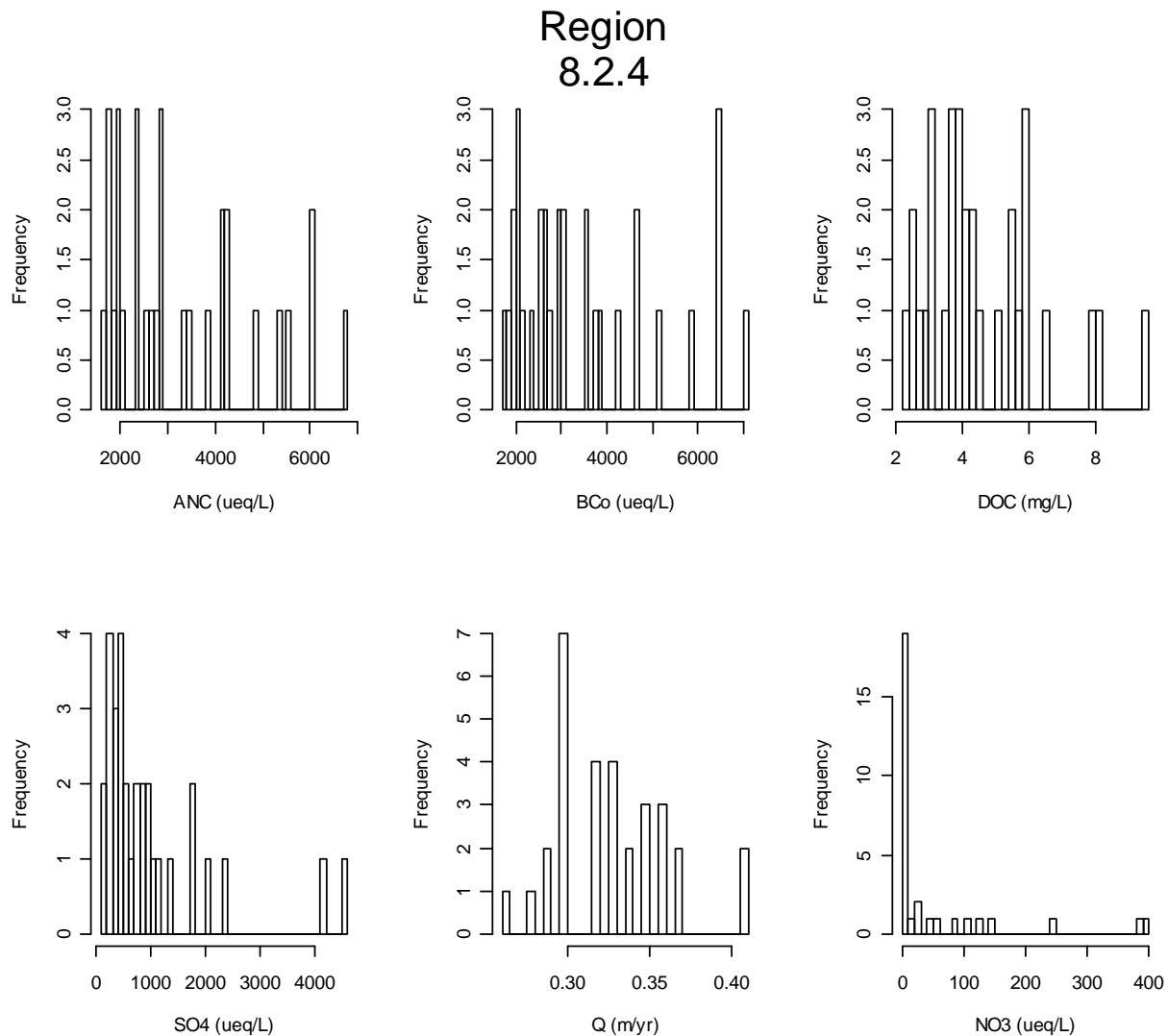


Figure C-39. Region 8.2.4 Water Quality Data Summary

Region 8.3 Southeastern USA Plains

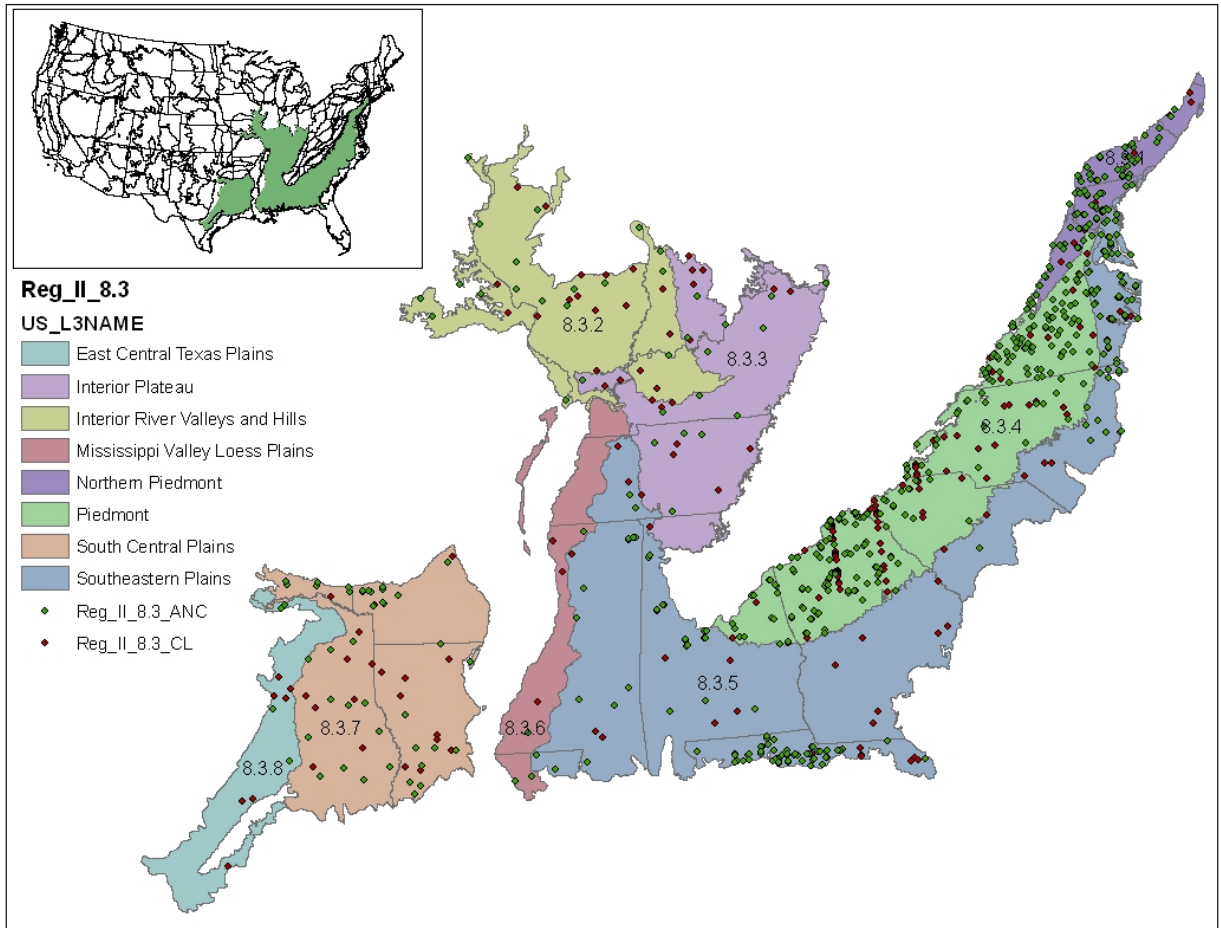


Figure C-40. Region 8.3

Region 8.3.1 Northern Piedmont

The Northern Piedmont is a transitional region of low rounded hills, irregular plains, and open valleys in contrast to the low mountains of Ecoregions 5.3.1, 8.4.4, and 8.4.1 to the north and west and the flatter coastal plains of Ecoregions 8.3.5 and 8.5.1 to the east. It is underlain by a mix of metamorphic, igneous, and sedimentary rocks, with soils that are mostly Alfisols and some Ultisols. Potential natural vegetation here was predominantly Appalachian oak forest as compared to the mostly oak-hickory-pine forests of the Piedmont (8.3.4) ecoregion to the southwest. The region now contains a higher proportion of cropland compared to the Piedmont.

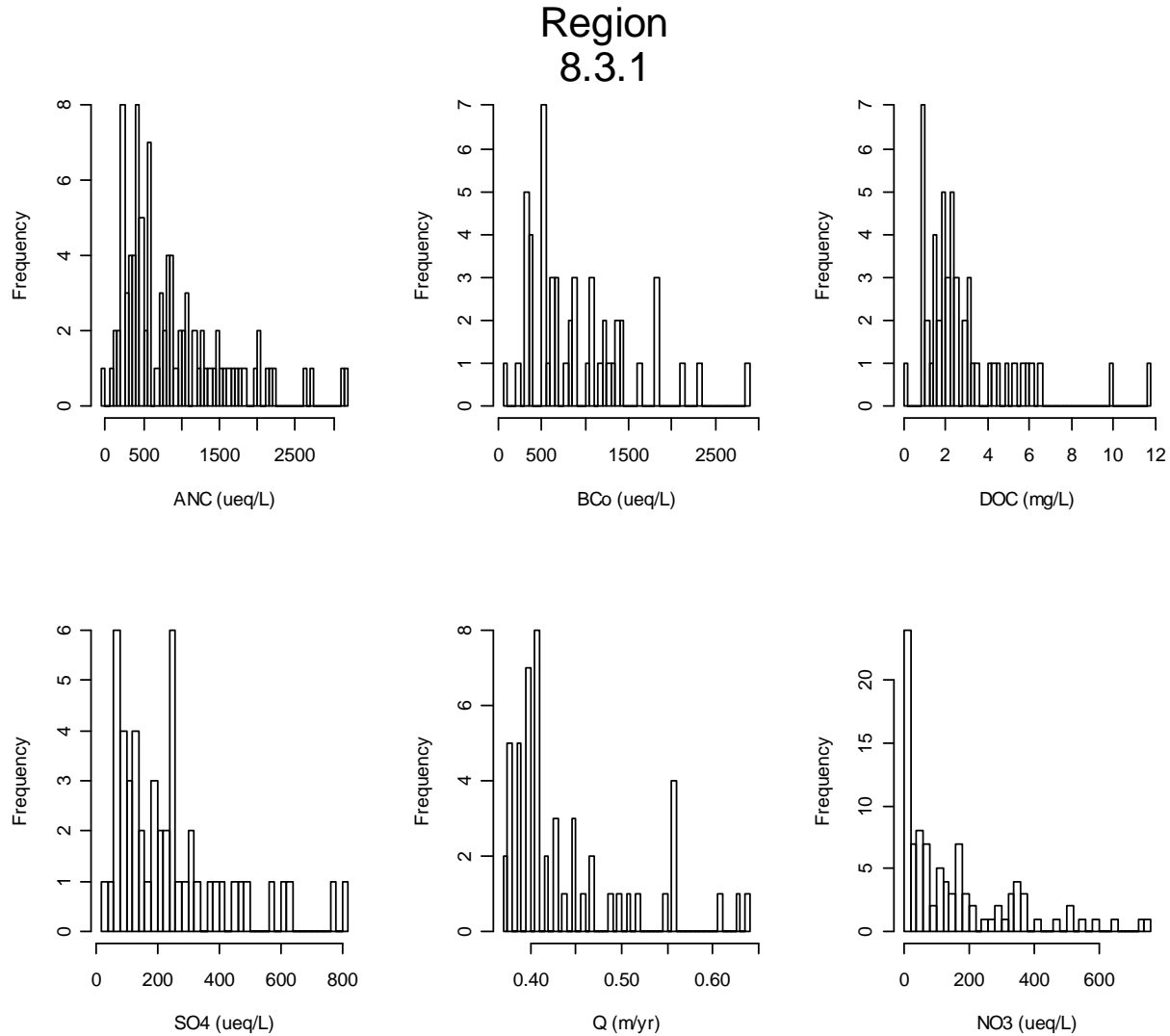


Figure C-41. Region 8.3.1 Water Quality Data Summary

Region 8.3.2 Interior River Valleys and Hills

The Interior River Lowland is made up of many wide, flat-bottomed terraced valleys, forested valley slopes, and dissected glacial till plains. In contrast to the generally rolling to slightly irregular plains in adjacent ecological regions to the north (8.2.3), east (8.2.4) and west (9.2.4, 9.2.3), where most of the land is cultivated for corn and soybeans, a little less than half of this area is in cropland, about 30 percent is in pasture, and the remainder is in forest. Bottomland deciduous forests and swamp forests were common on wet lowland sites, with mixed oak and oak-hickory forests on uplands. Paleozoic sedimentary rock is typical and coal mining occurs in several areas.

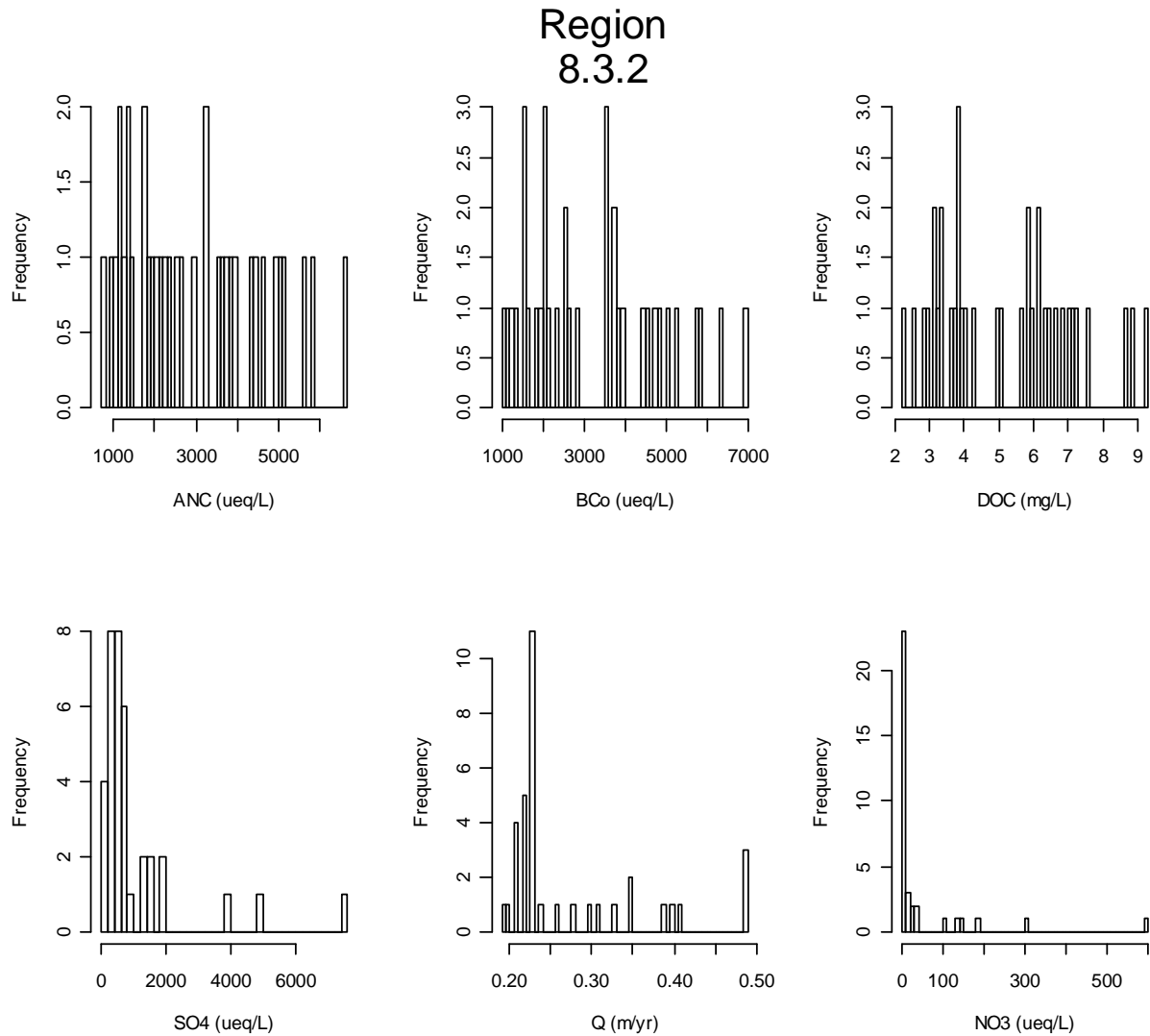


Figure C-42. Region 8.3.2 Water Quality Data Summary

Region 8.3.3 Interior Plateau

The Interior Plateau is a diverse ecoregion extending from southern Indiana and Ohio to northern Alabama. Rock types are distinctly different from the coastal plain sediments and alluvial deposits of ecoregions to the west, and elevations are lower than the Appalachian ecoregions (8.4.4, 8.4.1, 8.4.9) to the east. Mississippian to Ordovician-age limestone, chert, sandstone, siltstone and shale compose the landforms of open hills, irregular plains, and tablelands. The natural vegetation is primarily oak-hickory forest, with some areas of bluestem prairie and cedar glades. The region has a diverse fish fauna.

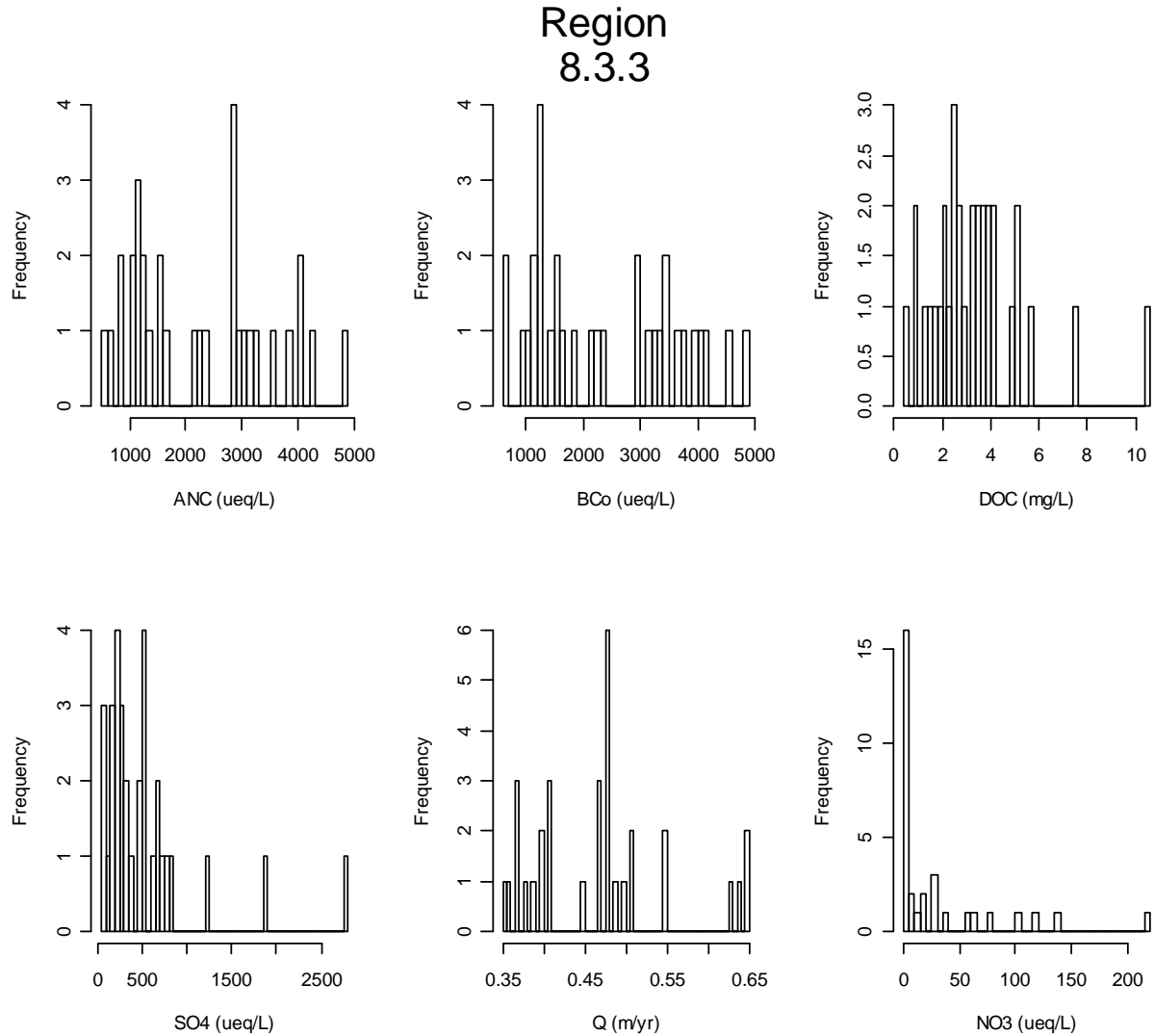


Figure C-43. Region 8.3.3 Water Quality Data Summary

Region 8.3.4 Piedmont

Considered the non-mountainous portion of the old Appalachians Highland by physiographers, the northeast-southwest trending Piedmont ecoregion comprises a transitional area between the mostly mountainous ecoregions of the Appalachians to the northwest and the relatively flat coastal plain to the southeast. It is a complex mosaic of Precambrian and Paleozoic metamorphic and igneous rocks, with moderately dissected irregular plains and some hills. The soils tend to be finer-textured than in coastal plain regions (8.5.1, 8.3.5). Once largely cultivated, much of this region has reverted to successional pine and hardwood woodlands, with an increasing conversion to an urban and suburban land cover.

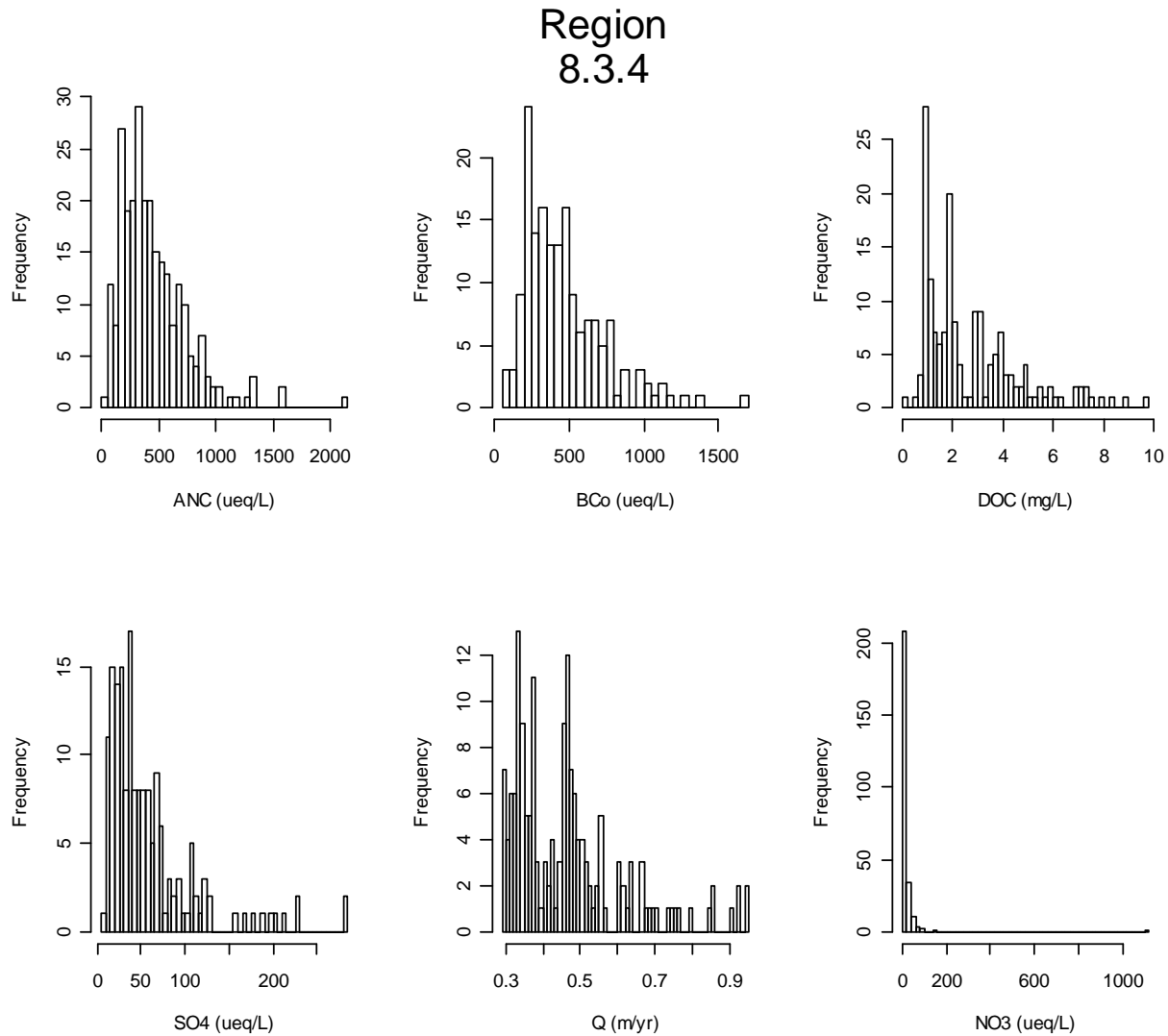


Figure C-44. Region 8.3.4 Water Quality Data Summary

Region 8.3.5 Southeastern Plains

These irregular plains have a mosaic of cropland, pasture, woodland, and forest. Natural vegetation was predominantly longleaf pine, with smaller areas of oak-hickory-pine and Southern mixed forest. The Cretaceous or Tertiary-age sands, silts, and clays of the region contrast geologically with the older metamorphic and igneous rocks of the Piedmont (8.3.4), and with the Paleozoic limestone, chert, and shale found in the Interior Plateau (8.3.3). Elevations and relief are greater than in the Southern Coastal Plain (8.5.3), but generally less than in much of the Piedmont. Streams in this area are relatively low-gradient and sandy-bottomed.

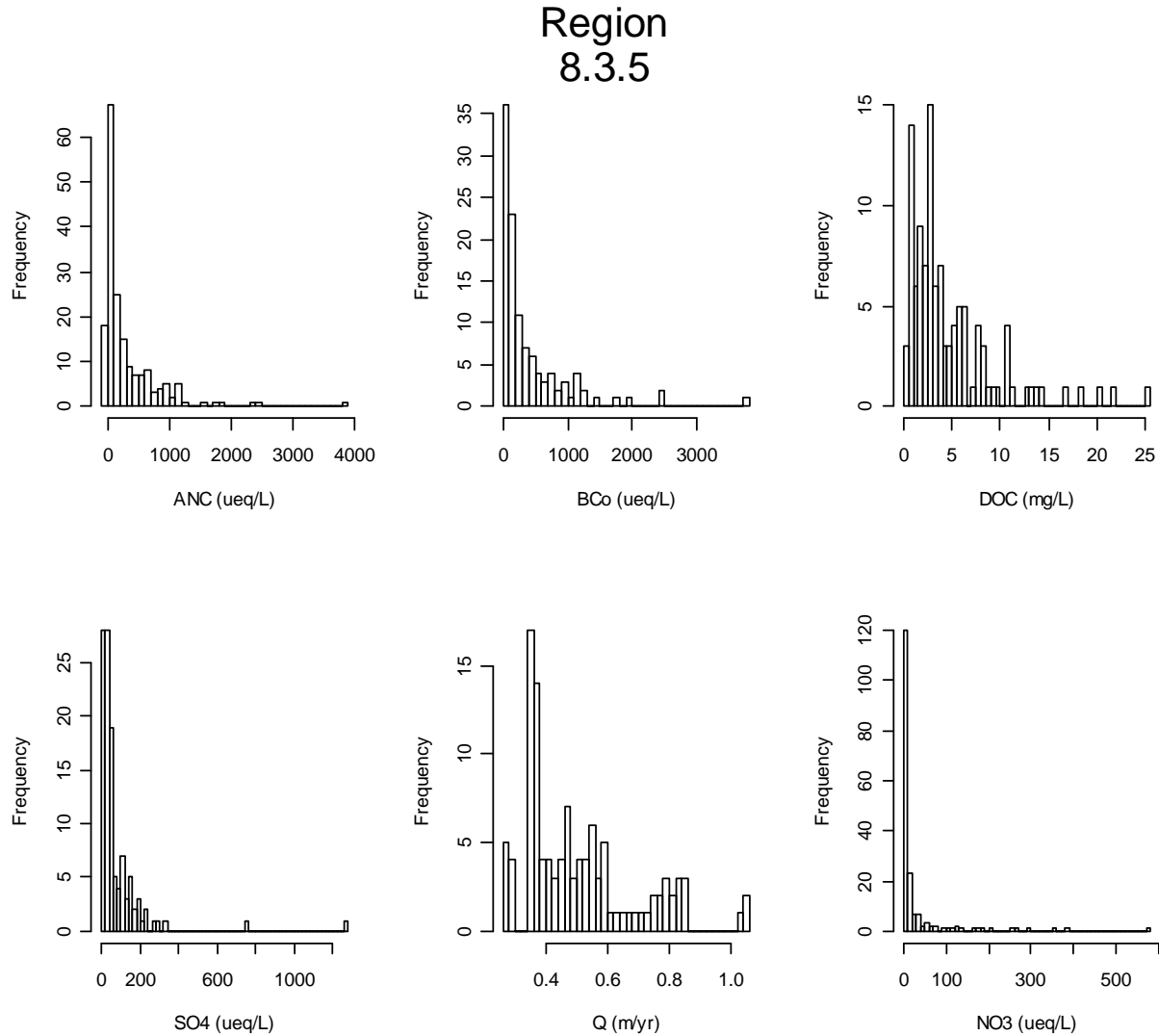


Figure C-45. Region 8.3.5 Water Quality Data Summary

Region 8.3.6 Mississippi Valley Loess Plains

This ecoregion stretches from near the Ohio River in western Kentucky to Louisiana. It consists primarily of irregular plains, some gently rolling hills, and near the Mississippi River, bluffs. Thick loess is one of the distinguishing characteristics. The bluff hills in the western portion contain soils that are deep, steep, silty, and erosive. Flatter topography is found to the east, and streams tend to have less gradient and siltier substrates than in the Southeastern Plains ecoregion (8.3.5). To the east, upland forests dominated by oak, hickory, and both loblolly and shortleaf pine, and to the west on bluffs some mixed and southern mesophytic forests, were the dominant natural vegetation. Agriculture is now the typical land cover in the Kentucky and Tennessee portion of the region, while in Mississippi there is a mosaic of forest and cropland.

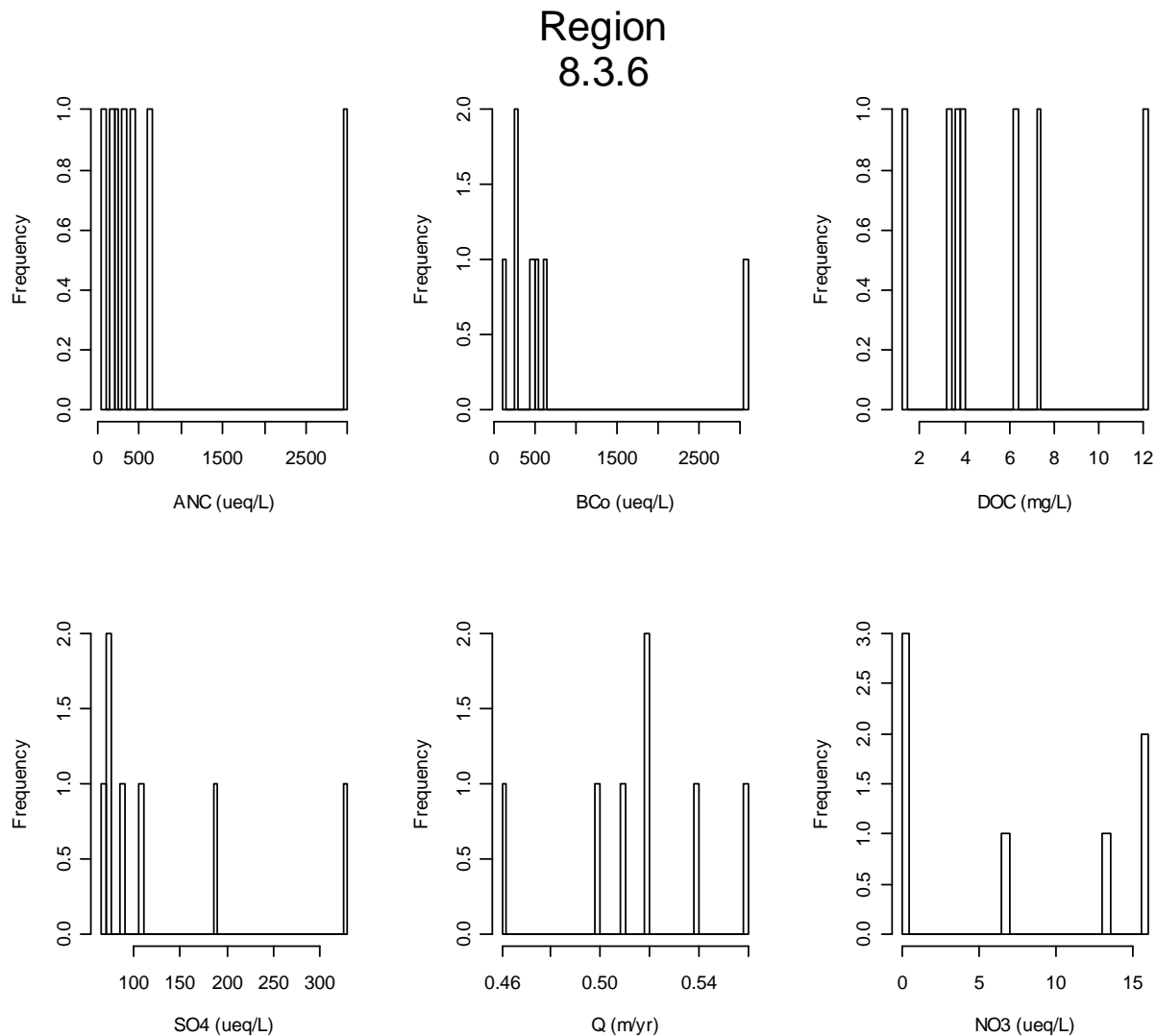


Figure C-46. Region 8.3.6 Water Quality Data Summary

Region 8.3.7 South Central Texas Plains

Locally termed the “piney woods”, this region of mostly irregular plains represents the western edge of the southern coniferous forest belt. Once blanketed by a mix of pine and hardwood forests, much of the region is now in loblolly and shortleaf pine plantations. Only about one sixth of the region is in cropland, primarily within the Red River floodplain, while about two thirds of the region is in forests and woodland. Lumber, pulpwood, oil and gas production are major economic activities.

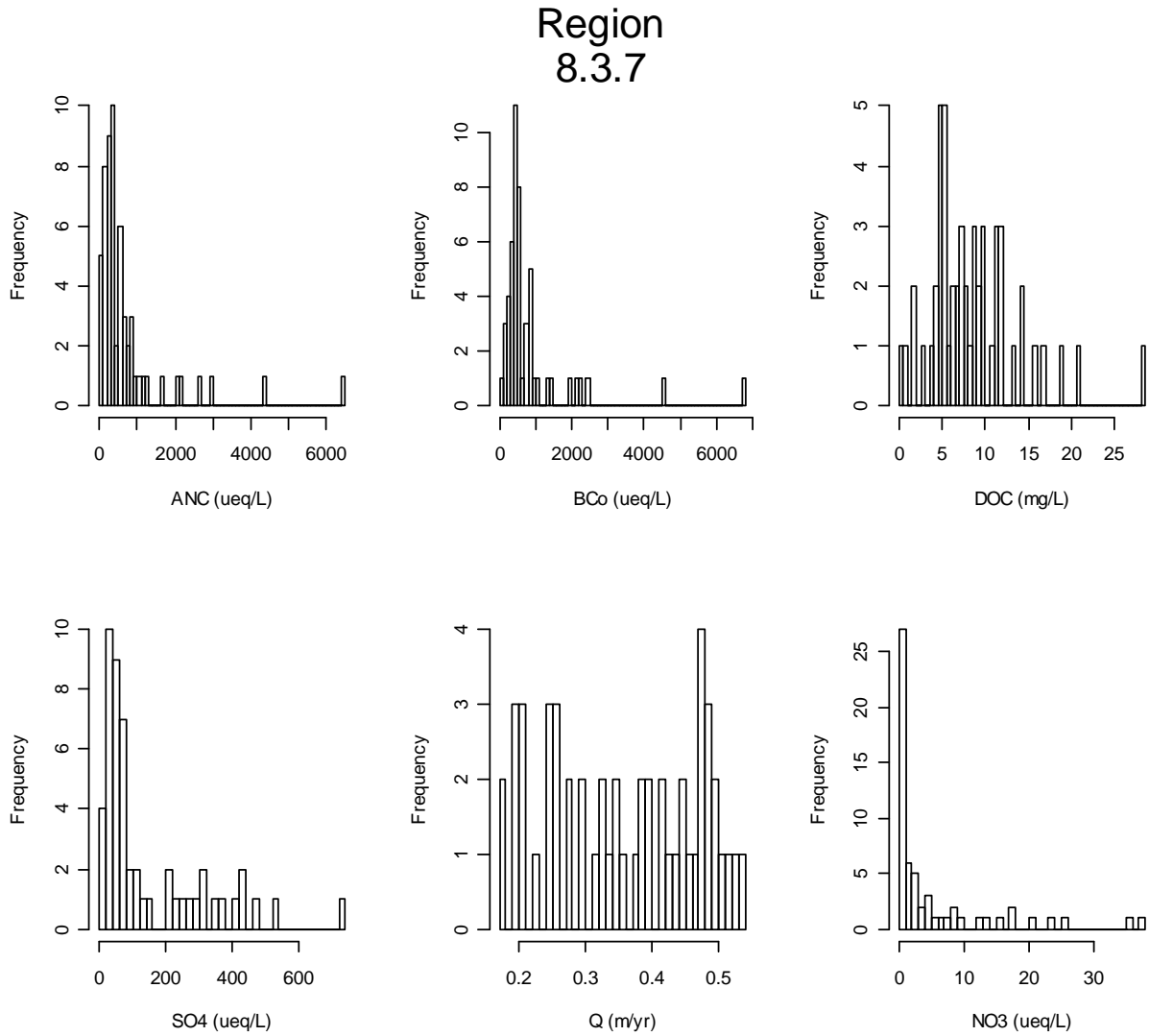


Figure C-47. Region 8.3.7 Water Quality Data Summary

Region 8.3.8 East Central Texas Plains

Also called the Post Oak Savanna or the Claypan Area, this region of irregular plains was originally covered by post oak savanna vegetation, in contrast to the more open prairie-type regions to the north, south, and west and the pine forests to the east. The boundary with Ecoregion 8.3.7 is a subtle transition of soils and vegetation. Many areas have a dense, underlying clay pan affecting water movement and available moisture for plant growth. The bulk of this region is now used for pasture and range.

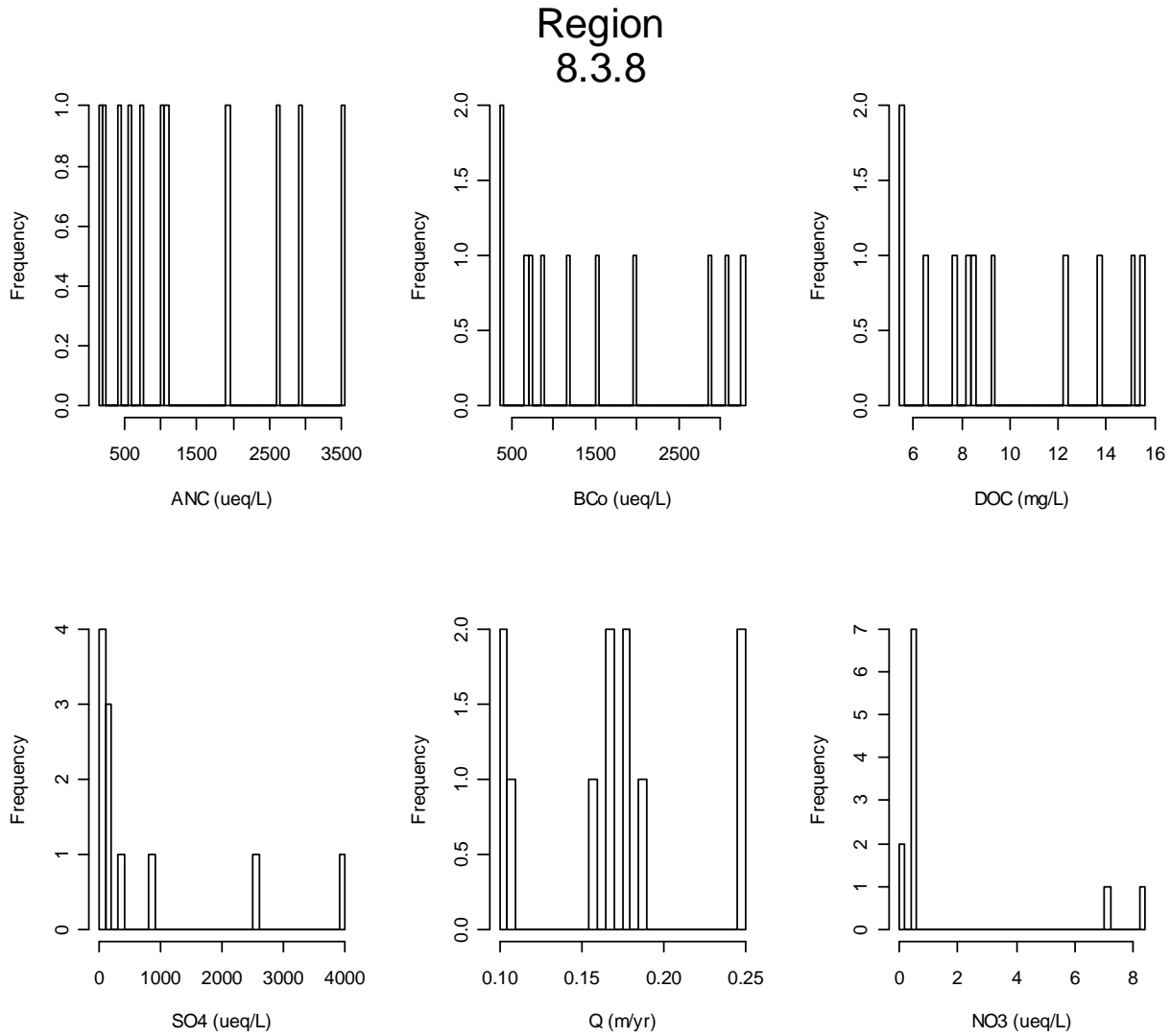


Figure C-48. Region 8.3.8 Water Quality Data Summary

Region 8.4 Ozark/Ouchita-Appalachian Forests

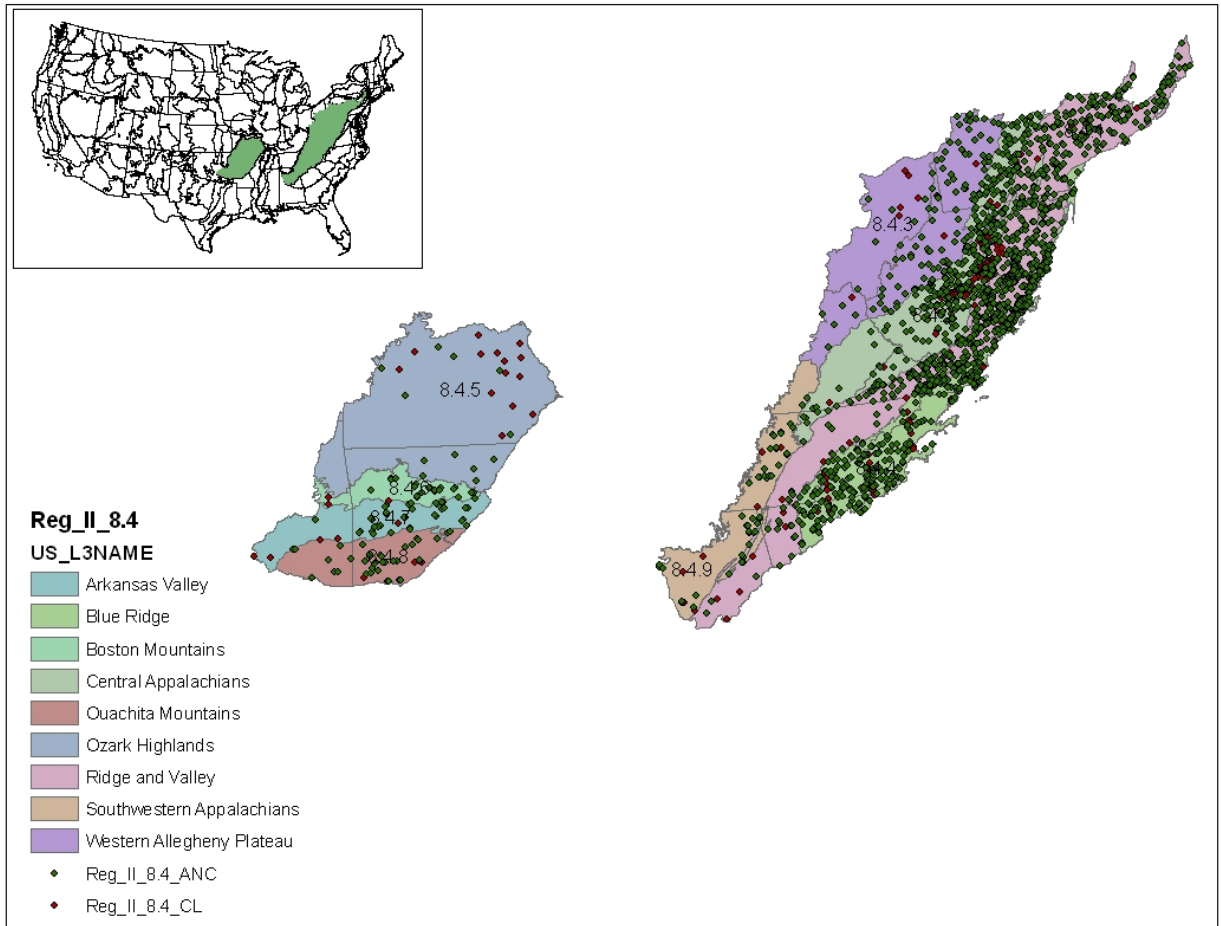


Figure C-49. Region 8.4

Region 8.4.1 Ridge and Valley

This northeast-southwest trending, relatively low-lying, but diverse ecoregion is sandwiched between generally higher, more rugged mountainous regions with greater forest cover. As a result of extreme folding and faulting events, the region's roughly parallel ridges and valleys have a variety of widths, heights, and geologic materials, including limestone, dolomite, shale, siltstone, sandstone, chert, mudstone, and marble. Springs and caves are relatively numerous. Present-day forests cover about 50% of the region. The ecoregion has a great diversity of aquatic habitats and species of fish.

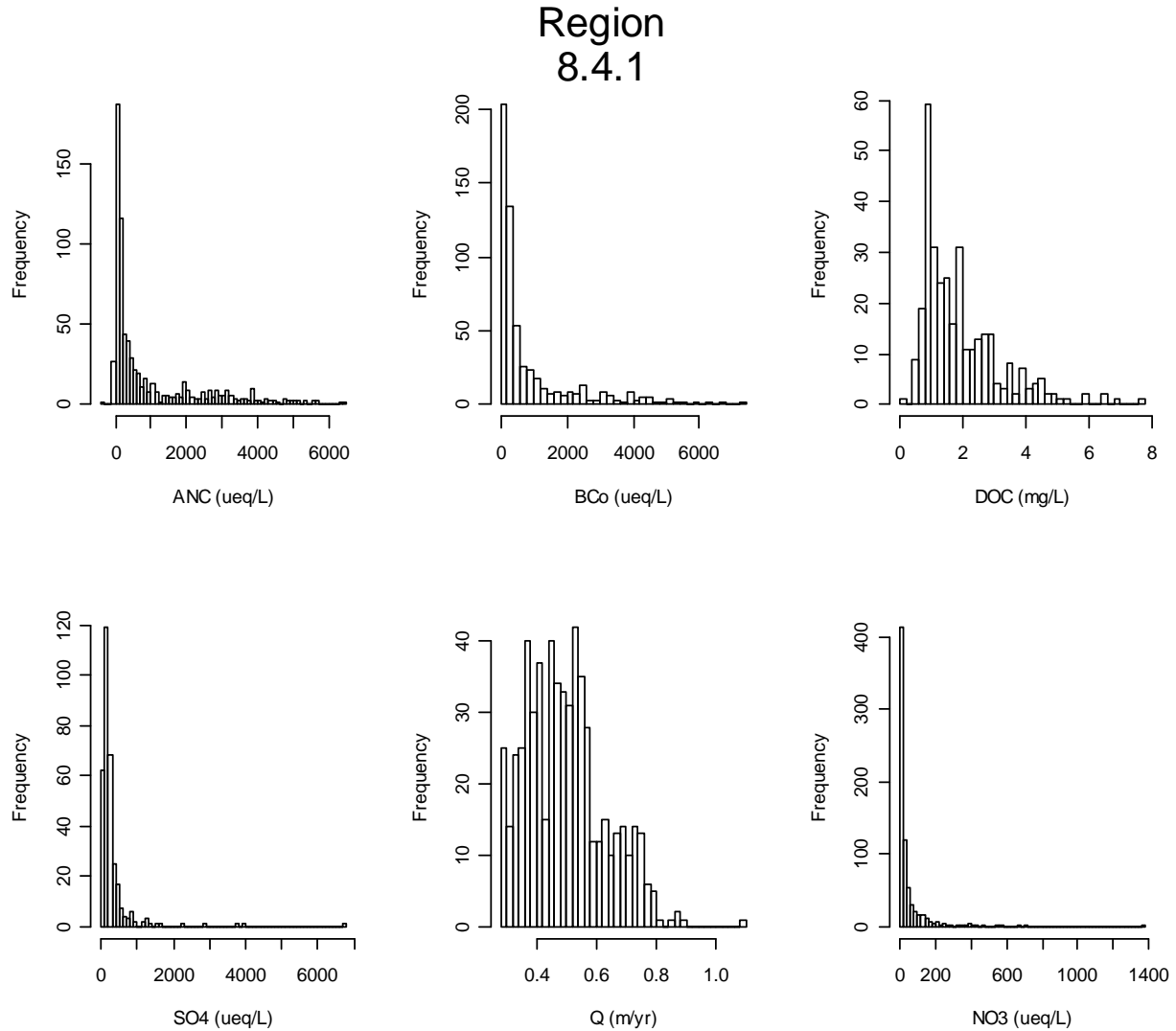


Figure C-50. Region 8.4.1 Water Quality Data Summary

Region 8.4.2 Central Appalachians

The Central Appalachian ecoregion, stretching from central Pennsylvania to northern Tennessee, is primarily a high, dissected, rugged plateau composed of sandstone, shale, conglomerate, and coal. The rugged terrain, cool climate, and infertile soils limit agriculture, resulting in a mostly forested land cover. The high hills and low mountains are covered by a mixed mesophytic forest with areas of Appalachian oak and northern hardwood forest. Bituminous coal mines are common, and have caused the siltation and acidification of streams.

Region 8.4.2

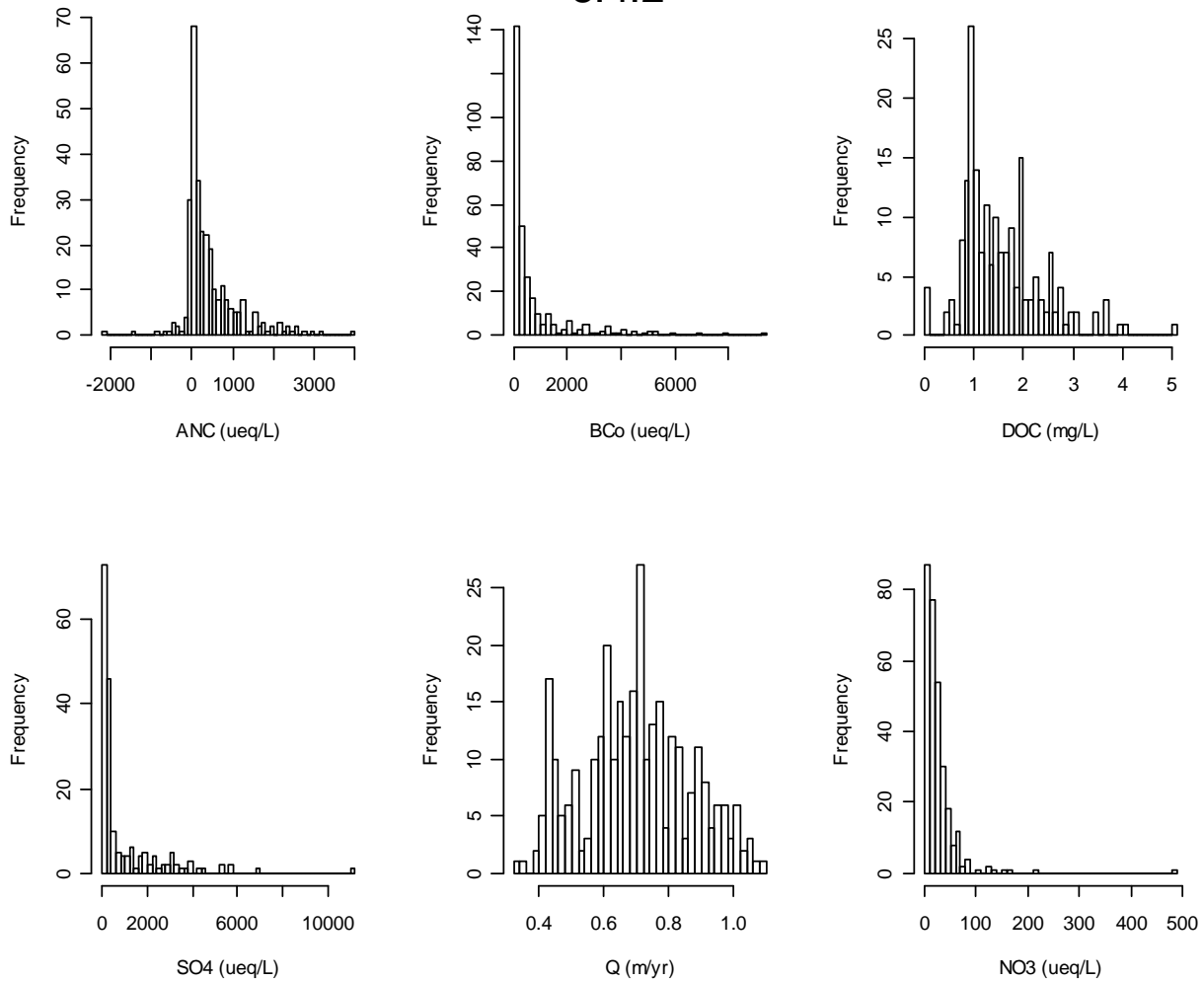


Figure C-51. Region 8.4.2 Water Quality Data Summary

Region 8.4.3 Western Allegheny Plateau

The hilly and wooded terrain of the Western Allegheny Plateau was not muted by glaciation and is more rugged than the agricultural till plains of Ecoregions 8.1.10 and 8.2.4 to the north and west, but is less rugged and not as forested as Ecoregion 8.4.2 to the east and south. Extensive mixed mesophytic forests and mixed oak forests originally grew in the Western Allegheny Plateau and, today, most of its rounded hills remain in forest; dairy, livestock, and general farms as well as residential developments are concentrated in the valleys. Horizontally-bedded sedimentary rock underlying the region has been mined for bituminous coal.

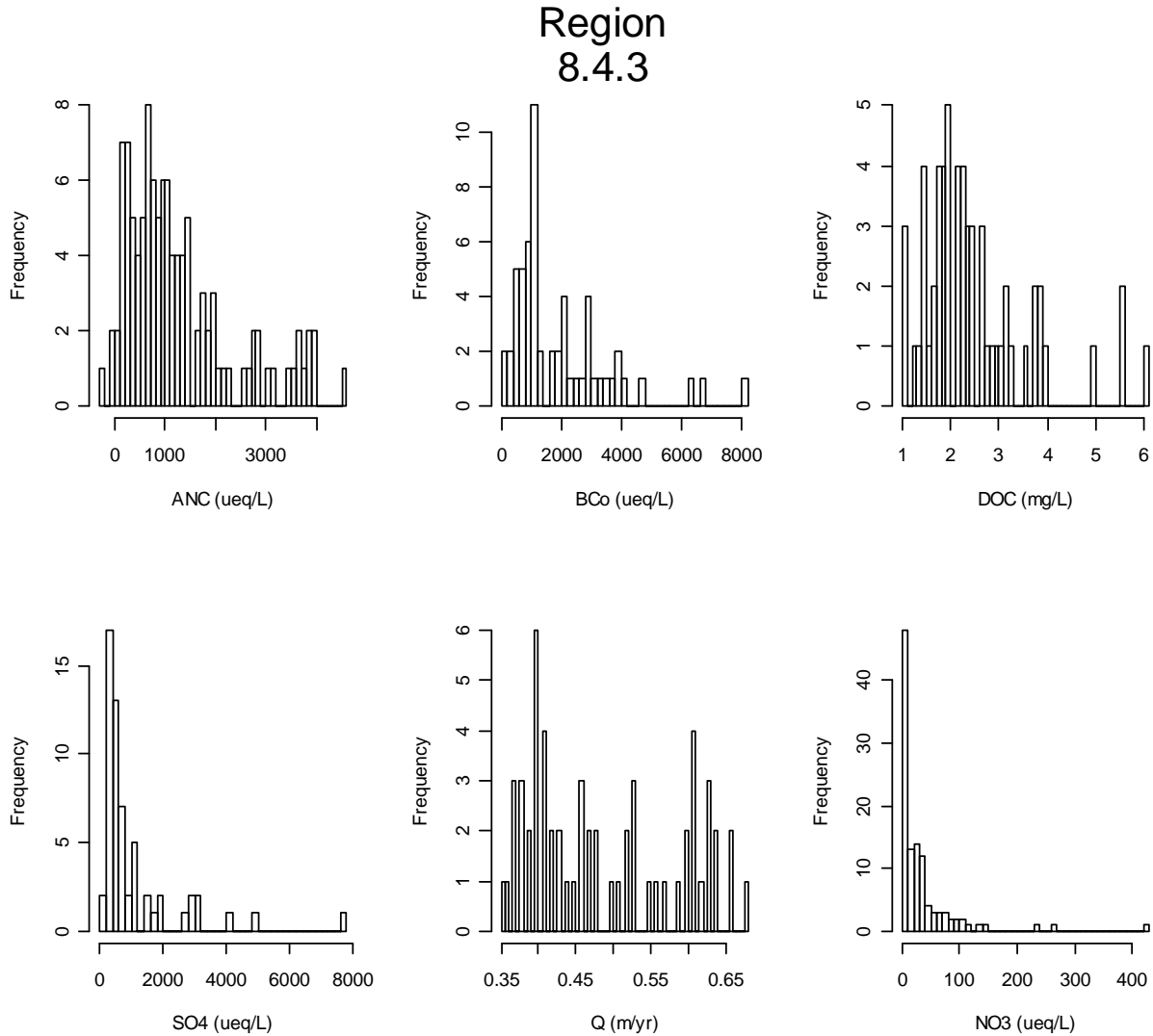


Figure C-52. Region 8.4.3 Water Quality Data Summary

Region 8.4.4 Blue Ridge

The Blue Ridge extends from southern Pennsylvania to northern Georgia, varying from narrow ridges to hilly plateaus to more massive mountainous areas, with high peaks reaching over 6600 feet. The mostly forested slopes, high-gradient, cool, clear streams, and rugged terrain occur primarily on metamorphic rocks, with minor areas of igneous and sedimentary geology. Annual precipitation of over 100 inches can occur in the wettest areas, while dry basins can average as little as 40 inches. The southern Blue Ridge is one of the richest centers of biodiversity in the eastern U.S. It is one of the most floristically diverse ecoregions, and includes Appalachian oak forests, northern hardwoods, and, at the highest elevations, Southeastern spruce-fir forests. Shrub, grass, and heath balds, hemlock, cove hardwoods, and oak-pine communities are also significant.

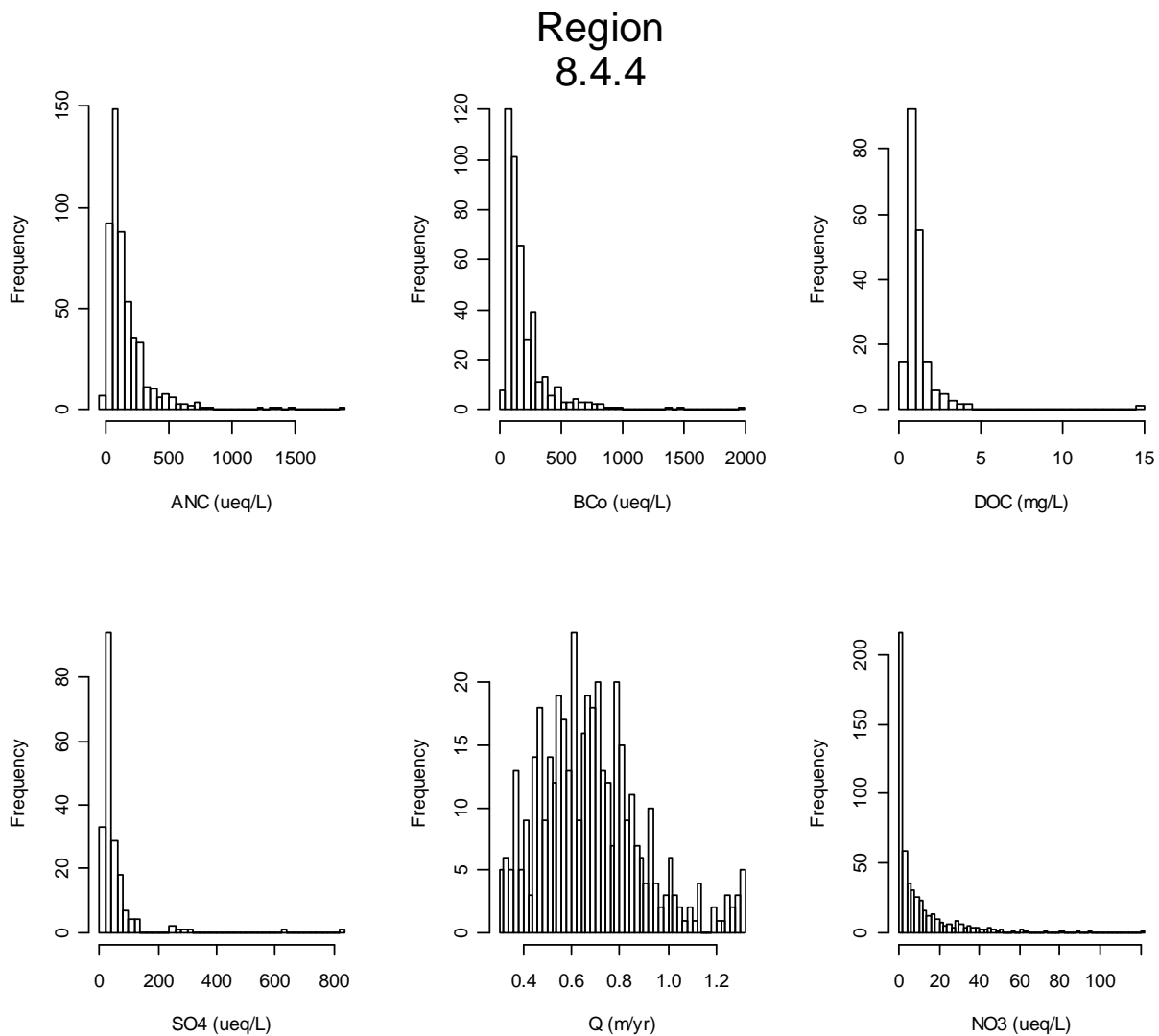


Figure C-53. Region 8.4.4 Water Quality Data Summary

Region 8.4.5 Ozark Highlands

The Ozark Highlands ecoregion has a more irregular physiography and is generally more forested than adjacent regions, with the exception of the Boston Mountains (8.4.6) to the south. Soils are mostly derived from cherty carbonate rocks. Cambrian and Ordovician dolomite and sandstone comprise the dominant bedrock in the interior of the region with Mississippian limestone underlying the western outer regions. Karst features, including caves, springs, and spring-fed streams are found throughout most of the Ozark Highlands. The majority of the region is forested; oak is the predominant forest type but mixed stands of oak and pine are also common, with pine concentrations greatest to the southeast. Less than one fourth of the core of this region has been cleared for pasture and cropland, but half or more of the periphery, while not as agricultural as bordering ecological regions, is in cropland and pasture.

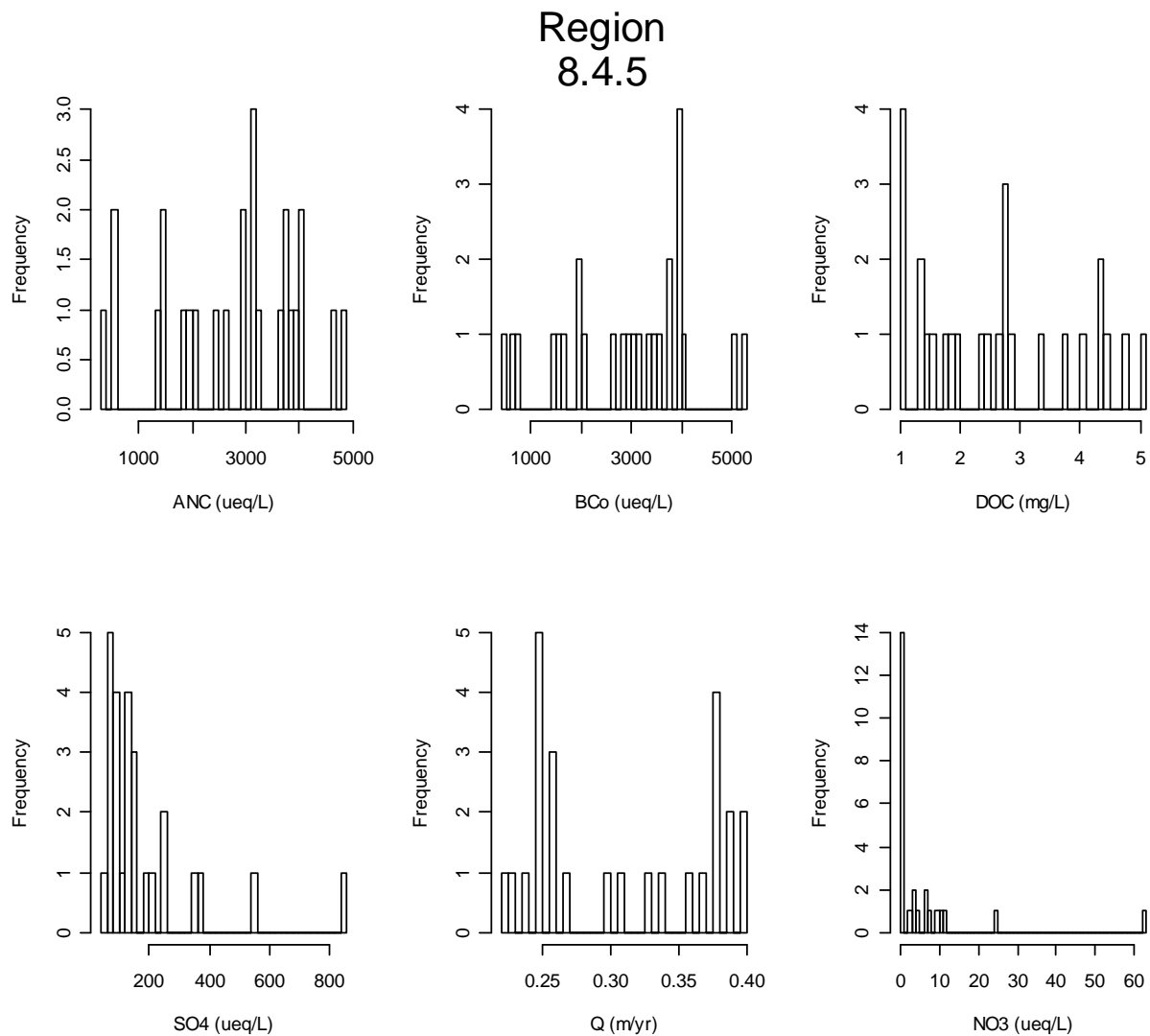


Figure C-54. Region 8.4.5 Water Quality Data Summary

Region 8.4.6 Boston Mountains

In contrast to the nearby Ouachita Mountains (8.4.8) region which comprises folded and faulted linear ridges mostly covered by pine forests, the Boston Mountains ecological region consists of a deeply dissected sandstone and shale plateau, originally covered by oak-hickory forests. Red oak, white oak, and hickory remain the dominant vegetation types in this region, although shortleaf pine and eastern red cedar are found in many of the lower areas and on some south- and west-facing slopes. The region is sparsely populated and recreation is a principal land use.

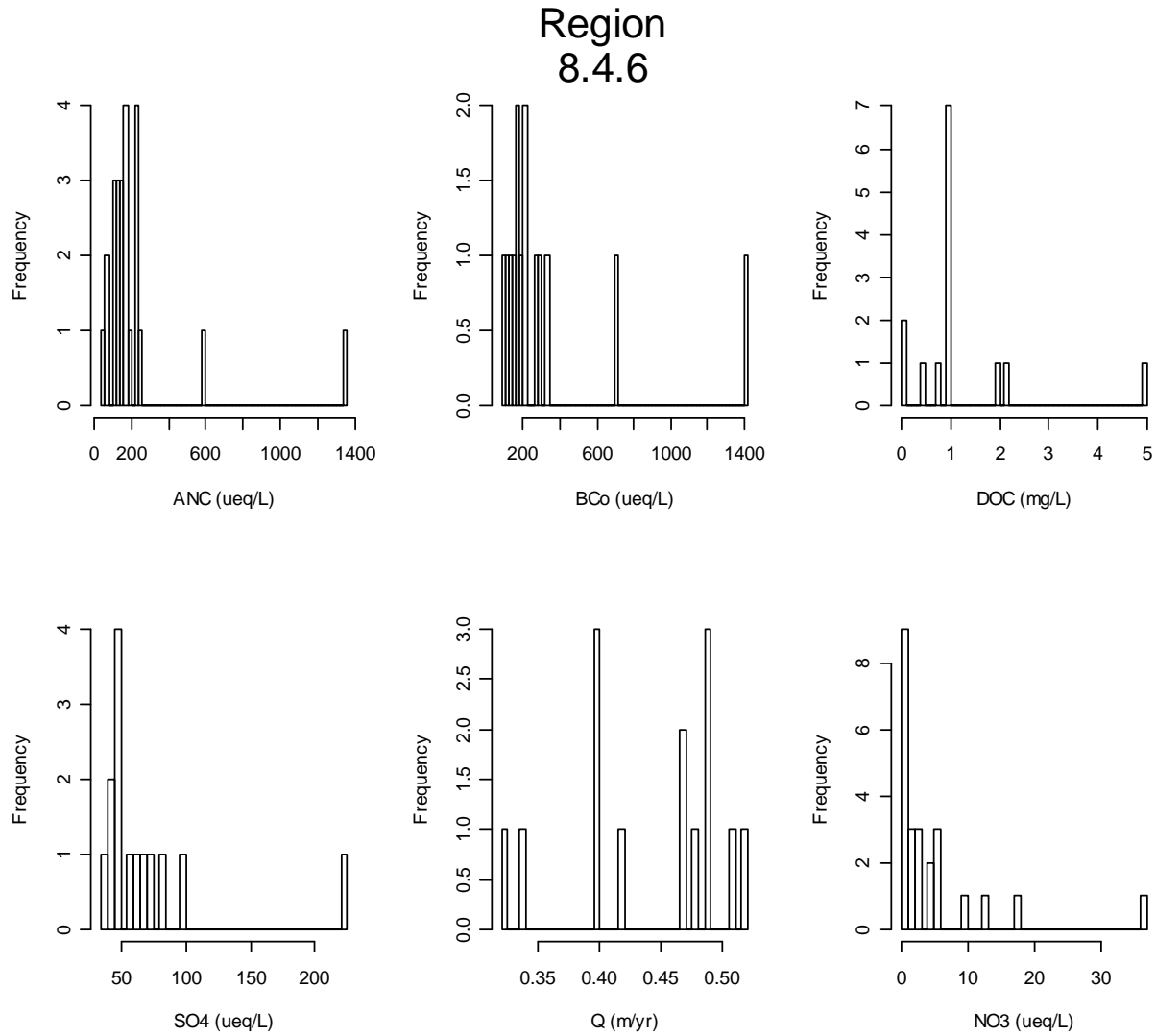


Figure C-55. Region 8.4.6 Water Quality Data Summary

Region 8.4.7 Arkansas Valley

A region of mostly forested valleys and ridges, the physiography of the Arkansas Valley is much less irregular than that of the Boston Mountains (8.4.6) to the north and the Ouachita Mountains (8.4.8) to the south, but is more irregular than the ecological regions to the west and east. About one fourth of the region is grazed and roughly one tenth is cropland. In the Arkansas Valley, even streams that have been relatively unimpacted by human activities have considerably lower dissolved oxygen levels, and hence support different biological communities, than those of most of the adjacent regions.

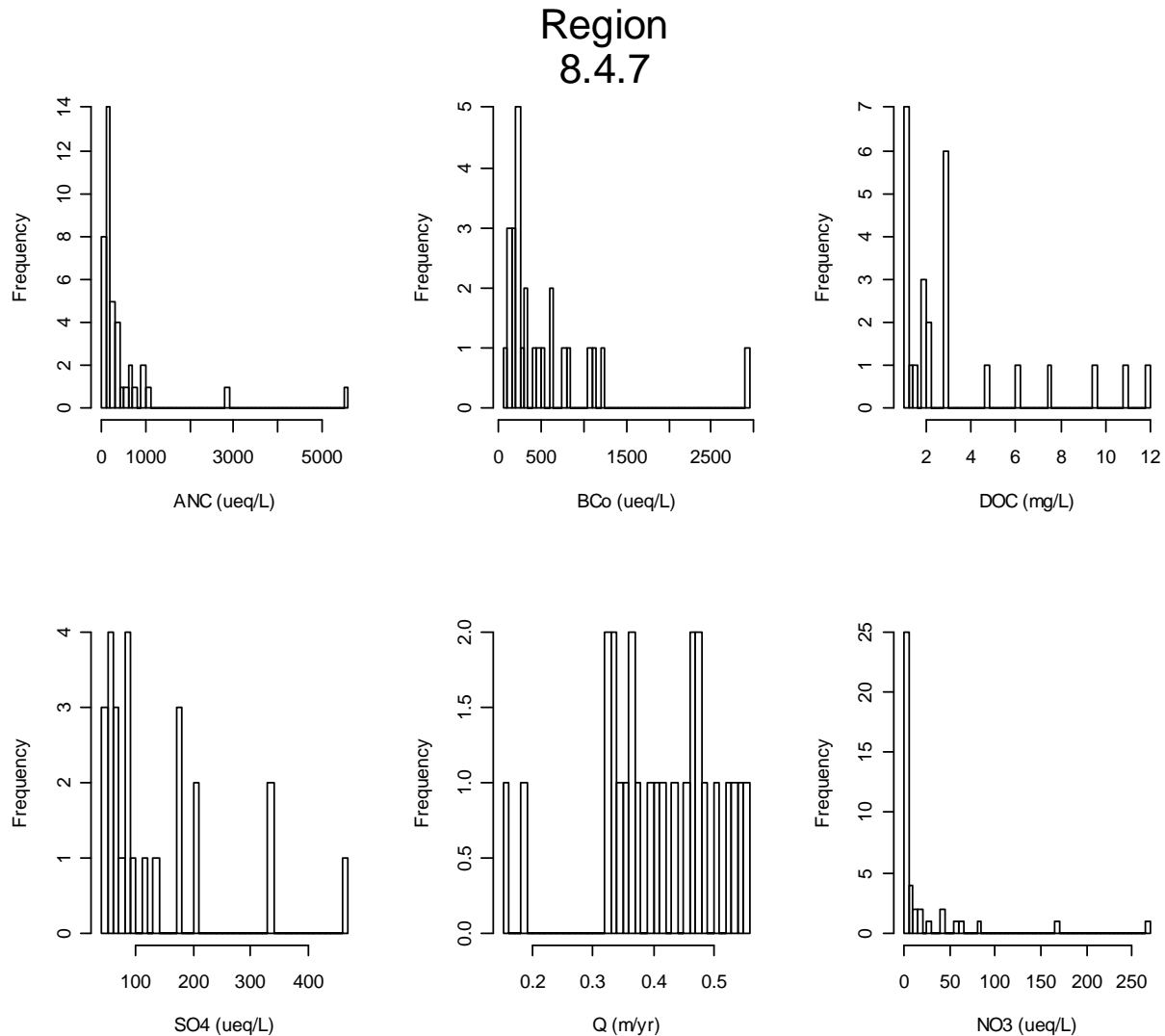


Figure C-56. Region 8.4.7 Water Quality Data Summary

Region 8.4.8 Ouchita Mountains

The Ouachita Mountains ecological region is made up of sharply defined east-west trending ridges, formed through erosion of compressed sedimentary rock formations. The Ouachitas are structurally different from the Boston Mountains (8.4.6), more folded and rugged than the lithologically distinct Ozark Highlands (8.4.5), and physiographically unlike the Arkansas Valley (8.4.7), South Central Plains (8.3.7), and Mississippi Alluvial Plain (8.5.2). Potential natural vegetation is oak-hickory-pine forest, which contrasts with the oak-hickory forest that dominates Ecoregion 8.4.5 and the northern part of the Boston Mountains (8.4.6). Most of this region is now in loblolly and shortleaf pine. Commercial logging is the major land use in the region.

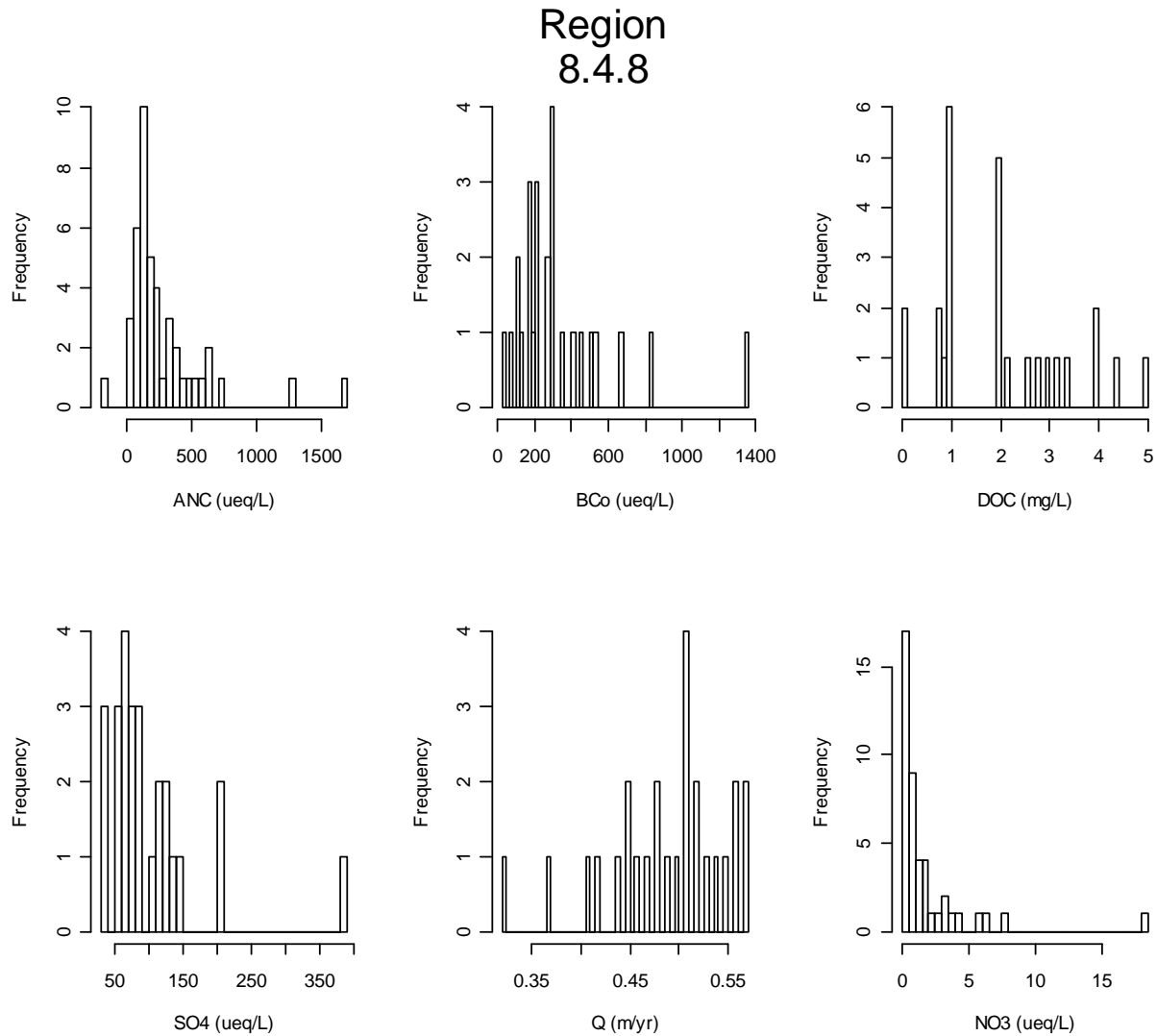


Figure C-57. Region 8.4.8 Water Quality Data Summary

Region 8.4.9 Southwestern Appalachians

Stretching from Kentucky to Alabama, these open low mountains contain a mosaic of forest and woodland with some cropland and pasture. The eastern boundary of the ecoregion, along the more abrupt escarpment where it meets the Ridge and Valley (8.4.1), is relatively smooth and only slightly notched by small, eastward flowing streams. Much of the western boundary, next to the Interior Plateau (8.3.3), is more crenulated, with a rougher escarpment that is more deeply incised. The mixed mesophytic forest is restricted mostly to the deeper ravines and escarpment slopes, and the upland forests are dominated by mixed oaks with shortleaf pine. Ecoregion 8.4.9 has less agriculture than the adjacent Ecoregion 8.3.3. Coal mining occurs in several parts of the region.

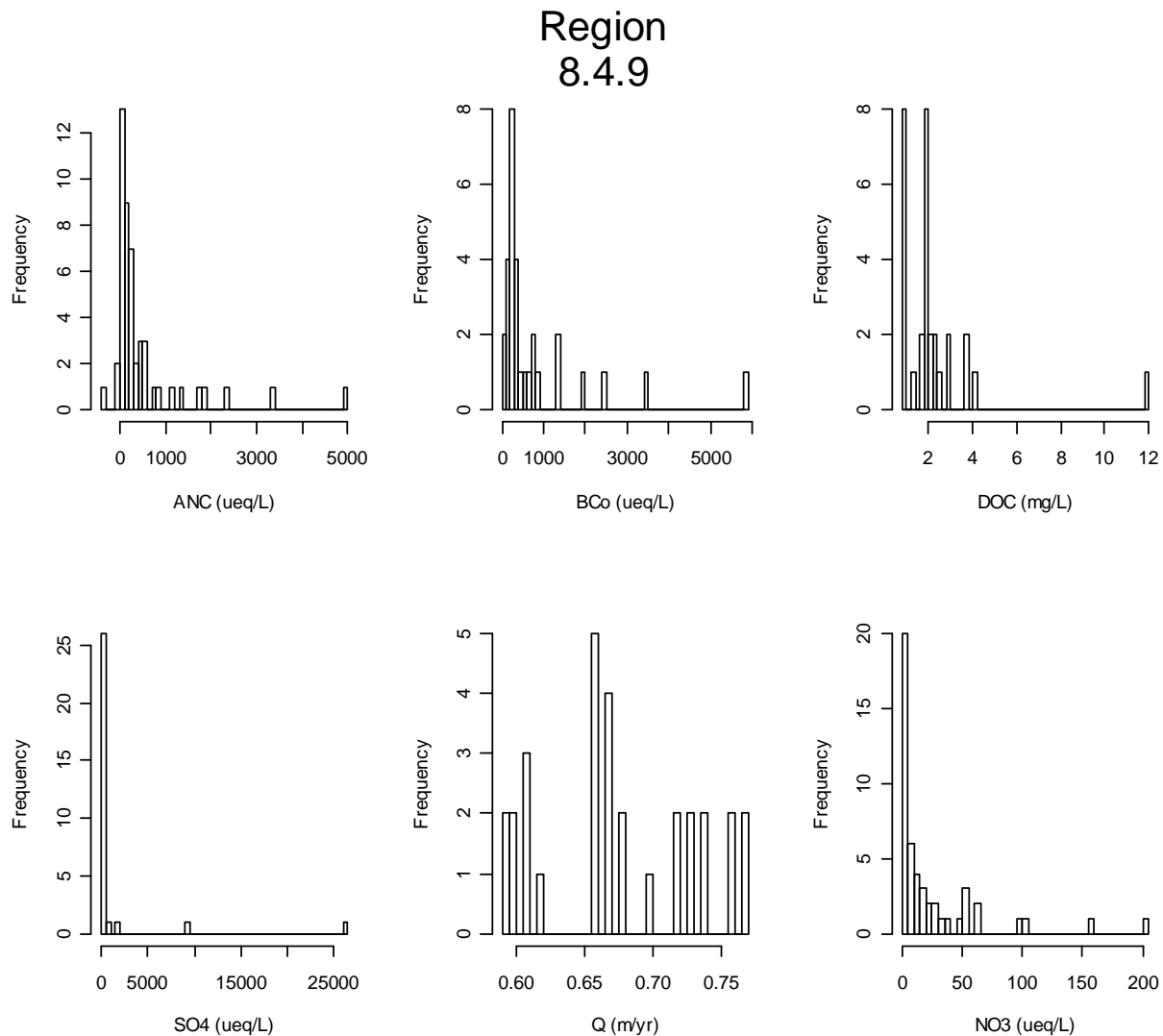


Figure C-58. Region 8.4.9 Water Quality Data Summary

Region 8.5 Mississippi Alluvial and Southeastern USA Coastal Plains

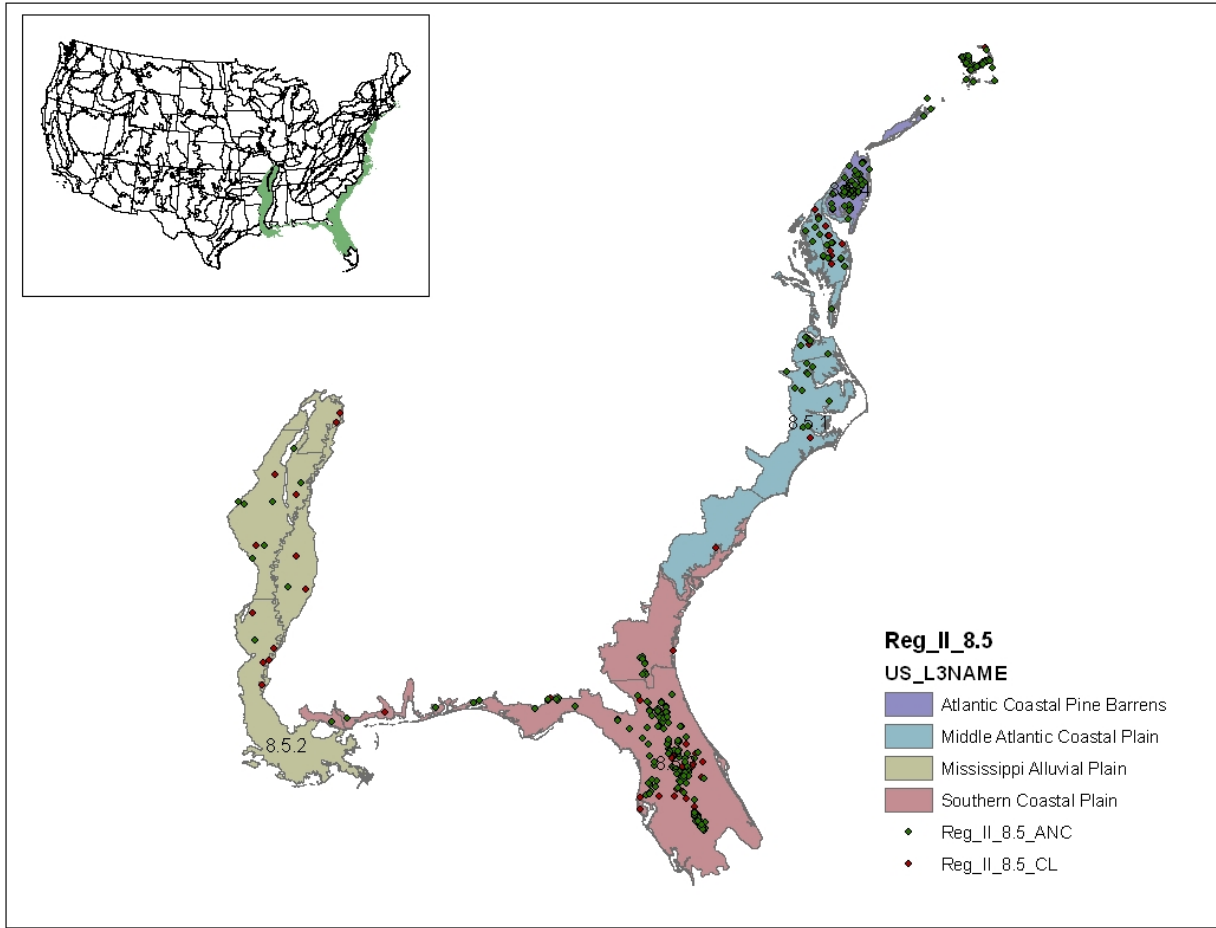


Figure C-59. Region 8.5

Region 8.5.1 Middle Atlantic Coastal Plain

The Middle Atlantic Coastal Plain ecoregion stretches from Delaware to the South Carolina/Georgia border and consists of low elevation flat plains, with many swamps, marshes, and estuaries. Forest cover in the region, once dominated by longleaf pine in the Carolinas, is now mostly loblolly and some shortleaf pine, with patches of oak, gum, and cypress near major streams, as compared to the mainly longleaf-slash pine forests of the warmer Southern Coastal Plain (8.5.3). Its low terraces, marshes, dunes, barrier islands, and beaches are underlain by unconsolidated sediments. Poorly drained soils are common, and the region has a mix of coarse and finer textured soils compared to the mostly coarse soils in the majority of Ecoregion 8.5.3. The Middle Atlantic Coastal Plain is typically lower, flatter, more poorly drained, and more marshy than Ecoregion 8.3.5. Less cropland occurs in the southern portion of the region than in the central and northern parts.

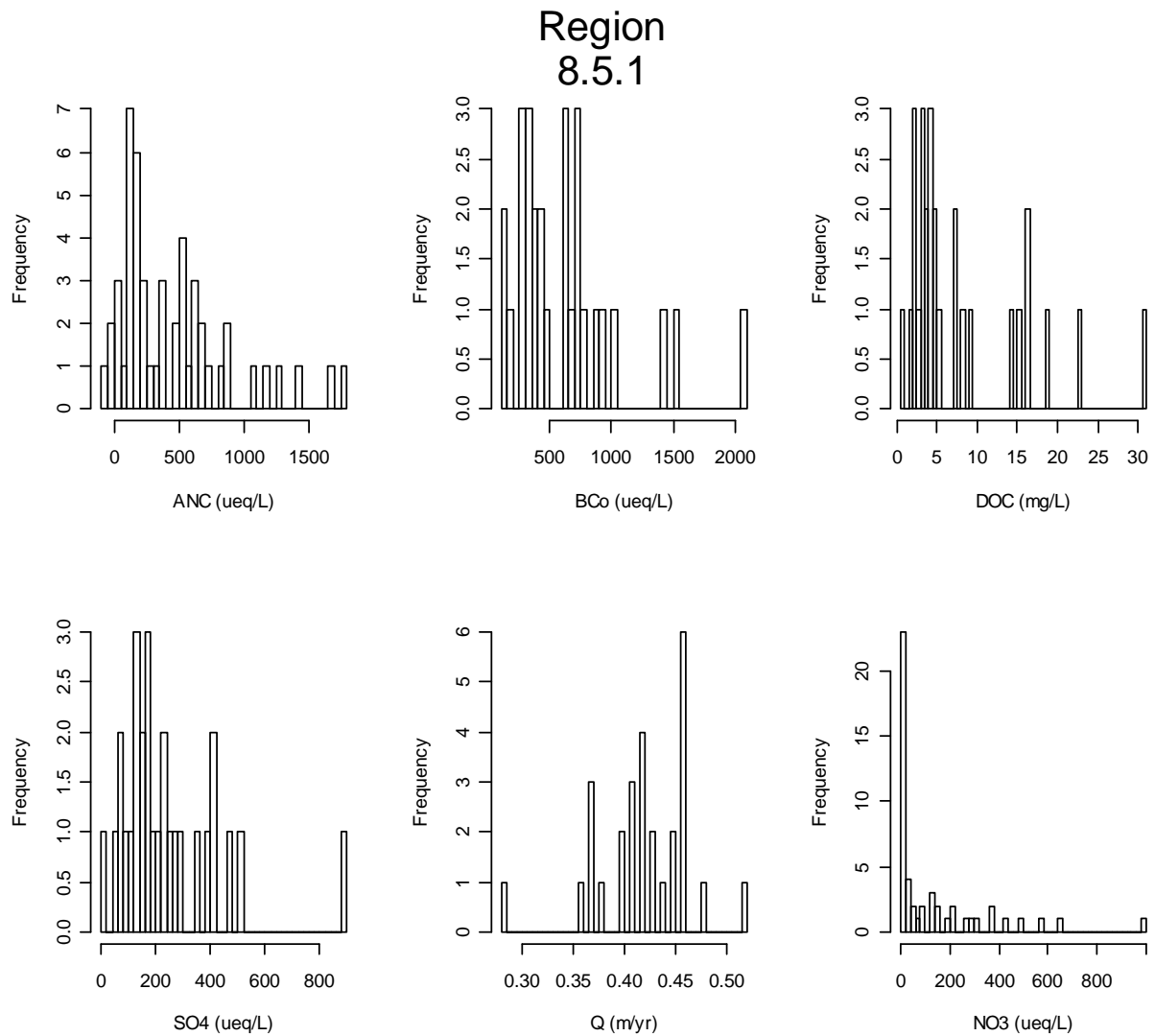


Figure C-60. Region 8.5.1 Water Quality Data Summary

Region 8.5.2 Mississippi Alluvial Plain

This riverine ecoregion extends from southern Illinois, at the confluence of the Ohio River with the Mississippi River, south to the Gulf of Mexico. It is mostly a broad, flat alluvial plain with river terraces, swales, and levees providing the main elements of relief. Soils are typically finer-textured and more poorly drained than the upland soils of adjacent Ecoregions 8.3.7 and 8.3.6, although there are some areas of coarser, better-drained soils. Winters are mild and summers are hot, with temperatures and precipitation increasing from north to south. Bottomland deciduous forest vegetation covered the region before much of it was cleared for cultivation. Presently, most of the northern and central parts of the region are in cropland and receive heavy treatments of insecticides and herbicides. Soybeans, cotton, and rice are the major crops.

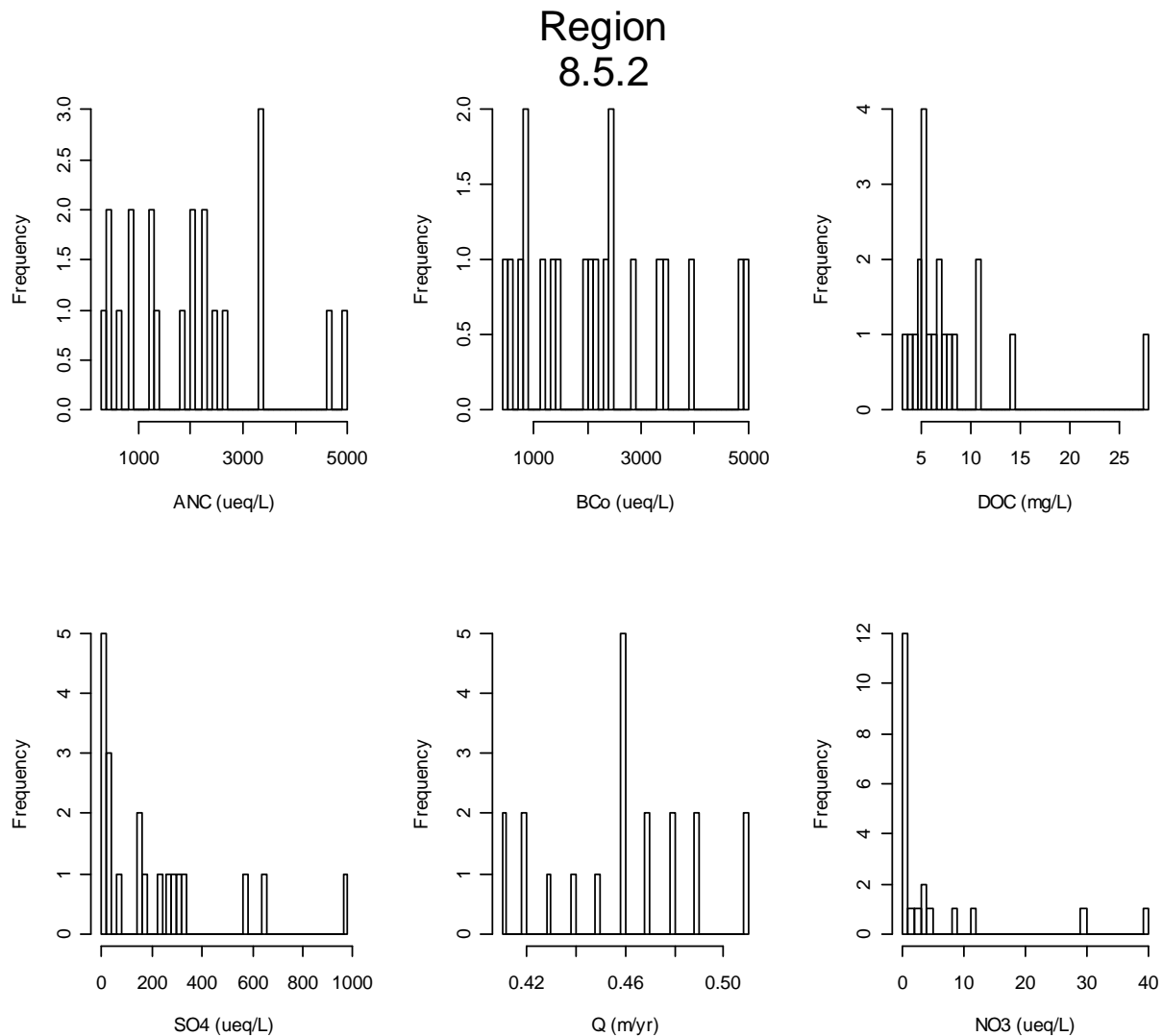


Figure C-61. Region 8.5.2 Water Quality Data Summary

Region 8.5.3 Southern Coastal Plains

The Southern Coastal Plain consists of mostly flat plains, but it is a heterogeneous region containing barrier islands, coastal lagoons, marshes, and swampy lowlands along the Gulf and Atlantic coasts. In Florida, an area of discontinuous highlands contains numerous lakes. This ecoregion is lower in elevation with less relief and wetter soils than the Southeastern Plains (8.3.5). It is warmer, more heterogeneous, and has a longer growing season and coarser textured soils than the Middle Atlantic Coastal Plain (8.5.1). Once covered by a variety of forest communities that included trees of longleaf pine, slash pine, pond pine, beech, sweetgum, southern magnolia, white oak, and laurel oak, land cover in the region is now mostly slash and loblolly pine with oak-gum-cypress forest in some low lying areas, citrus groves in Florida, pasture for beef cattle, and urban.

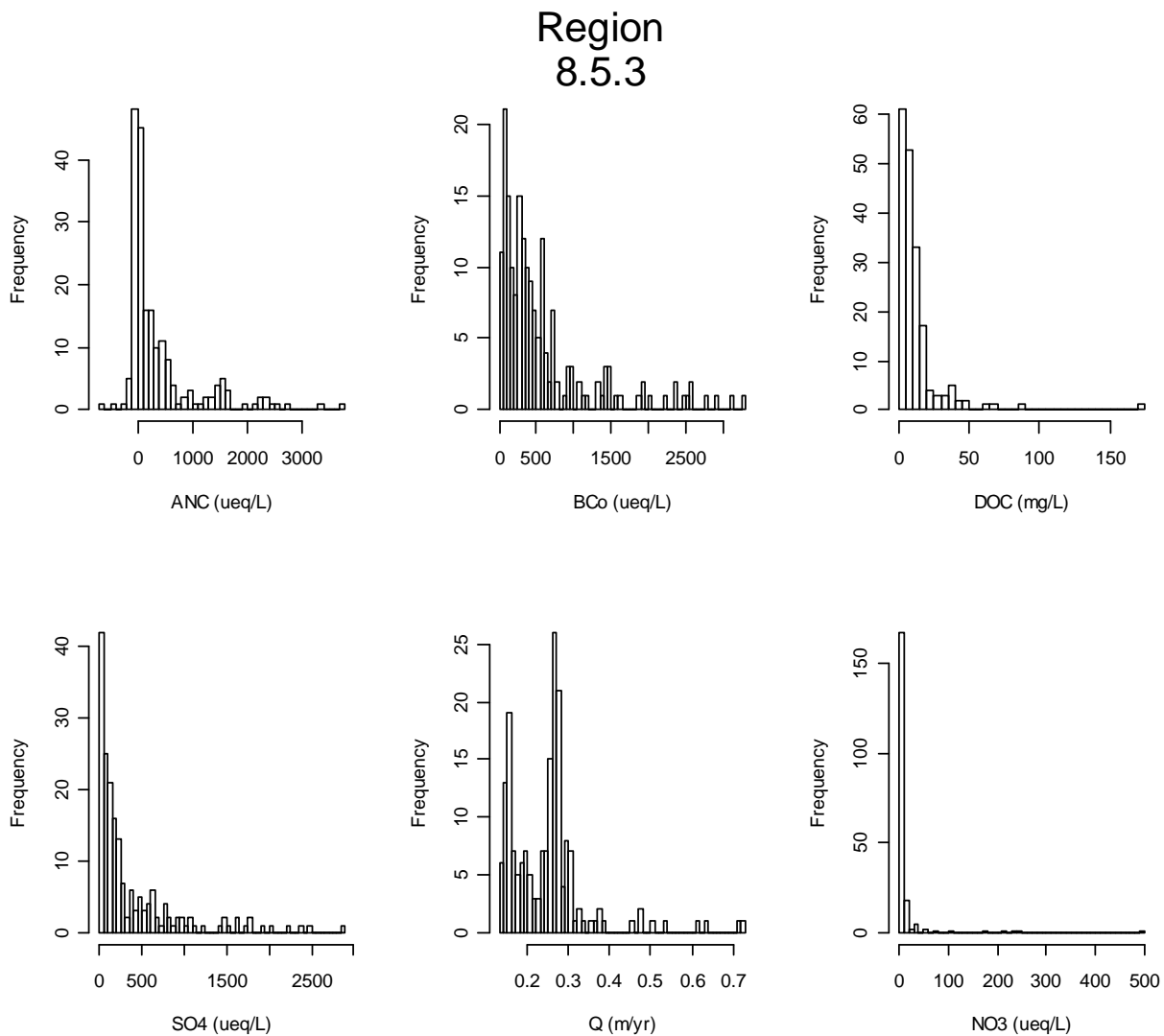


Figure C-62. Region 8.5.3 Water Quality Data Summary

Region 8.5.4 Atlantic Coastal Pine Barrens

This is a transitional ecoregion, distinguished from the coastal ecoregion (8.5.1) to the south by its coarser-grained soils, cooler climate, and Northeastern oak-pine potential natural vegetation. The climate is milder than the coastal ecoregion (8.1.7) to the north that contains Appalachian oak forests and some northern hardwoods forests. The physiography of this ecoregion is not as flat as that of the Middle Atlantic Coastal Plain (8.5.1), but it is not as irregular as that of the Northeastern Coastal Zone (8.1.7). The shore characteristics of sandy beaches, grassy dunes, bays, marshes, and scrubby oak-pine forests are more like those to the south, in contrast to the more rocky, jagged, forested coastline found to the north.

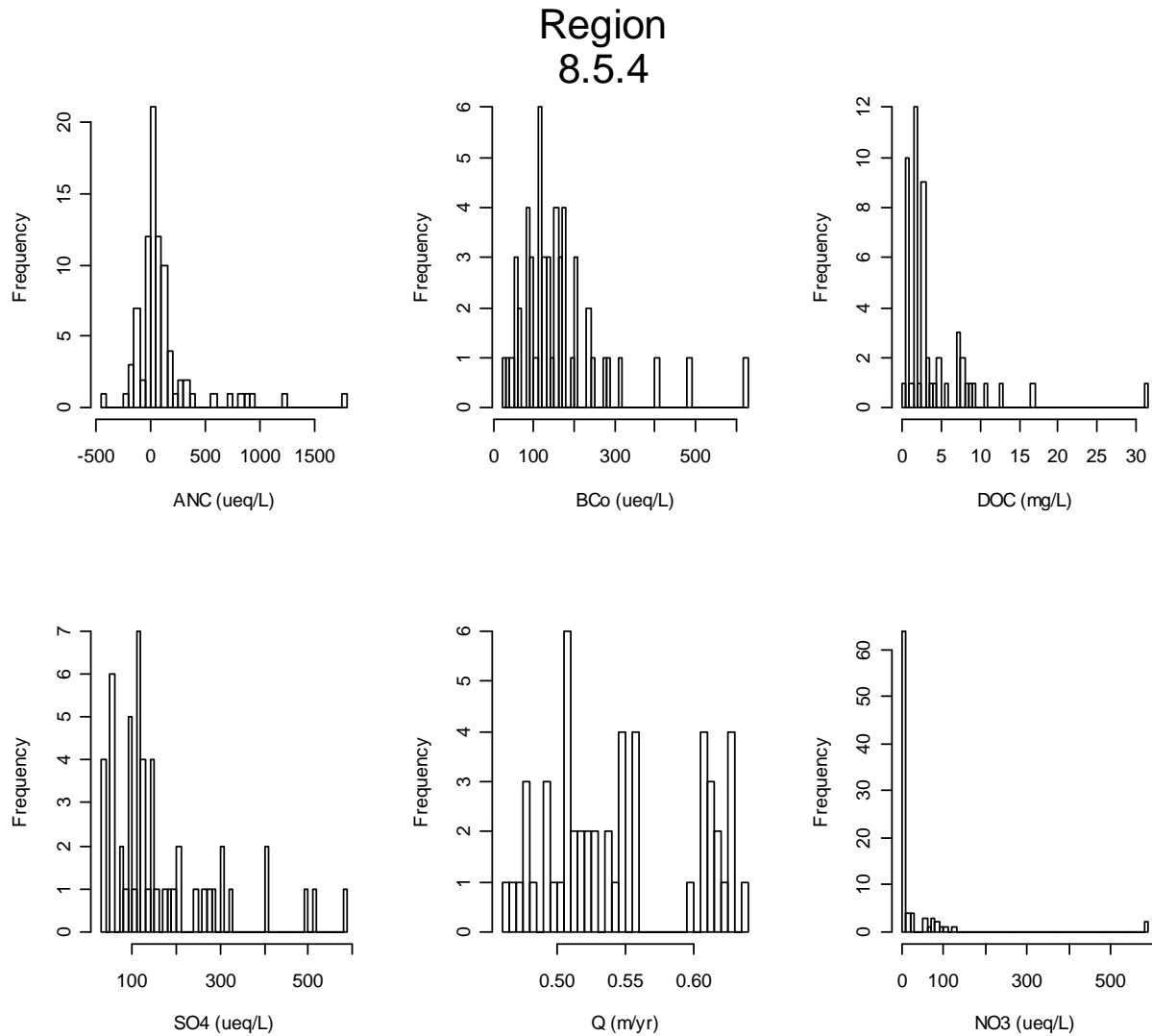


Figure C-63. Region 8.5.4 Water Quality Data Summary

Region 9.2 Temperate Prairies

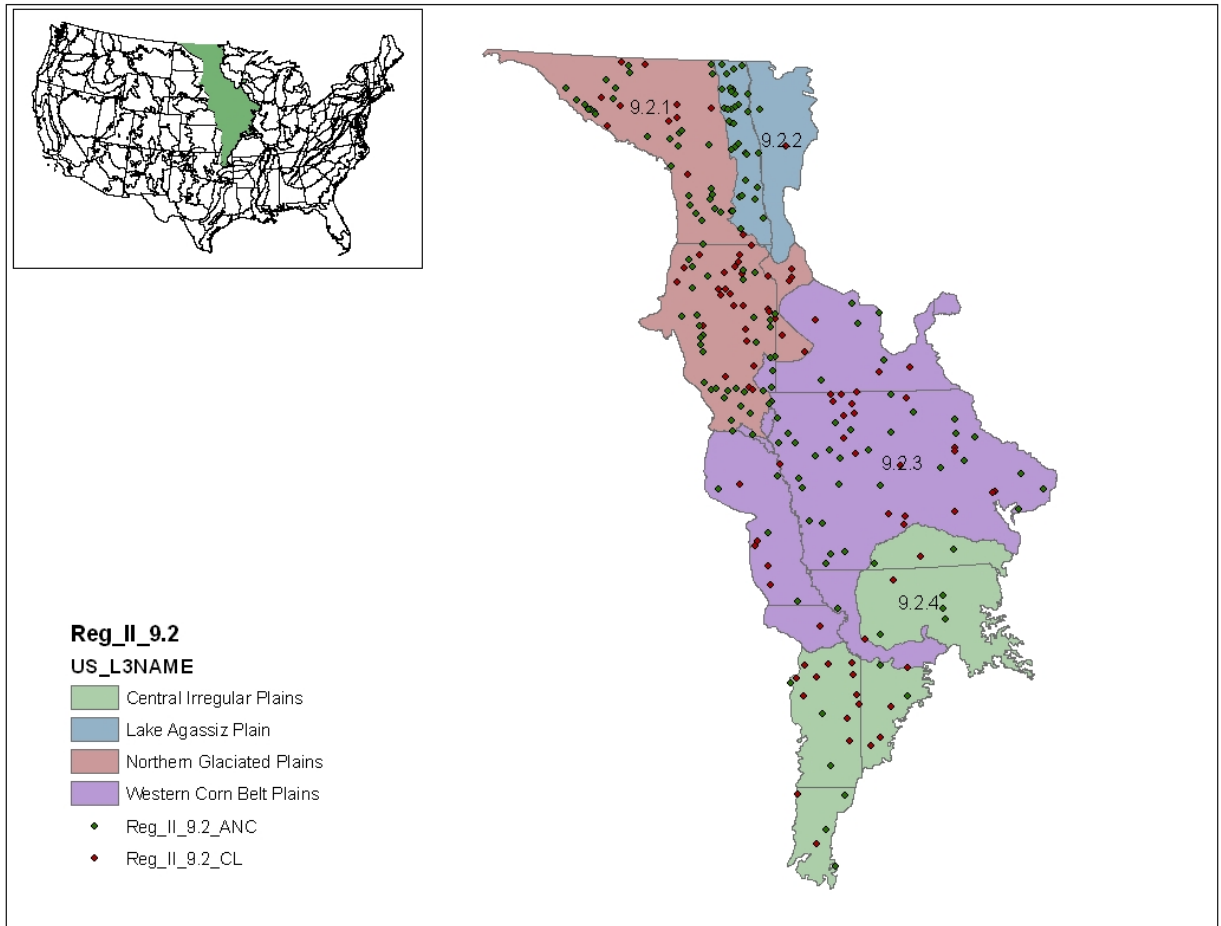


Figure C-64. Region 9.2

Region 9.2.1 Northern Glaciated Plains

The Northern Glaciated Plains ecoregion is characterized by a flat to gently rolling landscape composed of glacial drift. The subhumid conditions foster a grassland transitional between tall and shortgrass prairie. High concentrations of temporary and seasonal wetlands create favorable conditions for waterfowl nesting and migration. Although the till soils are very fertile, agricultural success is subject to annual climatic fluctuations.

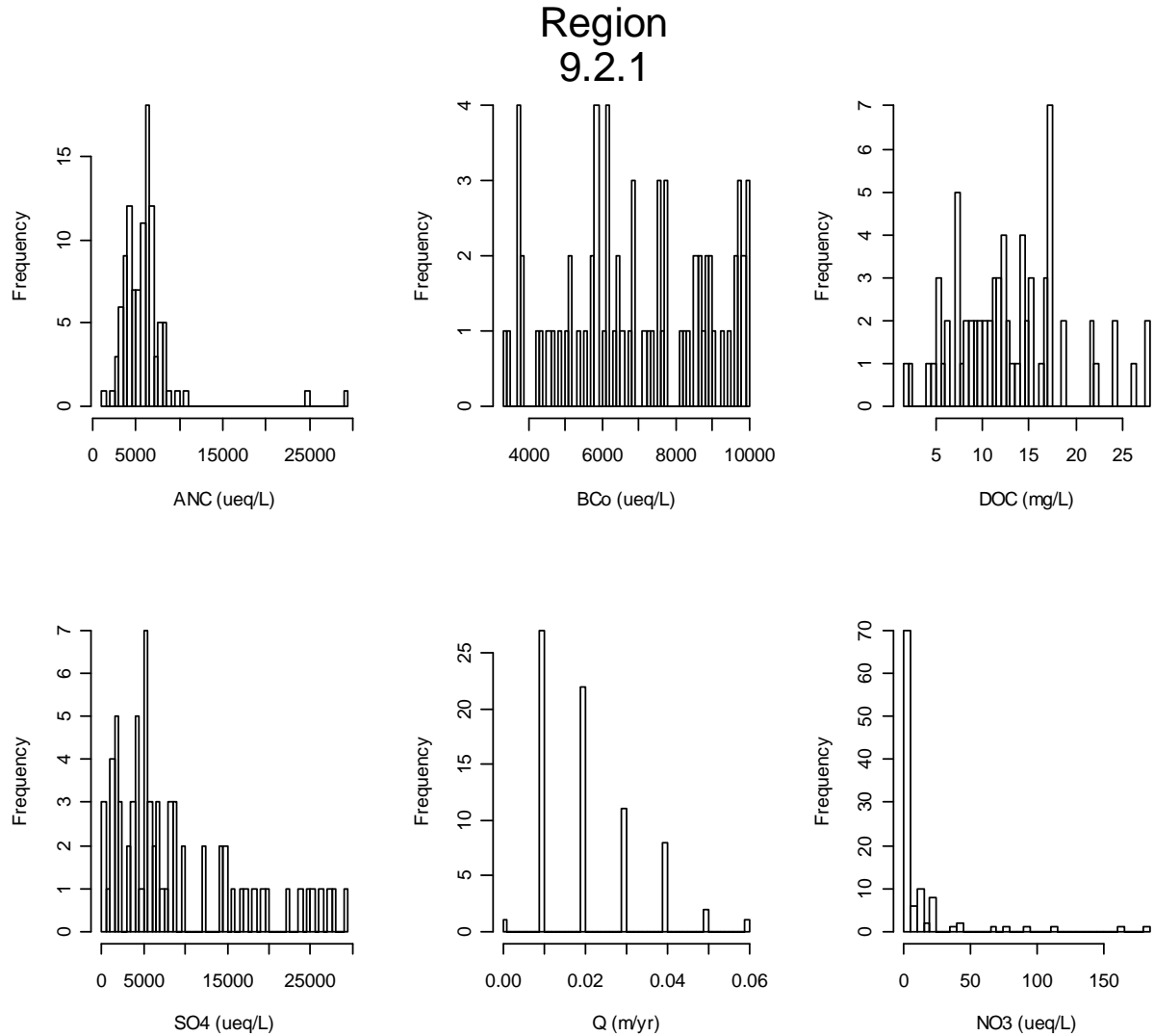


Figure C-65. Region 9.2.1 Water Quality Data Summary

Region 9.2.2 Lake Agassiz Plains

Glacial Lake Agassiz was the last in a series of proglacial lakes to fill the Red River valley in the three million years since the beginning of the Pleistocene. Thick beds of lake sediments on top of glacial till create the extremely flat floor of the Lake Agassiz Plain. The historic tallgrass prairie has been replaced by intensive row crop agriculture. The preferred crops in the northern half of the region are potatoes, beans, sugar beets, and wheat; soybeans, sugar beets, and corn predominate in the south.

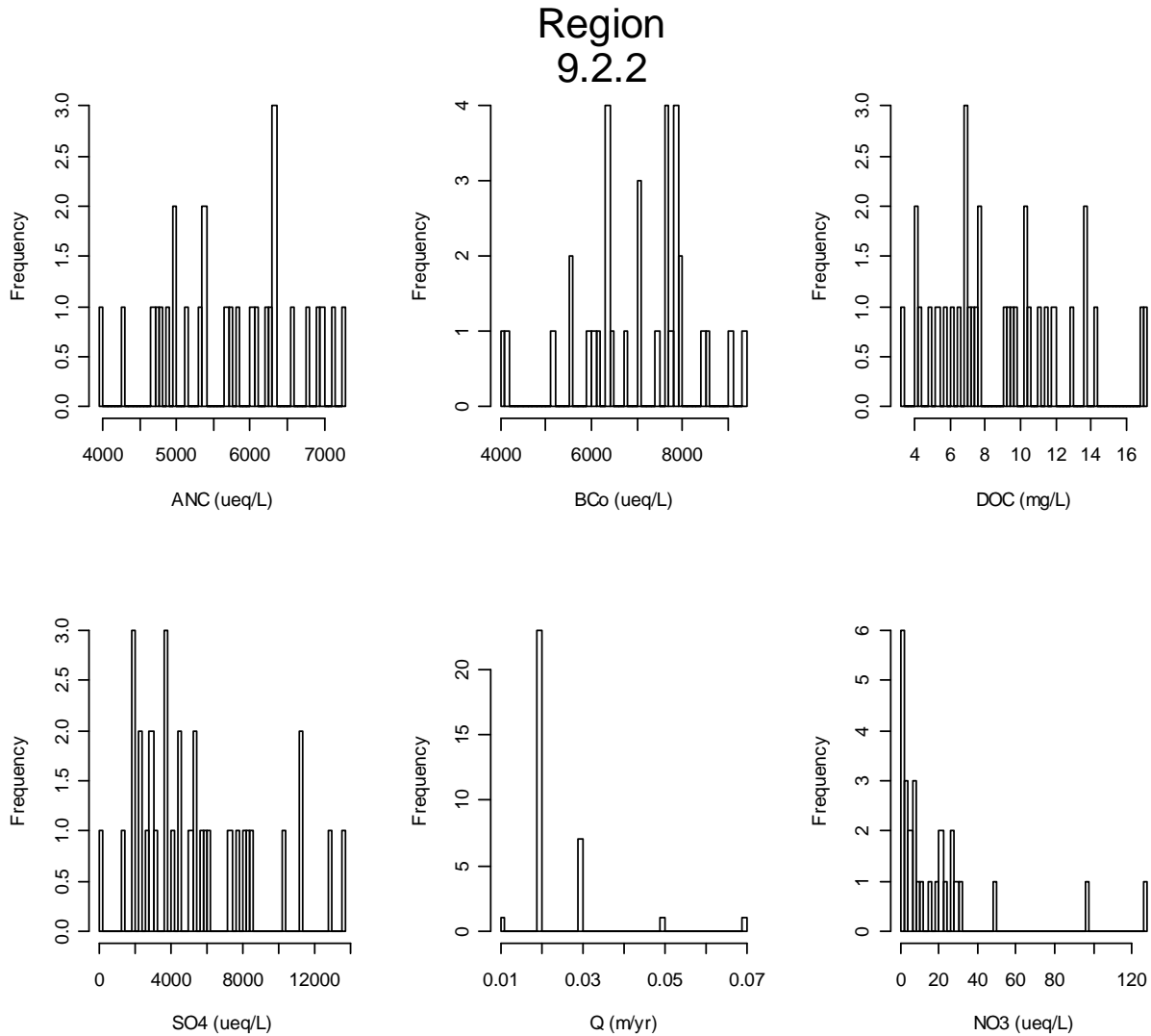


Figure C-66. Region 9.2.2 Water Quality Data Summary

Region 9.2.3 Western Corn Belt Plains

Once mostly covered with tallgrass prairie, over 80 percent of the Western Corn Belt Plains is now used for cropland agriculture and much of the remainder is in forage for livestock. A combination of nearly level to gently rolling glaciated till plains and hilly loess plains, an average annual precipitation of 26 to 37 inches, which occurs mainly in the growing season, and fertile, warm, moist soils make this one of the most productive areas of corn and soybeans in the world. Agricultural practices have contributed to environmental issues, including surface and groundwater contamination from fertilizer and pesticide applications as well as concentrated livestock production.

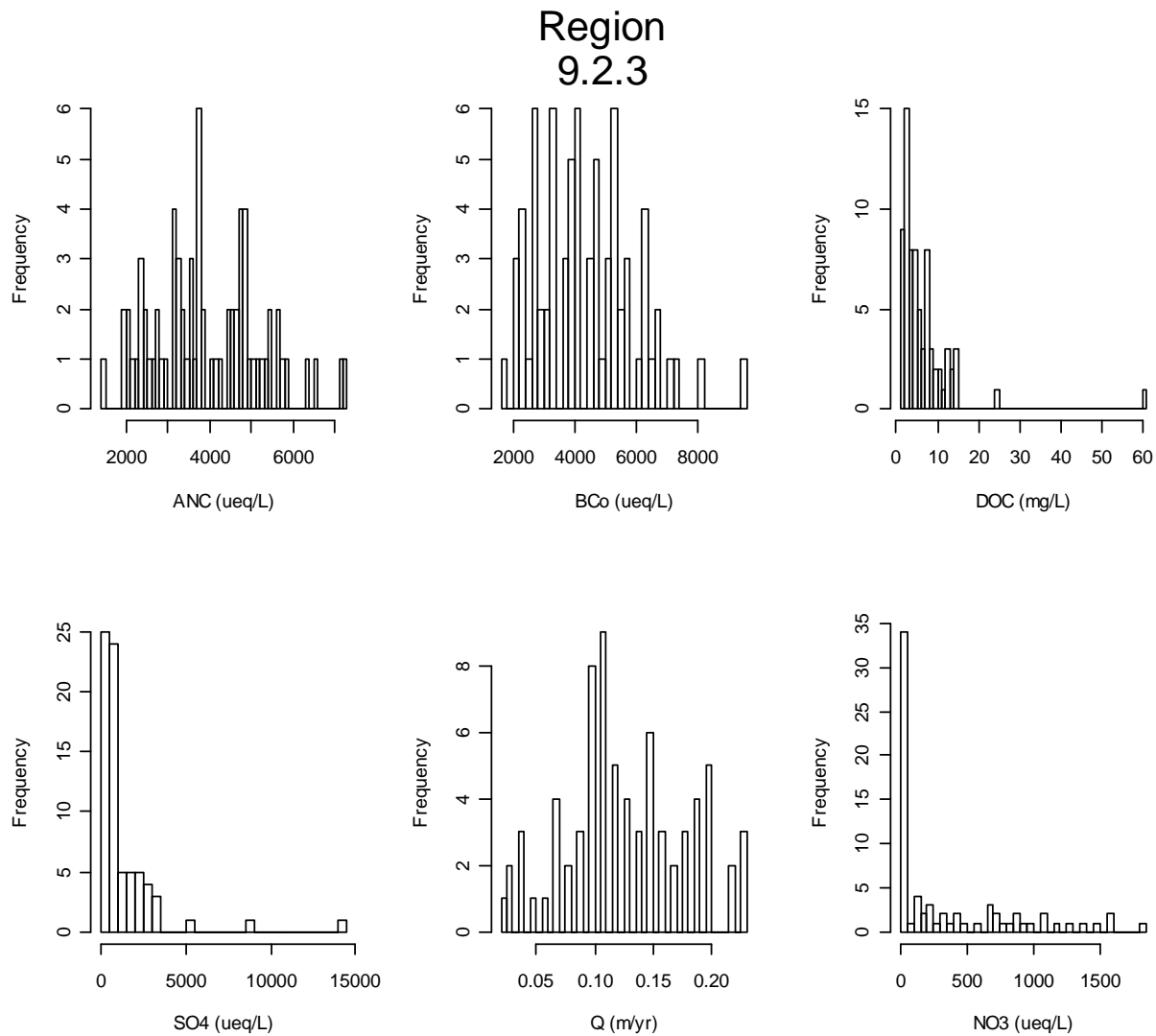


Figure C-67. Region 9.2.3 Water Quality Data Summary

Region 9.2.4 Central Irregular Plains

The Central Irregular Plains have a mix of land use and are topographically more irregular than the Western Corn Belt Plains (9.2.3) to the north, where most of the land is in crops. The region, however, is less irregular and less forest covered than the ecoregions to the south and east. The potential natural vegetation of this ecological region is a grassland/forest mosaic with wider forested strips along the streams compared to Ecoregion 9.2.3 to the north. The mix of land use activities in the Central Irregular Plains includes mining operations of high-sulfur bituminous coal. The disturbance of these coal strata in southern Iowa and northern Missouri has degraded water quality and affected aquatic biota.

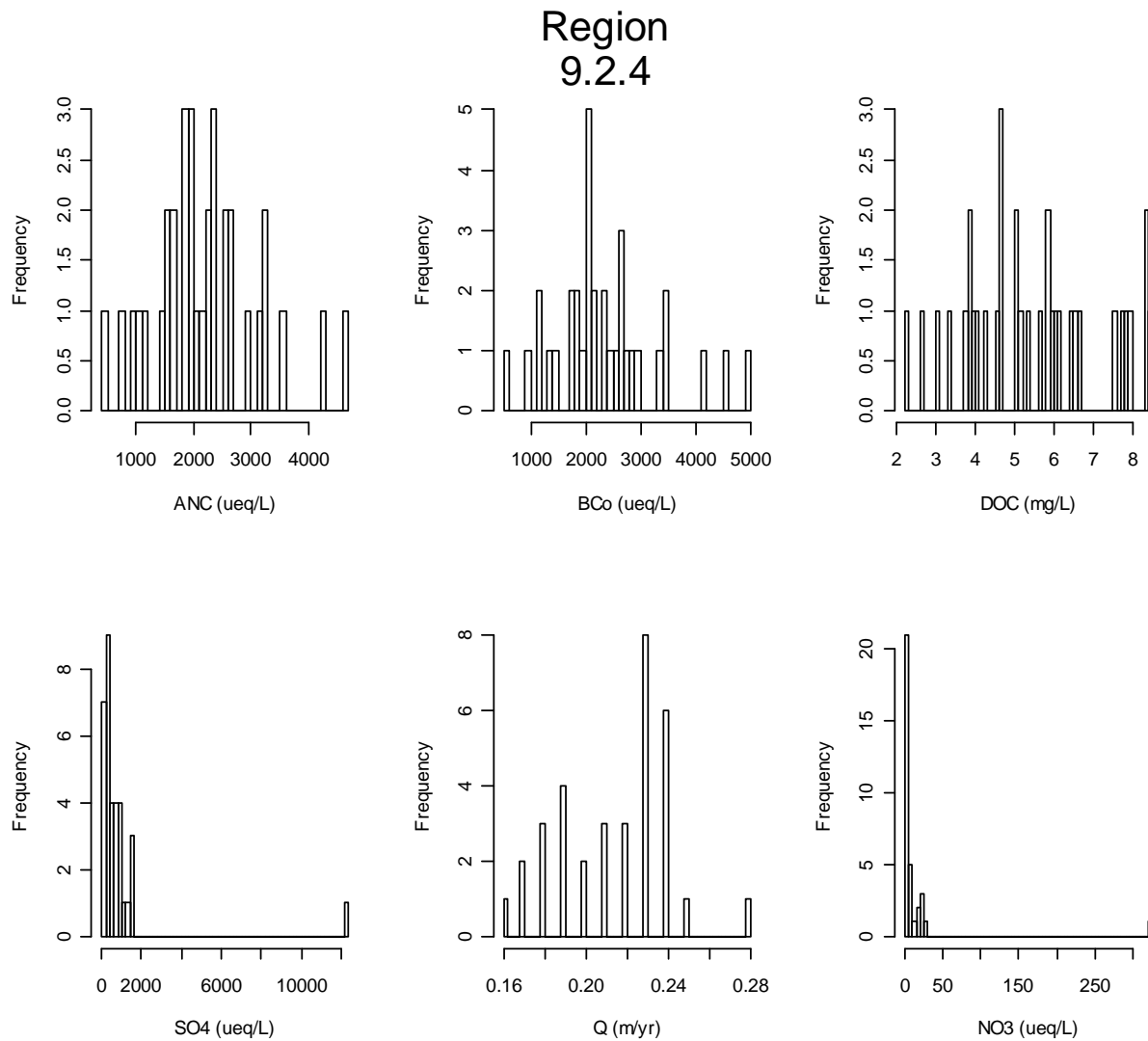


Figure C-68. Region 9.2.4 Water Quality Data Summary

Region 9.3 West-Central Semi-Arid Prairies

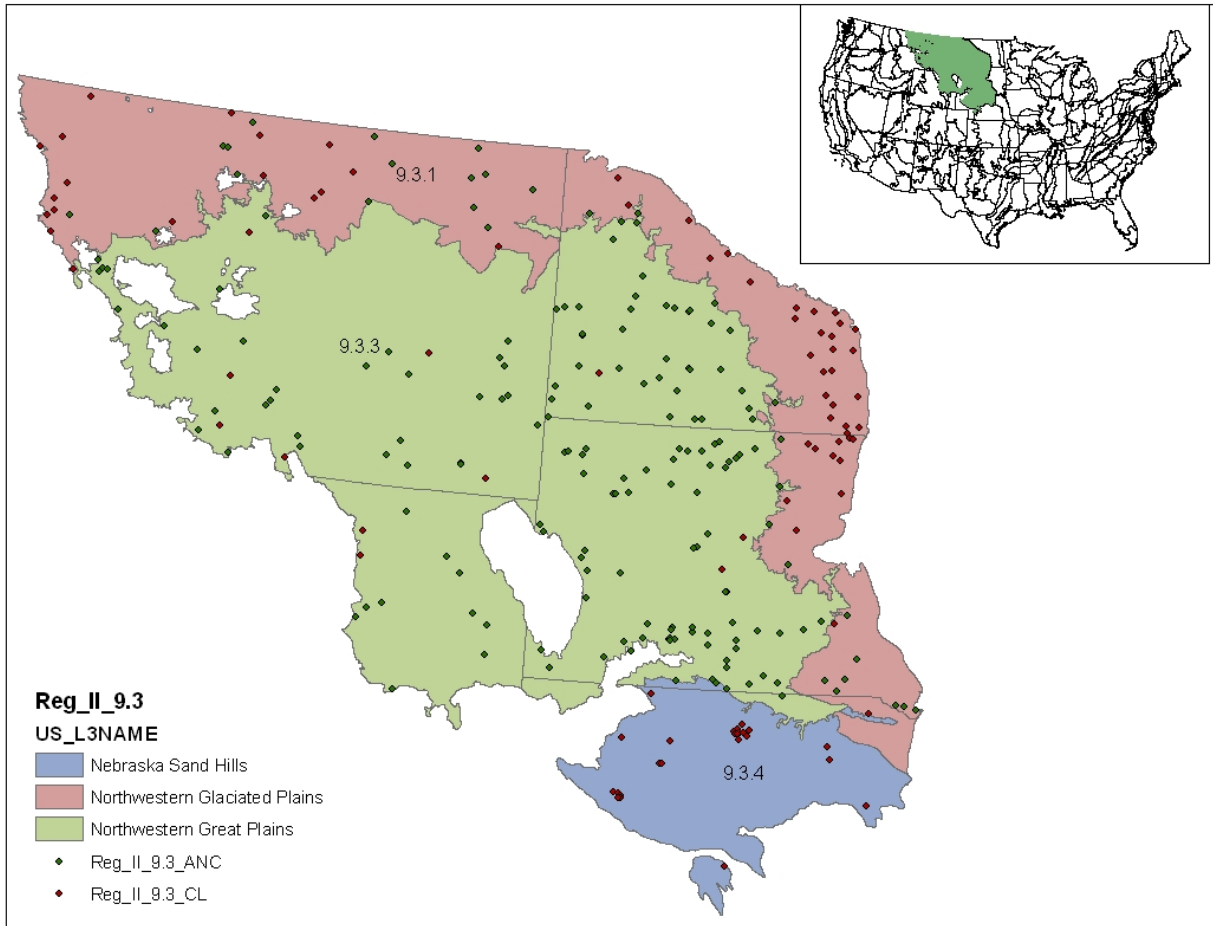


Figure C-69. Region 9.3

Region 9.3.1 Northwestern Glaciated Plains

The Northwestern Glaciated Plains ecoregion is a transitional region between the generally more level, moister, more agricultural Northern Glaciated Plains (9.2.1) to the east and the generally more irregular, dryer, Northwestern Great Plains (9.3.3) to the west and southwest. The western and southwestern boundary roughly coincides with the limits of continental glaciation. Pocking this ecoregion is a moderately high concentration of semi-permanent and seasonal wetlands, locally referred to as Prairie Potholes.

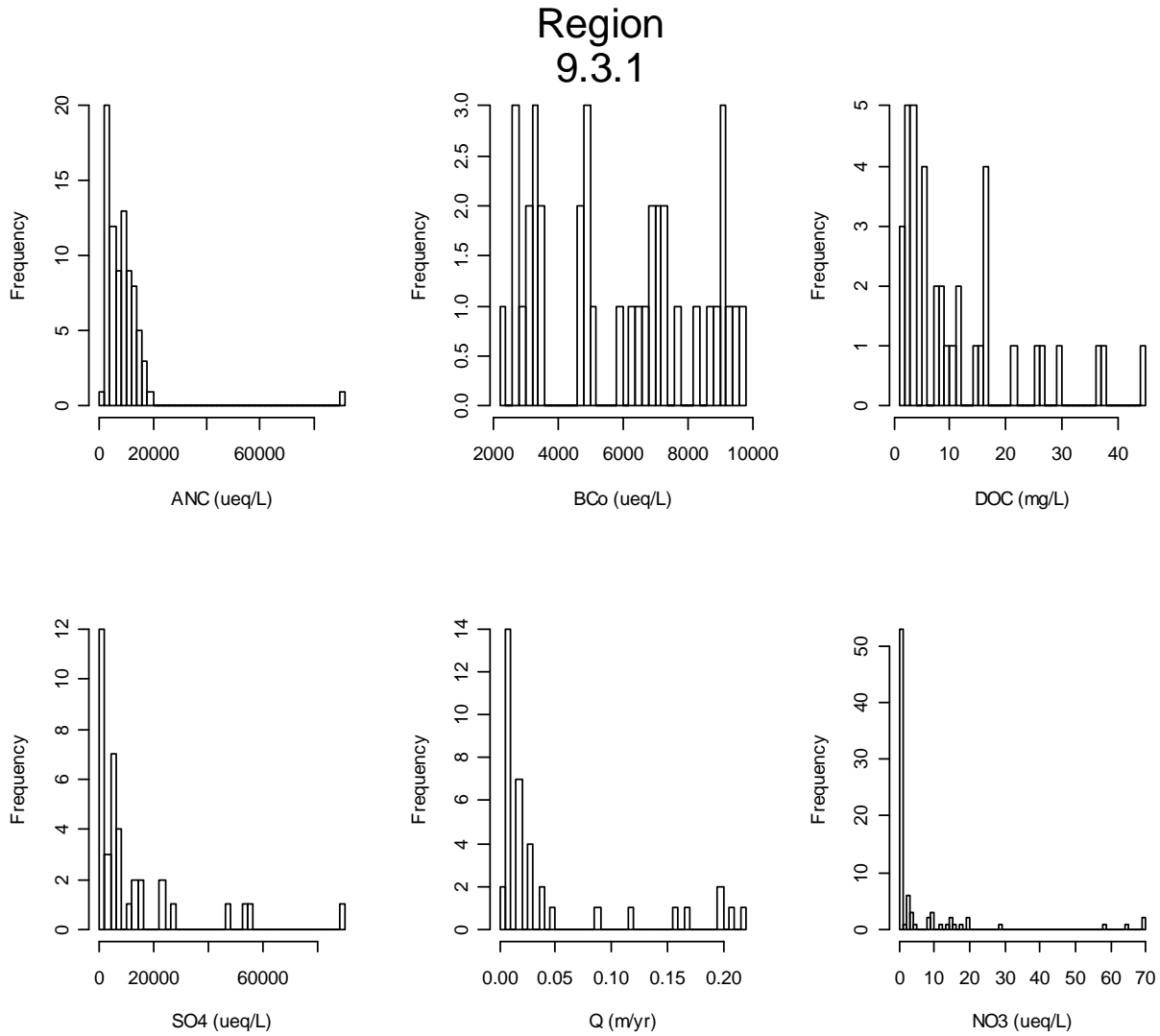


Figure C-70. Region 9.3.1 Water Quality Data Summary

Region 9.3.3 Northwestern Great Plains

The Northwestern Great Plains ecoregion encompasses the Missouri Plateau section of the Great Plains that is mostly unglaciated. It is a semiarid rolling plain of shale, siltstone, and sandstone punctuated by occasional buttes and badlands. Rangeland is common, but spring wheat and alfalfa farming also occur; native grasslands, persist in areas of steep or broken topography. Agriculture is restricted by the erratic precipitation and limited opportunities for irrigation.

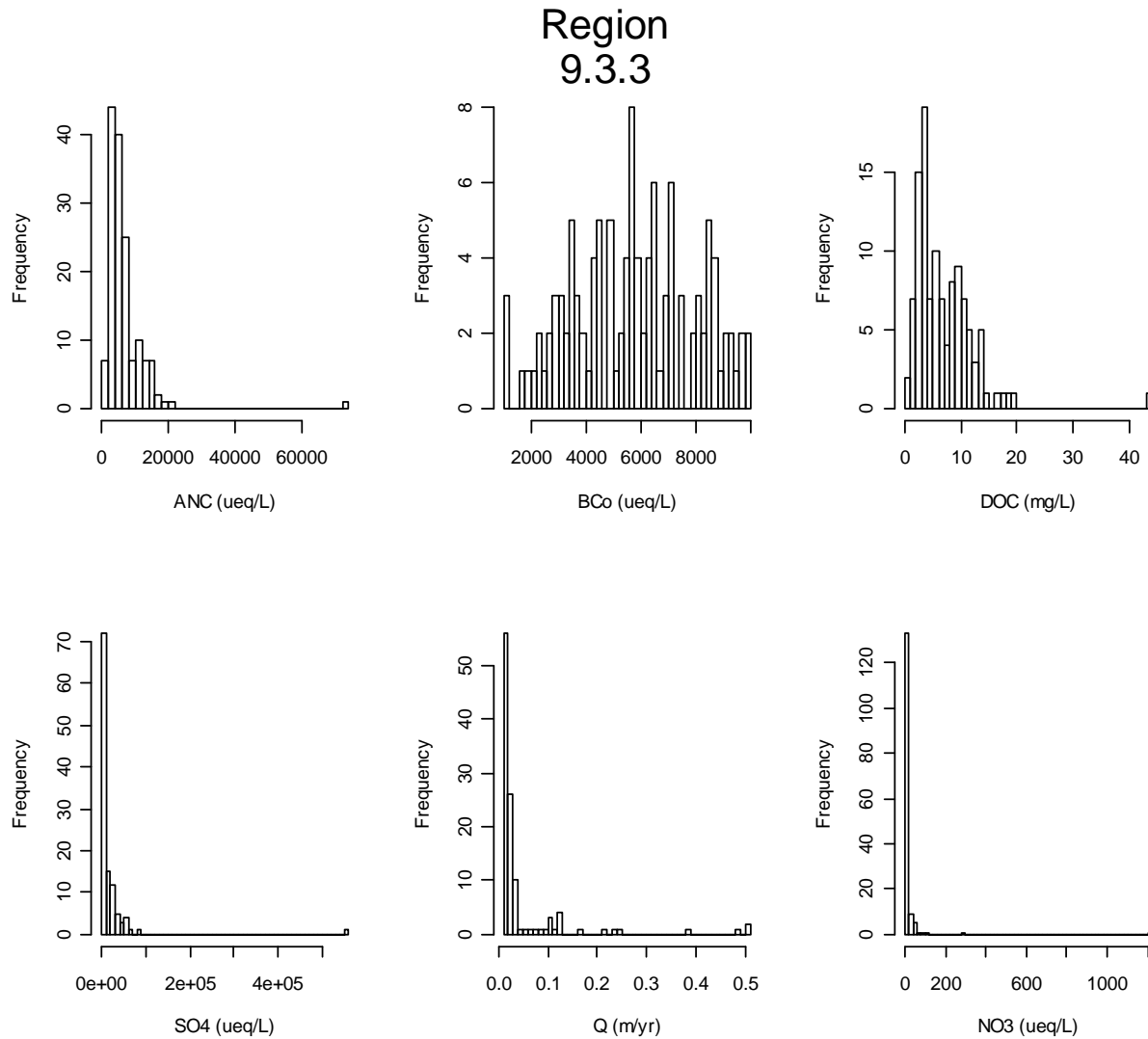


Figure C-71. Region 9.3.3 Water Quality Data Summary

Region 9.3.4 Nebraska San Hills

The Nebraska Sandhills comprise one of the most distinct and homogenous ecoregions in North America. One of the largest areas of grass stabilized sand dunes in the world, this region is generally devoid of cropland agriculture and except for some riparian areas in the north and east, and the region is treeless. Large portions of this ecoregion contain numerous lakes and wetlands and have a lack of streams. The area is sparsely populated; however, large cattle ranches are found throughout the region.

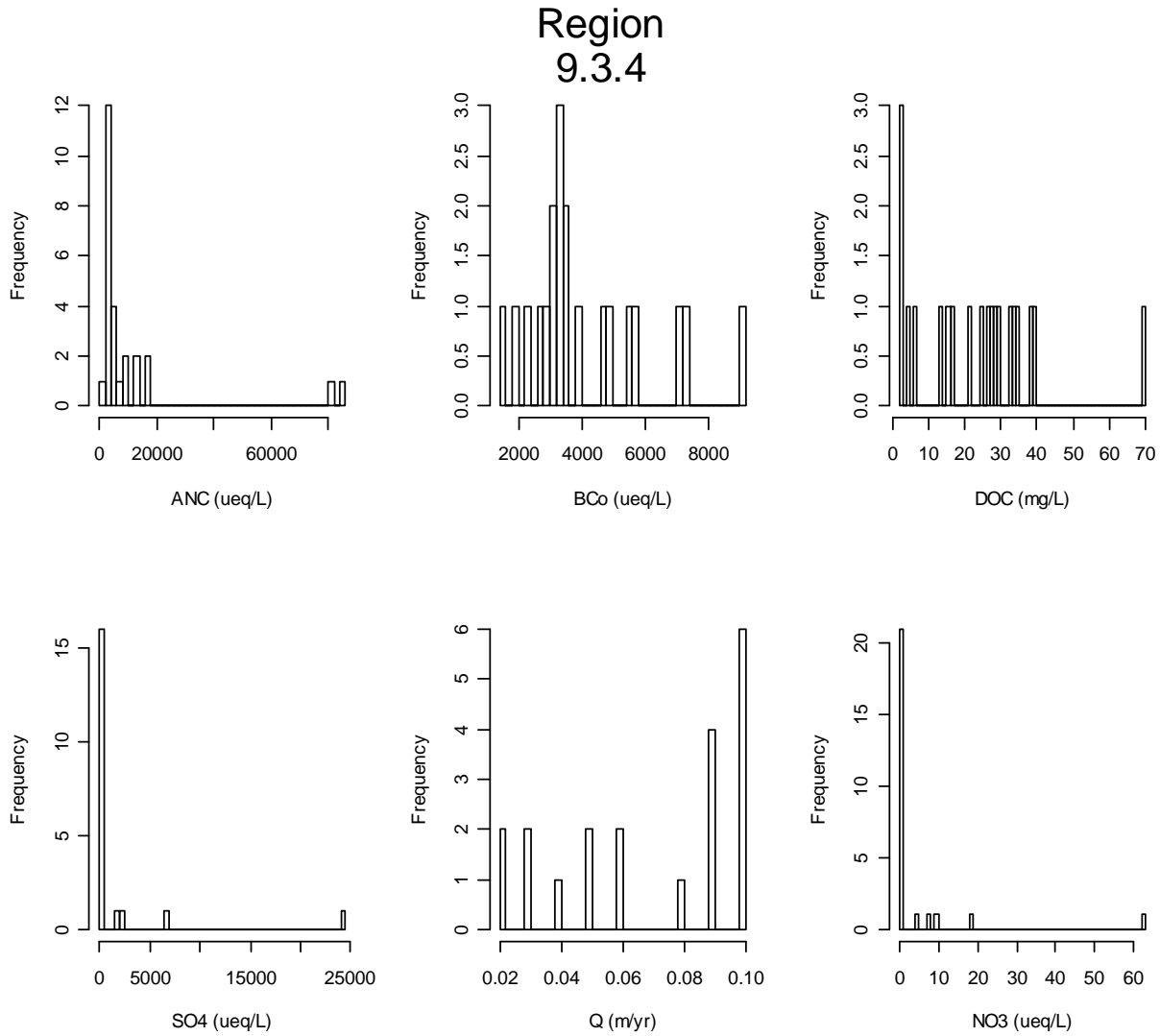


Figure C-72. Region 9.3.4 Water Quality Data Summary

Region 9.4 South Central Semi-Arid Prairies

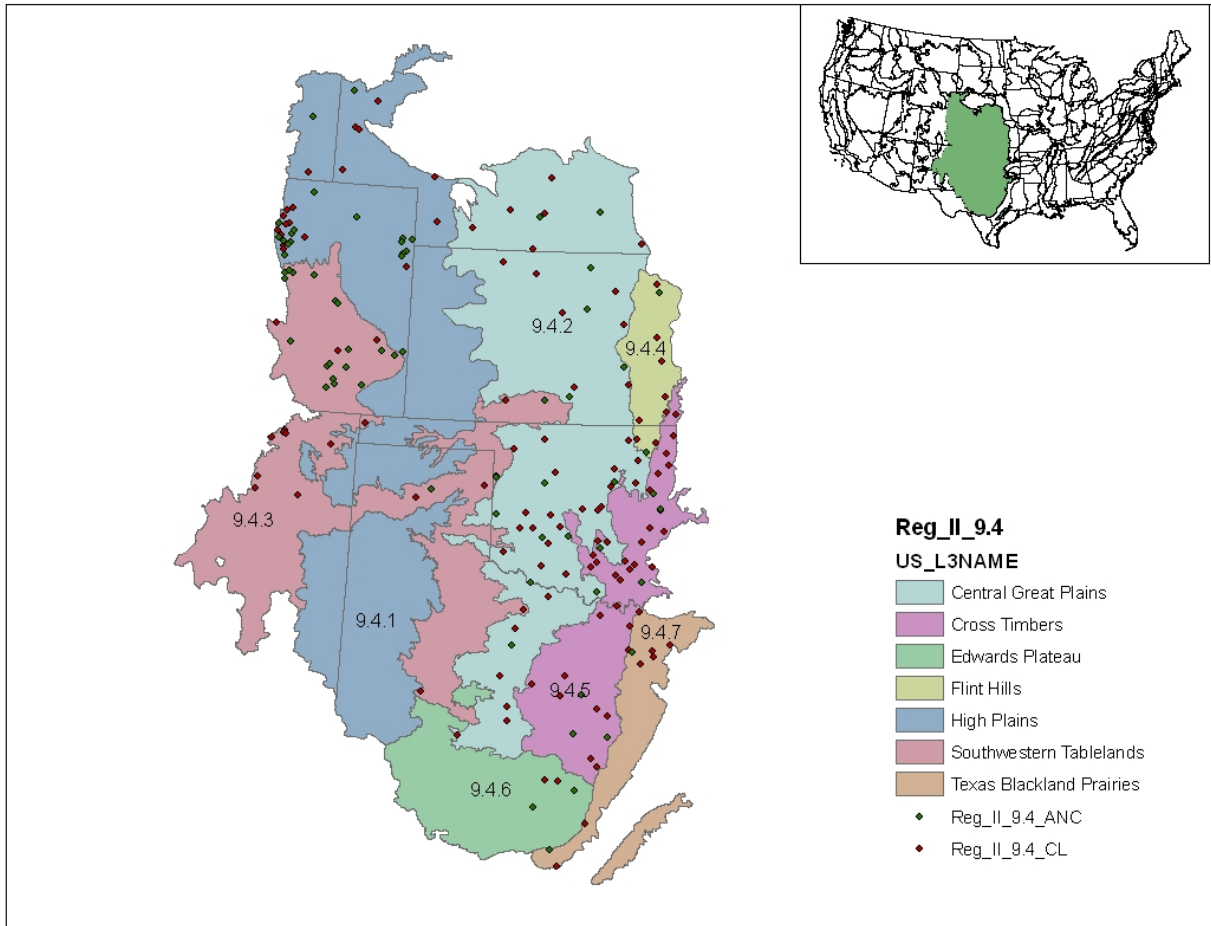


Figure C-73. Region 9.4

Region 9.4.1 High Plains

Higher and drier than the Central Great Plains (9.4.2) to the east, and in contrast to the irregular, mostly grassland or grazing land of the Northwestern Great Plains (9.3.3) to the north, much of the High Plains is characterized by smooth to slightly irregular plains having a high percentage of cropland. Grama-buffalo grass is the potential natural vegetation in this region as compared to mostly wheatgrass-needlegrass to the north, Trans-Pecos shrub savanna to the south, and taller grasses to the east. The northern boundary of this ecological region is also the approximate northern limit of winter wheat and sorghum and the southern limit of spring wheat.

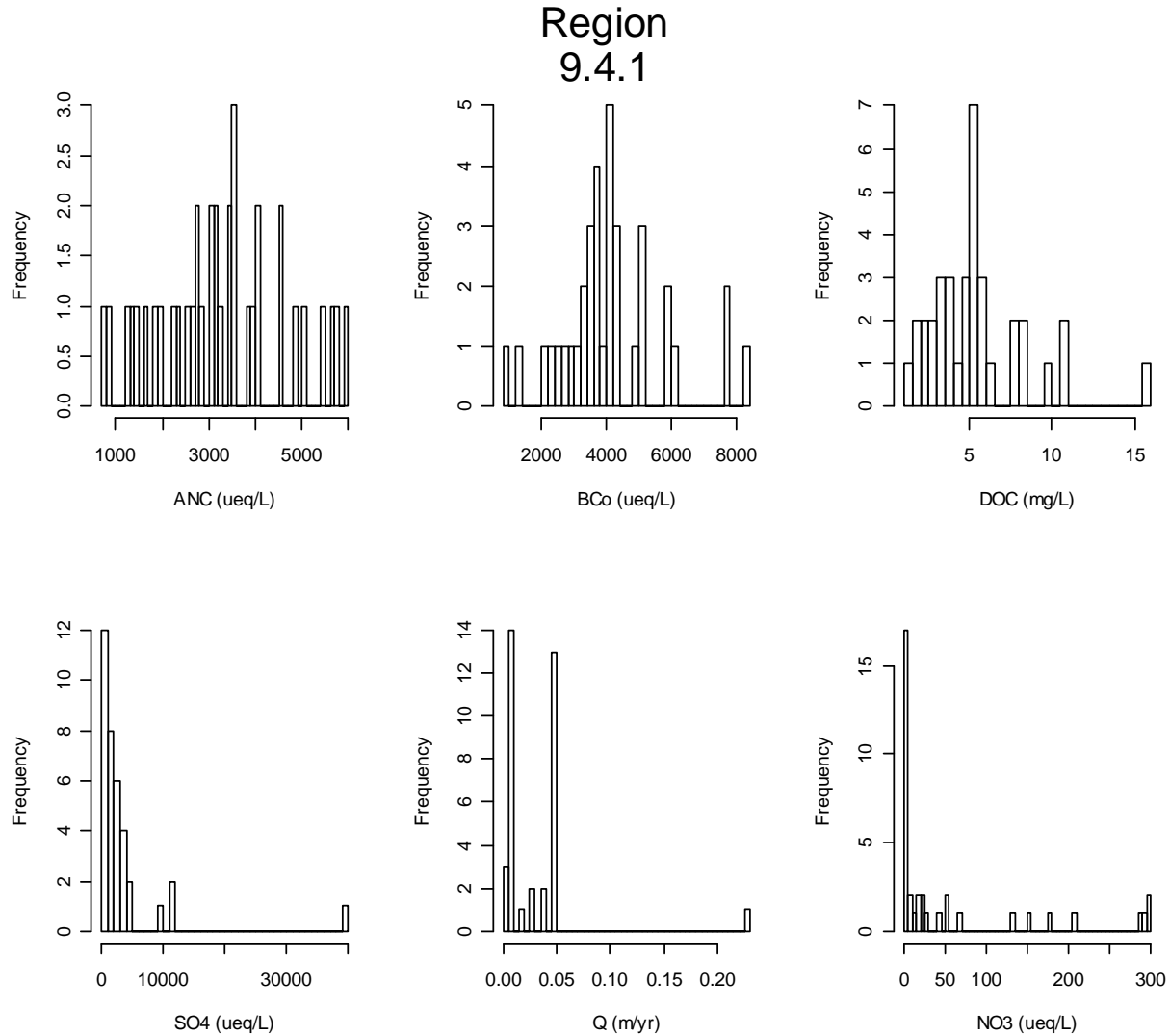


Figure C-74. Region 9.4.1 Water Quality Data Summary

Region 9.4.2 Central Great Plains

The Central Great Plains are slightly lower, receive more precipitation, and are somewhat more irregular than the High Plains (9.4.1) to the west. Once grassland, with scattered low trees and shrubs in the south, much of this ecological region is now cropland, the eastern boundary of the region marking the eastern limits of the major winter wheat growing area of the United States. Subsurface salt deposits and leaching contribute to high salinity found in some streams.

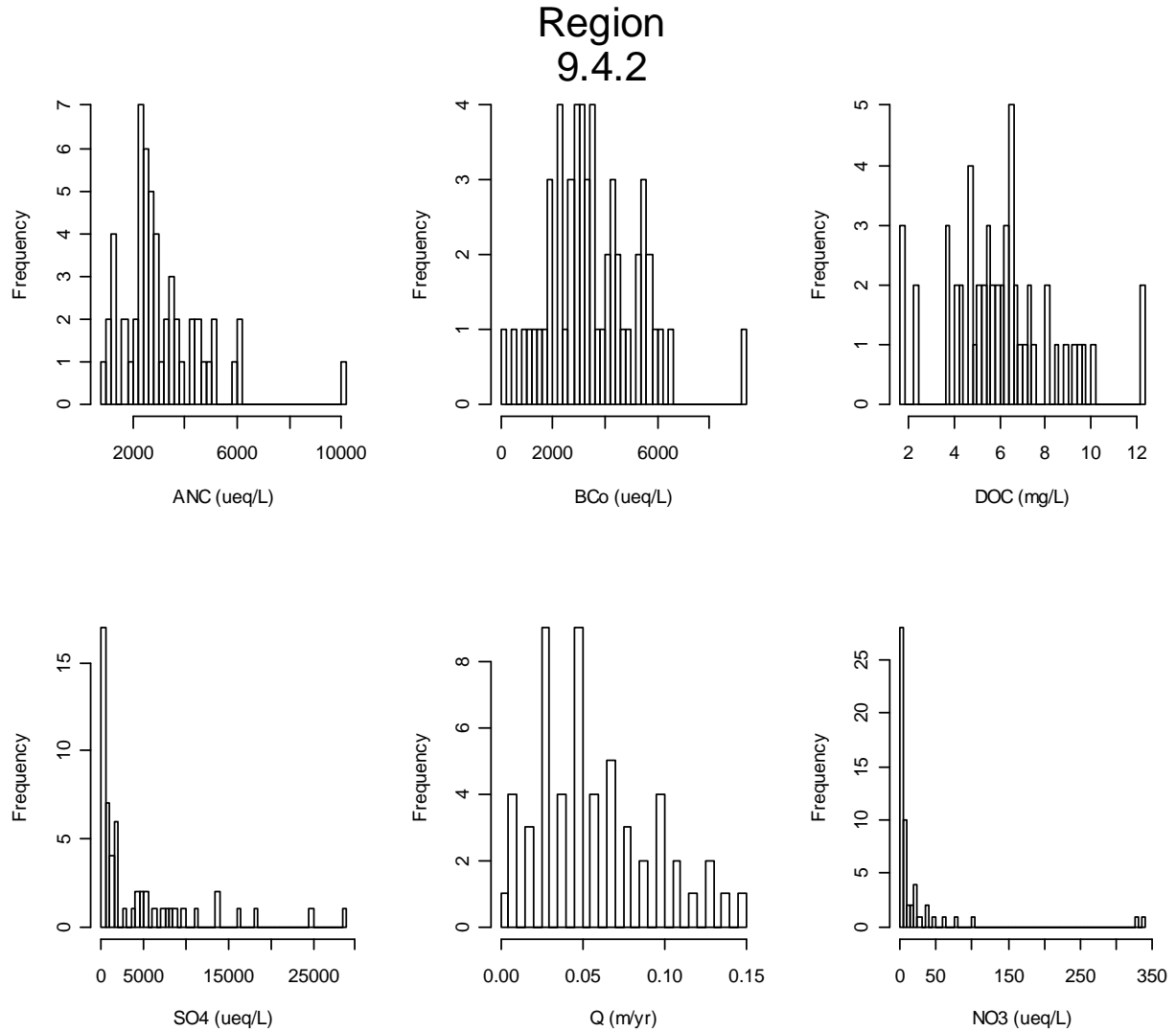


Figure C-75. Region 9.4.2 Water Quality Data Summary

Region 9.4.3 Southwestern Tablelands

The southwestern Tablelands flank the High Plains (9.4.1) with red hued canyons, mesas, badlands, and dissected river breaks. Unlike most adjacent Great Plains ecological regions, little of the Southwestern Tablelands is in cropland. Much of this region is in sub-humid grassland and semiarid range land. The potential natural vegetation is grama-buffalo grass with some mesquite-buffalo grass in the southeast, juniper-scrub oak-midgrass savanna on escarpment bluffs, and shinnery (midgrass prairie with open low and shrubs) along the Canadian River.

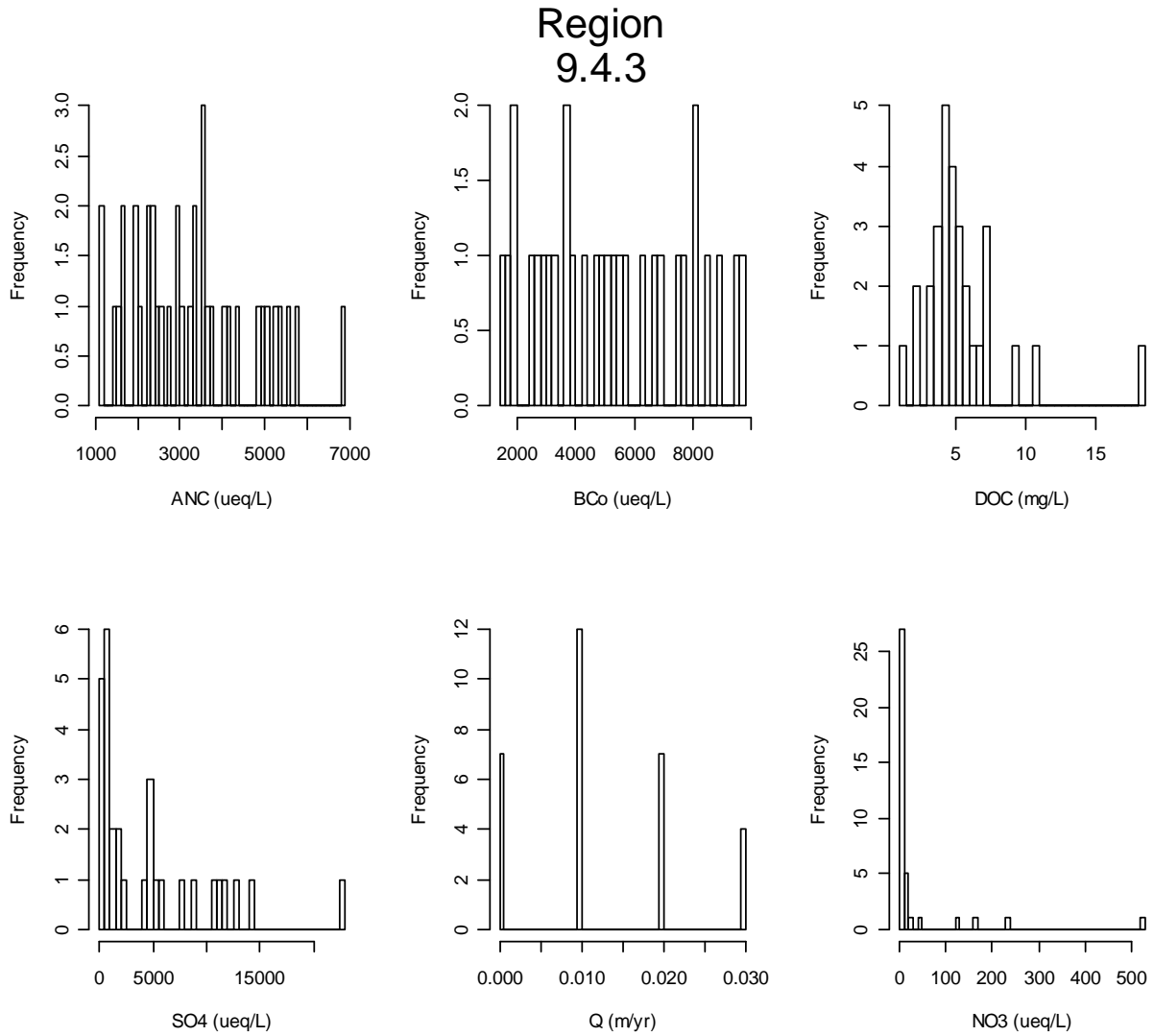


Figure C-76. Region 9.4.3 Water Quality Data Summary

Region 9.4.4 Flint Hills

The Flint Hills is a region of rolling hills with relatively narrow steep valleys, and is composed of shale and cherty limestone with rocky soils. In contrast to surrounding ecological regions that are mostly in cropland, most of the Flint Hills region is grazed by beef cattle. The Flint Hills mark the western edge of the tallgrass prairie, and contain the largest remaining intact tallgrass prairie in the Great Plains.

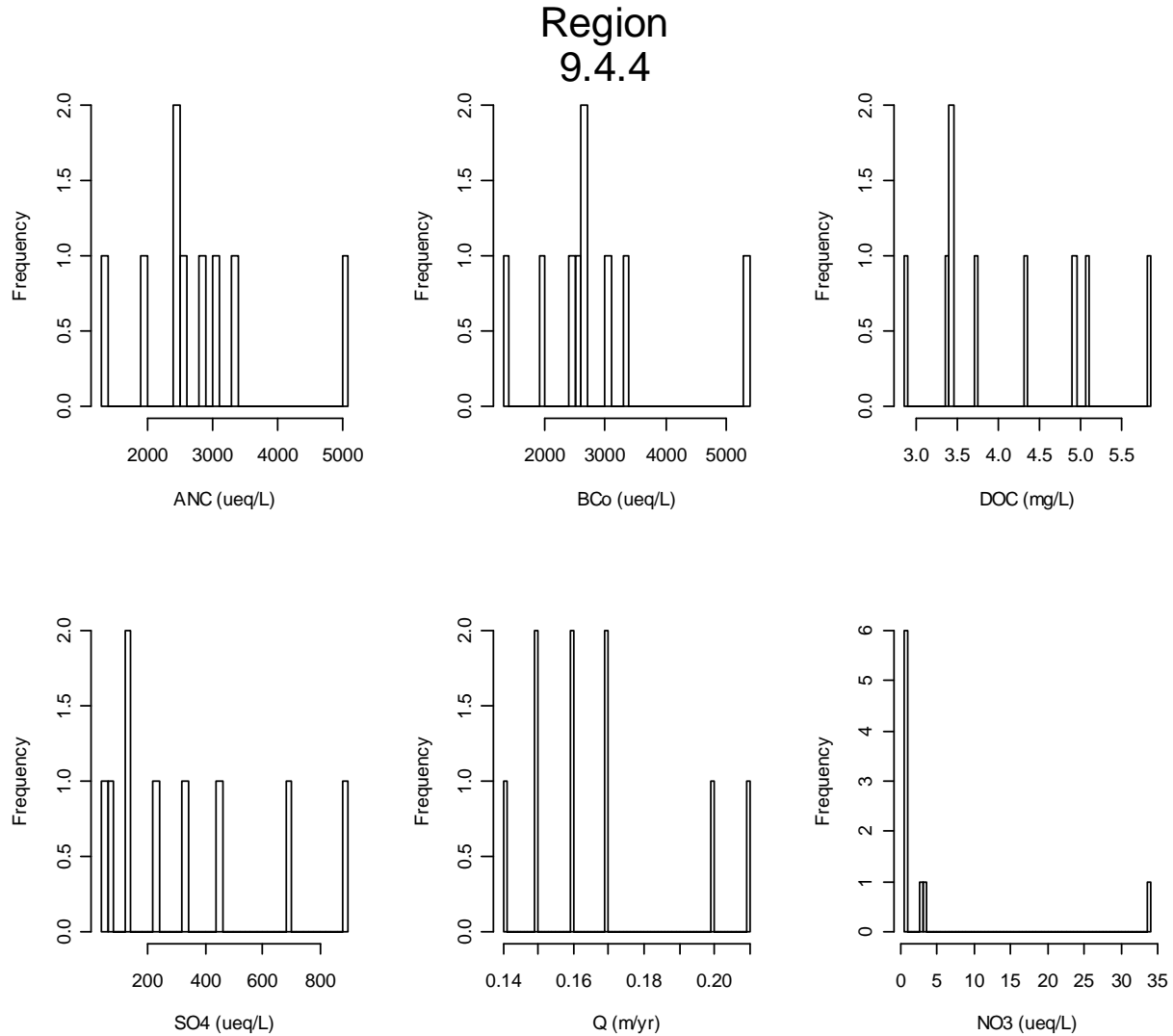


Figure C-77. Region 9.4.4 Water Quality Data Summary

Region 9.4.5 Cross Timbers

The Cross Timbers ecoregion is a transition area between the once prairie, now winter wheat growing regions to the west, and the forested low mountains or hills of eastern Oklahoma and Texas. The region does not possess the arability and suitability for crops such as corn and soybeans that are common in the Central Irregular Plains (9.2.4) to the northeast. Transitional “cross-timbers” (little bluestem grassland with scattered blackjack oak and post oak trees) is the native vegetation, and presently rangeland and pastureland comprise the predominant land cover, with some areas of woodland. Oil extraction has been a major activity in this region for over eighty years.

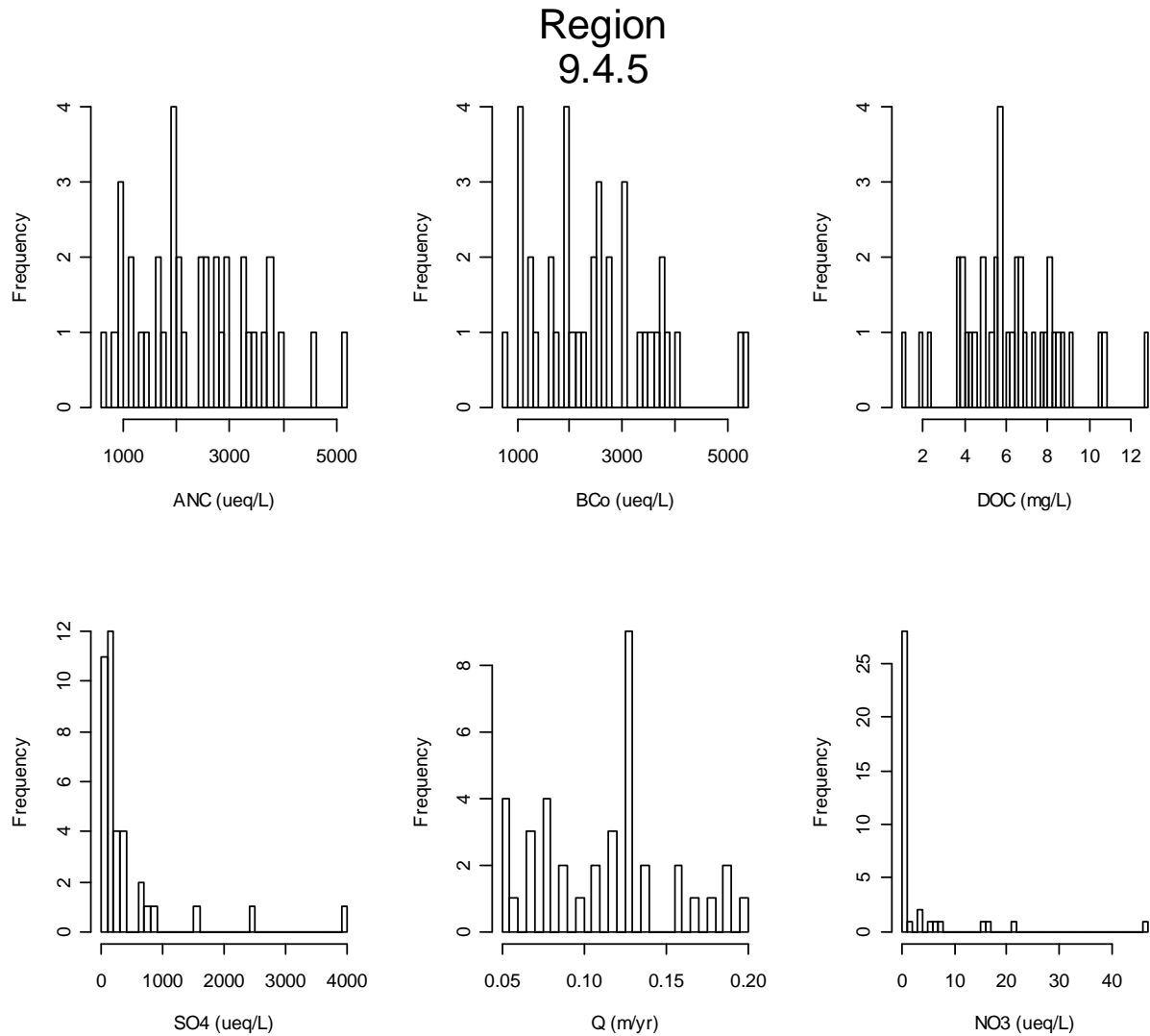


Figure C-78. Region 9.4.5 Water Quality Data Summary

Region 9.4.6 Edwards Plateau

This ecoregion is largely a dissected limestone plateau that is hillier in the south and east where it is easily distinguished from bordering ecological regions by a sharp fault line. The region contains a sparse network of perennial streams, but due to karst topography and resultant underground drainage they are relatively clear and cool compared to those of surrounding areas. Originally covered by juniper-oak savanna and mesquite-oak savanna, most of the region is used for grazing beef cattle, sheep, goats, and wildlife. Hunting leases are a major source of income.

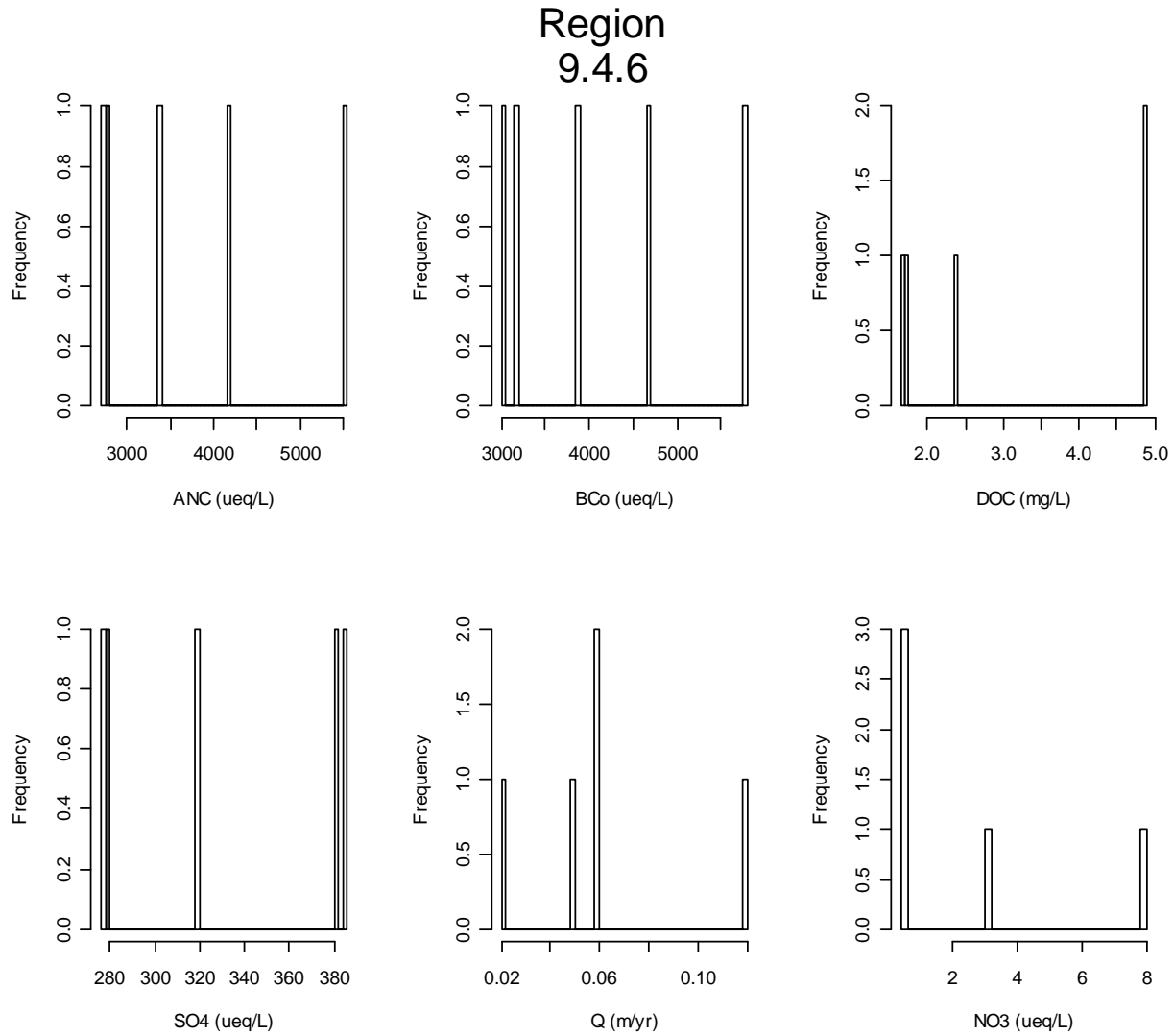


Figure C-79. Region 9.4.6 Water Quality Data Summary

Region 9.4.7 Texas Blackland Prairies

The Texas Blackland Prairies form a disjunct ecological region, distinguished from surrounding regions by its fine-textured, clayey soils and predominantly prairie potential natural vegetation. This region now contains a higher percentage of cropland than adjacent regions, and pasture and forage production for livestock is common. Large areas of the region are being converted to urban and industrial uses.

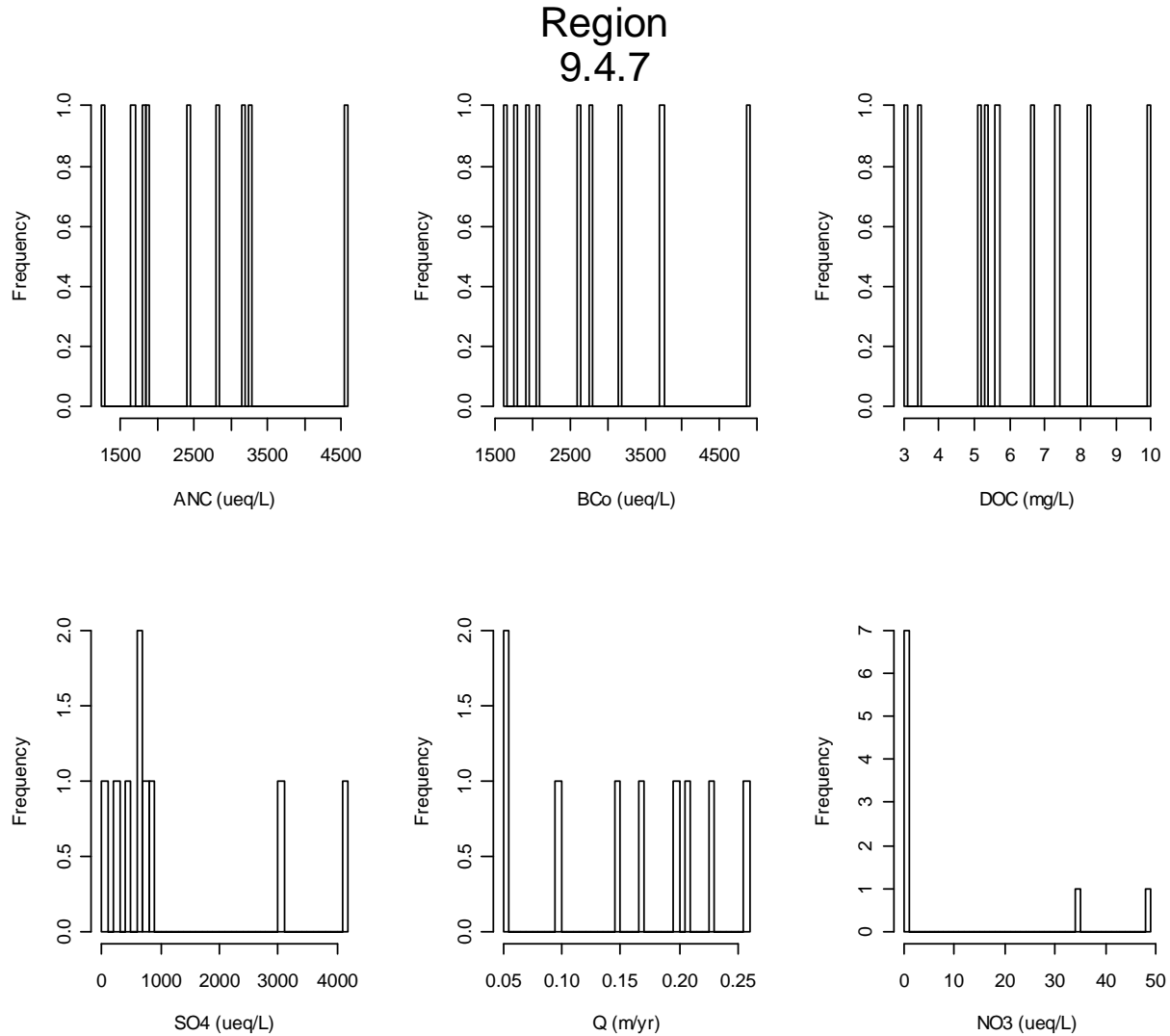


Figure C-80. Region 9.4.7 Water Quality Data Summary

Region 9.5 Texas-Louisiana Coastal Plain

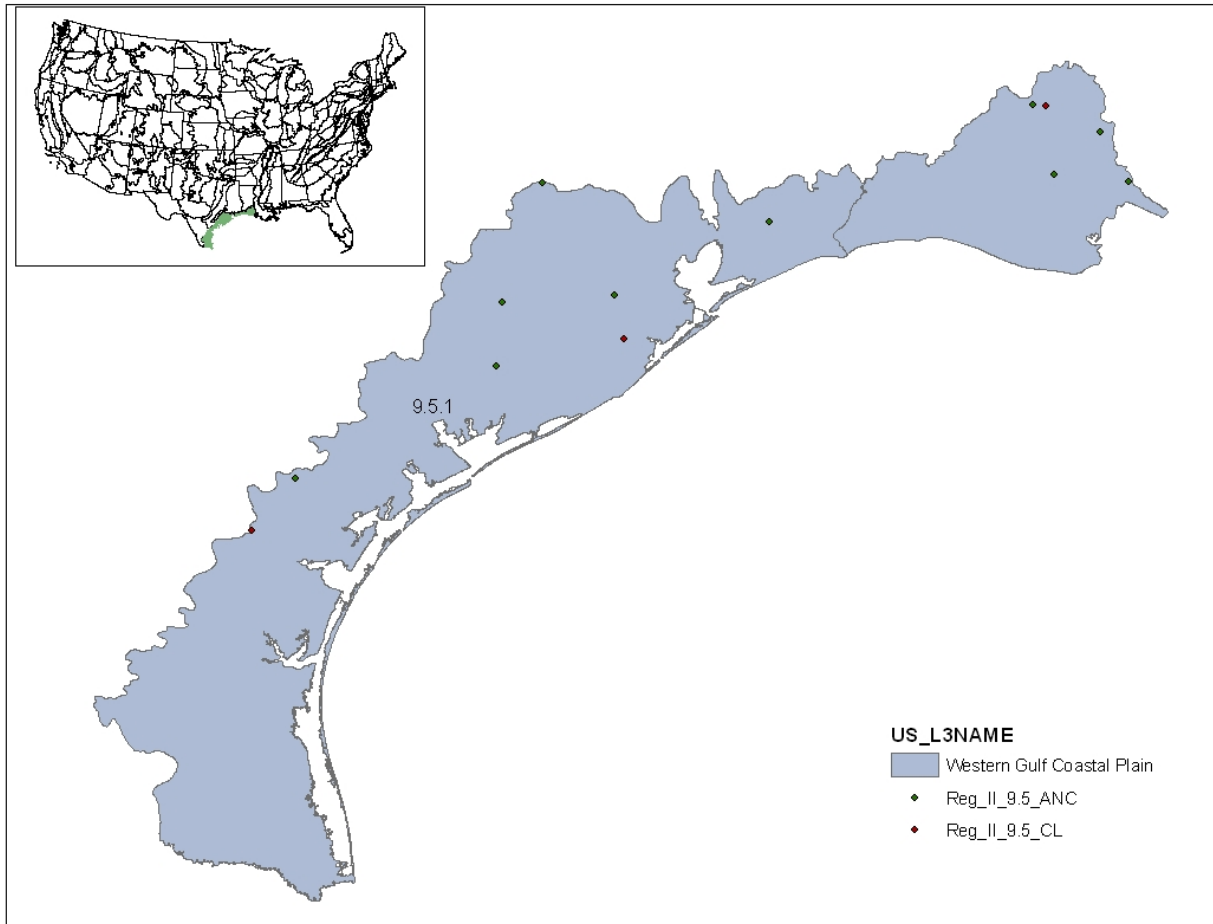


Figure C-81. Region 9.5

Region 9.5.1 Western Gulf Coastal Plain

The principal distinguishing characteristics of the Western Gulf Coastal Plain are its relatively flat coastal plain topography and mainly grassland potential natural vegetation. Inland from this region the plains are older, more irregular, and have mostly forest or savanna-type vegetation potentials. Largely because of these characteristics, a higher percentage of the land is in cropland than in bordering ecological regions. Urban and industrial land uses have expanded greatly in recent decades, and oil and gas production is common.

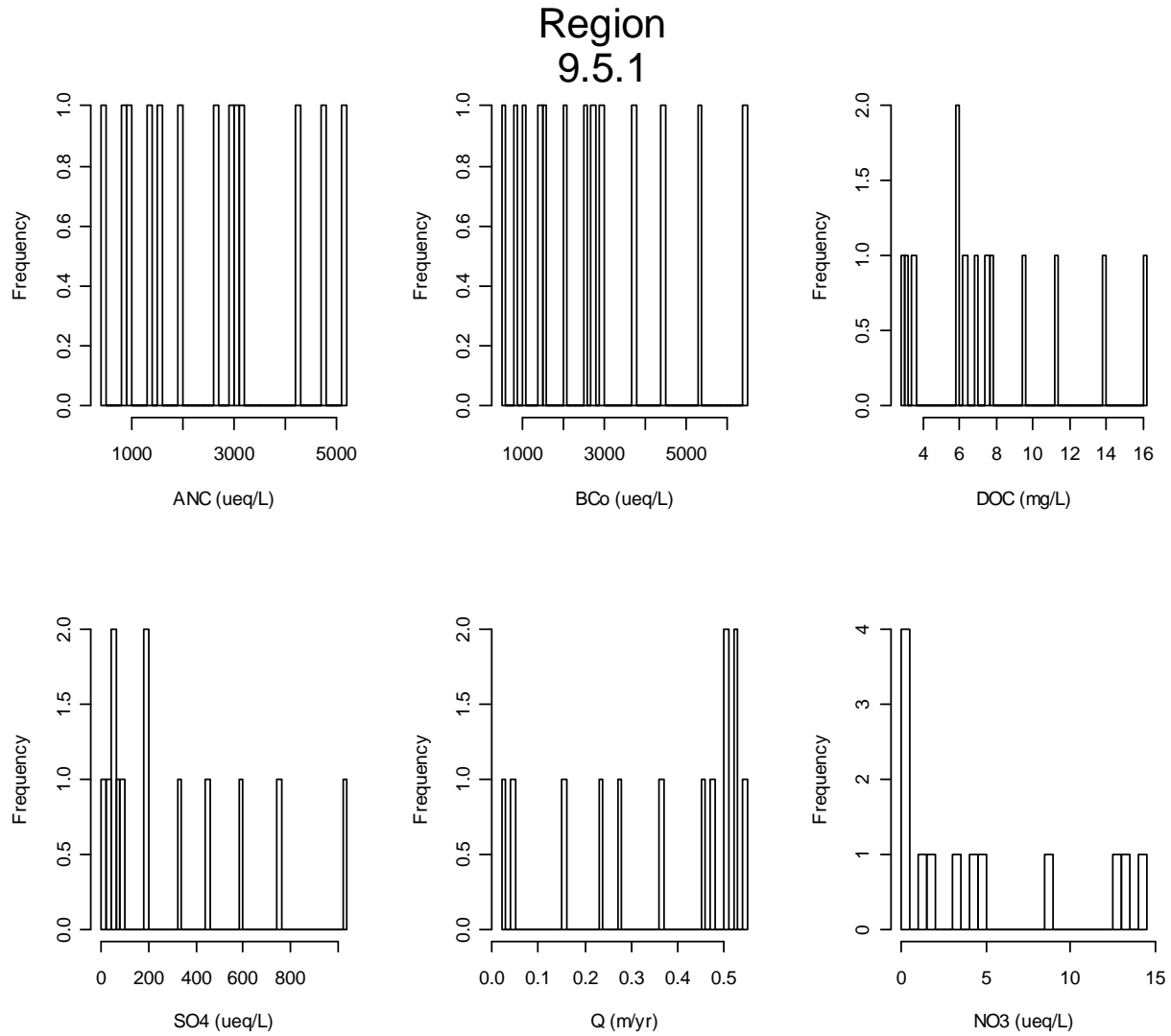


Figure C-82. Region 9.5.1 Water Quality Data Summary

Region 9.6 Tamaulipas-Texas Semi-Arid Plain

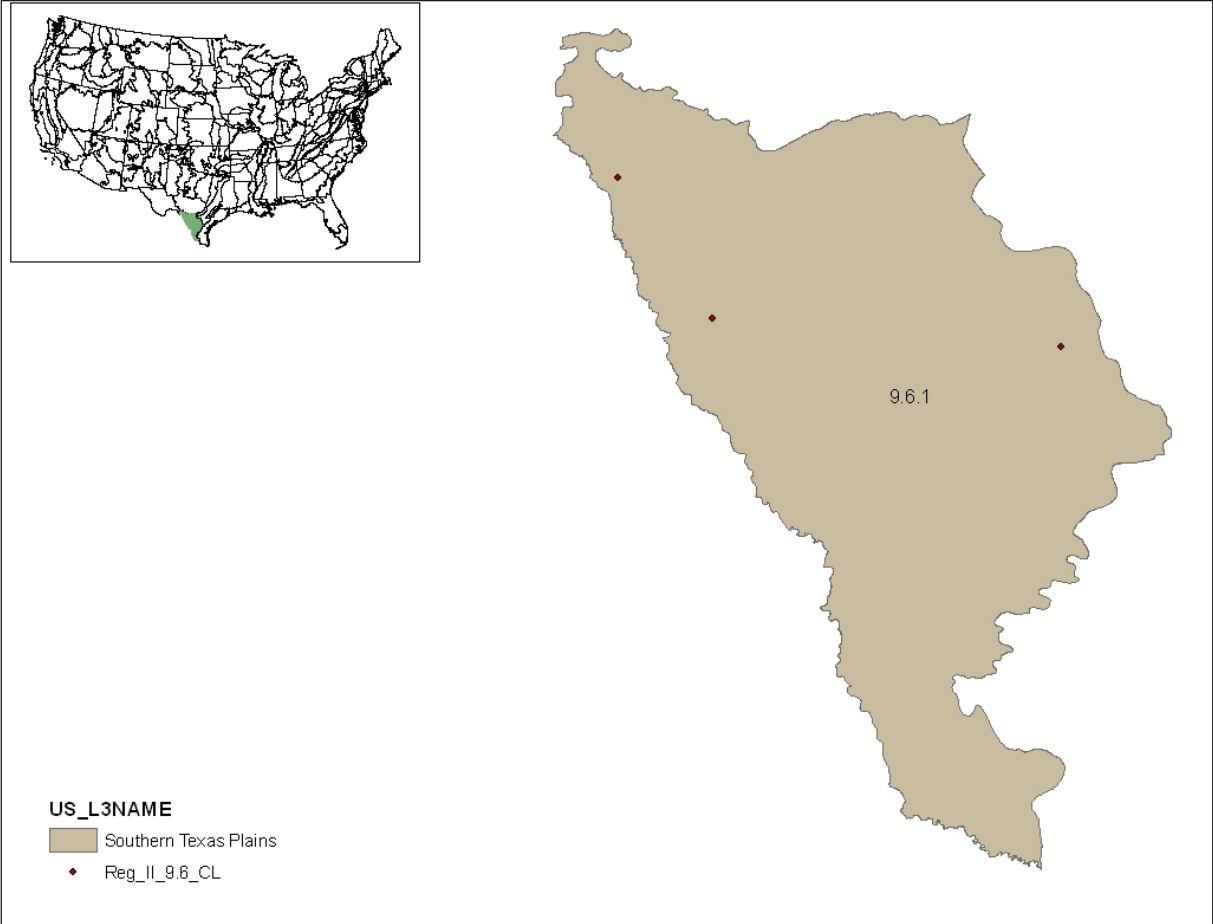


Figure C-83. Region 9.6

Region 9.6.1 Southern Texas Plains

This rolling to moderately dissected plain was once covered with grassland and savanna vegetation that varied during wet and dry cycles. Following long continued grazing and fire suppression, thorny brush, such as mesquite, is now the predominant vegetation type. Also known as the Tamualipan Thornscrub, or the “brush country”, as it is called locally, the subhumid to dry region has its greatest extent in Mexico. It is generally lower in elevation with warmer winters than the Chihuahuan Deserts (10.2.10) to the northwest, and it contains a high and distinct diversity of plant and animal life. Oil and natural gas production activities are widespread.

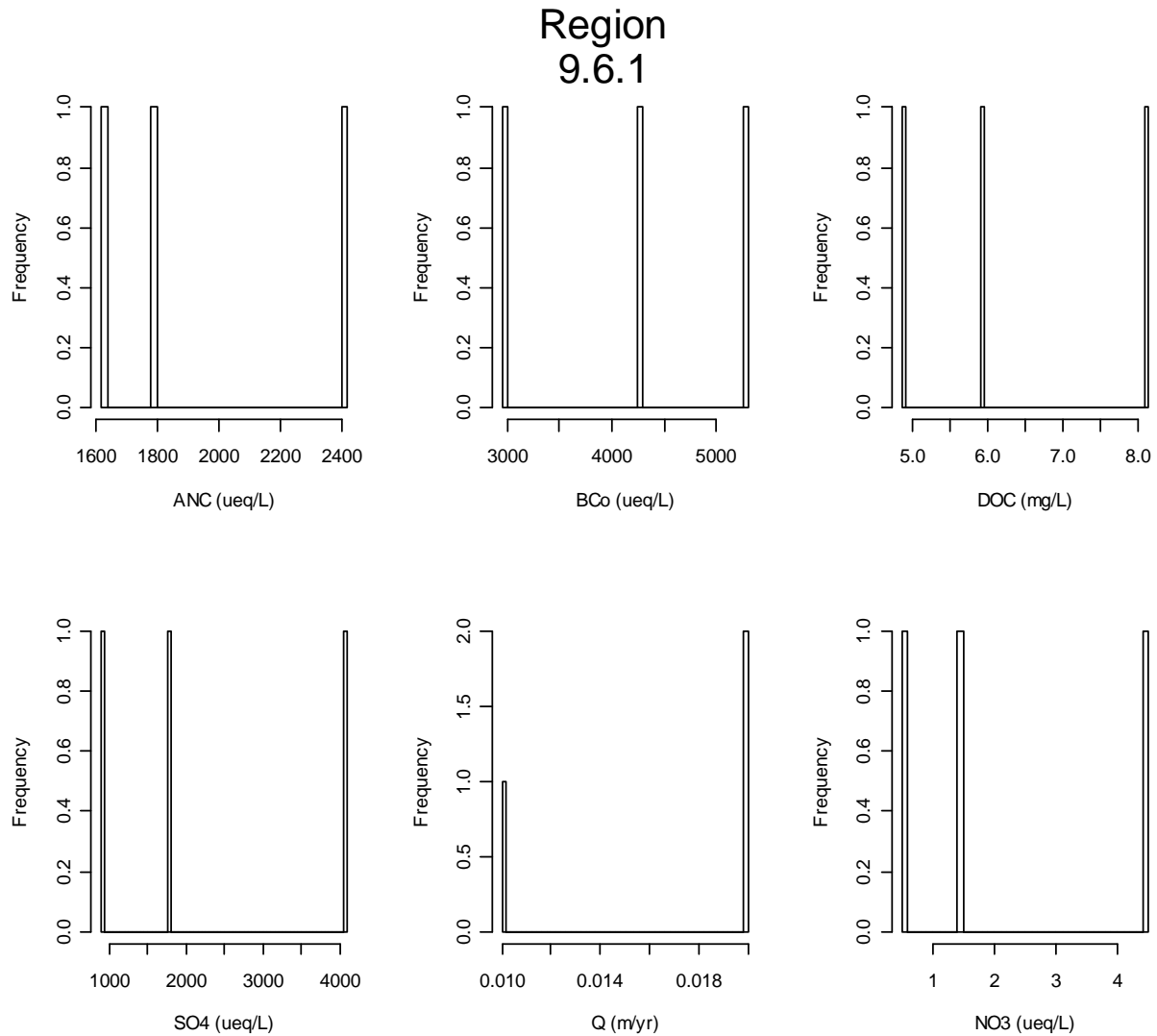


Figure C-84. Region 9.6.1 Water Quality Data Summary

Region 10.1 Cold Deserts

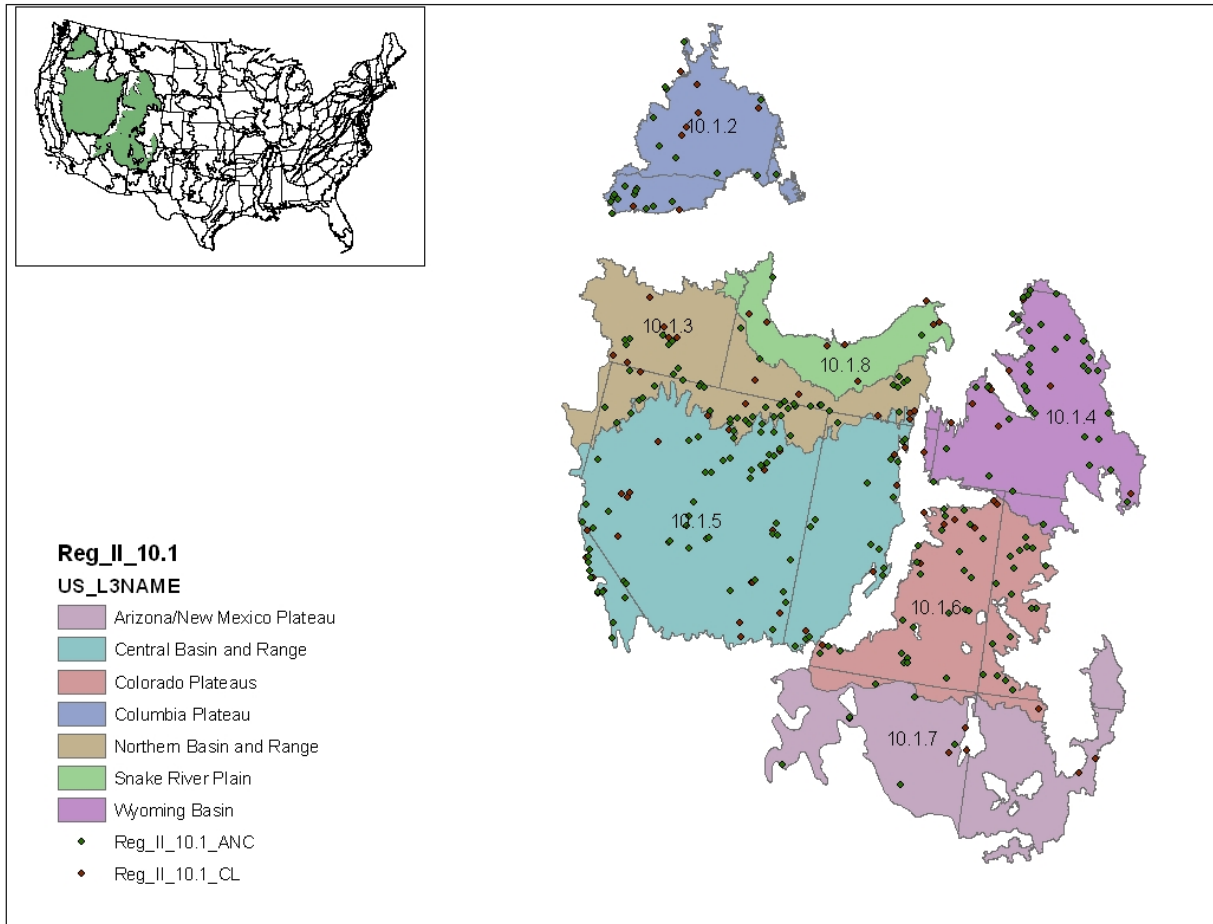


Figure C-85. Region 10.1

Region 10.1.2 Columbia Plateau

The Columbia Plateau is an arid sagebrush steppe and grassland, surrounded on all sides by moister, predominantly forested, mountainous ecological regions. This region is underlain by basalt up to two miles thick. It is covered in some places by loess soils that have been extensively cultivated for wheat, particularly in the eastern portions of the region where precipitation amounts are greater. During the glaciation of the Pleistocene era, parts of the area were scoured to bedrock by huge floods from breached ice dams.

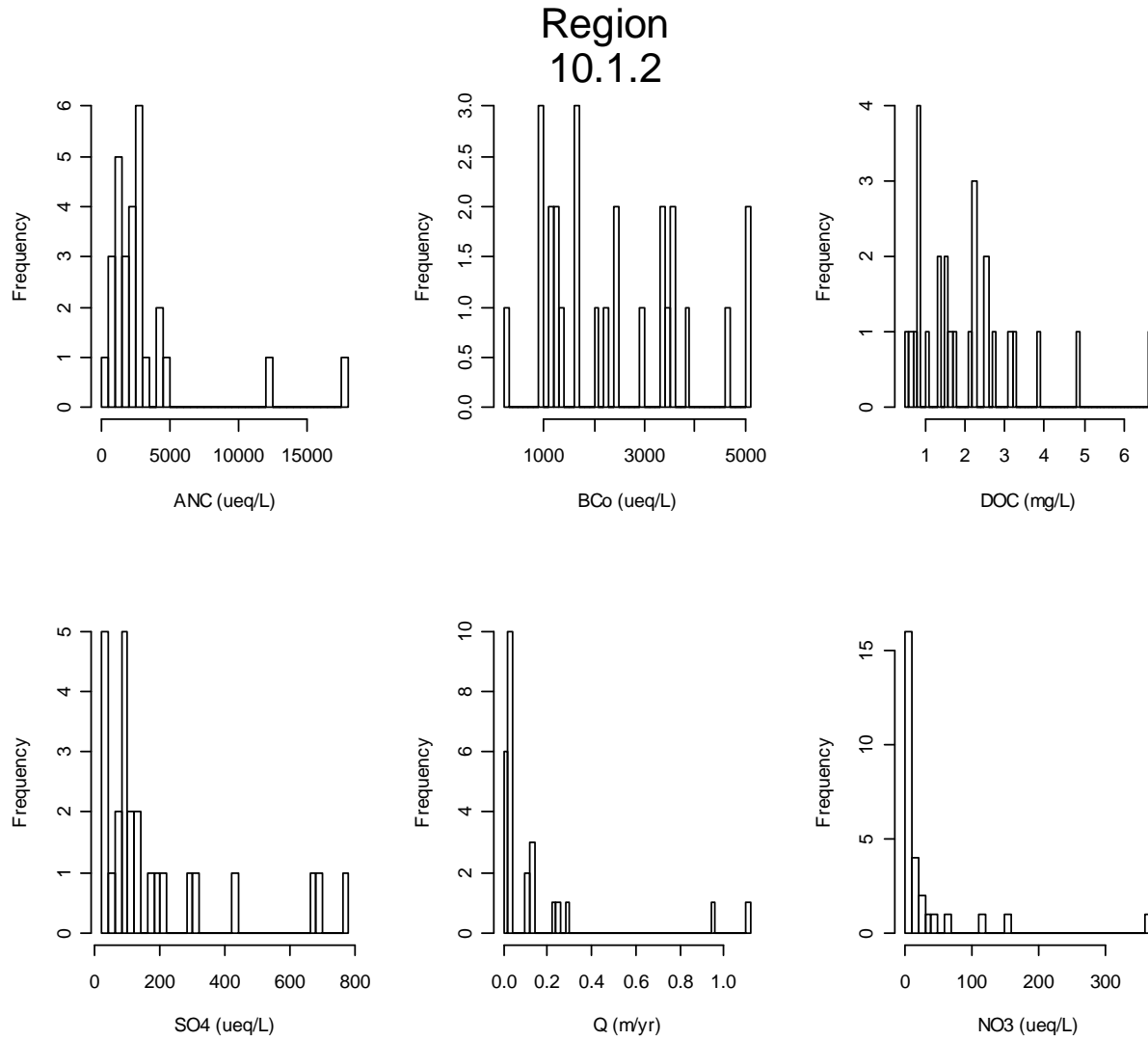


Figure C-86. Region 10.1.2 Water Quality Data Summary

Region 10.1.3 Northern Basin and Range

This ecoregion contains tablelands, dissected lava plains, valleys, alluvial fans, and scattered mountains. Overall, it is higher and cooler than the Snake River Plain (10.1.8) to the east and has more available moisture and a cooler climate than the Central Basin and Range (10.1.5) to the south. The region has more extensive basins and fewer mountain ranges than the Central Basin and Range. Non-mountain areas have sagebrush steppe vegetation; cool season grasses and Mollisols are more common than in the hotter-drier basins of the Central Basin and Range where Aridisols are dominated by sagebrush, shadscale, and greasewood. Ranges are covered in mountain sagebrush, mountain brush, and Idaho fescue at lower and mid-elevations; Douglas-fir, and aspen are common at higher elevations. Soils are less suitable for agriculture than those in the Columbia Plateau (10.1.2) and the Snake River Plain. Rangeland is common and dryland and irrigated agriculture occur in eastern basins.

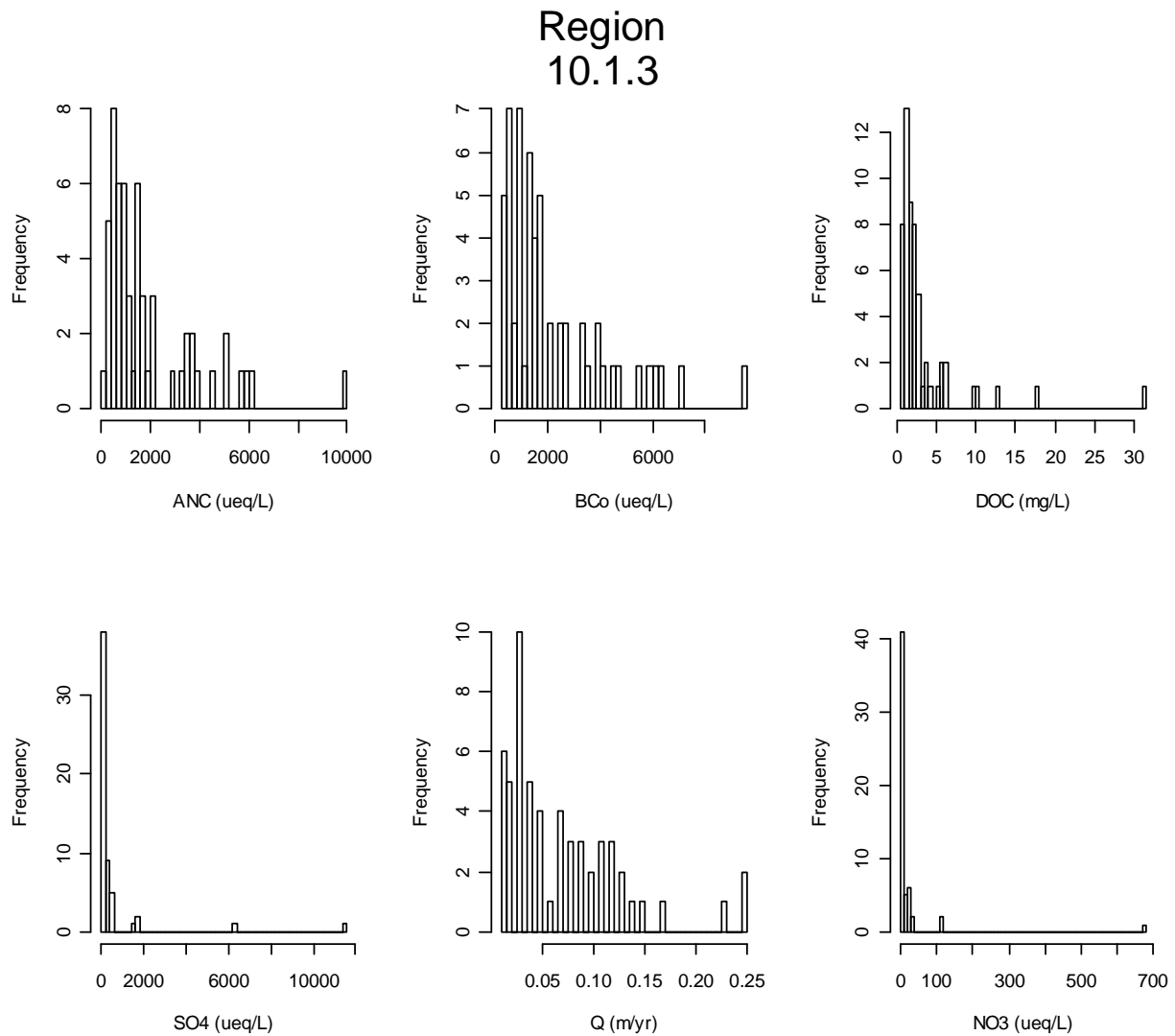


Figure C-87. Region 10.1.3 Water Quality Data Summary

Region 10.1.4 Wyoming Basin

This ecoregion is a broad intermontane basin interrupted by hills and low mountains and dominated by arid grasslands and shrublands. Nearly surrounded by forest covered mountains, the region is somewhat drier than the Northwestern Great Plains (9.3.3) to the northeast and does not have the extensive cover of pinyon-juniper woodland found in the Colorado Plateaus (10.16) to the south. Much of the region is used for livestock grazing, although many areas lack sufficient vegetation to support this activity. The region contains major producing natural gas and petroleum fields. The Wyoming Basin also has extensive coal deposits along with areas of trona, bentonite, clay, and uranium mining.

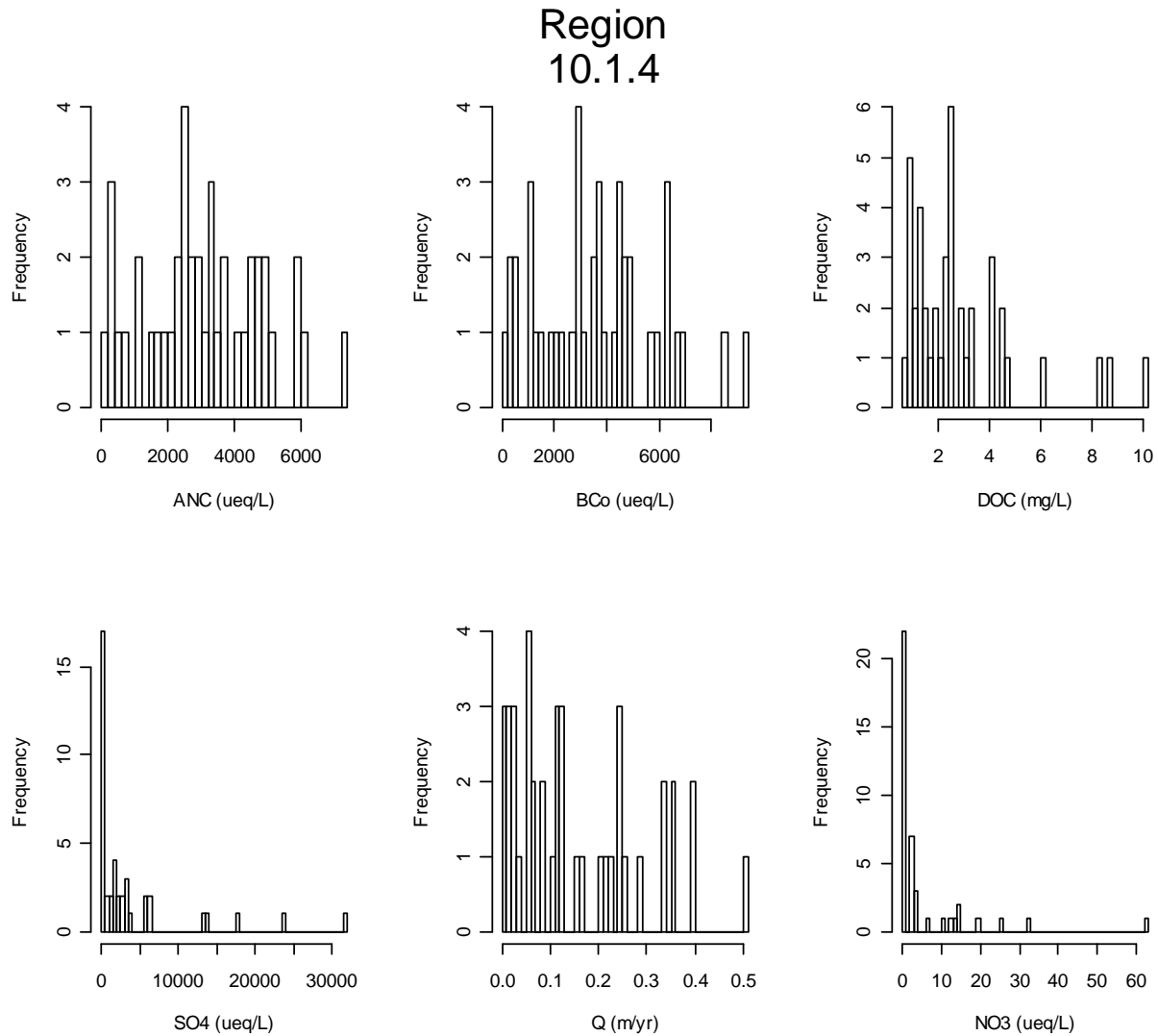


Figure C-88. Region 10.1.4 Water Quality Data Summary

Region 10.1.5 Central Basin and Range

The Central Basin and Range ecoregion is internally drained and is characterized by a mosaic of xeric basins, scattered low and high mountains, and salt flats. It has a hotter and drier climate, more shrubland, and more mountain ranges than the Northern Basin and Range (10.1.3) ecoregion to the north. Basins are covered by Great Basin sagebrush or saltbush-greasewood vegetation that grow in Aridisols; cool season grasses are less common than in the Mollisols of the Snake River Plain (10.1.8) and Northern Basin and Range. The region is not as hot as the Mojave Basin and Range (10.2.1) ecoregion to the south and it has a greater percent of land that is grazed.

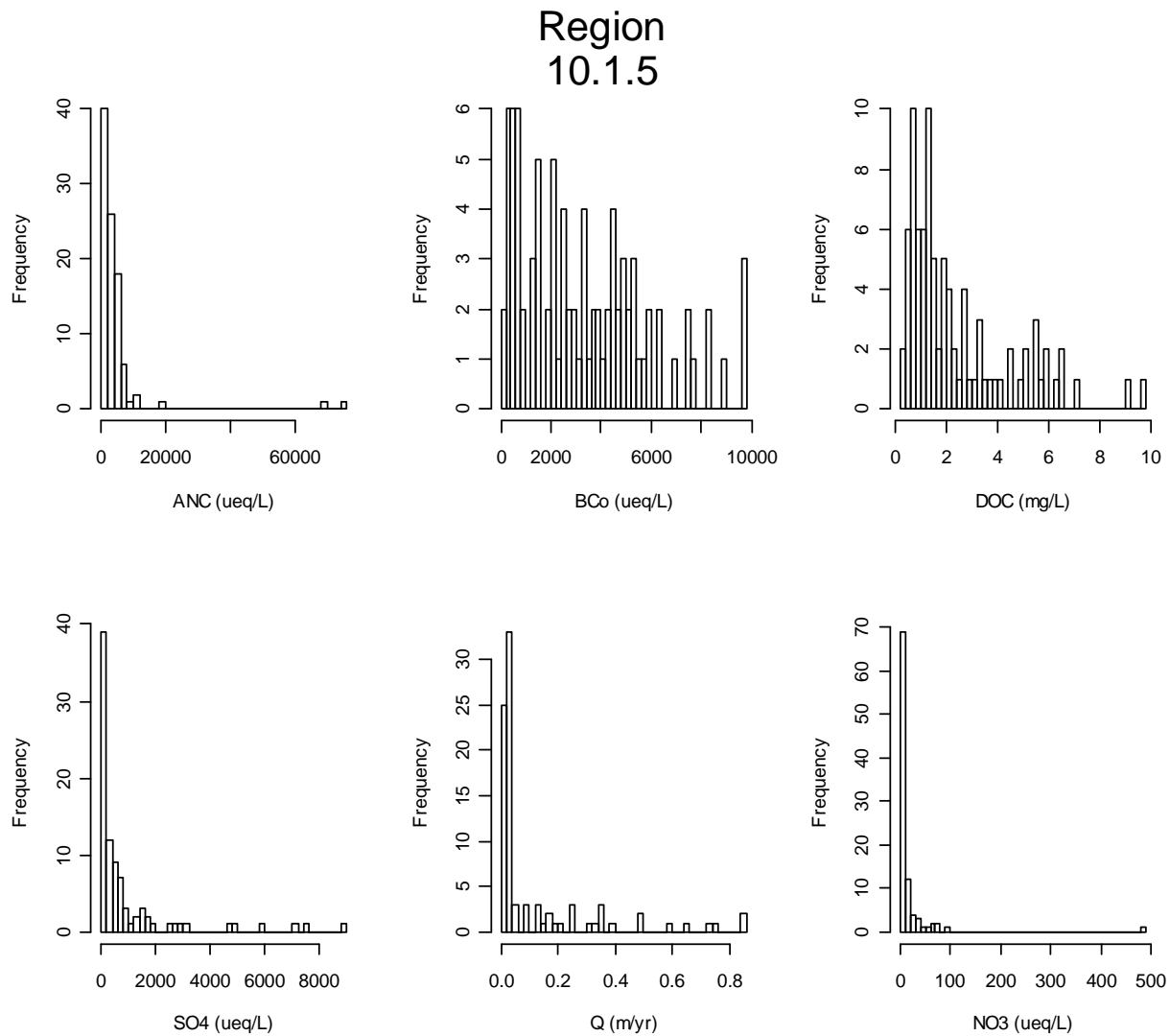


Figure C-89. Region 10.1.5 Water Quality Data Summary

Region 10.1.6 Colorado Plateaus

Ecoregion 10.1.6 is an uplifted, eroded, and deeply dissected tableland. Its benches, mesas, buttes, salt valleys, cliffs, and canyons are formed in and underlain by thick layers of sedimentary rock. Precipitous side-walls mark abrupt changes in local relief, often from 1,000 to 2,000 feet. The region contains a greater extent of pinyon-juniper and Gambel oak woodlands than the Wyoming Basin (10.1.4) to the north. There are also large low lying areas containing saltbrush-greasewood (typical of hotter drier areas), which are generally not found in the higher Arizona/New Mexico Plateau (10.1.7) to the south where grasslands are common. Summer moisture from thunderstorms supports warm season grasses not found in the Central Basin and Range (10.1.5) to the west. Many endemic plants occur and species diversity is greater than in Ecoregion 10.1.5. Several national parks are located in this ecoregion and attract many visitors to view their arches, spires, and canyons.

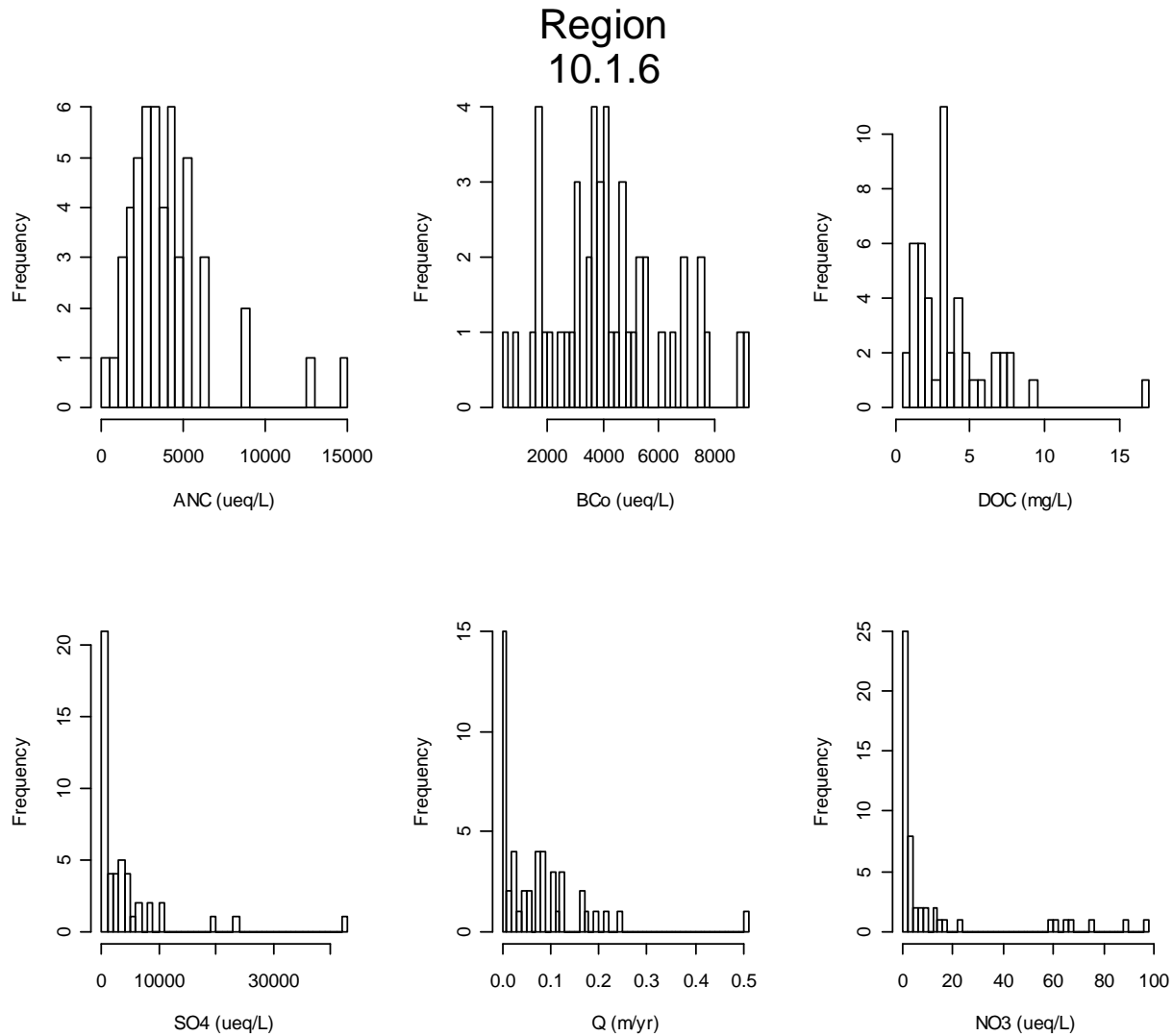


Figure C-90. Region 10.1.6 Water Quality Data Summary

Region 10.1.7 Arizona/New Mexico Plateau

The Arizona/New Mexico Plateau represents a large transitional region between the semiarid grasslands and low relief tablelands of the Southwestern Tablelands (9.4.3) in the east, the drier shrublands and woodland covered higher relief tablelands of the Colorado Plateau (10.1.6) in the north, and the lower, hotter, less vegetated Mojave Basin and Range (10.2.1) in the west and Chihuahuan Deserts (10.2.10) in the southeast. Higher, forest-covered, mountainous ecoregions border the region on the northeast (6.2.14) and south (13.1.1). Local relief in the region varies from a few feet on plains and mesa tops to well over 1000 feet along tableland side slopes.

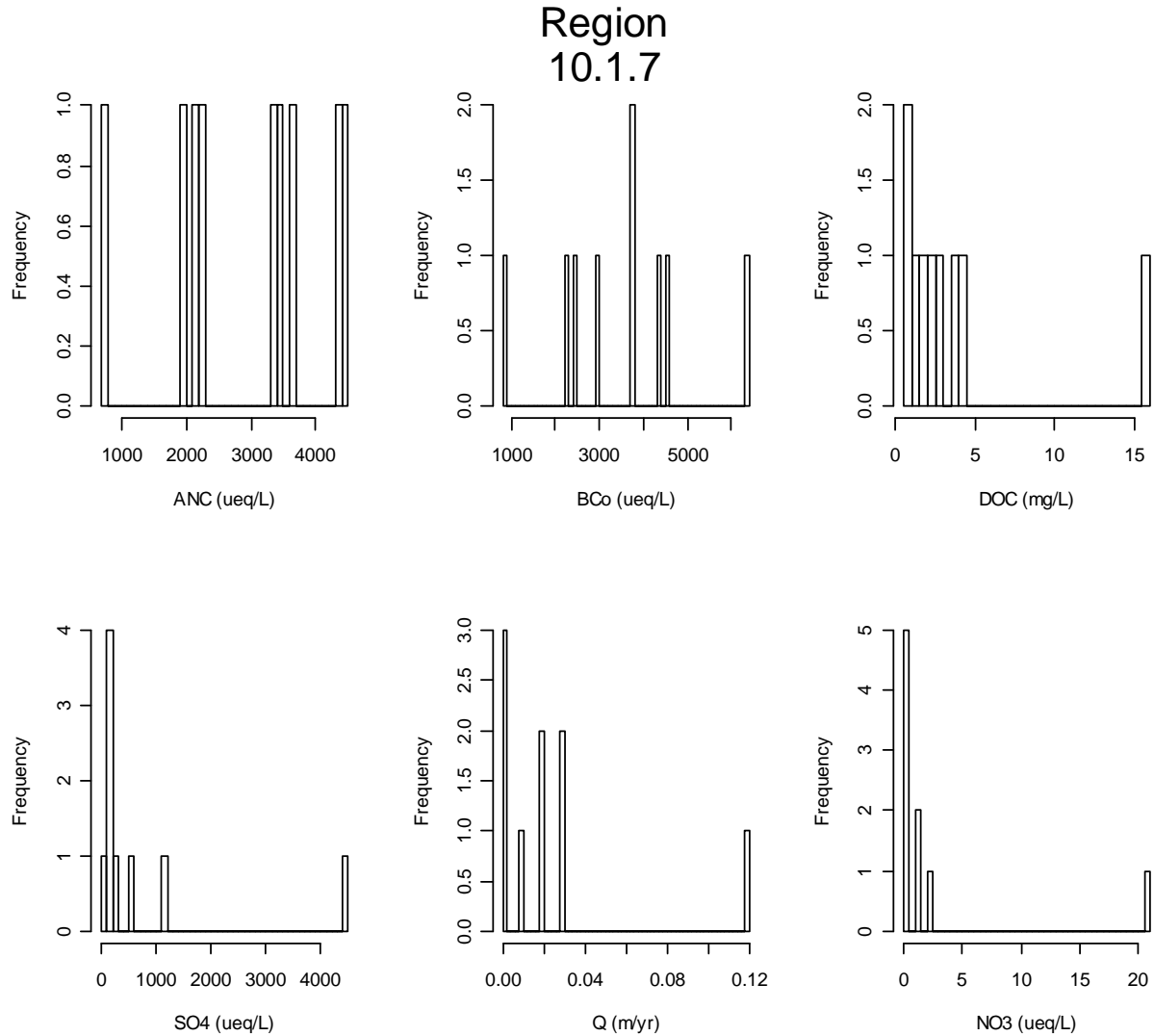


Figure C-91. Region 10.1.7 Water Quality Data Summary

Region 10.1.8 Snake River Plain

This portion of the xeric intermontane western United States is considerably lower and more gently sloping than the surrounding ecoregions. Mostly because of the available water for irrigation, a large percent of the alluvial valleys bordering the Snake River are in agriculture, with sugar beets, potatoes, alfalfa, and vegetables being the principal crops. Cattle feedlots and dairy operations are also common in the river plain. Except for the scattered barren lava fields, most of the plains and low hills in the ecoregion have sagebrush-grassland vegetation, now used mostly for cattle grazing.

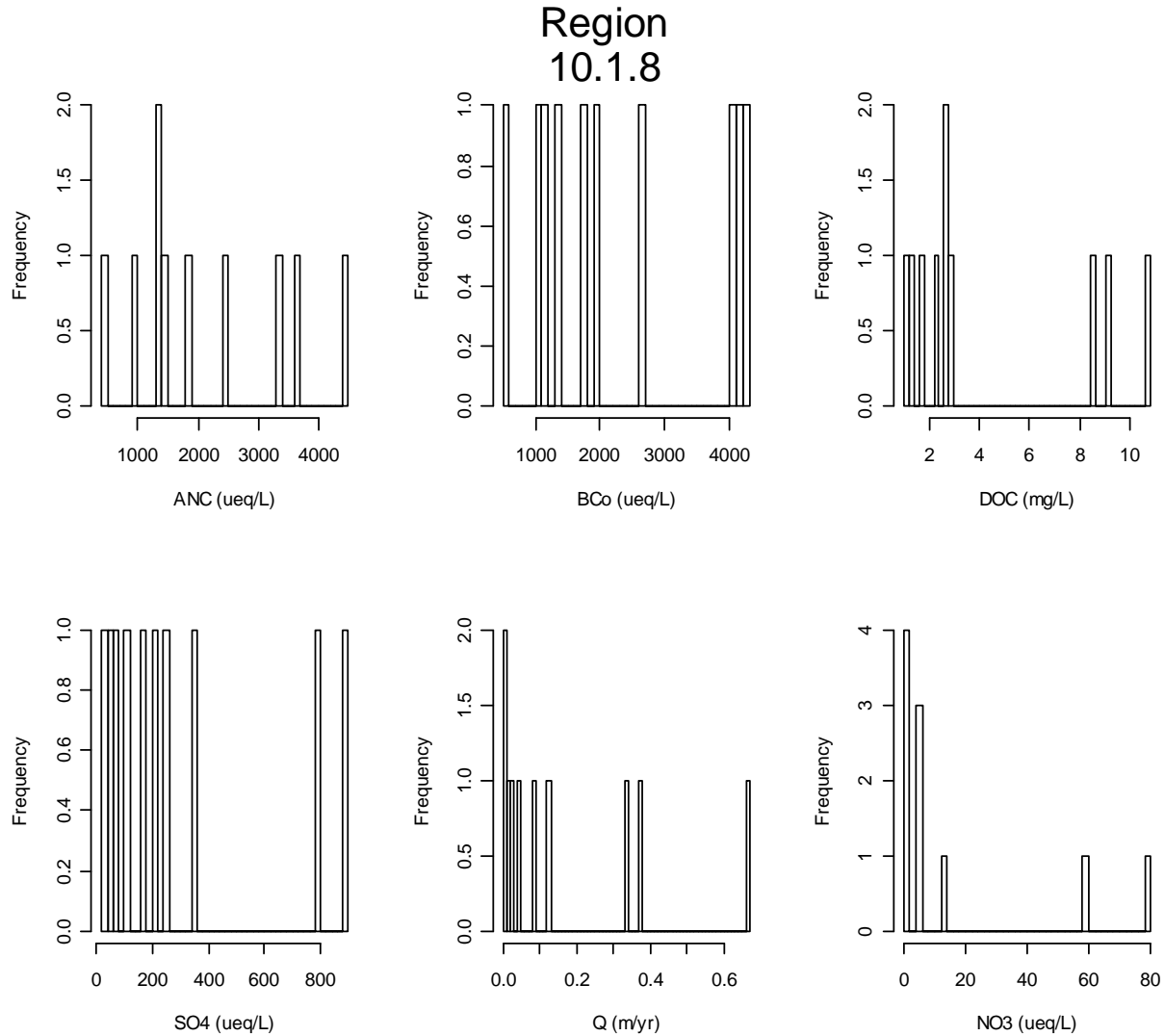


Figure C-92. Region 10.1.8 Water Quality Data Summary

Region 10.2 Warm Deserts

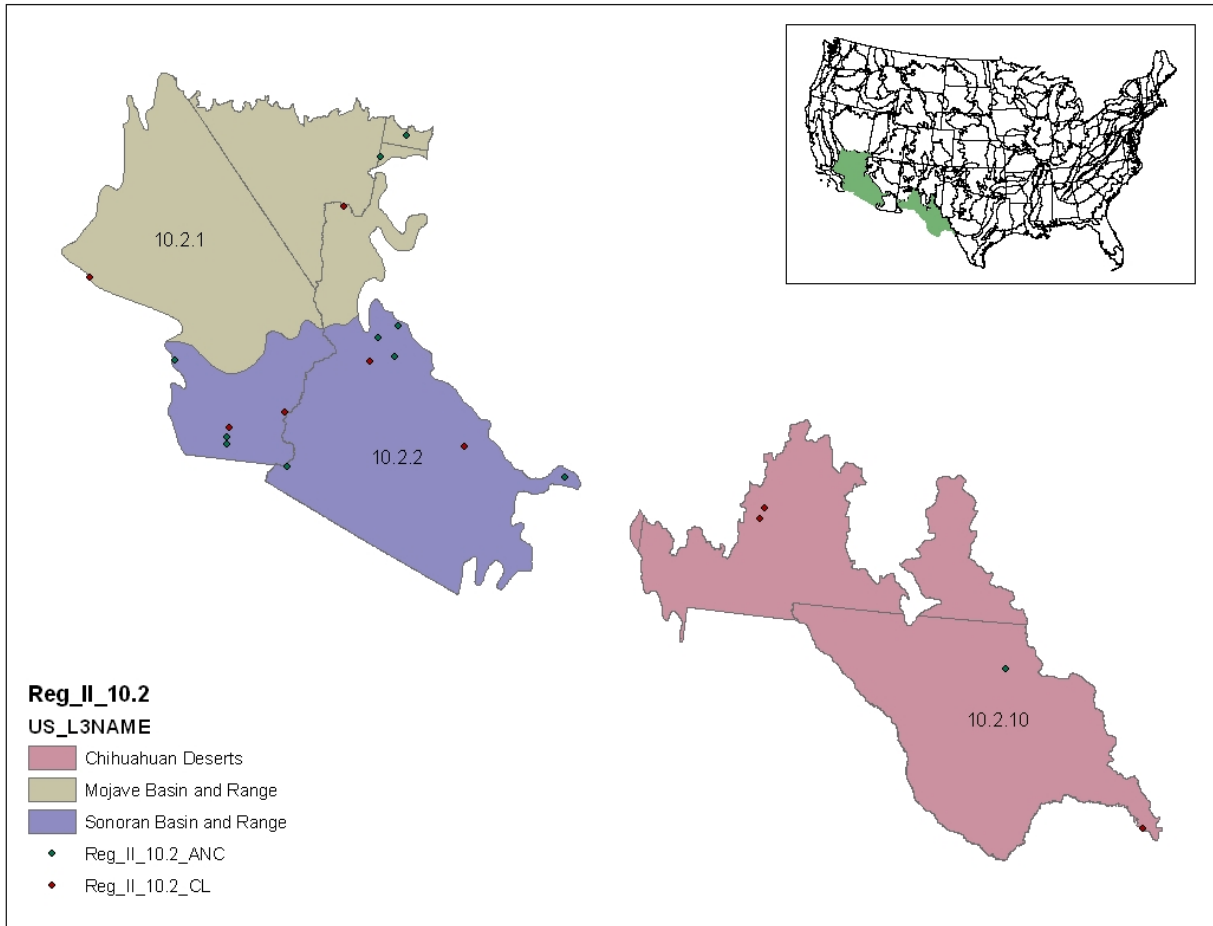


Figure C-93. Region 10.2

Region 10.2.1 Mojave Basin and Range

This ecoregion contains broad basins and scattered mountains that are generally lower, warmer, and drier, than those of the Central Basin and Range (10.1.5). Its creosote bush-dominated shrub community is distinct from the saltbush–greasewood and sagebrush–grass associations that occur to the north in the Central Basin and Range (10.1.5) and Northern Basin and Range (10.1.3); it is also differs from the palo verde–cactus shrub and saguaro cactus that occur in the Sonoran Basin and Range (10.2.2) to the south. Most of this region is federally owned and grazing is constrained by the lack of water and forage for livestock. Heavy use of off-road vehicles and motorcycles in some areas has made the soils susceptible to wind and water erosion.

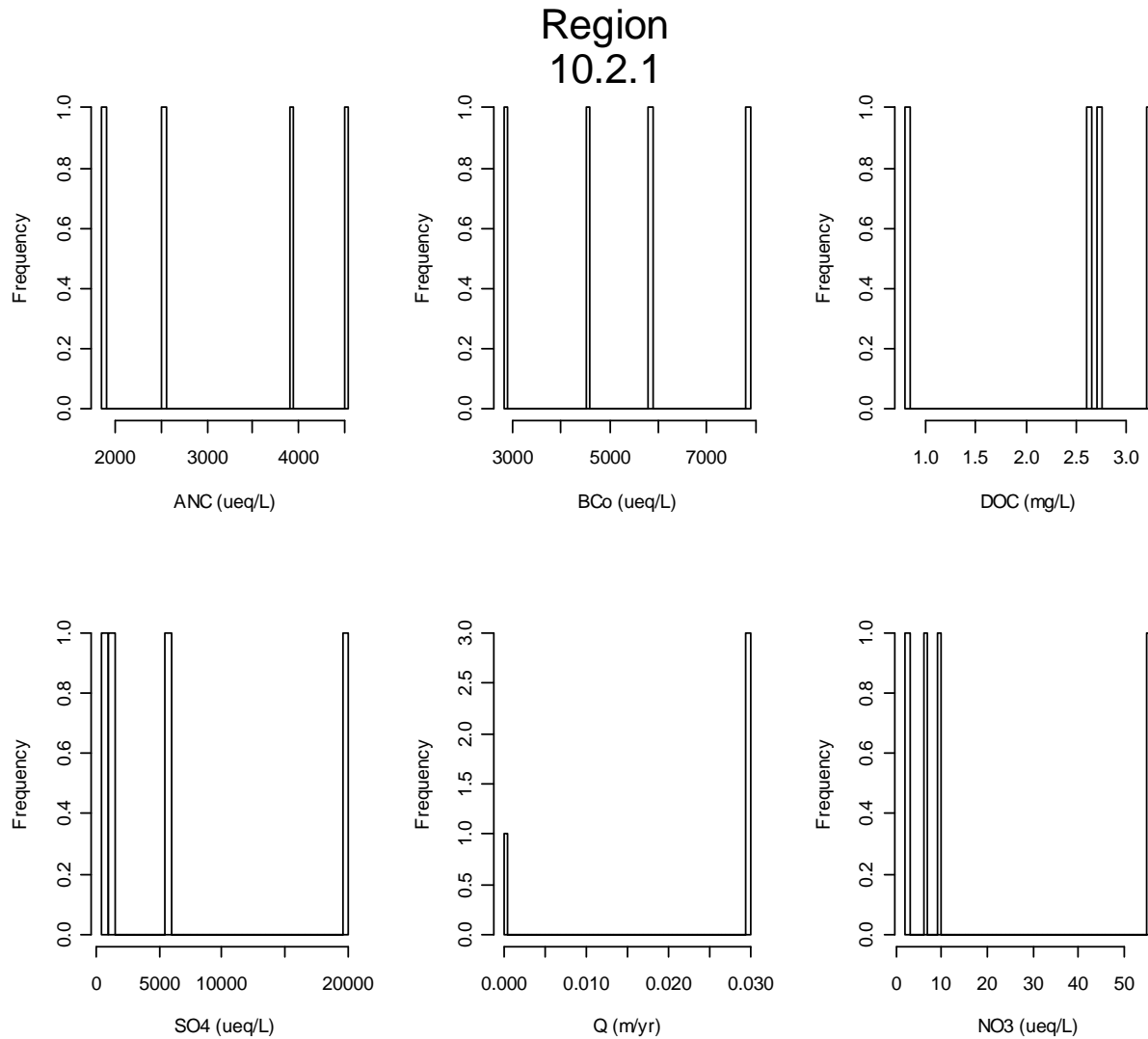


Figure C-94. Region 10.2.1 Water Quality Data Summary

Region 10.2.2 Sonoran Basin and Range

Similar in topography to the Mojave Basin and Range (10.2.1) to the north, this ecoregion contains scattered low mountains and has large tracts of federally owned land, a large portion of which is used for military training. However, the Sonoran Basin and Range is slightly hotter than the Mojave and contains large areas of palo verde-cactus shrub and giant saguaro cactus, whereas the potential natural vegetation in the Mojave is largely creosote bush. Winter rainfall decreases from west to east, while summer rainfall decreases from east to west.

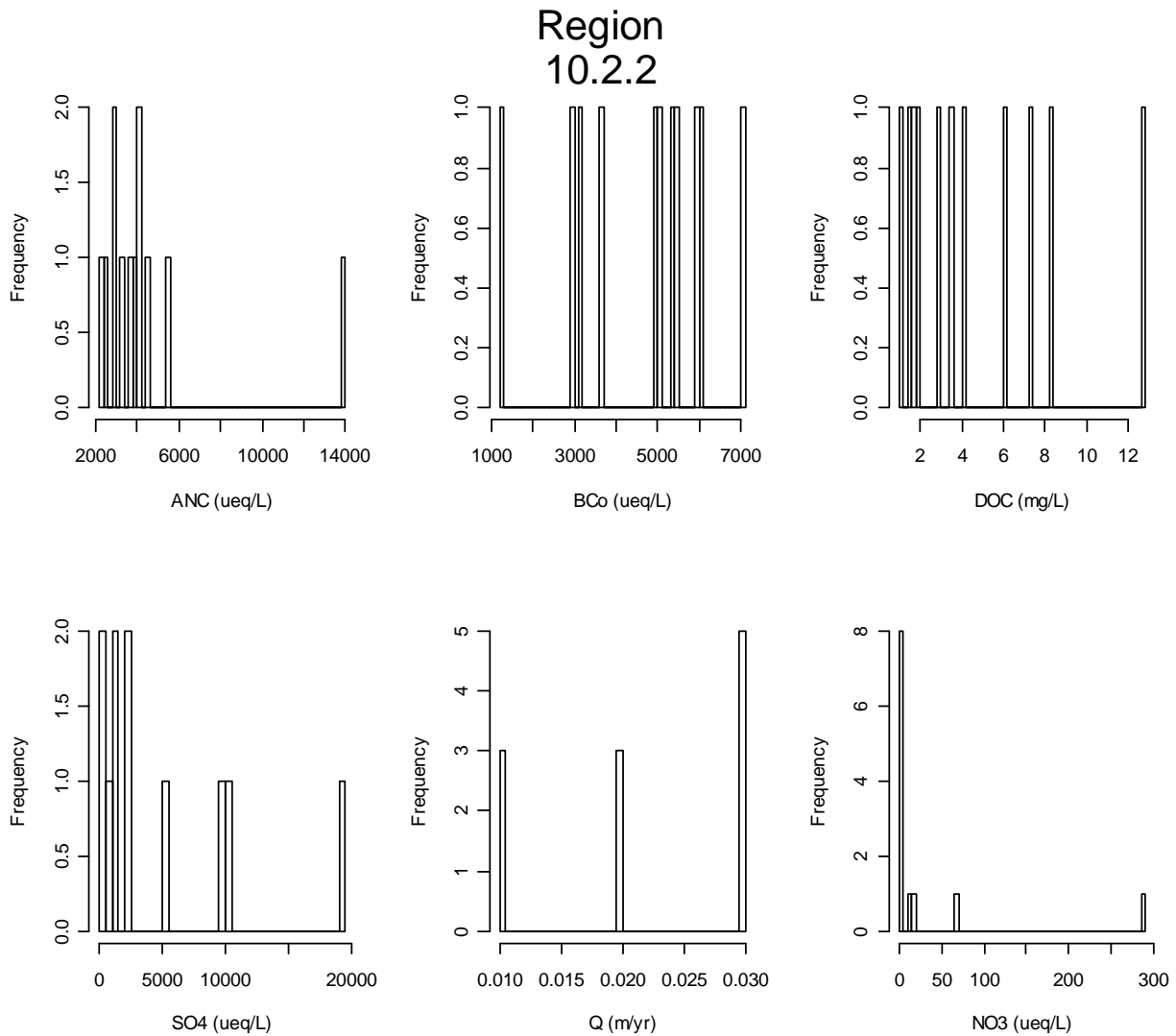


Figure C-95. Region 10.2.2 Water Quality Data Summary

Region 10.2.10 (10.2.4) Chihuahuan Deserts

This desert ecoregion extends from the Madrean Archipelago (12.1.1) in southeastern Arizona to the Edwards Plateau (9.4.6) in south-central Texas. The physiography is generally a continuation of basin and range terrain that is typical of the Mojave Basin and Range (10.2.1) and the Central Basin and Range (10.1.5) to the west and northwest, although the patterns of alternating mountains and valleys is not as pronounced as in Ecoregions 10.1.5 and 10.2.1. Vegetative cover is predominantly desert grassland and shrubland, except on the higher mountains where oak, juniper, and pinyon woodlands occur. The extent of desert shrubland is increasing across lowlands and mountain foothills due to the gradual desertification caused in part by historical grazing pressure.

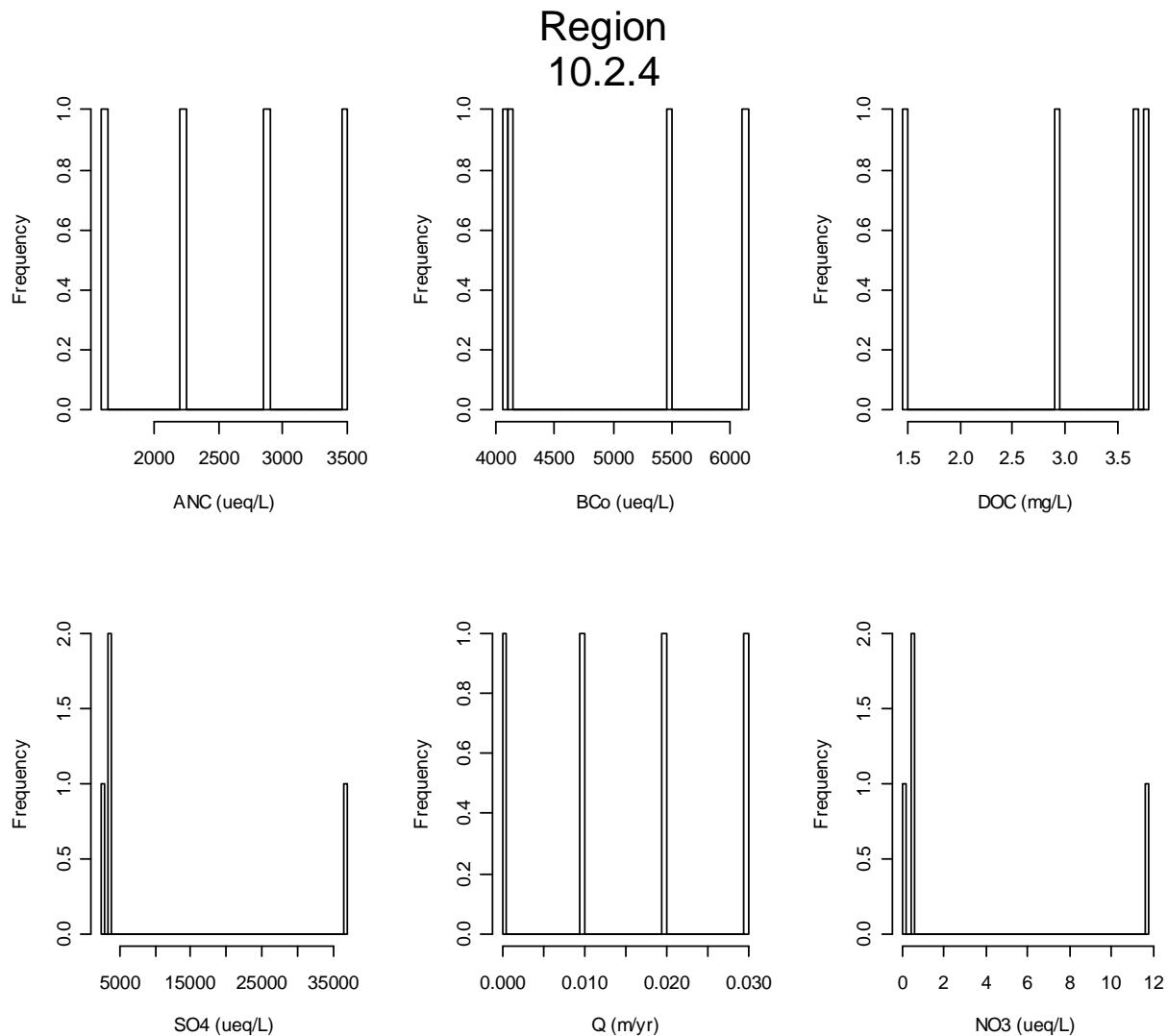


Figure C-96. Region 10.2.4 Water Quality Data Summary

Region 11.1 Mediterranean California

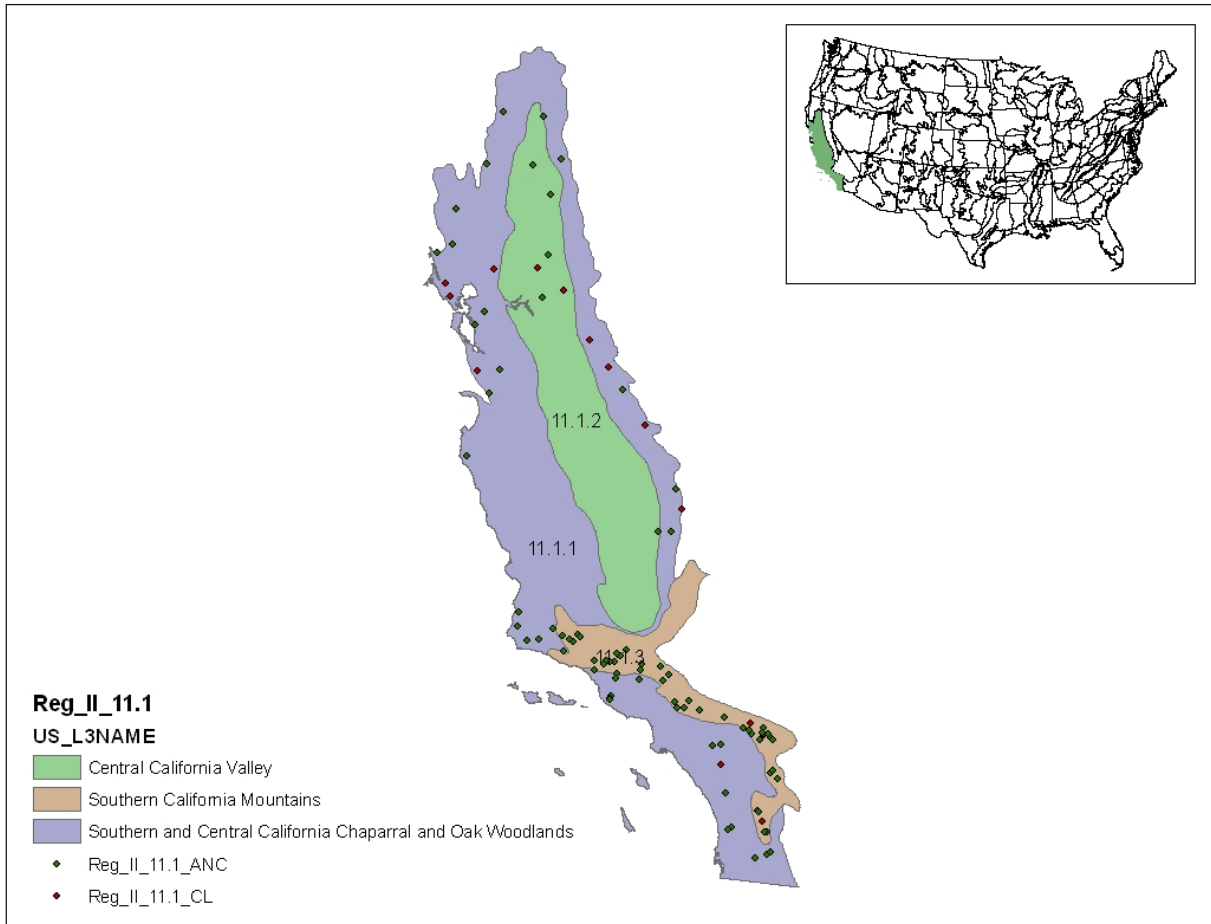


Figure C-97. Region 11.1

Region 11.1.1 Southern and Central California Chaparral and Oak Woodlands

The primary distinguishing characteristic of this ecoregion is its Mediterranean climate of hot dry summers and cool moist winters, and associated vegetative cover comprising mainly chaparral and oak woodlands; grasslands occur in some lower elevations and patches of pine are found at higher elevations. Most of the region consists of open low mountains or foothills, but there are areas of irregular plains in the south and near the border of the adjacent Central California Valley ecoregion. Large parts of the region are grazed by domestic livestock; relatively little land has been cultivated, although some valleys are or were important agricultural centers.

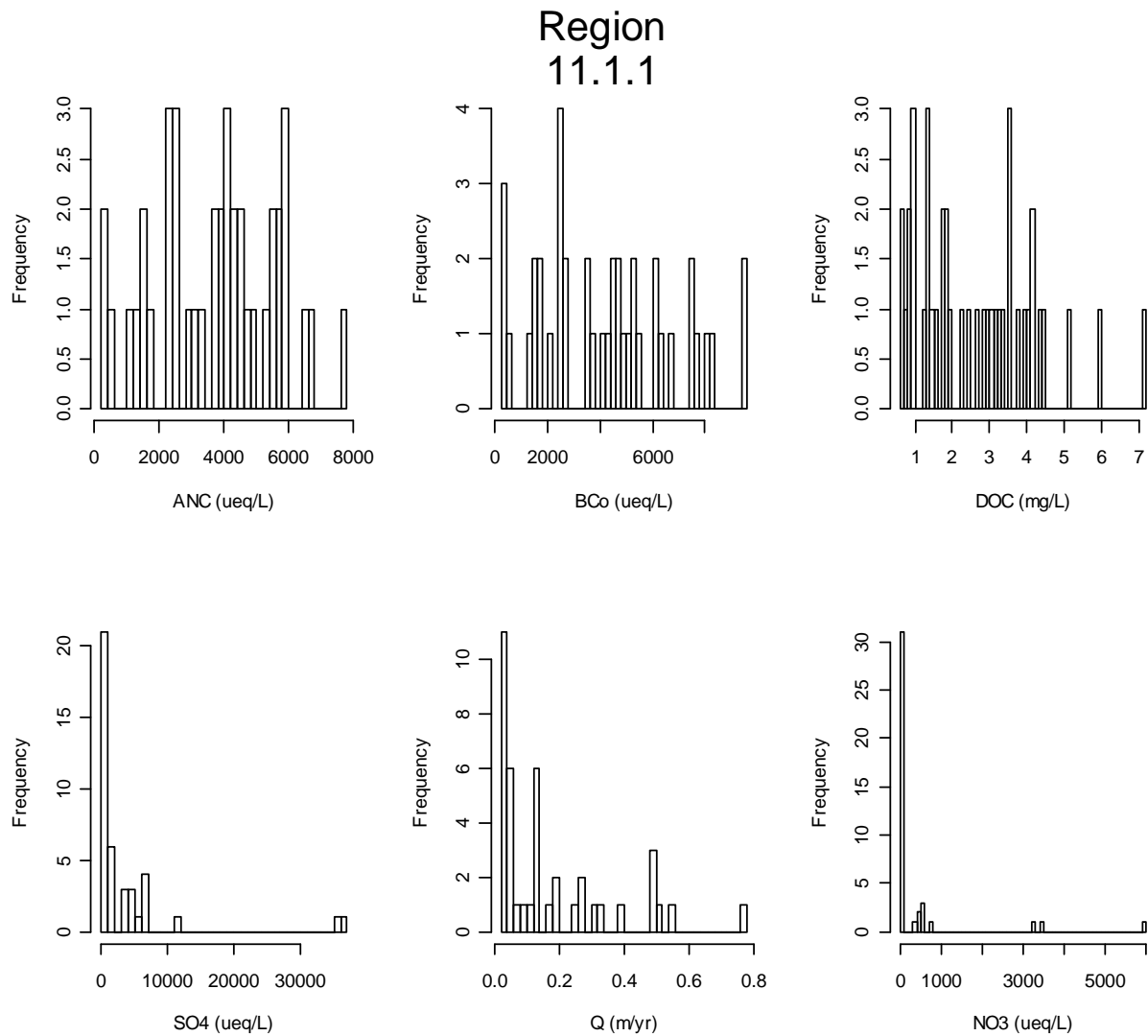


Figure C-98. Region 11.1.1 Water Quality Data Summary

Region 11.1.2 Central California Valley

This region is characterized by flat, intensively farmed plains having long, hot dry summers and mild winters, distinguish the Central California Valley from its neighboring ecoregions that are either hilly or mountainous, forest or shrub covered, and generally nonagricultural. Nearly half of the region is in cropland, about three fourths of which is irrigated. Environmental concerns in the region include salinity due to evaporation of irrigation water, groundwater contamination from heavy use of agricultural chemicals, wildlife habitat loss, and urban sprawl.

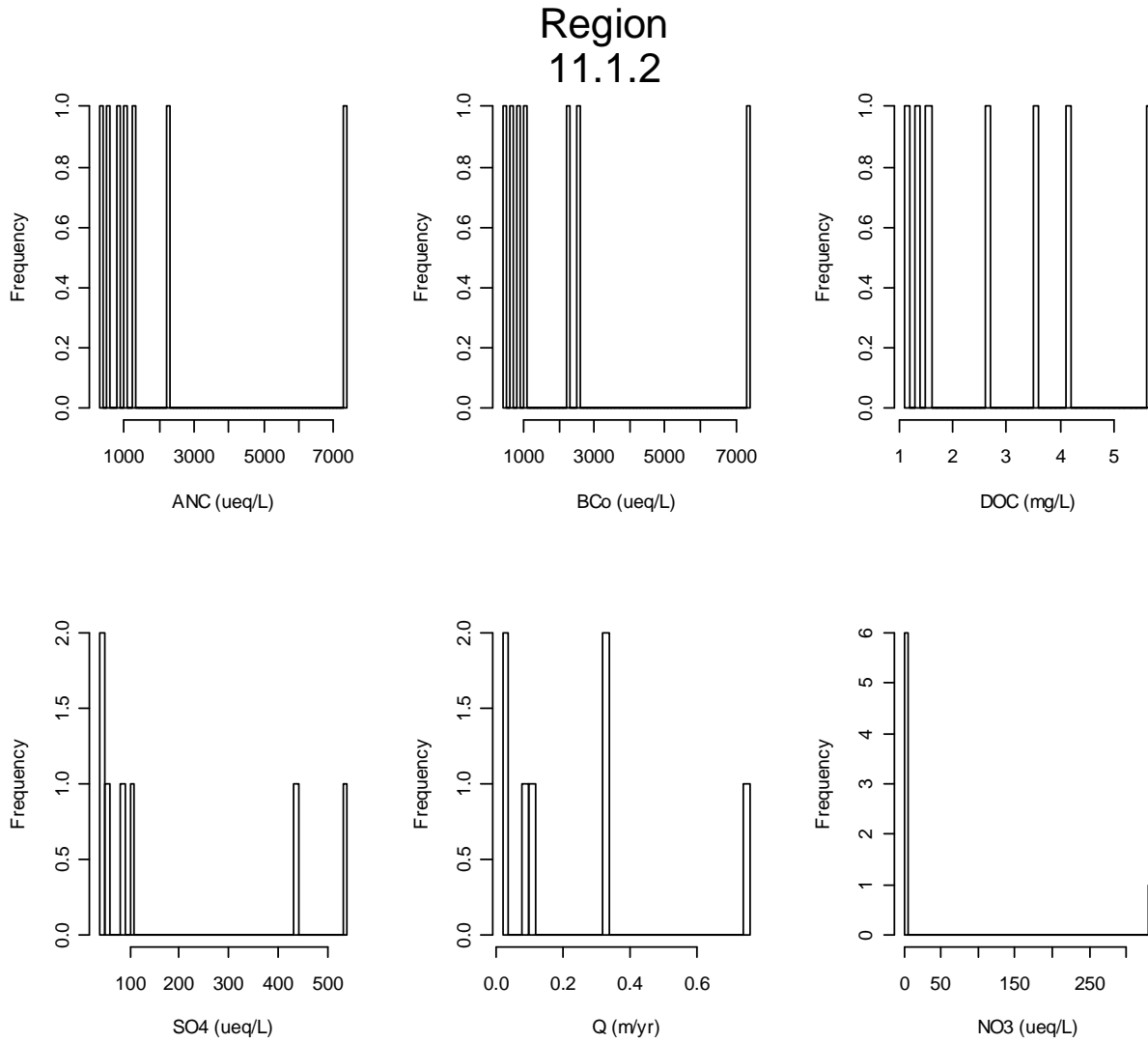


Figure C-99. Region 11.1.2 Water Quality Data Summary

Region 11.1.3 Southern California Mountains

Like the other ecoregions in central and southern California, the Southern California Mountains has a Mediterranean climate of hot dry summers and moist cool winters. Although Mediterranean types of vegetation such as chaparral and oak woodlands predominate in this region, the elevations are considerably higher, the summers are slightly cooler, and precipitation amounts are greater than in adjacent ecoregions, resulting in more dense vegetation and some large areas of coniferous woodlands. Severe erosion problems are common where the vegetation cover has been destroyed by fire or overgrazing.

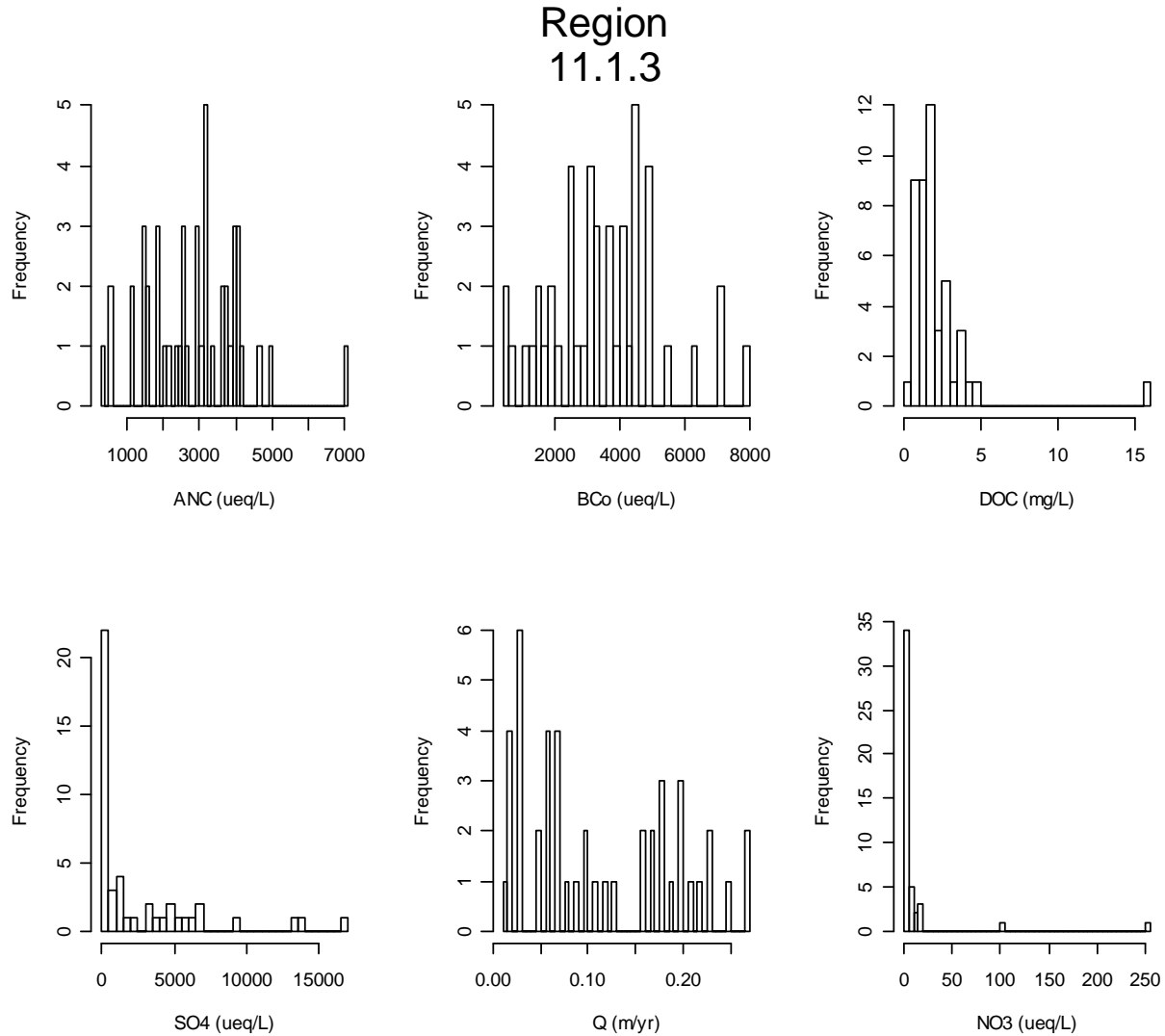


Figure C-100. Region 11.1.3 Water Quality Data Summary

Region 12.1 Western Sierra Madre Piedmont

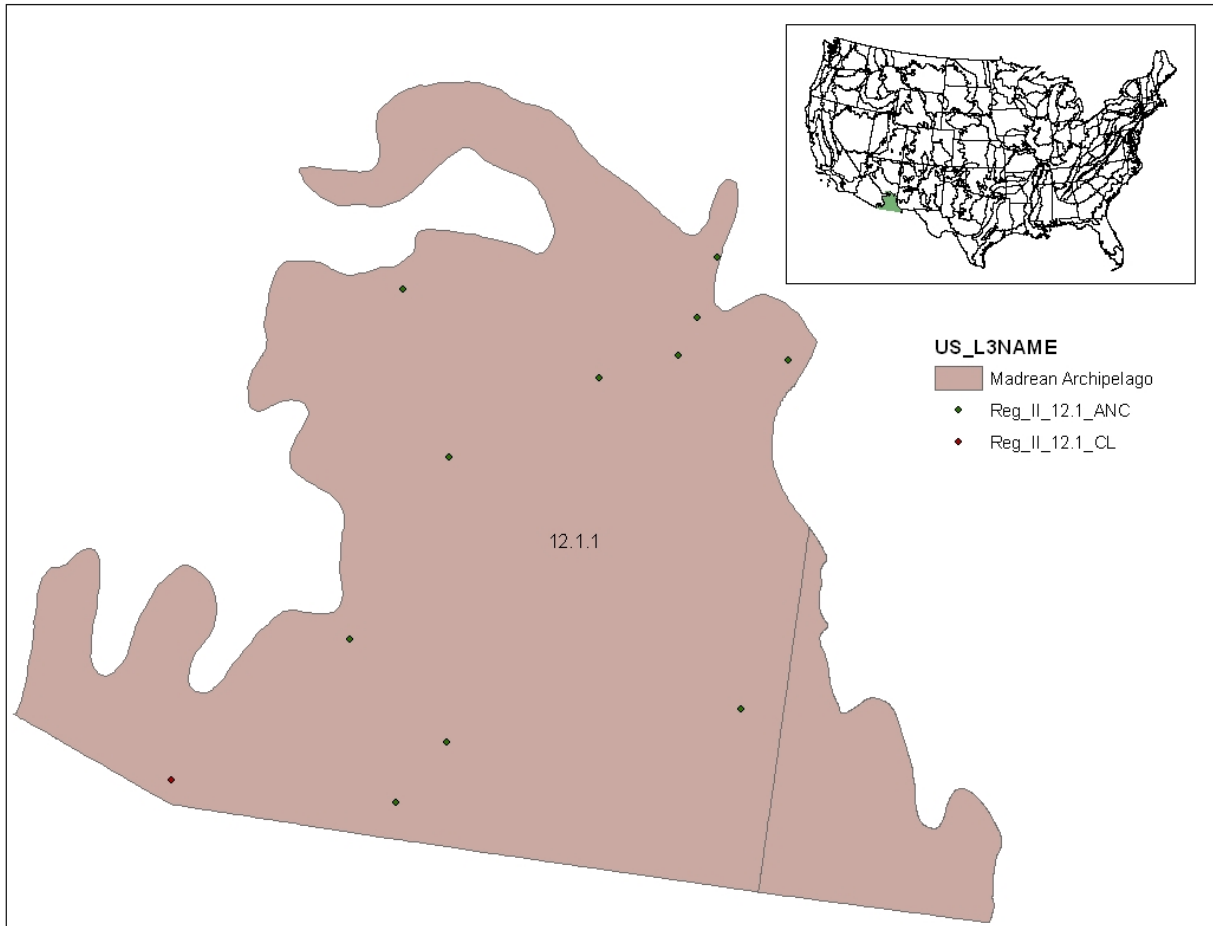


Figure C-101. Region 12.1

Region 12.1.1 Madrean Archipelago

Also known as the Sky Islands in the United States, this is a region of basins and ranges with medium to high local relief, typically 3,000 to 5,000 feet. Native vegetation in the region is mostly grama-tobosa shrubsteppe in the basins and oak-juniper woodlands on the ranges, except at higher elevations where ponderosa pine is predominant. The region has ecological significance as both a barrier and bridge between two major cordilleras of North America, the Rocky Mountains and the Sierra Madre Occidental.

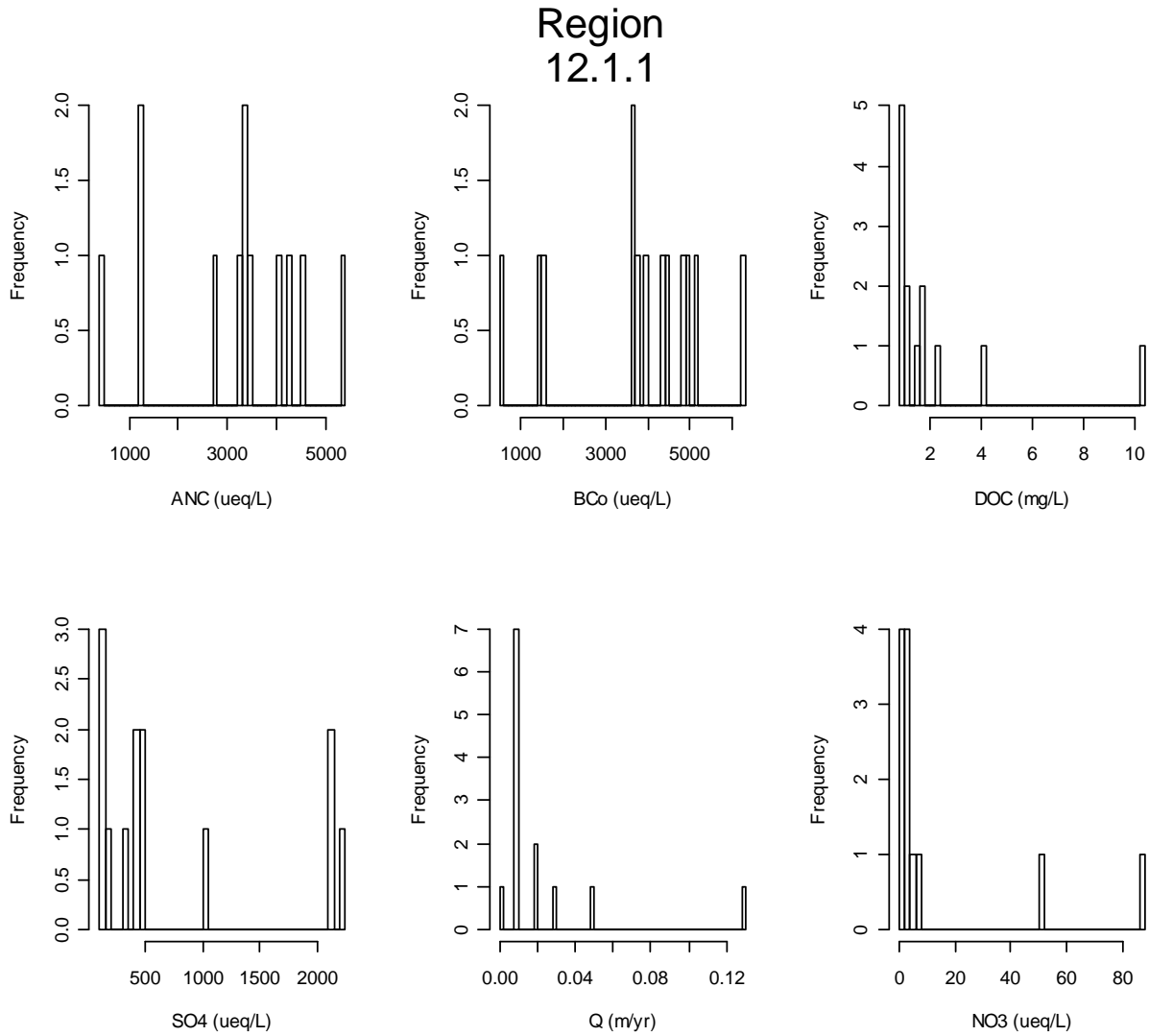


Figure C-102. Region 12.1.1 Water Quality Data Summary

Region 13.1 Upper Gila Mountains

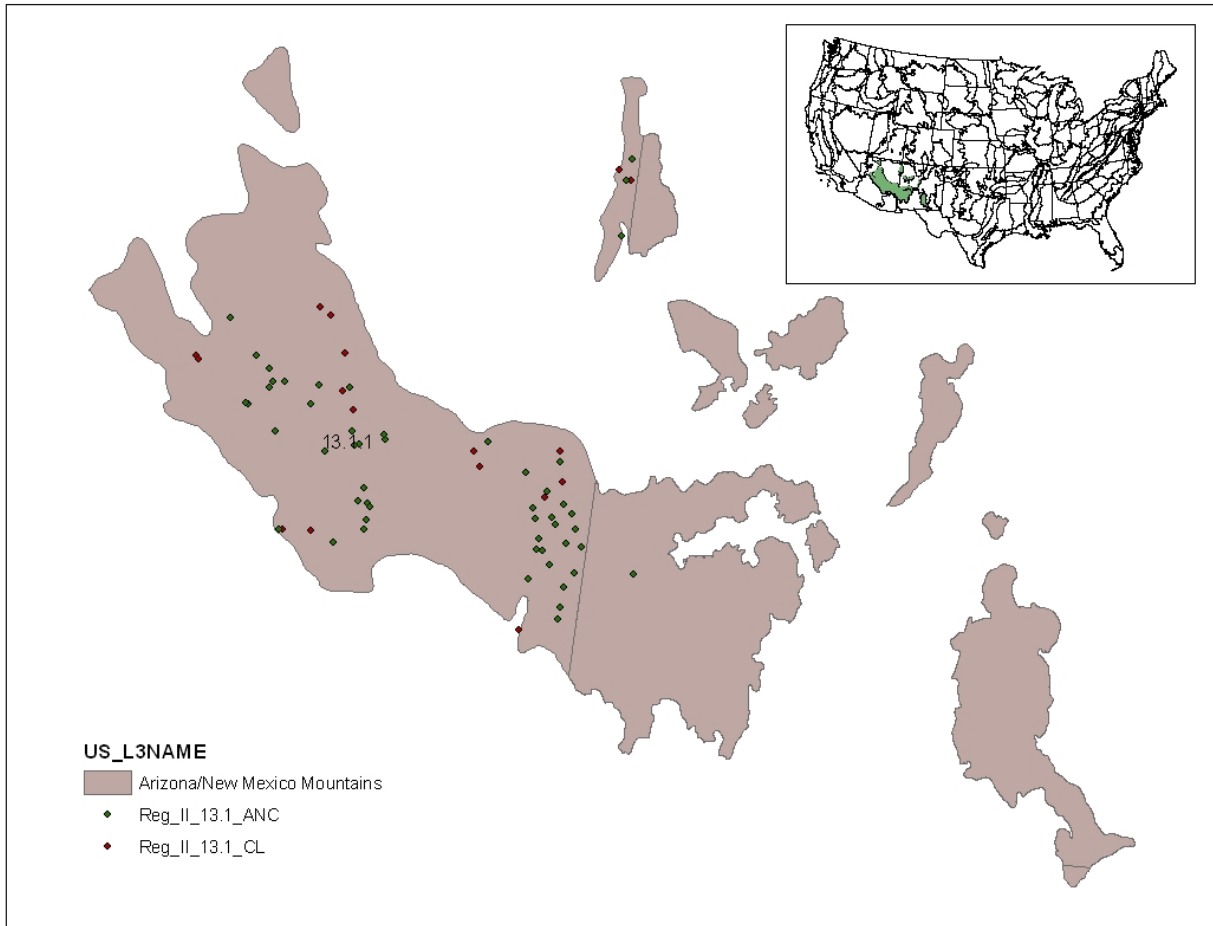


Figure C-103. Region 13.1

Region 13.1.1 Arizona/New Mexico Mountains

The Arizona/New Mexico Mountains are distinguished from neighboring mountainous ecoregions by their lower elevations and associated vegetation indicative of drier, warmer environments, which is due in part to the region's more southerly location. Forests of spruce, fir, and Douglas-fir, that are common in the Southern Rockies (6.2.14) and the Uinta and Wasatch Mountains (6.2.13), are only found in a few high elevation parts of this region. Chaparral is common on the lower elevations, pinyon-juniper and oak woodlands are found on lower and middle elevations, and the higher elevations are mostly covered with open to dense ponderosa pine forests. These mountains are the northern extent of some Mexican plant and animal species.

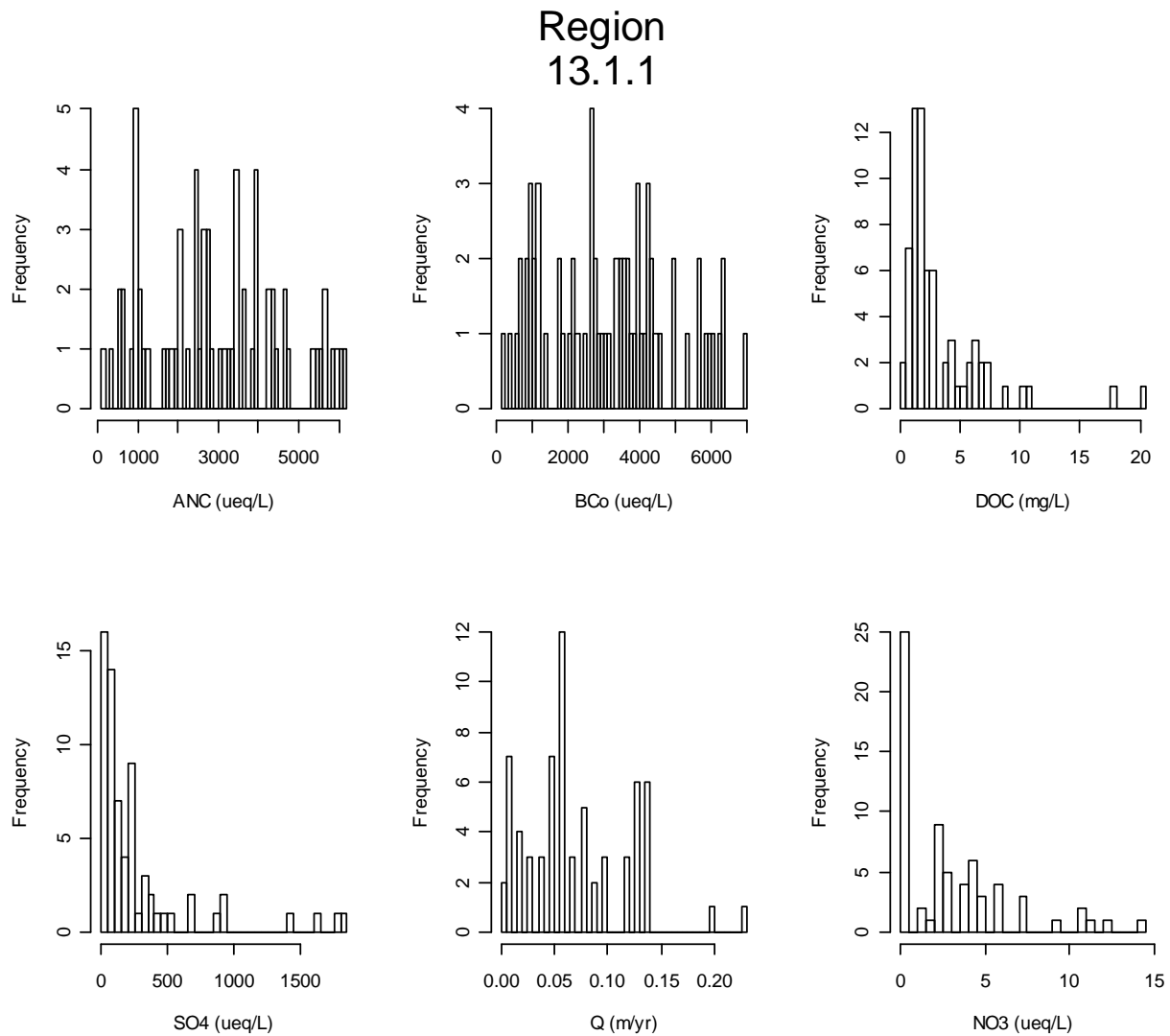


Figure C-104. Region 13.1.1 Water Quality Data Summary

Region 15.4 Everglades

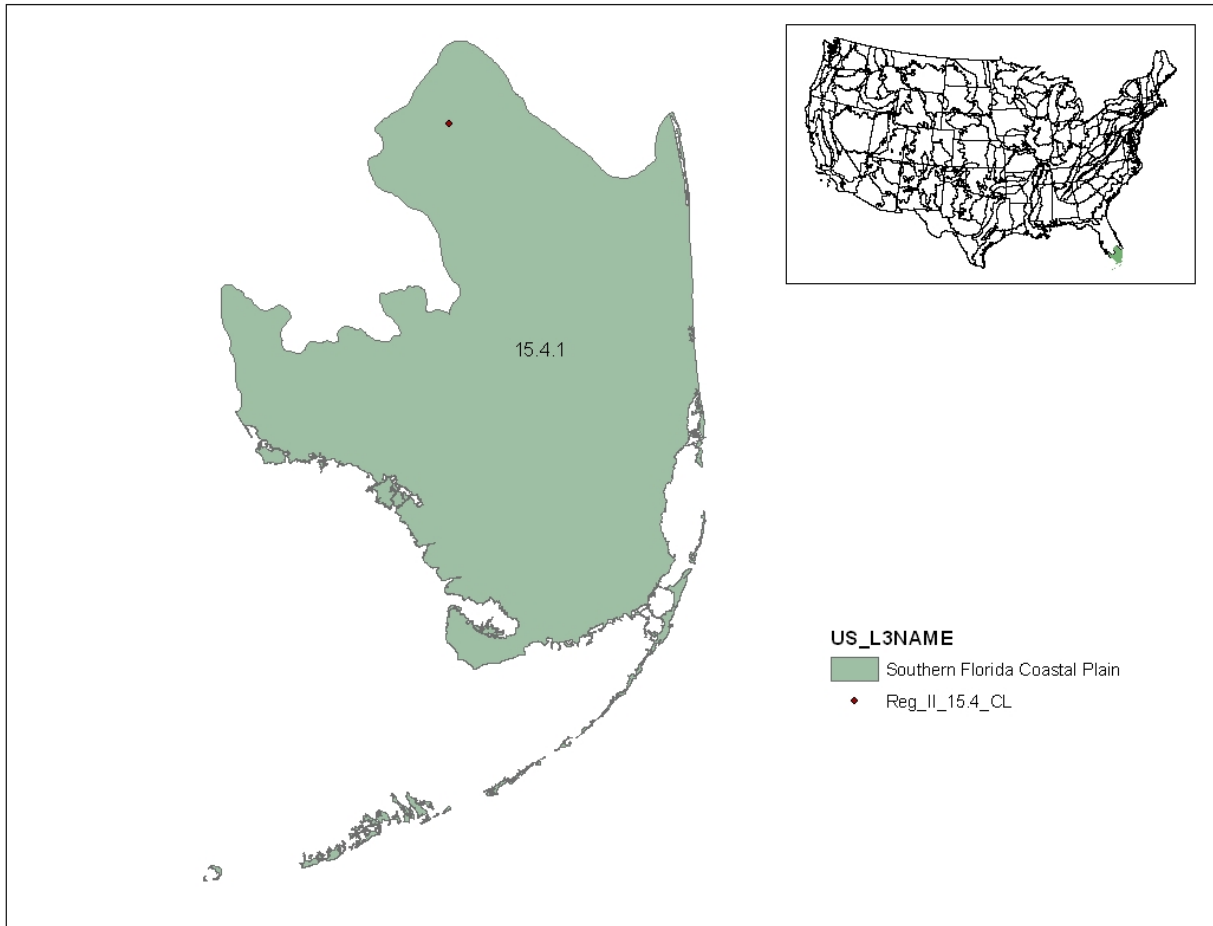


Figure C-105. Region 15.4

Region 15.4.1 Southern Florida Coastal Plain

The frost free climate of the Southern Florida Coastal Plain makes it distinct from other ecoregions in the conterminous United States. This region is characterized by flat plains with wet soils, marsh and swamp land cover with everglades and palmetto prairie vegetation types. Relatively slight differences in elevation and landform have important consequences for vegetation and the diversity of habitat types. Although portions of this region are in parks, game refuges, and Indian reservations, a large part of the region has undergone extensive hydrological and biological alteration.

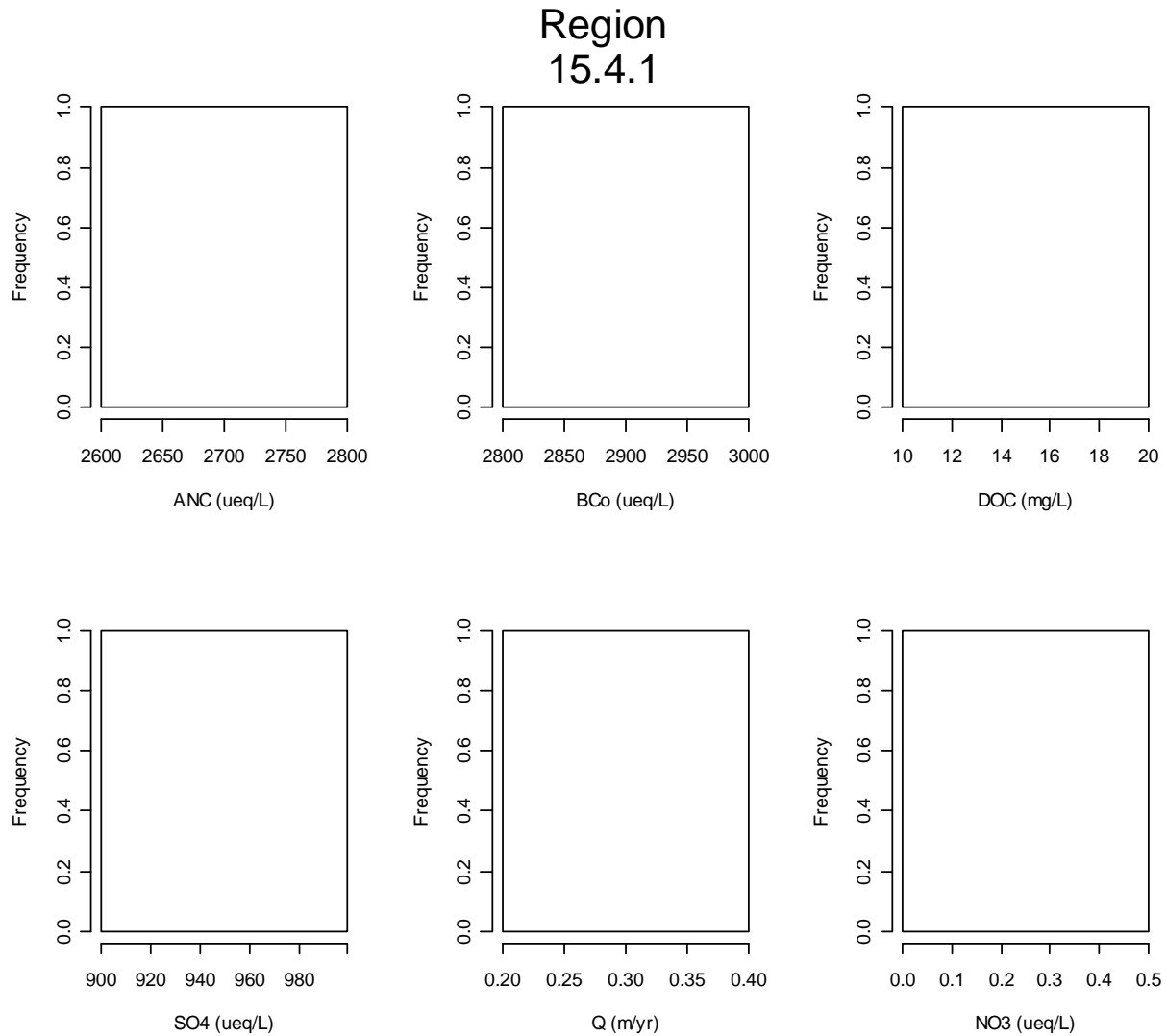


Figure C-106. Region 15.4.1 Water Quality Data Summary

Note: There is only one data point for this region.

References

US EPA. 2010. Primary Distinguishing Characteristics Of Level III Ecoregions Of The Continental United States, July, 2010. U.S. Environmental Protection Agency, Washington, DC. Available at http://www.epa.gov/wed/pages/ecoregions/level_iii_iv.htm.

Appendix D

Maps and calculation procedures for alternative standards

This appendix includes supplemental information that is referred to in section 7.5, *Considerations associated with alternative standards*. Section D.1 provides the calculation procedures used in calculating the AAI values; D.2 provides maps of ecoregions not likely meeting alternative standards and summary tables of all related calculations; D.3 provides the critical loads for all acid sensitive ecoregions, calculated AAI values and critical loads for relatively non-acid sensitive regions, and CMAQ deposition values and transference ratios for each region; and D.4 provides further explanation of calculations in the context of combinations of NO_y and SO_x, concentrations and associated deposition, as well as illustrating the effect of Neco on calculations.

D.1 Analytical approach and data sources

Results of this assessment are based on calculating AAIs for alternative standards using the range of levels (20, 35, 50, 75) and nth percentiles (70, 75, 80, 85, 90) discussed in section 7.4. Because we have modeled data only as a source of deposition and concentration fields, CMAQ output for concentration fields, transference ratios, and deposition values enables applications for calculating AAI values using equation 7-11.

$$ANC_{calc} = \{ANC_{lim} + CL_r/Q_r\} - NHx/Q_r - T_{NOy} [NOy]/Q_r - T_{SOx} [SOx]/Q_r \quad (7-11)$$

Calculations procedures:

1. Assemble current deposition and concentration fields using the annual average value of each grid cell and then averaged over the grid cells of the ecoregion of interest.

$$Ndep = NHxdep + NOydep$$

All depositions are in values of meq/m²-yr

2. Calculate CL_{I(ANClim,%)};

$$CL_{I(ANC,\%)} = ([BC^*_0]_{anclim,\%} - [ANC_{lim}])Q_{ANClim,\%} + Neco$$

Where the ANClim,% refers to the specified target ANC level and the specific water body representing the nth percentile critical load in the ecoregion.

$([BC]_{0,\%}^*$ is calculated with water quality data (major cations, NO₃ and SO₄) as described in Appendix B)

$$Neco = \sum (Ndep - Nleach_i)/n$$

3. Determine if $Neco > Ndep$
4. Calculate deposition exceedance, and check for Neco conditions:
 $DEPex = Ndep + Sdep - (([BC]_{0,\%}^* - [ANC_{lim}])Q\% + Neco\%), Ndep > Neco$
 $DEPex = Sdep - ([BC]_{0,\%}^* - [ANC_{lim}])Q\%, Ndep < Neco$
5. Calculate an AAI value, which essentially is a design value at the ecoregion level:
Calculated AAI = Level (as ANClim) - DEPex/QR

As described in section 7.2, this calculation procedure using deposition exceedances is the basis for deriving equation 7-11, and the AAI calculations using this approach is identical, algebraically, to using equation 7-11 directly.

Data sources used in the exceedance analyses.

The AAI calculations require estimates of current time frame N and S deposition, observed water quality major cations (CA, Mg, K) and strong anions (NO₃, SO₄) and runoff rates, summarized in Table D-1. The 2005 and emissions sensitivity CMAQ simulations were applied at 12 km horizontal grid cell resolution and provided all deposition and concentration estimates. Water quality data were based on TIME/LTM and other data bases as described in chapter 2. The representative critical loads for each ecoregion are provided in Table D.2.

Table D-1. Data sources for calculating AAI's.

| Parameter | Description | Data source | Notes |
|-------------------|---|--|--|
| Ndep | Sum of wet and dry NO _y and NH _x deposition | 2005 12 CMAQ base case | meq/(m ² -yr), average of all 12 km grid cells within ecoregion |
| NH _x | Sum of wet and dry NH _x deposition | 2005 12 CMAQ base case | meq/(m ² -yr), average of all 12 km grid cells within ecoregion |
| Sdep | Sum of wet and dry SO ₂ and SO ₄ deposition | 2005 12 CMAQ base case | meq/(m ² -yr), average of all 12 km grid cells within ecoregion |
| Nleach | Outflow water column concentration of NO ₃ | TIME/LTM and STORET data bases (Table 2-4) | μeq/l; average of all water bodies in an ecoregion |
| BC* _{0%} | Preindustrial base cation levels | TIME/LTM and STORET data bases (Table 2-4) | μeq/l; based on the % water body |
| Q | Annual runoff rate | USGS (Table 2-4) | m/yr; based on the % water body |
| Q _r | Ecoregion representative Annual runoff rate | USGS (Table 2-4) | m/yr; based on the 50 % water body |

D.2 Maps and tables of ecoregions not meeting alternative standards.

Figures D-1 through D-9 are illustrative maps of ecoregions likely not meeting alternative standards based on current (2005) conditions and an emissions sensitivity simulation of approximately 42% and 48% SO_x and NO_x emission reductions across the U.S. Table D-2a –D-2d include all of the calculated AAI values for the range alternative standards considered.

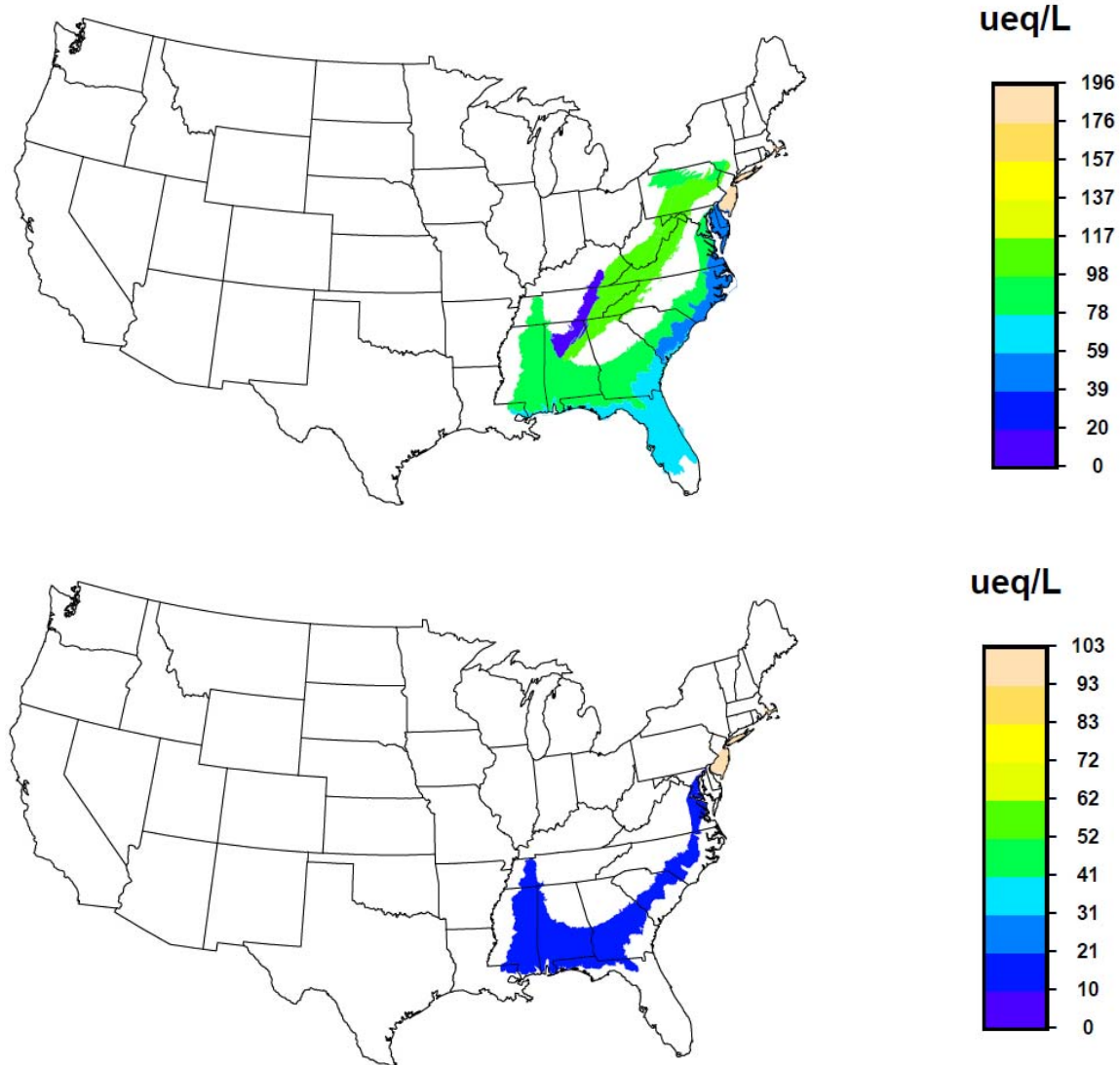


Figure D-1. Acid sensitive ecoregion level III areas likely not meeting the standard when the level = 35 $\mu\text{eq/L}$ and the form is based on the 70th percentile water body; based on CMAQ 2005

(top) and emissions sensitivity(bottom) simulations. The legend reflects the magnitude of the exceedance relative to the specified level of the standard.

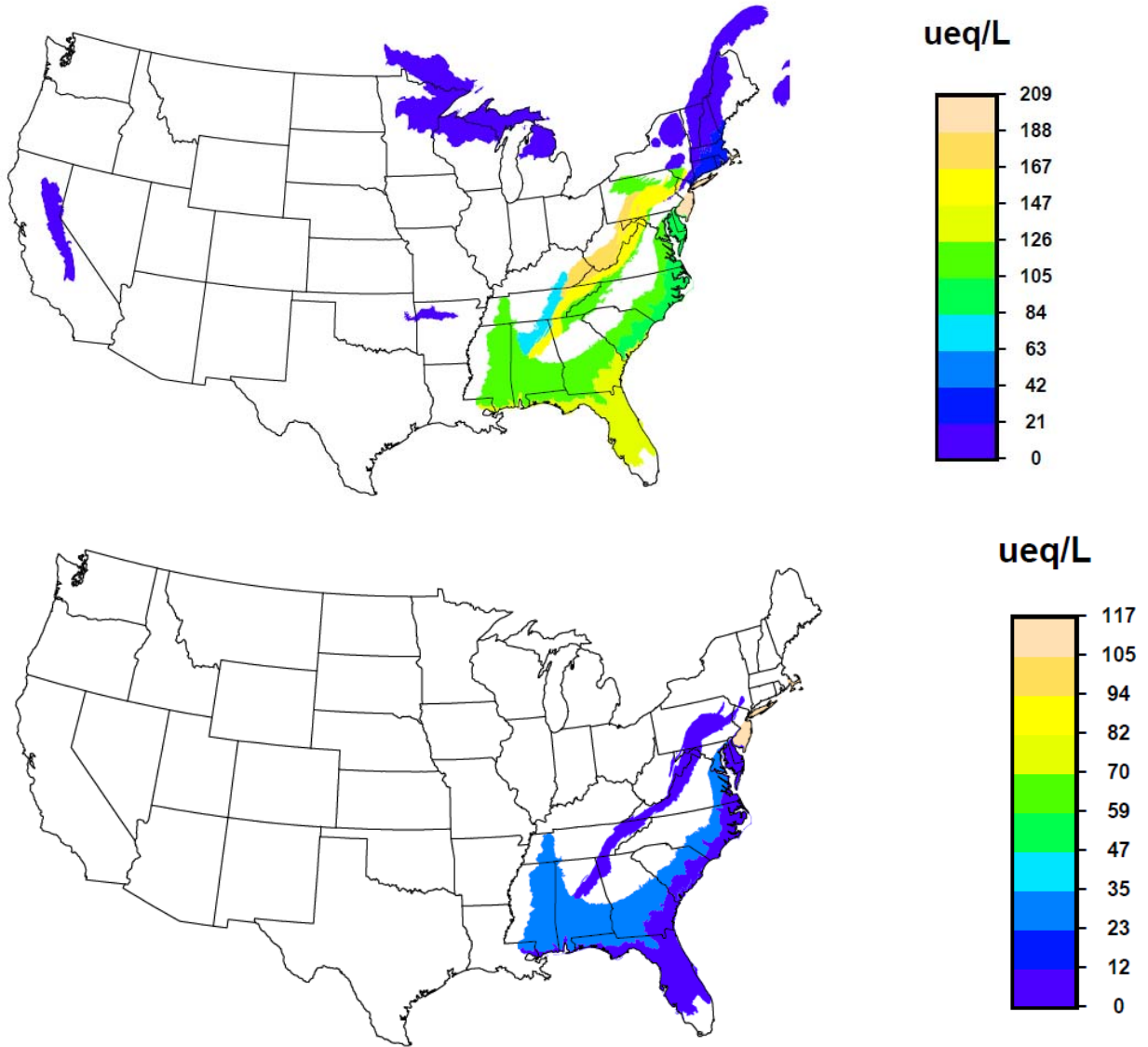


Figure D-2. Acid sensitive ecoregion level III areas likely not meeting the standard when the level = 35 $\mu\text{eq/L}$ and the form is based on the 80th percentile water body; based on CMAQ 2005 (top) and emissions sensitivity(bottom) simulations. The legend reflects the magnitude of the exceedance relative to the specified level of the standard.

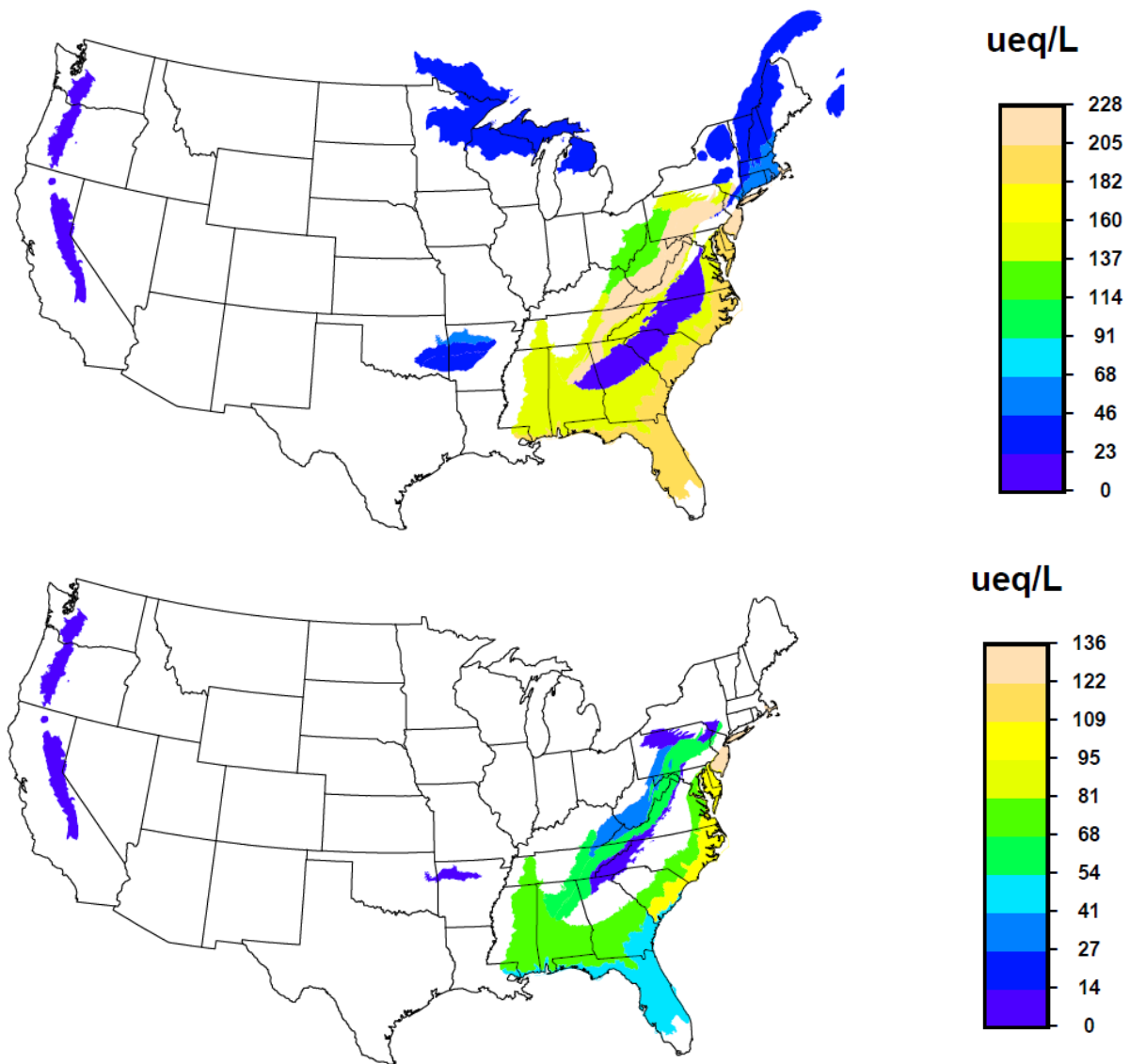


Figure D-3. Acid sensitive ecoregion level III areas likely not meeting the standard when the level = 35 µeq/L and the form is based on the 90th percentile water body; based on CMAQ 2005 (top) and emissions sensitivity(bottom) simulations. The legend reflects the magnitude of the exceedance relative to the specified level of the standard.

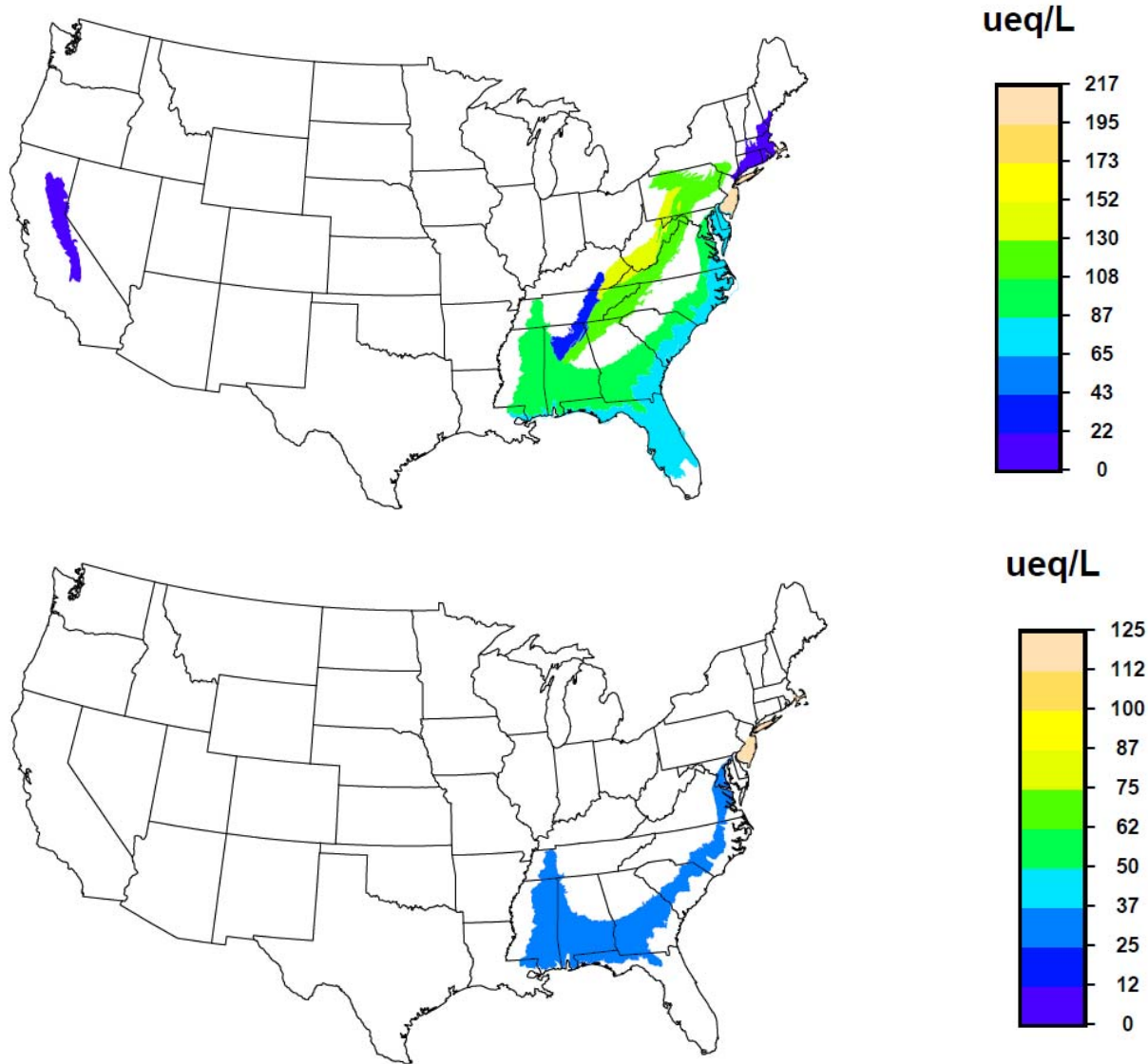


Figure D-4. Acid sensitive ecoregion level III areas likely not meeting the standard when the level = 50 $\mu\text{eq/L}$ and the form is based on the 70th percentile water body; based on CMAQ 2005 (top) and emissions sensitivity(bottom) simulations. The legend reflects the magnitude of the exceedance relative to the specified level of the standard.

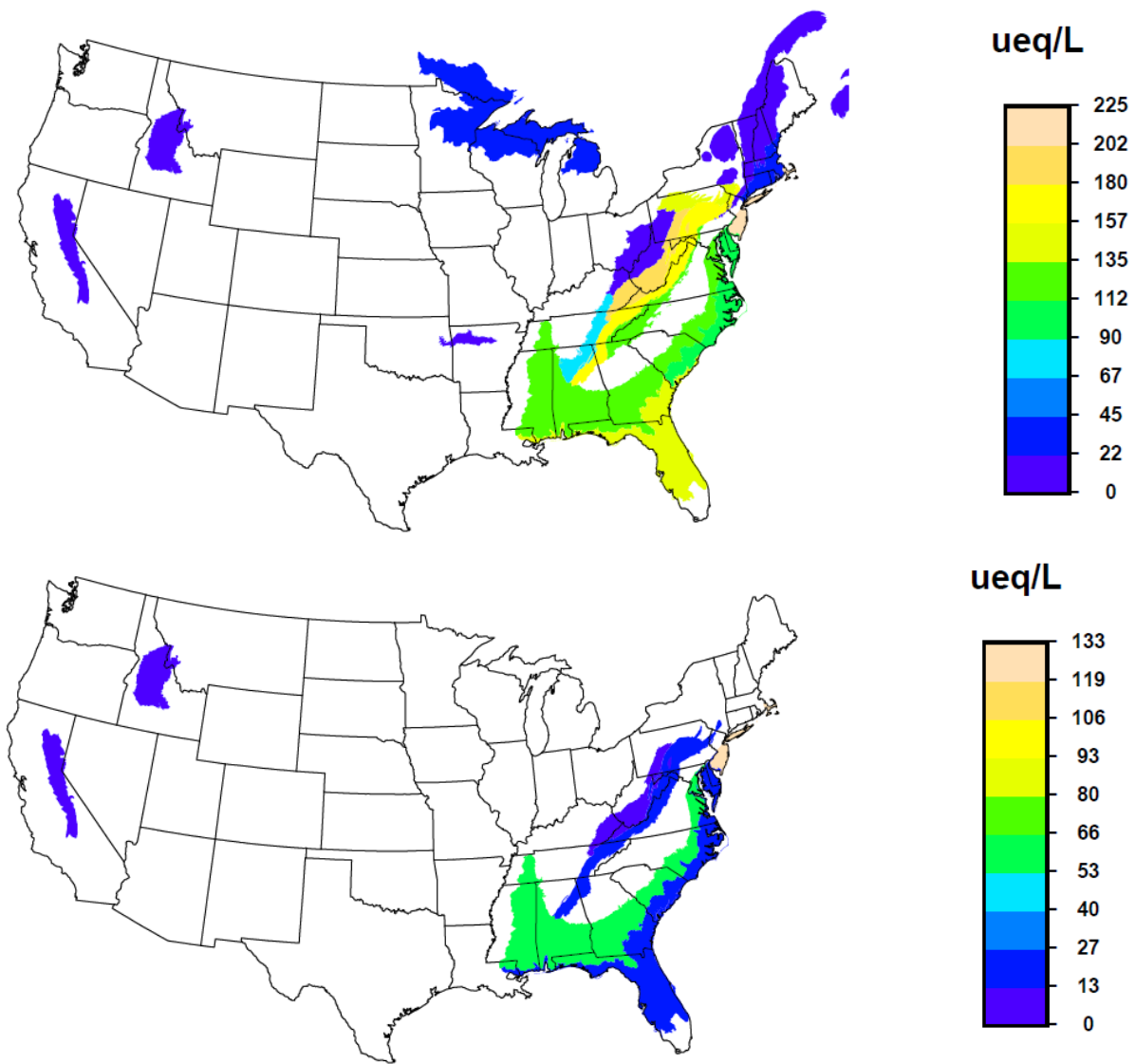


Figure D-5. Acid sensitive ecoregion level III areas likely not meeting the standard when the level = 50 µeq/L and the form is based on the 80th percentile water body; based on CMAQ 2005 (top) and emissions sensitivity(bottom) simulations. The legend reflects the magnitude of the exceedance relative to the specified level of the standard.

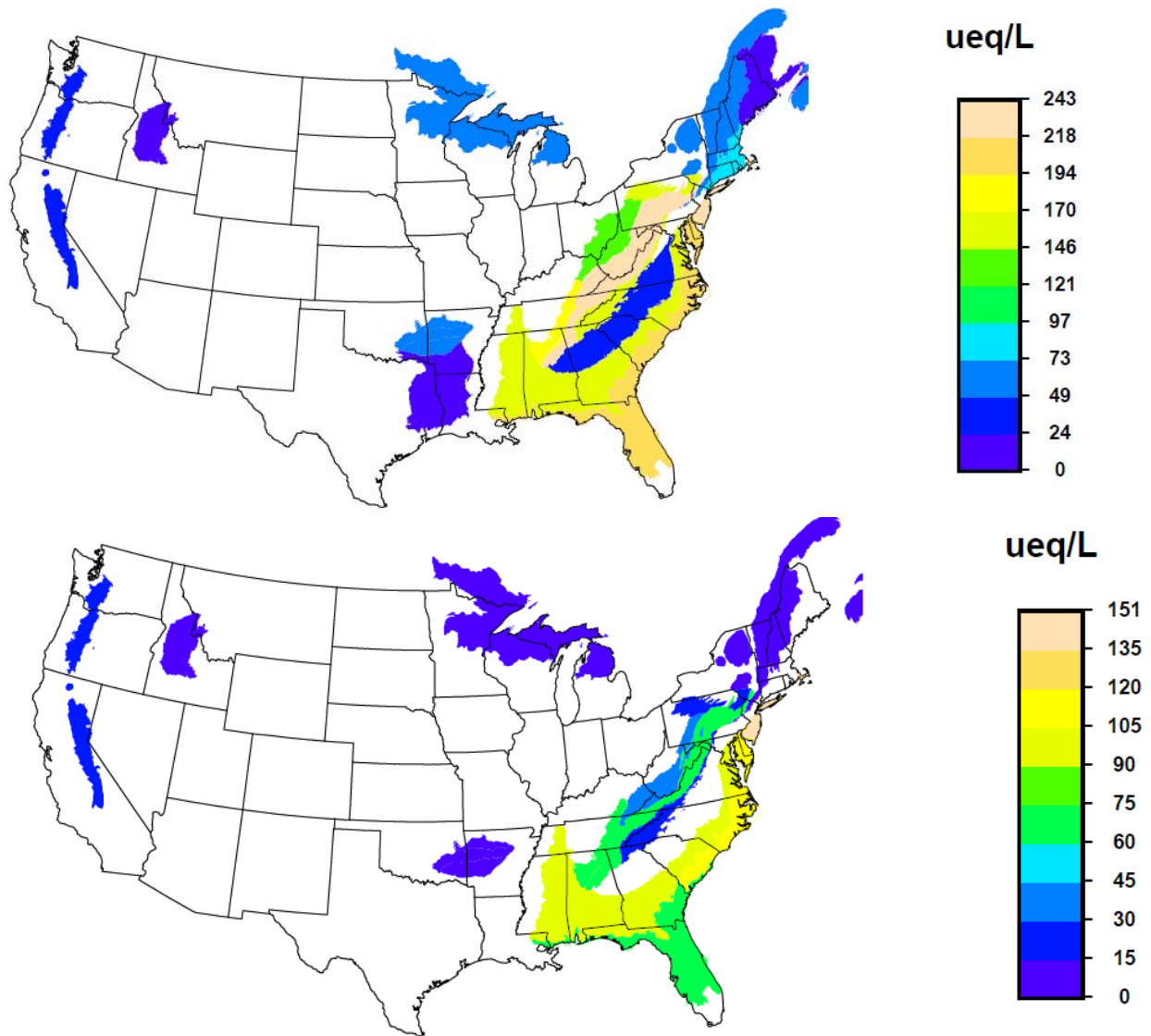


Figure D-6. Acid sensitive ecoregion level III areas likely not meeting the standard when the level = 50 $\mu\text{eq/L}$ and the form is based on the 90th percentile water body; based on CMAQ 2005 (top) and emissions sensitivity(bottom) simulations. The legend reflects the magnitude of the exceedance relative to the specified level of the standard.

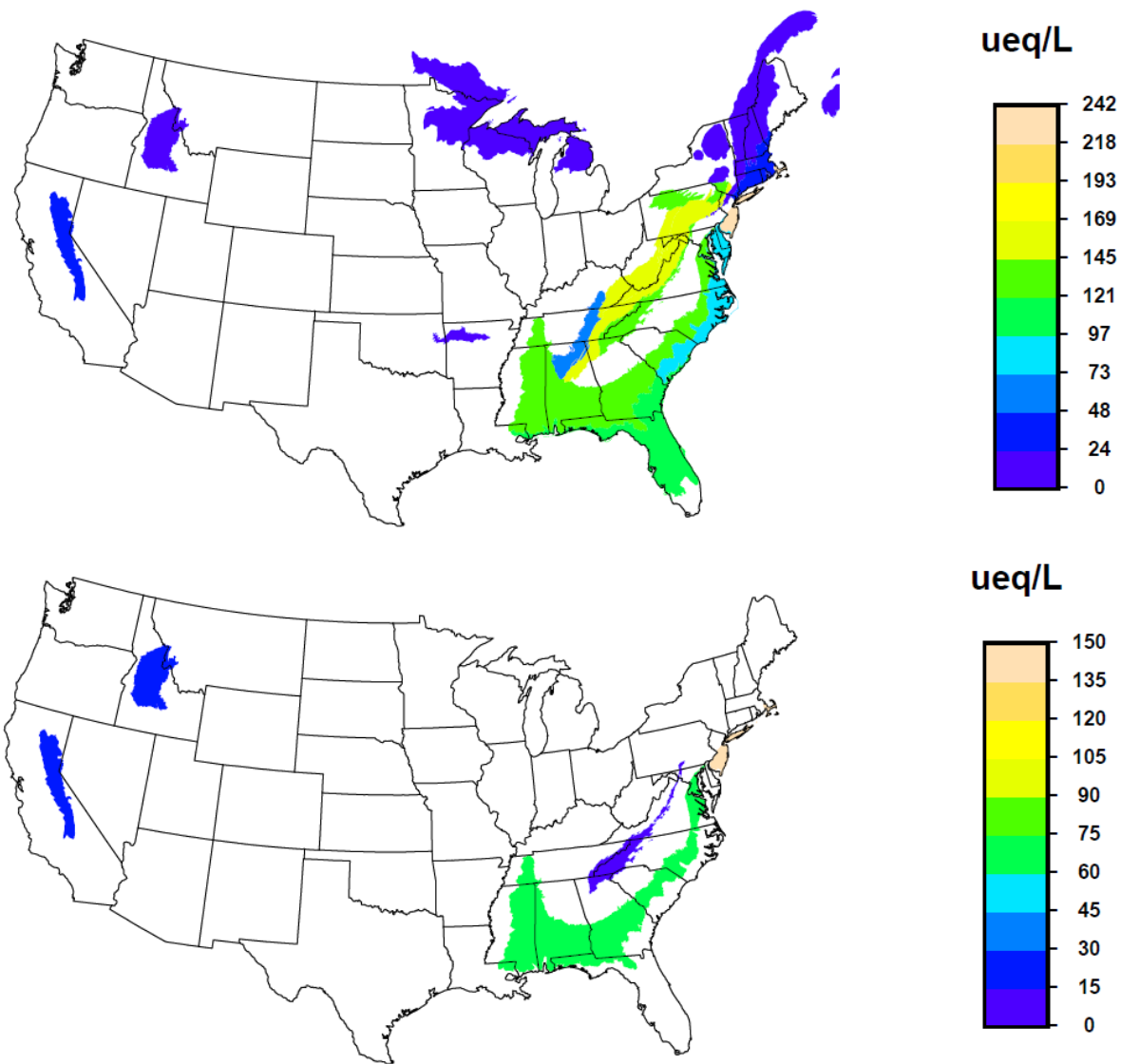


Figure D-7. Acid sensitive ecoregion level III areas likely not meeting the standard when the level = 75 $\mu\text{eq/L}$ and the form is based on the 70th percentile water body; based on CMAQ 2005 (top) and emissions sensitivity(bottom) simulations. The legend reflects the magnitude of the exceedance relative to the specified level of the standard.

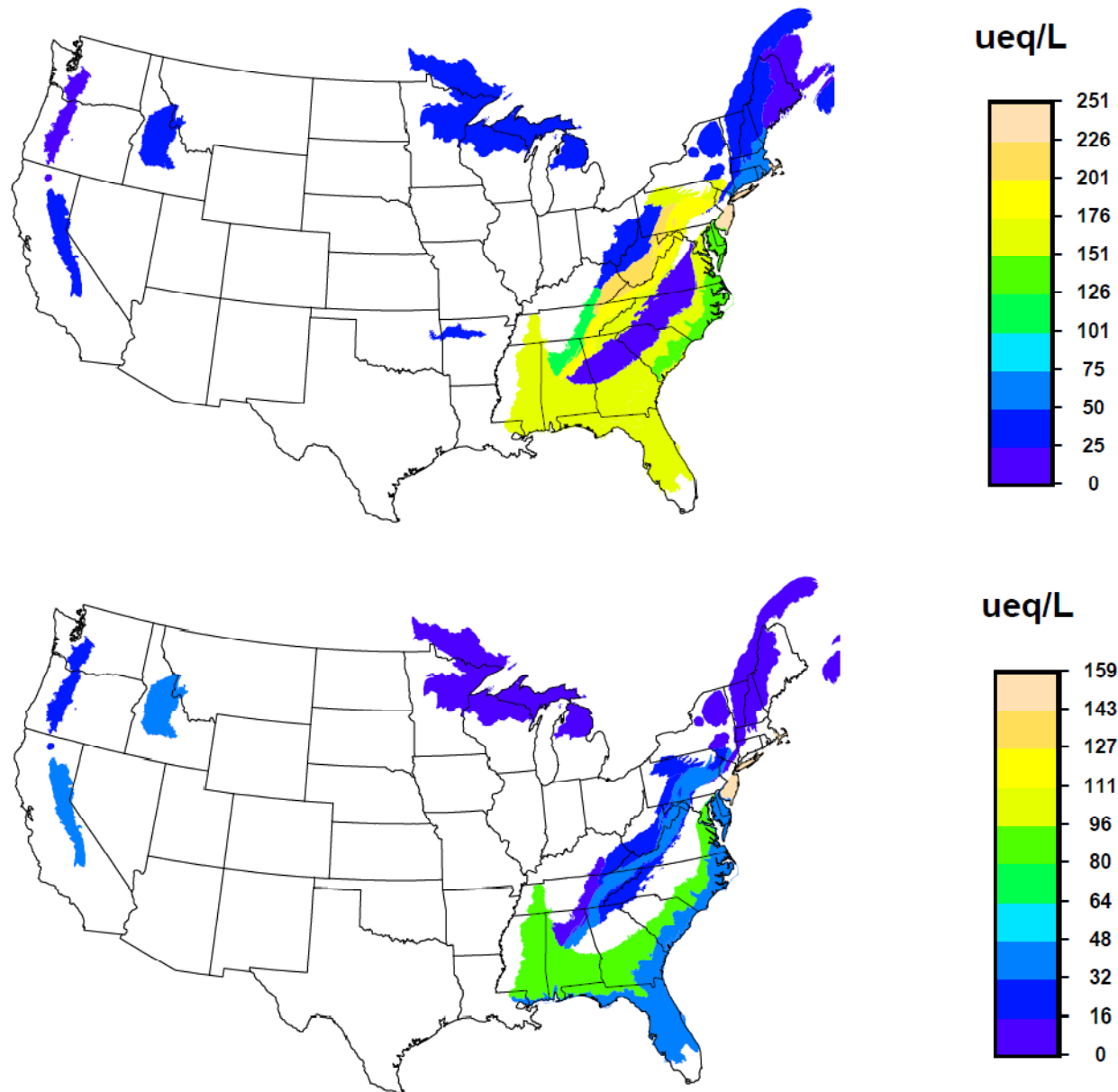


Figure D-8. Acid sensitive ecoregion level III areas likely not meeting the standard when the level = 75 $\mu\text{eq/L}$ and the form is based on the 80th percentile water body; based on CMAQ 2005 (top) and emissions sensitivity(bottom) simulations. The legend reflects the magnitude of the exceedance relative to the specified level of the standard.

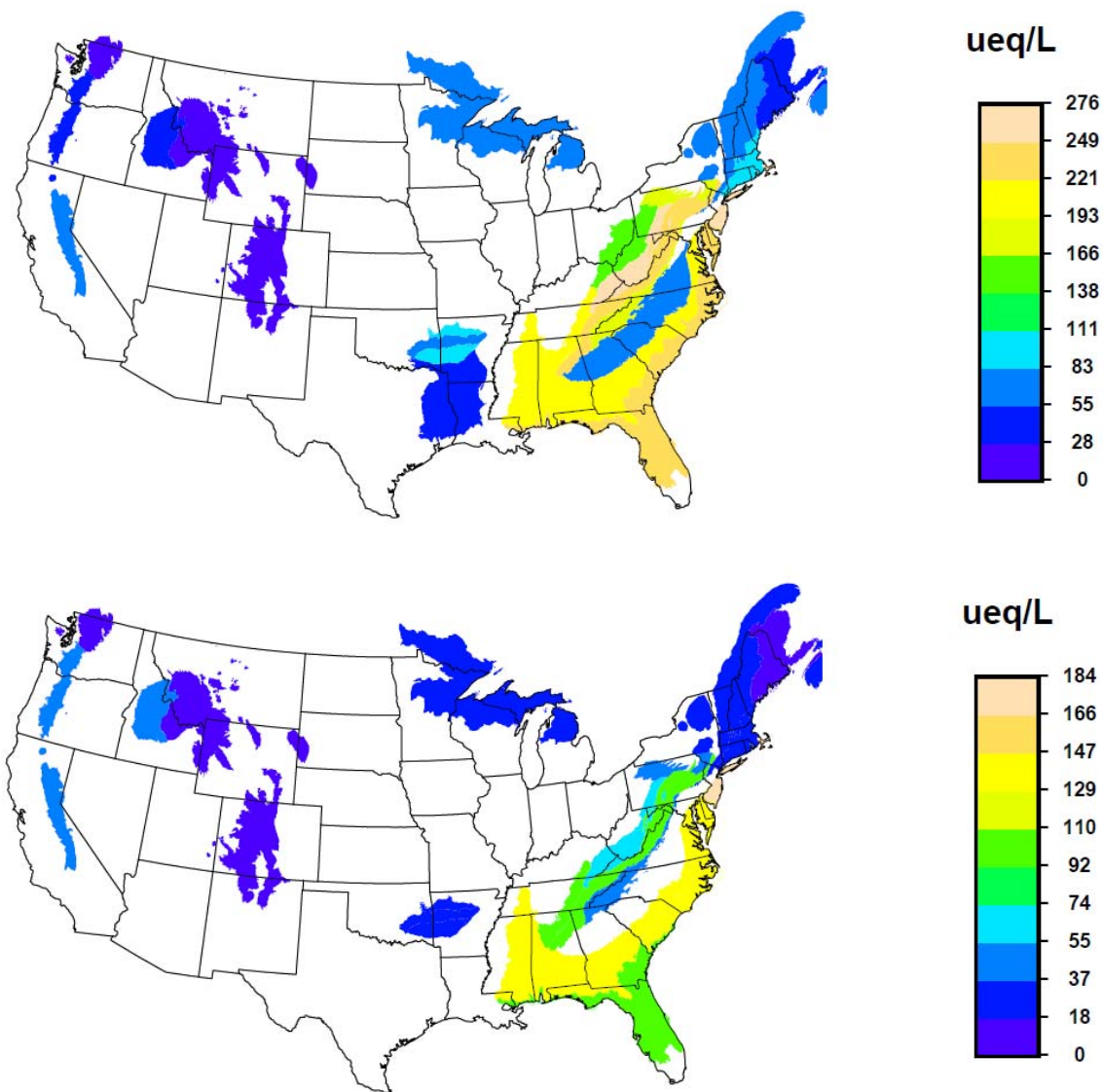


Figure D-9. Acid sensitive ecoregion level III areas likely not meeting the standard when the level = 75 $\mu\text{eq/L}$ and the form is based on the 90th percentile water body; based on CMAQ 2005 (top) and emissions sensitivity(bottom) simulations. The legend reflects the magnitude of the exceedance relative to the specified level of the standard.

Table D-2a. Calculated AAI values for sensitive ecoregions across the range of nth percentiles for a Level of 20 µeq/L: pairs of 2005 base and emissions sensitivity (42% and 48% NOx and SOx reduction). Highlighted cell pairs: Yellow-Green (likely not meeting 2005; likely meeting with emissions reductions); Yellow-Red (likely not meeting 2005 and after emissions reductions)

| | | 70 th | | 75 th | | 80 th | | 85 th | | 90 th | |
|--------|--|------------------|-------|------------------|-------|------------------|-------|------------------|-------|------------------|--------|
| | | | | | | | | | | | |
| 6.2.4 | Canadian Rockies | 933.4 | 935.8 | 740.3 | 742.7 | 685.6 | 688 | 551.0 | 553.4 | 84.5 | 86.9 |
| 6.2.3 | Columbia Mountains/Northern Rockies | 353.5 | 359.5 | 267.3 | 273.2 | 190.3 | 196.3 | 136.5 | 142.5 | 106.3 | 112.2 |
| 6.2.7 | Cascades | 90.2 | 92.7 | 72.2 | 74.7 | 46.2 | 48.6 | 31.3 | 33.8 | 19.1 | 21.6 |
| 8.5.4 | Atlantic Coastal Pine Barrens | -154.6 | -62.5 | -172.7 | -80.6 | -174.6 | -82.5 | -182.4 | -90.2 | -193.6 | -101.5 |
| 5.3.1 | Northern Appalachian and Atlantic Maritime Highlands | 58.3 | 102.9 | 49.0 | 93.6 | 33.6 | 78.2 | 21.3 | 65.9 | 6.4 | 51 |
| 6.2.10 | Middle Rockies | 180.0 | 187.9 | 122.1 | 130 | 99.0 | 106.9 | 81.6 | 89.5 | 69.4 | 77.3 |
| 8.1.3 | Northern Appalachian Plateau and Uplands | 227.0 | 342.3 | 173.4 | 288.7 | 165.7 | 281 | 120.4 | 235.7 | 85.6 | 200.9 |
| 8.1.7 | Northeastern Coastal Zone | 42.0 | 117.5 | 22.6 | 98.1 | 9.3 | 84.8 | -4.4 | 71.1 | -23.6 | 51.9 |
| 5.3.3 | North Central Appalachians | -60.8 | 79.5 | -74.4 | 66 | -87.4 | 52.9 | -97.8 | 42.6 | -112.5 | 27.9 |
| 8.1.8 | Maine/New Brunswick Plains and Hills | 89.7 | 110.1 | 84.4 | 104.7 | 71.0 | 91.4 | 65.5 | 85.9 | 48.5 | 68.9 |
| 6.2.5 | North Cascades | 138.4 | 139.8 | 130.7 | 132.1 | 112.9 | 114.2 | 93.8 | 95.2 | 65.8 | 67.2 |
| 5.2.1 | Northern Lakes and Forests | 51.4 | 97.9 | 38.7 | 85.2 | 25.9 | 72.4 | 14.1 | 60.6 | 3.8 | 50.3 |
| 6.2.15 | Idaho Batholith | 66.8 | 70.3 | 62.0 | 65.4 | 59.3 | 62.8 | 48.0 | 51.5 | 41.6 | 45.1 |
| 8.4.1 | Ridge and Valley | -72.3 | 76.2 | -95.1 | 53.4 | -117.6 | 30.9 | -143.7 | 4.8 | -177.8 | -29.3 |
| 8.4.2 | Central Appalachians | -78.3 | 109.2 | -109.0 | 78.4 | -147.0 | 40.5 | -169.5 | 17.9 | -186.2 | 1.3 |
| 8.4.3 | Western Allegheny Plateau | 412.4 | 694.3 | 280.7 | 562.6 | 47.4 | 329.3 | -20.8 | 261.1 | -97.9 | 184 |
| 6.2.13 | Wasatch and Uinta Mountains | 297.8 | 323.8 | 255.3 | 281.4 | 230.6 | 256.7 | 174.6 | 200.6 | 136.6 | 162.6 |
| 8.5.1 | Middle Atlantic Coastal Plain | -17.2 | 75.4 | -29.5 | 63.1 | -64.0 | 28.5 | -131.6 | -39.1 | -169.4 | -76.9 |
| 6.2.12 | Sierra Nevada | 49.1 | 59.2 | 38.2 | 48.2 | 28.1 | 38.2 | 22.2 | 32.2 | 12.6 | 22.6 |
| 6.2.14 | Southern Rockies | 120.6 | 129.4 | 98.5 | 107.4 | 85.7 | 94.6 | 67.6 | 76.4 | 50.8 | 59.7 |
| 8.4.4 | Blue Ridge | -65.5 | 68.8 | -73.5 | 60.8 | -83.3 | 51 | -93.1 | 41.3 | -104.9 | 29.4 |
| 8.3.5 | Southeastern Plains | -51.2 | 21 | -59.2 | 13 | -73.1 | -0.9 | -91.0 | -18.9 | -106.7 | -34.5 |
| 8.3.4 | Piedmont | 131.6 | 266.5 | 102.7 | 237.5 | 72.7 | 207.6 | 45.7 | 180.6 | 11.8 | 146.7 |
| 8.4.9 | Southwestern Appalachians | 35.3 | 131.9 | -18.5 | 78.1 | -29.4 | 67.2 | -69.8 | 26.7 | -121.5 | -25 |
| 8.4.6 | Boston Mountains | 65.1 | 119.3 | 65.1 | 119.3 | 27.7 | 81.9 | 8.7 | 62.8 | -24.4 | 29.7 |
| 8.4.7 | Arkansas Valley | 90.1 | 129.6 | 82.5 | 122 | 66.2 | 105.7 | 50.7 | 90.2 | -1.0 | 38.5 |
| 8.5.3 | Southern Coastal Plain | -31.2 | 102.6 | -61.8 | 71.9 | -105.1 | 28.6 | -143.2 | -9.4 | -154.9 | -21.2 |
| 8.4.8 | Ouachita Mountains | 89.3 | 140.5 | 74.6 | 125.9 | 64.6 | 115.8 | 51.3 | 102.6 | -3.3 | 47.9 |
| 8.3.7 | South Central Plains | 287.1 | 346.3 | 279.6 | 338.8 | 213.3 | 272.6 | 136.4 | 195.7 | 47.3 | 106.6 |

Table D-2b. Calculated AAI values for sensitive ecoregions across the range of nth percentiles for a Level of 35 µeq/L: pairs of 2005 base and emissions sensitivity (42% and 48% NO_x and SO_x reduction). Highlighted cell pairs: Yellow-Green (likely not meeting 2005; likely meeting with emissions reductions); Yellow-Red (likely not meeting 2005 and after emissions reductions)

| | | 70% | | 75% | | 80% | | 85% | | 90% | |
|--------|--|--------|-------|--------|-------|--------|-------|--------|-------|--------|--------|
| 6.2.4 | Canadian Rockies | 934.4 | 936.8 | 736.5 | 738.9 | 692.4 | 694.8 | 556.9 | 559.2 | 80.9 | 83.2 |
| 6.2.3 | Columbia Mountains/Northern Rockies | 342.8 | 348.8 | 257.3 | 263.2 | 188.0 | 194 | 122.5 | 128.5 | 106.8 | 112.8 |
| 6.2.7 | Cascades | 92.1 | 94.6 | 74.7 | 77.1 | 47.8 | 50.3 | 30.7 | 33.2 | 21.4 | 23.9 |
| 8.5.4 | Atlantic Coastal Pine Barrens | -160.7 | -68.5 | -173.7 | -81.5 | -174.3 | -82.1 | -180.7 | -88.5 | -192.9 | -100.7 |
| 5.3.1 | Northern Appalachian and Atlantic Maritime Highlands | 58.8 | 103.5 | 46.2 | 90.8 | 32.1 | 76.7 | 20.1 | 64.7 | 3.4 | 48 |
| 6.2.10 | Middle Rockies | 179.1 | 187 | 121.7 | 129.6 | 99.2 | 107.1 | 81.0 | 88.9 | 63.3 | 71.2 |
| 8.1.3 | Northern Appalachian Plateau and Uplands | 225.5 | 340.7 | 173.7 | 289 | 163.9 | 279.2 | 121.4 | 236.7 | 87.3 | 202.6 |
| 8.1.7 | Northeastern Coastal Zone | 42.3 | 117.8 | 23.2 | 98.8 | 8.9 | 84.4 | -6.1 | 69.4 | -24.2 | 51.3 |
| 5.3.3 | North Central Appalachians | -59.8 | 80.6 | -71.8 | 68.6 | -88.7 | 51.7 | -95.3 | 45.1 | -114.3 | 26.1 |
| 8.1.8 | Maine/New Brunswick Plains and Hills | 89.5 | 109.9 | 84.6 | 105 | 72.1 | 92.5 | 65.9 | 86.3 | 47.1 | 67.5 |
| 6.2.5 | North Cascades | 144.4 | 145.8 | 125.1 | 126.4 | 110.3 | 111.7 | 86.5 | 87.8 | 71.6 | 73 |
| 5.2.1 | Northern Lakes and Forests | 52.7 | 99.2 | 39.6 | 86.1 | 25.7 | 72.2 | 14.3 | 60.8 | 1.0 | 47.5 |
| 6.2.15 | Idaho Batholith | 60.2 | 63.6 | 56.7 | 60.1 | 53.7 | 57.2 | 49.6 | 53.1 | 39.8 | 43.2 |
| 8.4.1 | Ridge and Valley | -72.3 | 76.2 | -94.0 | 54.5 | -116.3 | 32.1 | -144.8 | 3.7 | -175.4 | -26.9 |
| 8.4.2 | Central Appalachians | -80.3 | 107.1 | -107.3 | 80.1 | -143.2 | 44.2 | -173.0 | 14.4 | -182.0 | 5.4 |
| 8.4.3 | Western Allegheny Plateau | 415.2 | 697.1 | 281.4 | 563.3 | 46.2 | 328.1 | -22.1 | 259.8 | -94.1 | 187.8 |
| 6.2.13 | Wasatch and Uinta Mountains | 287.3 | 313.4 | 243.0 | 269 | 221.8 | 247.9 | 184.4 | 210.5 | 126.3 | 152.4 |
| 8.5.1 | Middle Atlantic Coastal Plain | -16.2 | 76.4 | -32.0 | 60.5 | -61.4 | 31.1 | -133.2 | -40.7 | -163.4 | -70.9 |
| 6.2.12 | Sierra Nevada | 47.4 | 57.4 | 40.5 | 50.5 | 30.6 | 40.7 | 21.8 | 31.8 | 13.8 | 23.8 |
| 6.2.14 | Southern Rockies | 120.2 | 129 | 102.3 | 111.2 | 87.3 | 96.2 | 66.4 | 75.3 | 53.1 | 62 |
| 8.4.4 | Blue Ridge | -65.4 | 69 | -71.6 | 62.7 | -82.4 | 52 | -93.6 | 40.7 | -104.6 | 29.7 |
| 8.3.5 | Southeastern Plains | -55.5 | 16.6 | -63.4 | 8.8 | -72.1 | 0.1 | -96.2 | -24 | -107.9 | -35.7 |
| 8.3.4 | Piedmont | 131.2 | 266 | 96.1 | 231 | 72.6 | 207.4 | 43.7 | 178.6 | 14.0 | 148.9 |
| 8.4.9 | Southwestern Appalachians | 31.1 | 127.7 | -12.2 | 84.3 | -29.1 | 67.5 | -71.4 | 25.1 | -121.3 | -24.8 |
| 8.4.6 | Boston Mountains | 65.1 | 119.3 | 65.1 | 119.3 | 28.9 | 83 | 8.7 | 62.9 | -21.2 | 33 |
| 8.4.7 | Arkansas Valley | 89.3 | 128.8 | 85.7 | 125.2 | 71.4 | 110.9 | 50.6 | 90.1 | -2.0 | 37.5 |
| 8.5.3 | Southern Coastal Plain | -29.1 | 104.6 | -61.7 | 72 | -106.5 | 27.3 | -138.6 | -4.9 | -150.8 | -17 |
| 8.4.8 | Ouachita Mountains | 89.5 | 140.8 | 78.9 | 130.1 | 67.4 | 118.7 | 49.3 | 100.5 | -4.8 | 46.5 |
| 8.3.7 | South Central Plains | 291.9 | 351.1 | 275.4 | 334.6 | 210.4 | 269.7 | 133.1 | 192.4 | 47.3 | 106.6 |

Table D-2c. Calculated AAI values for sensitive ecoregions across the range of nth percentiles for a Level of 50 µeq/L: pairs of 2005 base and emissions sensitivity (42% and 48% NOx and SOx reduction).

Highlighted cell pairs: Yellow-Green (likely not meeting 2005; likely meeting with emissions reductions); Yellow-Red (likely not meeting 2005 and after emissions reductions)

| | | 70% | | 75% | | 80% | | 85% | | 90% | |
|--------|--|--------|-------|--------|-------|--------|-------|--------|-------|--------|--------|
| 6.2.4 | Canadian Rockies | 935.5 | 937.8 | 732.7 | 735 | 699.2 | 701.6 | 562.7 | 565.1 | 79.4 | 81.8 |
| 6.2.3 | Columbia Mountains/Northern Rockies | 327.0 | 333 | 262.1 | 268.1 | 192.3 | 198.2 | 132.6 | 138.5 | 106.4 | 112.4 |
| 6.2.7 | Cascades | 93.0 | 95.4 | 72.5 | 74.9 | 51.7 | 54.2 | 29.2 | 31.7 | 23.9 | 26.4 |
| 8.5.4 | Atlantic Coastal Pine Barrens | -166.7 | 74.5 | -174.0 | 81.8 | -174.7 | 82.5 | -176.5 | 84.3 | -192.7 | -100.5 |
| 5.3.1 | Northern Appalachian and Atlantic Maritime Highlands | 57.0 | 101.6 | 44.0 | 88.7 | 30.8 | 75.4 | 17.0 | 61.7 | 1.1 | 45.7 |
| 6.2.10 | Middle Rockies | 178.2 | 186.1 | 119.5 | 127.4 | 97.5 | 105.4 | 81.6 | 89.5 | 56.9 | 64.8 |
| 8.1.3 | Northern Appalachian Plateau and Uplands | 223.9 | 339.2 | 174.1 | 289.4 | 162.2 | 277.5 | 122.4 | 237.7 | 89.0 | 204.3 |
| 8.1.7 | Northeastern Coastal Zone | 42.1 | 117.6 | 23.9 | 99.4 | 8.7 | 84.2 | -7.2 | 68.3 | -24.8 | 50.7 |
| 5.3.3 | North Central Appalachians | -58.7 | 81.7 | -69.2 | 71.1 | -87.5 | 52.9 | -95.5 | 44.9 | -115.8 | 24.6 |
| 8.1.8 | Maine/New Brunswick Plains and Hills | 90.1 | 110.5 | 84.8 | 105.2 | 73.4 | 93.8 | 65.1 | 85.5 | 45.8 | 66.2 |
| 6.2.5 | North Cascades | 148.3 | 149.7 | 123.8 | 125.2 | 116.8 | 118.2 | 93.0 | 94.4 | 69.7 | 71.1 |
| 5.2.1 | Northern Lakes and Forests | 54.0 | 100.5 | 39.8 | 86.3 | 24.7 | 71.1 | 14.1 | 60.6 | -0.2 | 46.3 |
| 6.2.15 | Idaho Batholith | 59.3 | 62.8 | 53.6 | 57.1 | 43.9 | 47.4 | 40.6 | 44 | 37.5 | 40.9 |
| 8.4.1 | Ridge and Valley | -75.2 | 73.3 | -94.4 | 54.1 | -116.8 | 31.6 | -144.0 | 4.5 | -172.8 | -24.3 |
| 8.4.2 | Central Appalachians | -82.0 | 105.5 | -105.5 | 82 | -140.5 | 46.9 | -172.1 | 15.3 | -182.1 | 5.3 |
| 8.4.3 | Western Allegheny Plateau | 418.0 | 699.9 | 282.2 | 564.1 | 43.2 | 325.1 | -23.4 | 258.5 | -90.3 | 191.6 |
| 6.2.13 | Wasatch and Uinta Mountains | 276.9 | 303 | 230.6 | 256.7 | 199.4 | 225.5 | 194.2 | 220.3 | 109.5 | 135.6 |
| 8.5.1 | Middle Atlantic Coastal Plain | -15.2 | 77.4 | -34.6 | 58 | -58.8 | 33.8 | -134.8 | 42.3 | -157.4 | 64.9 |
| 6.2.12 | Sierra Nevada | 44.9 | 55 | 39.0 | 49 | 32.0 | 42.1 | 24.3 | 34.3 | 13.7 | 23.8 |
| 6.2.14 | Southern Rockies | 124.1 | 133 | 112.6 | 121.5 | 85.2 | 94.1 | 67.9 | 76.7 | 58.1 | 66.9 |
| 8.4.4 | Blue Ridge | -65.3 | 69 | -72.9 | 61.5 | -82.7 | 51.6 | -92.5 | 41.8 | -102.8 | 31.5 |
| 8.3.5 | Southeastern Plains | -57.5 | 14.7 | -65.2 | 7 | -77.2 | 5.1 | -102.6 | 30.4 | -112.7 | 40.6 |
| 8.3.4 | Piedmont | 125.8 | 260.6 | 99.6 | 234.5 | 74.2 | 209.1 | 40.1 | 175 | 14.8 | 149.7 |
| 8.4.9 | Southwestern Appalachians | 26.9 | 123.4 | -6.0 | 90.5 | -28.8 | 67.7 | -73.1 | 23.5 | -121.1 | -24.6 |
| 8.4.6 | Boston Mountains | 65.1 | 119.2 | 65.1 | 119.2 | 30.0 | 84.2 | 8.7 | 62.9 | -17.9 | 36.2 |
| 8.4.7 | Arkansas Valley | 88.8 | 128.3 | 88.4 | 127.9 | 76.6 | 116.1 | 50.5 | 90 | 0.7 | 40.2 |
| 8.5.3 | Southern Coastal Plain | -27.5 | 106.2 | -55.8 | 77.9 | -101.9 | 31.8 | -134.7 | -1 | -151.7 | -18 |
| 8.4.8 | Ouachita Mountains | 89.8 | 141 | 83.1 | 134.4 | 70.3 | 121.5 | 47.2 | 98.5 | -6.2 | 45 |
| 8.3.7 | South Central Plains | 296.7 | 355.9 | 271.2 | 330.5 | 209.4 | 268.7 | 129.8 | 189.1 | 47.3 | 106.6 |

Table D-2d. Calculated AAI values for sensitive ecoregions across the range of nth percentiles for a Level of 75 µeq/L: pairs of 2005 base and emissions sensitivity (42% and 48% NOx and SOx reduction). Highlighted cell pairs: Yellow-Green (likely not meeting 2005; likely meeting with emissions reductions)

| reductions); Yellow-Red (likely not meeting 2005 and after emissions reductions) | | | | | | | | | | | |
|--|--|--------|-------|--------|-------|--------|-------|--------|-------|--------|--------|
| | | 70% | | 75% | | 80% | | 85% | | 90% | |
| 6.2.4 | Canadian Rockies | 937.2 | 939.5 | 726.3 | 728.7 | 710.5 | 712.9 | 572.5 | 574.9 | 63.5 | 77.1 |
| 6.2.3 | Columbia Mountains/Northern Rockies | 316.6 | 322.6 | 268.7 | 274.7 | 201.8 | 207.7 | 130.5 | 136.5 | 40.3 | 103.6 |
| 6.2.7 | Cascades | 89.4 | 91.9 | 70.1 | 72.6 | 49.9 | 52.4 | 36.2 | 38.7 | 11.3 | 26.8 |
| 8.5.4 | Atlantic Coastal Pine Barrens | -166.7 | -74.6 | -173.5 | -81.3 | -176.4 | -84.2 | -176.7 | -84.6 | -205.6 | -201.3 |
| 5.3.1 | Northern Appalachian and Atlantic Maritime Highlands | 56.3 | 100.9 | 43.4 | 88 | 27.6 | 72.2 | 14.6 | 59.3 | -25.3 | -3 |
| 6.2.10 | Middle Rockies | 176.6 | 184.5 | 125.2 | 133.1 | 98.0 | 105.9 | 83.1 | 91 | 32.7 | 52.8 |
| 8.1.3 | Northern Appalachian Plateau and Uplands | 225.3 | 340.6 | 174.6 | 289.9 | 159.3 | 274.5 | 128.5 | 243.7 | -35.2 | 86.6 |
| 8.1.7 | Northeastern Coastal Zone | 43.0 | 118.5 | 25.0 | 100.5 | 8.1 | 83.6 | -5.2 | 70.3 | -47.4 | -25.2 |
| 5.3.3 | North Central Appalachians | -56.9 | 83.5 | -73.1 | 57.3 | -85.3 | 55 | -92.8 | 47.6 | -128.1 | -112.5 |
| 8.1.8 | Maine/New Brunswick Plains and Hills | 87.9 | 108.2 | 83.2 | 103.6 | 71.7 | 92.1 | 62.5 | 82.9 | 15.2 | 43.3 |
| 6.2.5 | North Cascades | 145.6 | 147 | 125.1 | 126.5 | 116.0 | 117.4 | 95.4 | 96.7 | 24.4 | 73.2 |
| 5.2.1 | Northern Lakes and Forests | 54.9 | 101.4 | 41.0 | 87.5 | 26.2 | 72.7 | 12.8 | 59.3 | -17.4 | -2.9 |
| 6.2.15 | Idaho Batholith | 55.7 | 59.2 | 44.9 | 48.3 | 38.8 | 42.3 | 30.1 | 33.5 | 13.6 | 27.5 |
| 8.4.1 | Ridge and Valley | -73.1 | 75.4 | -95.5 | 53 | -116.5 | 32 | -142.2 | 6.3 | -203.2 | -169.4 |
| 8.4.2 | Central Appalachians | -81.7 | 105.7 | -106.4 | 81.1 | -137.9 | 49.6 | -169.5 | 18 | -263.2 | -180.3 |
| 8.4.3 | Western Allegheny Plateau | 422.7 | 704.6 | 283.4 | 565.3 | 41.2 | 323.1 | -25.6 | 256.3 | -183.9 | -84 |
| 6.2.13 | Wasatch and Uinta Mountains | 259.6 | 285.6 | 210.6 | 236.7 | 186.2 | 212.3 | 168.0 | 194 | 71.9 | 102.8 |
| 8.5.1 | Middle Atlantic Coastal Plain | -13.5 | 79 | -38.8 | 53.7 | -54.4 | 38.1 | -137.4 | -44.9 | -218.4 | -148.5 |
| 6.2.12 | Sierra Nevada | 45.9 | 55.9 | 39.6 | 49.6 | 30.8 | 40.8 | 23.9 | 33.9 | -6.9 | 12.5 |
| 6.2.14 | Southern Rockies | 127.1 | 135.9 | 112.6 | 121.4 | 92.2 | 101.1 | 78.3 | 87.2 | 46.6 | 64.8 |
| 8.4.4 | Blue Ridge | -64.8 | 59.5 | -74.7 | 59.6 | -83.3 | 51 | -92.9 | 41.4 | -116.5 | -104.8 |
| 8.3.5 | Southeastern Plains | -59.8 | 12.3 | -68.9 | 3.2 | -89.3 | -17.1 | -109.0 | -36.8 | -142.1 | -126.5 |
| 8.3.4 | Piedmont | 126.1 | 261 | 98.6 | 233.5 | 70.2 | 205 | 37.6 | 172.5 | -50.6 | 13 |
| 8.4.9 | Southwestern Appalachians | 19.9 | 116.4 | 4.4 | 100.9 | -28.4 | 68.2 | -75.8 | 20.7 | 3741.4 | -120.8 |
| 8.4.6 | Boston Mountains | 65.0 | 119.2 | 65.0 | 119.2 | 31.9 | 86.1 | 8.8 | 62.9 | -12.5 | -12.5 |
| 8.4.7 | Arkansas Valley | 93.8 | 133.3 | 87.0 | 126.5 | 85.3 | 124.8 | 50.4 | 89.9 | -7.4 | 5.2 |
| 8.5.3 | Southern Coastal Plain | -31.0 | 102.7 | -60.7 | 73 | -94.4 | 39.3 | -132.0 | 1.7 | -182.4 | -156.6 |
| 8.4.8 | Ouachita Mountains | 90.2 | 141.5 | 90.2 | 141.5 | 75.1 | 126.3 | 43.8 | 95 | -44.9 | -8.7 |
| 8.3.7 | South Central Plains | 304.7 | 363.9 | 264.3 | 323.5 | 220.8 | 280.1 | 124.3 | 183.6 | 20.9 | 47.3 |

D.3 Data summary tables

Tables D-3a and b includes critical load values for all acid sensitive areas; Table D-4 includes 2005 calculated AAI values and critical loads for relatively non-acid sensitive areas; Table D-5 includes CMAQ deposition values and transference ratios for each ecoregion.

| EcoRegion Level III | | 70% | 75% | 80% | 85% | 90% | 70% | 75% | 80% | 85% | 90% |
|---------------------|--|--------|--------|--------|--------|--------|--------|--------|--------|--------|--------|
| Number | Description | ANC 35 | ANC 20 |
| 5.2.1 | No. Lakes and Forests | 79.1 | 74.7 | 70.1 | 66.3 | 61.9 | 83.6 | 79.4 | 75.2 | 71.3 | 67.8 |
| 5.3.1 | No. Appalachian/ Atlantic Maritime Highlands | 120.4 | 112.3 | 103.4 | 95.8 | 85.1 | 129.6 | 123.6 | 113.9 | 106.0 | 96.6 |
| 5.3.3 | No. Central Appalachians | 132.4 | 125.8 | 116.5 | 112.9 | 102.4 | 140.1 | 132.6 | 125.4 | 119.7 | 111.7 |
| 6.2.10 | Middle Rockies | 82.0 | 60.8 | 52.5 | 45.7 | 39.1 | 87.9 | 66.5 | 57.9 | 51.5 | 47.0 |
| 6.2.12 | Sierra Nevada | 55.0 | 50.5 | 44.1 | 38.3 | 33.1 | 66.0 | 58.8 | 52.3 | 48.4 | 42.1 |
| 6.2.13 | Wasatch and Uinta Mountains | 90.5 | 81.3 | 76.9 | 69.0 | 56.9 | 95.9 | 87.0 | 81.8 | 70.1 | 62.2 |
| 6.2.14 | Southern Rockies | 75.4 | 66.2 | 58.4 | 47.7 | 40.8 | 83.3 | 71.9 | 65.3 | 56.0 | 47.3 |
| 6.2.15 | Idaho Batholith | 41.2 | 38.9 | 36.9 | 34.1 | 27.5 | 55.8 | 52.5 | 50.7 | 43.1 | 38.8 |
| 6.2.3 | Columbia Mtns/ No. Rockies | 172.9 | 131.7 | 98.4 | 66.9 | 59.4 | 185.2 | 143.8 | 106.8 | 80.9 | 66.3 |
| 6.2.4 | Canadian Rockies | 893.1 | 703.5 | 661.2 | 531.3 | 75.2 | 906.5 | 721.5 | 669.1 | 540.1 | 93.1 |
| 6.2.5 | No. Cascades | 227.7 | 194.4 | 169.0 | 128.0 | 102.4 | 243.2 | 230.0 | 199.3 | 166.5 | 118.3 |
| 6.2.7 | Cascades | 131.0 | 104.1 | 62.8 | 36.6 | 22.3 | 151.0 | 123.5 | 83.4 | 60.6 | 41.8 |
| 8.1.3 | No. Appalachian Plateau and Uplands | 256.8 | 230.1 | 225.1 | 203.2 | 185.6 | 265.3 | 237.7 | 233.7 | 210.4 | 192.5 |
| 8.1.7 | NE Coastal Zone | 168.7 | 156.7 | 147.6 | 138.2 | 126.8 | 177.9 | 165.7 | 157.3 | 148.7 | 136.6 |
| 8.1.8 | Maine/NBrunswick Plains and Hills | 112.8 | 109.5 | 101.0 | 96.7 | 84.0 | 123.2 | 119.5 | 110.4 | 106.7 | 95.1 |
| 8.3.4 | Piedmont | 208.4 | 193.1 | 182.8 | 170.3 | 157.3 | 215.1 | 202.5 | 189.4 | 177.7 | 162.9 |
| 8.3.5 | Southeastern Plains | 87.6 | 83.7 | 79.4 | 67.3 | 61.5 | 97.3 | 93.3 | 86.4 | 77.4 | 69.6 |
| 8.3.7 | South Central Plains | 213.4 | 207.2 | 182.7 | 153.6 | 121.2 | 217.2 | 214.4 | 189.4 | 160.5 | 126.9 |
| 8.4.1 | Ridge and Valley | 133.0 | 122.9 | 112.6 | 99.3 | 85.1 | 140.0 | 129.4 | 119.0 | 106.9 | 91.0 |
| 8.4.2 | Central Appalachians | 161.6 | 146.9 | 127.4 | 111.3 | 106.4 | 170.8 | 154.1 | 133.5 | 121.3 | 112.3 |
| 8.4.3 | Western Allegheny Plateau | 445.6 | 384.9 | 278.0 | 247.0 | 214.3 | 451.2 | 391.3 | 285.4 | 254.4 | 219.3 |
| 8.4.4 | Blue Ridge | 122.9 | 119.9 | 114.8 | 109.3 | 104.0 | 130.1 | 126.2 | 121.5 | 116.8 | 111.1 |
| 8.4.6 | Boston Mountains | 137.3 | 137.3 | 121.4 | 112.6 | 99.5 | 143.8 | 143.8 | 127.5 | 119.1 | 104.7 |
| 8.4.7 | Arkansas Valley | 139.0 | 137.3 | 130.4 | 120.4 | 95.0 | 146.7 | 143.0 | 135.1 | 127.6 | 102.7 |
| 8.4.8 | Ouachita Mountains | 138.3 | 133.3 | 127.9 | 119.3 | 93.8 | 145.3 | 138.4 | 133.6 | 127.4 | 101.6 |

Table D-3a. Representative critical loads for acid sensitive ecoregions - Level values of 35 and 20 $\mu\text{eq/L}$.

| | | | | | | | | | | | |
|-------|-------------------------------|-------|-------|-------|-------|------|-------|-------|-------|-------|------|
| 8.4.9 | Southwestern Appalachians | 177.6 | 149.3 | 138.4 | 110.8 | 78.3 | 190.1 | 155.0 | 148.0 | 121.6 | 88.0 |
| 8.5.1 | Middle Atlantic Coastal Plain | 145.9 | 138.6 | 125.0 | 91.8 | 77.8 | 152.4 | 146.7 | 130.7 | 99.5 | 82.0 |
| 8.5.3 | Southern Coastal Plain | 100.9 | 92.5 | 81.0 | 72.7 | 69.6 | 104.2 | 96.4 | 85.2 | 75.4 | 72.4 |
| 8.5.4 | Atlantic Coastal Pine Barrens | 85.4 | 78.4 | 78.1 | 74.7 | 68.1 | 96.6 | 86.9 | 85.9 | 81.8 | 75.8 |

Table D-3b. Representative critical loads for acid sensitive ecoregions - Level values of 75 and 50 µeq/L.

| EcoRegion Level III | | 70% | 75% | 80% | 85% | 90% | 70% | 75% | 80% | 85% | 90% |
|---------------------|--|--------|--------|--------|--------|--------|--------|--------|--------|--------|--------|
| Number | Description | ANC 75 | ANC 50 |
| 5.2.1 | No. Lakes and Forests | 66.5 | 61.9 | 57.0 | 52.6 | 47.4 | 74.5 | 69.8 | 64.8 | 61.3 | 56.5 |
| 5.3.1 | No. Appalachian/ Atlantic Maritime Highlands | 93.4 | 85.1 | 75.1 | 66.9 | 55.7 | 109.7 | 101.4 | 93.0 | 84.3 | 74.1 |
| 5.3.3 | No. Central Appalachians | 112.0 | 103.1 | 96.3 | 92.3 | 81.4 | 124.8 | 119.0 | 108.9 | 104.5 | 93.3 |
| 6.2.10 | Middle Rockies | 66.3 | 47.3 | 37.2 | 31.7 | 20.4 | 76.1 | 54.4 | 46.3 | 40.4 | 31.2 |
| 6.2.12 | Sierra Nevada | 27.9 | 23.8 | 18.0 | 13.5 | 6.1 | 43.6 | 39.8 | 35.2 | 30.2 | 23.2 |
| 6.2.13 | Wasatch and Uinta Mountains | 76.4 | 66.2 | 61.1 | 57.2 | 43.6 | 85.2 | 75.6 | 69.0 | 68.0 | 50.2 |
| 6.2.14 | Southern Rockies | 58.3 | 50.8 | 40.3 | 33.1 | 26.2 | 69.7 | 63.7 | 49.6 | 40.6 | 35.6 |
| 6.2.15 | Idaho Batholith | 11.4 | 4.1 | 0.0 | -5.9 | -7.6 | 30.6 | 26.7 | 20.2 | 18.0 | 15.9 |
| 6.2.3 | Columbia Mtns/ No. Rockies | 141.0 | 118.0 | 85.8 | 51.5 | 38.6 | 158.1 | 126.8 | 93.2 | 64.5 | 52.0 |
| 6.2.4 | Canadian Rockies | 857.4 | 655.4 | 640.2 | 508.0 | 33.3 | 879.7 | 685.4 | 653.3 | 522.6 | 59.5 |
| 6.2.5 | No. Cascades | 161.0 | 125.6 | 110.0 | 74.4 | 36.2 | 208.6 | 166.4 | 154.3 | 113.4 | 73.3 |
| 6.2.7 | Cascades | 65.3 | 35.7 | 4.6 | -16.4 | -30.9 | 109.2 | 77.7 | 45.8 | 11.2 | 3.1 |
| 8.1.3 | No. Appalachian Plateau and Uplands | 236.1 | 210.0 | 202.1 | 186.2 | 164.6 | 248.2 | 222.6 | 216.5 | 196.0 | 178.7 |
| 8.1.7 | NE Coastal Zone | 143.9 | 132.6 | 121.9 | 113.5 | 100.9 | 159.1 | 147.6 | 138.1 | 128.0 | 117.0 |
| 8.1.8 | Maine/NBrunswick Plains and Hills | 84.5 | 81.3 | 73.5 | 67.2 | 54.1 | 103.0 | 99.4 | 91.7 | 86.0 | 72.9 |
| 8.3.4 | Piedmont | 188.7 | 176.7 | 164.4 | 150.2 | 139.5 | 199.5 | 188.1 | 177.0 | 162.2 | 151.1 |
| 8.3.5 | Southeastern Plains | 65.5 | 60.9 | 50.8 | 41.0 | 32.2 | 79.2 | 75.3 | 69.3 | 56.6 | 51.6 |
| 8.3.7 | South Central Plains | 203.1 | 187.9 | 171.5 | 135.2 | 106.2 | 209.5 | 199.9 | 176.7 | 146.7 | 115.6 |
| 8.4.1 | Ridge and Valley | 114.1 | 103.7 | 93.9 | 82.0 | 69.3 | 124.7 | 115.8 | 105.4 | 92.8 | 79.4 |
| 8.4.2 | Central Appalachians | 139.1 | 125.7 | 108.6 | 91.5 | 85.6 | 152.5 | 139.8 | 120.7 | 103.6 | 98.2 |
| 8.4.3 | Western Allegheny Plateau | 430.9 | 367.6 | 257.5 | 227.2 | 200.7 | 440.1 | 378.4 | 269.8 | 239.6 | 209.2 |
| 8.4.4 | Blue Ridge | 103.9 | 99.2 | 95.1 | 90.4 | 84.7 | 115.7 | 112.1 | 107.4 | 102.7 | 97.7 |
| 8.4.6 | Boston Mountains | 119.7 | 119.7 | 105.2 | 95.1 | 85.8 | 130.7 | 130.7 | 115.3 | 106.0 | 94.4 |
| 8.4.7 | Arkansas Valley | 121.9 | 118.6 | 117.8 | 101.0 | 79.1 | 131.6 | 131.4 | 125.7 | 113.1 | 89.0 |
| 8.4.8 | Ouachita Mountains | 119.8 | 119.8 | 112.6 | 97.9 | 73.1 | 131.4 | 128.2 | 122.2 | 111.3 | 86.1 |
| 8.4.9 | Southwestern Appalachians | 144.2 | 134.1 | 112.8 | 81.9 | 52.6 | 165.1 | 143.6 | 128.8 | 100.0 | 68.7 |
| 8.5.1 | Middle Atlantic Coastal Plain | 128.7 | 116.9 | 109.7 | 71.4 | 66.3 | 139.4 | 130.5 | 119.3 | 84.1 | 73.7 |
| 8.5.3 | Southern Coastal Plain | 90.1 | 82.5 | 73.8 | 64.1 | 57.8 | 97.4 | 90.2 | 78.3 | 69.9 | 65.5 |
| 8.5.4 | Atlantic Coastal Pine | 60.8 | 57.2 | 55.6 | 55.4 | 42.3 | 74.1 | 70.2 | 69.9 | 68.9 | 60.3 |

Table D-4. Critical Loads (meq/(m²-yr) and calculated AAI values for relatively less non-acid sensitive ecoregions (note all calculations based on n_{th} %percentile = 50).

| Region | Name | CL ₇₅ | CL ₅₀ | CL ₃₅ | CL ₂₀ | AAI ₇₅ | AAI ₅₀ | AAI ₃₅ | AAI ₂₀ |
|--------|---|------------------|------------------|------------------|------------------|-------------------|-------------------|-------------------|-------------------|
| 10.1.2 | Columbia Plateau | 112.8 | 113.5 | 113.8 | 114.2 | 3618.4 | 3618.4 | 3618.4 | 3618.4 |
| 10.1.3 | Northern Basin and Range | 60.2 | 64.4 | 66.1 | 66.9 | 877.6 | 932.5 | 950.5 | 951.3 |
| 10.1.4 | Wyoming Basin | 54.0 | 70.3 | 77.2 | 87.1 | 133.6 | 140.3 | 139.0 | 143.3 |
| 10.1.5 | Central Basin and Range | 79.3 | 86.1 | 89.6 | 92.2 | 1814.0 | 1989.3 | 2077.6 | 2141.6 |
| 10.1.6 | Colorado Plateaus | 147.2 | 149.2 | 150.4 | 151.6 | 2083.9 | 2093.0 | 2098.5 | 2104.0 |
| 10.1.7 | Arizona/New Mexico Plateau | 90.2 | 90.6 | 90.9 | 91.1 | 969.1 | 950.0 | 938.6 | 927.1 |
| 10.1.8 | Snake River Plain | 113.9 | 116.1 | 117.4 | 118.8 | 1133.5 | 1140.1 | 1144.0 | 1147.9 |
| 10.2.2 | Sonoran Desert | 100.0 | 100.6 | 101.0 | 101.3 | 3284.1 | 3287.5 | 3289.5 | 3291.6 |
| 11.1.1 | California Coastal Sage, Chaparral, and Oak Woodlands | 281.6 | 283.0 | 283.8 | 284.6 | 2174.8 | 2162.5 | 2155.1 | 2147.7 |
| 11.1.2 | Central California Valley | 174.3 | 184.0 | 189.9 | 195.7 | 361.8 | 366.0 | 368.5 | 371.1 |
| 11.1.3 | Southern and Baja California Pine-Oak Mountains | 386.4 | 392.0 | 393.9 | 395.9 | 3253.8 | 3285.5 | 3290.0 | 3294.5 |
| 12.1.1 | Madrean Archipelago | 71.0 | 71.3 | 71.4 | 71.6 | 3076.7 | 3073.1 | 3071.0 | 3068.8 |
| 13.1.1 | Arizona/New Mexico Mountains | 152.6 | 153.0 | 153.3 | 153.6 | 2032.3 | 2015.0 | 2004.6 | 1994.2 |
| 6.2.11 | Klamath Mountains | 755.3 | 766.3 | 772.9 | 782.4 | 1045.5 | 1035.2 | 1029.0 | 1026.7 |
| 6.2.8 | Eastern Cascades Slopes and Foothills | 184.9 | 196.7 | 201.6 | 230.2 | 335.6 | 329.3 | 322.2 | 352.7 |
| 6.2.9 | Blue Mountains | 209.5 | 212.7 | 222.3 | 223.1 | 867.3 | 855.6 | 880.7 | 869.0 |
| 7.1.7 | Strait of Georgia/Puget Lowland | 271.0 | 282.7 | 301.0 | 325.1 | 232.6 | 217.0 | 216.7 | 221.2 |
| 7.1.8 | Coast Range | 881.0 | 947.7 | 957.6 | 992.1 | 715.8 | 741.9 | 734.5 | 746.0 |
| 8.1.1 | Eastern Great Lakes and Hudson Lowlands | 637.2 | 653.3 | 662.9 | 672.6 | 974.0 | 978.8 | 981.8 | 984.7 |
| 8.1.10 | Erie Drift Plain | 888.1 | 896.3 | 901.2 | 906.1 | 1314.6 | 1305.5 | 1300.1 | 1294.6 |
| 8.1.4 | North Central Hardwood Forests | 396.2 | 401.2 | 402.6 | 404.0 | 1428.7 | 1426.9 | 1418.5 | 1410.1 |
| 8.1.5 | Driftless Area | 943.6 | 948.7 | 951.8 | 954.9 | 3951.7 | 3950.9 | 3950.4 | 3950.0 |
| 8.1.6 | S. Michigan/N. Indiana Drift Plains | 919.3 | 926.3 | 930.4 | 934.6 | 2620.3 | 2618.9 | 2618.1 | 2617.2 |
| 8.2.1 | Southeastern Wisconsin Till Plains | 878.9 | 884.5 | 887.8 | 891.1 | 3705.1 | 3707.2 | 3708.4 | 3709.6 |
| 8.2.3 | Central Corn Belt Plains | 1050.1 | 1058.0 | 1062.7 | 1067.5 | 3880.7 | 3889.9 | 3895.4 | 3900.9 |
| 8.2.4 | Eastern Corn Belt Plains | 931.2 | 939.8 | 944.9 | 950.1 | 2295.2 | 2297.0 | 2298.2 | 2299.3 |
| 8.3.1 | Northern Piedmont | 386.2 | 403.8 | 414.4 | 425.0 | 401.3 | 410.7 | 416.4 | 422.0 |
| 8.3.2 | Interior River Valleys and Hills | 574.0 | 581.0 | 585.1 | 589.3 | 1799.0 | 1804.5 | 1807.7 | 1811.0 |
| 8.3.3 | Interior Plateau | 803.4 | 815.5 | 822.7 | 829.9 | 1357.2 | 1357.7 | 1357.9 | 1358.2 |
| 8.4.5 | Ozark Highlands | 719.4 | 725.8 | 729.6 | 733.4 | 2202.4 | 2200.1 | 2198.7 | 2197.3 |
| 8.5.2 | Mississippi Alluvial Plain | 1039.4 | 1052.2 | 1059.9 | 1067.7 | 2069.5 | 2072.4 | 2074.2 | 2075.9 |
| 9.2.1 | Aspen Parkland/Northern Glaciated Plains | 154.1 | 154.8 | 155.3 | 155.7 | 6663.8 | 6690.8 | 6707.0 | 6723.1 |
| 9.2.2 | Lake Manitoba and Lake Agassiz Plain | 261.0 | 261.7 | 262.1 | 262.5 | 7748.4 | 7750.1 | 7751.1 | 7752.1 |
| 9.2.3 | Western Corn Belt Plains | 492.9 | 495.5 | 497.0 | 498.6 | 3006.8 | 3002.3 | 2999.6 | 2996.9 |
| 9.2.4 | Central Irregular Plains | 495.7 | 500.4 | 503.2 | 505.9 | 1800.5 | 1796.5 | 1794.0 | 1791.6 |
| 9.3.1 | Northwestern Glaciated Plains | 145.4 | 145.6 | 145.7 | 145.8 | 9116.2 | 9105.5 | 9099.0 | 9092.6 |
| 9.3.3 | Northwestern Great Plains | 173.9 | 174.5 | 174.9 | 175.3 | 5810.6 | 5812.9 | 5814.2 | 5815.6 |
| 9.3.4 | Nebraska Sand Hills | 354.4 | 355.8 | 356.6 | 357.5 | 4103.2 | 4096.8 | 4093.0 | 4089.2 |

Table D-4. Critical Loads (meq/(m²-yr) and calculated AAI values for relatively less non-acid sensitive ecoregions (note all calculations based on n_{th} %percentile = 50).

| Region | Name | CL ₇₅ | CL ₅₀ | CL ₃₅ | CL ₂₀ | AAI ₇₅ | AAI ₅₀ | AAI ₃₅ | AAI ₂₀ |
|---------------------|--|------------------|------------------|------------------|------------------|-------------------|-------------------|-------------------|-------------------|
| 9.4.1 | High Plains | 101.7 | 102.0 | 102.2 | 102.4 | 1632.4 | 1618.2 | 1609.7 | 1601.3 |
| 9.4.2 | Central Great Plains | 197.5 | 198.9 | 199.7 | 200.5 | 2340.2 | 2341.2 | 2341.8 | 2342.4 |
| 9.4.3 | Southwestern Tablelands | 86.5 | 86.7 | 86.9 | 87.0 | 5535.8 | 5538.1 | 5539.5 | 5540.8 |
| 9.4.5 | Cross Timbers | 309.4 | 312.6 | 314.5 | 316.5 | 1916.1 | 1918.2 | 1919.4 | 1920.7 |
| 9.5.1 | Western Gulf Coastal Plain | 738.9 | 750.9 | 758.0 | 765.1 | 1416.0 | 1416.0 | 1416.0 | 1416.0 |
| 15.4.1 ¹ | Southern Florida Coastal Plain | 281.6 | 283.0 | 301.0 | 316.5 | 931.9 | 913.4 | 986.0 | 1046.1 |
| 5.2.2 ¹ | Northern Minnesota Wetlands | 281.6 | 283.0 | 301.0 | 316.5 | 1166.4 | 1147.9 | 1220.5 | 1280.6 |
| 8.2.2 ¹ | Huron/Erie Lake Plains | 281.6 | 283.0 | 301.0 | 316.5 | 547.1 | 528.6 | 601.3 | 661.4 |
| 9.6.1 | Southern Texas Plains/Interior Plains and Hills with Xerophytic Shrub and Oak Forest | 281.6 | 283.0 | 301.0 | 316.5 | 1086.2 | 1067.7 | 1140.3 | 1200.4 |
| 10.2.1 ¹ | Mojave Basin and Range | 281.6 | 283.0 | 301.0 | 316.5 | 1291.0 | 1272.5 | 1345.1 | 1405.2 |
| 10.2.4 ¹ | Chihuahuan Desert | 281.6 | 283.0 | 301.0 | 316.5 | 1265.2 | 1246.7 | 1319.3 | 1379.4 |
| 7.1.9 ¹ | Willamette Valley | 281.6 | 283.0 | 301.0 | 316.5 | 1109.3 | 1090.9 | 1163.5 | 1223.6 |
| 8.3.6 ¹ | Mississippi Valley Loess Plains | 281.6 | 283.0 | 301.0 | 316.5 | 783.1 | 764.6 | 837.2 | 897.3 |
| 9.4.6 ¹ | Edwards Plateau | 281.6 | 283.0 | 301.0 | 316.5 | 1087.3 | 1068.8 | 1141.4 | 1201.5 |
| 9.4.4 ¹ | Flint Hills | 281.6 | 283.0 | 301.0 | 316.5 | 939.4 | 920.9 | 993.5 | 1053.6 |
| 9.4.7 ¹ | Texas Blackland Prairies | 281.6 | 283.0 | 301.0 | 316.5 | 835.5 | 817.0 | 889.7 | 949.7 |
| 8.3.8 ¹ | East Central Texas Plains | 281.6 | 283.0 | 301.0 | 316.5 | 881.2 | 862.7 | 935.3 | 995.4 |

1 – indicates relatively non-acidless- sensitive regions with data from less than 10 water bodies; CL and Qr values are based on median values of all the relatively non-acid sensitive regions with data from ≥ 10 water bodies with data.

Table D-5. CMAQ 2005 annual average depositions, transference ratios, and Neco vales. All depositions and Neco in meq/(m²-yr); T ratios in m/yr; Ndep = NOydep + NHxdep.

| EcoRgnIII 3III | Name | Total NDep | NHx Dep | SOx Dep | TSOx | TNOy | Neco ¹ |
|-------------------|---|---------------|------------|------------|------|------|-------------------|
| 10.1.2 | Columbia Plateau | 19.2 | 8.9 | 3.6 | 8.9 | 7.1 | 17.1 |
| 10.1.3 | Northern Basin and Range | 14.2 | 5.6 | 4.3 | 15.3 | 14.9 | 13.1 |
| 10.1.4 | Wyoming Basin | 15.7 | 4.7 | 8.3 | 13.3 | 11.9 | 14.8 |
| 10.1.5 | Central Basin and Range | 15.6 | 4.4 | 4.7 | 14.3 | 13.4 | 15.1 |
| 10.1.6 | Colorado Plateaus | 21.3 | 5.8 | 9.0 | 19.3 | 16.4 | 19.8 |
| 10.1.7 | Arizona/New Mexico Plateau | 19.3 | 4.7 | 7.5 | 14.1 | 12.2 | 18.7 |
| 10.1.8 | Snake River Plain | 33.1 | 21.6 | 6.2 | 14.8 | 7.6 | 27.3 |
| 10.2.1 | Mojave Basin and Range | 26.1 | 4.9 | 5.4 | 8.6 | 11.2 | NA |
| 10.2.2 | Sonoran Desert | 23.6 | 7.1 | 5.7 | 6.7 | 8.5 | NA |
| 10.2.4 | Chihuahuan Desert | 24.5 | 7.8 | 12.4 | 11.6 | 15.3 | 24.4 |
| 11.1.1 | California Coastal Sage, Chaparral, and Oak Woodlands | 45.8 | 11.4 | 14.6 | 9.8 | 7.5 | 32.7 |
| 11.1.2 | Central California Valley | 68.8 | 34.4 | 9.8 | 7.0 | 5.5 | 67.9 |
| 11.1.3 | Southern and Baja California Pine-Oak Mountains | 59.6 | 12.1 | 10.9 | 11.8 | 13.5 | 57.7 |
| 12.1.1 | Madrean Archipelago | 23.4 | 8.6 | 9.1 | 12.2 | 13.9 | 23.2 |
| 13.1.1 | Arizona/New Mexico Mountains | 24.6 | 6.5 | 8.6 | 18.1 | 18.1 | 24.4 |
| 15.4.1 | Southern Florida Coastal Plain | 64.6 | 10.1 | 40.8 | 17.6 | 12.9 | NA |
| 5.2.2 | Northern Minnesota Wetlands | 39.8 | 19.5 | 17.4 | 21.5 | 13.9 | NA |
| 6.2.11 | Klamath Mountains | 20.9 | 6.1 | 9.7 | 30.8 | 17.6 | 18.9 |
| 6.2.8 | Eastern Cascades Slopes and Foothills | 16.3 | 4.9 | 4.5 | 16.6 | 15.2 | 15.7 |
| 6.2.9 | Blue Mountains | 15.9 | 6.0 | 4.1 | 15.5 | 13.5 | 15.5 |
| 7.1.7 | Strait of Georgia/Puget Lowland | 50.3 | 22.7 | 25.4 | 15.5 | 5.0 | 42.7 |
| 7.1.8 | Coast Range | 25.2 | 7.5 | 20.9 | 39.6 | 14.4 | 17.2 |
| 7.1.9 | Willamette Valley | 51.8 | 27.8 | 17.0 | 15.7 | 4.6 | NA |
| 8.1.1 | Eastern Great Lakes and Hudson Lowlands | 82.1 | 35.3 | 70.4 | 20.1 | 10.8 | 78.7 |
| 8.1.10 | Erie Drift Plain | 111.6 | 37.6 | 140.1 | 20.6 | 10.9 | 90.0 |
| 8.1.4 | North Central Hardwood Forests | 70.8 | 38.5 | 34.2 | 17.4 | 7.9 | 69.2 |
| 8.1.5 | Driftless Area | 80.8 | 46.5 | 39.5 | 16.1 | 8.3 | 0.9 |
| 8.1.6 | S. Michigan/N. Indiana Drift Plains | 90.0 | 32.7 | 78.5 | 16.5 | 8.3 | 86.7 |
| 8.2.1 | Southeastern Wisconsin Till Plains | 81.0 | 37.6 | 51.2 | 14.6 | 6.9 | 51.7 |
| 8.2.2 | Huron/Erie Lake Plains | 95.0 | 38.1 | 89.5 | 16.7 | 7.9 | NA |
| 8.2.3 | Central Corn Belt Plains | 89.2 | 33.8 | 79.6 | 14.2 | 7.2 | -36.1 |
| 8.2.4 | Eastern Corn Belt Plains | 104.0 | 40.0 | 116.8 | 17.3 | 8.5 | 87.3 |
| 8.3.1 | Northern Piedmont | 110.0 | 37.9 | 108.6 | 13.4 | 6.8 | 39.1 |
| 8.3.2 | Interior River Valleys and Hills | 87.1 | 32.3 | 91.6 | 15.3 | 9.7 | 81.5 |
| 8.3.3 | Interior Plateau | 90.5 | 27.4 | 106.5 | 16.8 | 11.5 | 80.2 |
| 8.3.6 | Mississippi Valley Loess Plains | 80.6 | 27.7 | 55.4 | 15.5 | 11.5 | NA |
| 8.3.8 | East Central Texas Plains | 73.7 | 30.4 | 42.1 | 13.9 | 11.8 | NA |
| 8.4.5 | Ozark Highlands | 76.4 | 32.2 | 47.0 | 16.0 | 14.0 | 75.6 |

Table D-5. CMAQ 2005 annual average depositions, transference ratios, and Neco vales. All depositions and Neco in meq/(m²-yr); T ratios in m/yr; Ndep = NOydep + NHxdep.

| EcoRgnIII 3III | Name | Total NDep | NHx Dep | SOx Dep | TSOx | TNOy | Neco ¹ |
|-------------------|--|---------------|------------|------------|------|------|-------------------|
| 8.5.2 | Mississippi Alluvial Plain | 73.4 | 26.4 | 48.9 | 14.2 | 9.2 | 70.4 |
| 9.2.1 | Aspen Parkland/Northern Glaciated Plains | 46.3 | 29.2 | 15.9 | 17.1 | 10.1 | 46.0 |
| 9.2.2 | Lake Manitoba and Lake Agassiz Plain | 50.7 | 33.6 | 15.0 | 18.5 | 9.0 | 50.1 |
| 9.2.3 | Western Corn Belt Plains | 86.9 | 53.9 | 34.5 | 15.4 | 9.0 | 40.1 |
| 9.2.4 | Central Irregular Plains | 73.8 | 33.4 | 40.2 | 14.4 | 10.0 | 71.0 |
| 9.3.1 | Northwestern Glaciated Plains | 29.1 | 15.7 | 11.2 | 15.5 | 9.1 | 28.8 |
| 9.3.3 | Northwestern Great Plains | 23.4 | 10.2 | 10.3 | 17.4 | 12.5 | 22.9 |
| 9.3.4 | Nebraska Sand Hills | 43.6 | 23.4 | 12.4 | 18.7 | 13.7 | 43.4 |
| 9.4.1 | High Plains | 45.1 | 23.3 | 12.1 | 14.1 | 10.1 | 41.8 |
| 9.4.2 | Central Great Plains | 61.6 | 30.2 | 19.4 | 15.0 | 12.0 | 60.2 |
| 9.4.3 | Southwestern Tablelands | 32.6 | 12.1 | 10.9 | 13.7 | 12.7 | 32.5 |
| 9.4.4 | Flint Hills | 70.6 | 31.5 | 33.3 | 15.1 | 11.8 | NA |
| 9.4.5 | Cross Timbers | 66.3 | 24.2 | 25.0 | 11.2 | 10.5 | 65.9 |
| 9.4.6 | Edwards Plateau | 50.6 | 14.7 | 22.8 | 17.0 | 16.6 | NA |
| 9.4.7 | Texas Blackland Prairies | 81.7 | 33.1 | 43.5 | 11.6 | 8.7 | NA |
| 9.5.1 | Western Gulf Coastal Plain | 62.9 | 20.4 | 37.0 | 14.9 | 9.0 | 60.8 |
| 9.6.1 | Southern Texas Plains/Interior Plains and Hills with Xerophytic Shrub and Oak Forest | 46.2 | 13.3 | 27.4 | 15.7 | 15.5 | NA |
| 5.2.1 | Northern Lakes and Forests | 46.1 | 18.4 | 27.1 | 20.2 | 14.3 | 45.6 |
| 5.3.1 | Northern Appalachian and Atlantic Maritime Highlands | 56.7 | 17.9 | 48.5 | 25.1 | 15.9 | 52.2 |
| 5.3.3 | North Central Appalachians | 80.4 | 18.8 | 104.2 | 20.9 | 15.4 | 71.1 |
| 6.2.10 | Middle Rockies | 20.9 | 8.6 | 7.8 | 25.4 | 20.5 | 19.9 |
| 6.2.12 | Sierra Nevada | 35.9 | 11.3 | 11.1 | 30.5 | 25.0 | 35.2 |
| 6.2.13 | Wasatch and Uinta Mountains | 28.4 | 9.1 | 9.4 | 22.6 | 17.6 | 26.8 |
| 6.2.14 | Southern Rockies | 22.6 | 6.0 | 8.9 | 27.0 | 22.3 | 21.3 |
| 6.2.15 | Idaho Batholith | 18.5 | 7.4 | 5.8 | 26.7 | 21.4 | 17.8 |
| 6.2.3 | Columbia Mountains/Northern Rockies | 18.5 | 6.8 | 6.4 | 19.6 | 13.6 | 17.9 |
| 6.2.4 | Canadian Rockies | 19.6 | 7.1 | 11.7 | 17.3 | 17.4 | 15.6 |
| 6.2.5 | North Cascades | 27.2 | 8.0 | 12.2 | 35.8 | 22.0 | 25.0 |
| 6.2.7 | Cascades | 30.0 | 10.1 | 13.2 | 36.1 | 17.3 | 27.9 |
| 8.1.3 | Northern Appalachian Plateau and Uplands | 76.2 | 22.7 | 82.4 | 19.2 | 14.3 | 59.3 |
| 8.1.7 | Northeastern Coastal Zone | 82.4 | 21.5 | 81.7 | 17.9 | 7.1 | 77.7 |
| 8.1.8 | Maine/New Brunswick Plains and Hills | 36.4 | 10.9 | 39.3 | 29.7 | 18.3 | 35.8 |
| 8.3.4 | Piedmont | 84.5 | 27.6 | 82.0 | 15.3 | 10.4 | 80.1 |
| 8.3.5 | Southeastern Plains | 73.2 | 25.8 | 59.7 | 15.6 | 12.6 | 60.9 |
| 8.3.7 | South Central Plains | 72.1 | 24.4 | 44.5 | 16.7 | 13.4 | 70.4 |
| 8.4.1 | Ridge and Valley | 86.0 | 27.0 | 96.9 | 16.3 | 10.9 | 61.8 |
| 8.4.2 | Central Appalachians | 90.9 | 20.6 | 133.3 | 23.1 | 18.1 | 74.1 |
| 8.4.3 | Western Allegheny Plateau | 98.1 | 23.1 | 174.8 | 20.5 | 12.5 | 78.7 |

Table D-5. CMAQ 2005 annual average depositions, transference ratios, and Neco vales. All depositions and Neco in meq/(m²-yr); T ratios in m/yr; Ndep = NOydep + NHxdep.

| EcoRgnIII 3III | Name | Total NDep | NHx Dep | SOx Dep | TSOx | TNOy | Neco ¹ |
|---|-------------------------------|---------------|------------|------------|------|------|-------------------|
| 8.4.4 | Blue Ridge | 84.2 | 24.4 | 87.1 | 21.3 | 17.8 | 79.5 |
| 8.4.6 | Boston Mountains | 81.9 | 36.0 | 42.2 | 17.9 | 17.7 | 79.0 |
| 8.4.7 | Arkansas Valley | 75.5 | 35.2 | 37.3 | 14.5 | 12.2 | 66.0 |
| 8.4.8 | Ouachita Mountains | 72.0 | 27.1 | 40.6 | 16.8 | 16.8 | 71.0 |
| 8.4.9 | Southwestern Appalachians | 88.9 | 30.4 | 91.2 | 18.1 | 14.1 | 72.5 |
| 8.5.1 | Middle Atlantic Coastal Plain | 87.0 | 33.9 | 82.6 | 17.9 | 11.7 | 4.4 |
| 8.5.3 | Southern Coastal Plain | 66.2 | 15.3 | 51.2 | 18.4 | 13.6 | 62.9 |
| 8.5.4 | Atlantic Coastal Pine Barrens | 91.5 | 22.1 | 98.3 | 16.1 | 6.8 | 68.1 |
| 1- NA indicates a lessrelatively non-acid sensitive area with less than 10o water bodies with water chemistry data. | | | | | | | |

D.4 Relating exceedances to ambient air indicators: introducing trade-off curves

The exceedance calculations based on deposition reflect a straightforward approach to determine if the AAI is met, and serves the purpose of explaining current conditions with respect various combinations of alternative levels and forms of the standard. In practice, a state agency would use observed ambient concentrations of NO_y, SO₂ and SO₄ and calculate the AAI using equation

$$AAI = F1 - F2 - F3[NO_y] - F4[SO_x]$$

An alternative standard would be met if the calculated AAI is equal to or above the alternative standard level. An infinite amount of combinations of NO_y and SO_x concentrations can satisfy the condition that the calculated AAI be greater than or equal to the level of the standard. NO_x/SO_x tradeoff curves, using nitrogen and sulfur axes are used to illustrate the possible combinations of nitrogen and sulfur that could meet a target AAI. The following discussion on tradeoff curves illustrates how NH_x and Neco affect the AAI calculations, and demonstrate the range of tradeoff options between NO_y and SO_x for attaining a hypothetical standard.

NO_x and SO_x tradeoff curves are introduced using deposition axes to illustrate (Figure D-10) the basic concepts of combinations of NO_x and SO_x deposition and the role of Neco and NH_x deposition. The tradeoff curve is based on the critical load equation described earlier,

$$CL_{ANClim}(N + S) = ([BC]_0^* - [ANC_{lim}])Q + Neco \quad (D-1)$$

expressed in terms of nitrogen (zero sulfur deposition) and sulfur (zero nitrogen deposition) deposition only:

$$CL_{ANClim}(Nmax) = ([BC]_0^* - [ANC_{lim}])Q + Neco \quad (D-2a)$$

$$CL_{ANClim}(Smax) = ([BC]_0^* - [ANC_{lim}])Q \quad (D-2b)$$

Equations D-2a and D-2b provide the x and y intercepts of the basic tradeoff curve (Figure D-10). Neco reflects how much nitrogen deposition can be neutralized before it contributes to acidification so, as the two equations imply, Neco can only affect nitrogen deposition.

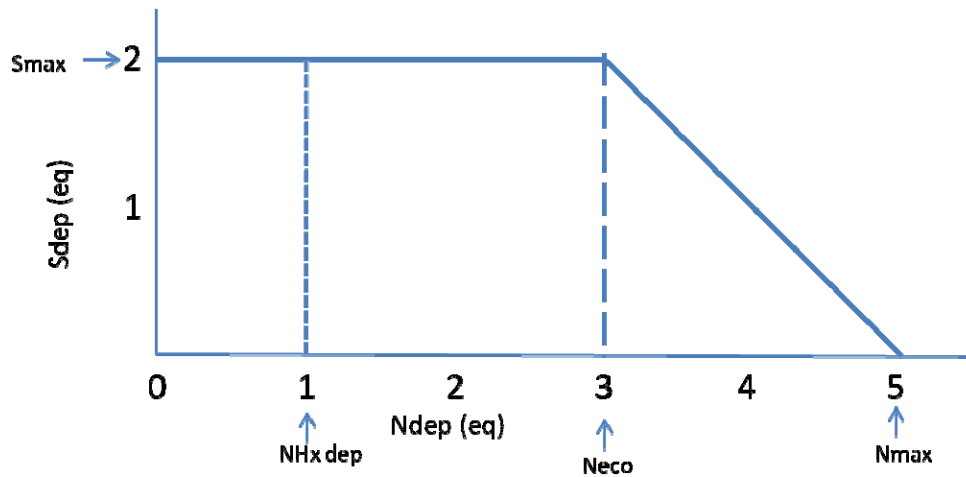


Figure D-10. Hypothetical tradeoff diagram for acidifying nitrogen and sulfur deposition. The solid horizontal and diagonal lines represent the combinations of nitrogen and sulfur deposition to meet a target ANC. Deposition values within the area bounded by these lines do not exceed the target critical load and values outside the borders exceed a critical load. When all units are transformed to equivalent charge, there is a 1:1 slope in the region where nitrogen deposition exceeds Neco which illustrates the area of tradeoffs between nitrogen and sulfur deposition.

Because, NHx is not treated as an ambient air indicator, NHx deposition is extracted from the tradeoff curve by reducing the available pool of Neco and changing the total nitrogen to a NOy deposition axis (Figure D-11):

$$CL_{ANClim}(NO_{ymax}) = ([BC]_0^* - [ANC_{lim}])Q + Neco - NHx$$

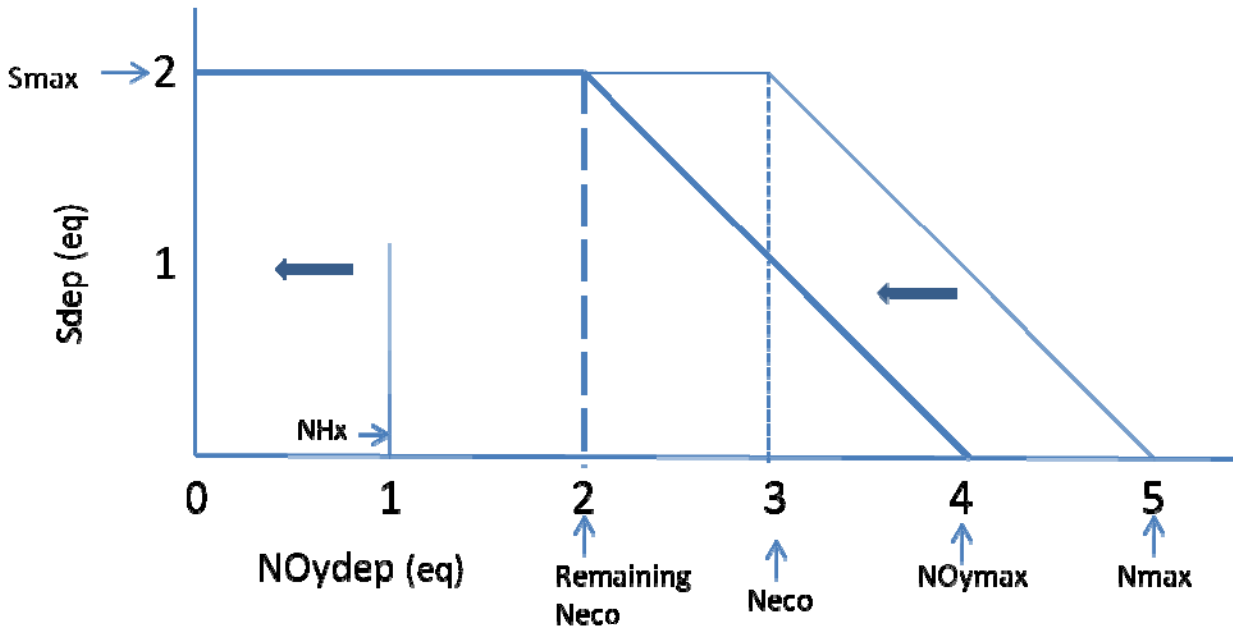


Figure D-11. Deposition tradeoff diagram for sulfur and the oxidized fraction of total nitrogen deposition with 1 equivalent unit of NH_x deposition removed. The removal of one equivalent unit of NH_x from Figure D-10 shifts the original diagram to the left and defines the amount of allowable maximum NO_y deposition, which is simply the difference between N_{max} and NH_x in Figure D-10.

The deposition axes can be directly converted to concentration axes using the transference ratios, T_{SO_x} and T_{NO_y} :

$$[\text{SO}_x]_{\text{max}} = \text{Dep}(\text{SO}_x)_{\text{max}} / T_{\text{SO}_x} \text{ and}$$

$$[\text{NO}_y]_{\text{max}} = \text{Dep}(\text{NO}_y)_{\text{max}} / T_{\text{NO}_y} .$$

With tradeoff curves expressed in NO_x and SO_x concentrations (Figure D-11), a variety of scenarios with respect to exceedances can be explained. More thorough explanations covering the development of tradeoff curves follow.

Additional Explanation of Developing Tradeoff Curves

The “basic” acid-base charge balance equation,

$$CL(\text{Acidify}) = BC_{\text{dep}} + BC_{\text{w}} + N_{\text{up}} + N_{\text{de}} + N_{\text{i}} - BC_{\text{cup}} - ANCL_{\text{limit}} \quad (\text{D-3})$$

Where $CL(\text{Acidity})$ represents the deposition flux of nitrogen and sulfur beyond which a prescribed $ANCL_{\text{limit}}$ is not met. The BC terms represent the contribution of major cations due to weathering (BC_{w}) and atmospheric deposition (BC_{dep}) and loss through plant uptake (BC_{cup}). We assume that BC_{cup} is negligible and combine cation contributions due to weathering and deposition to define BC_{co} :

$$BC_{\text{co}} = BC_{\text{dep}} + BC_{\text{w}}$$

BC_{co} integrates at the watershed level of deposition of BC from the air and weathering processes. The N terms represent the ecosystems capacity for neutralizing nitrogen deposition through plant uptake, denitrification and immobilization, largely through adsorption, which collectively is represented by the term, N_{eco} .

$$N_{\text{eco}} = N_{\text{up}} + N_{\text{de}} + N_{\text{i}}$$

N_{eco} is estimated by subtracting measured surface water outflow nitrate (leached nitrogen) from total nitrogen deposition (oxidized and reduced). Substituting the expressions for BC_{co} and N_{eco} into equation (1) and accounting for catchment runoff, Q to retain mass consistency between deposition fluxes and concentrations yields the basic critical load expression for a specific ANC target at the catchment level:

$$CL_{ANC_{\text{lim}}}(N + S) = ([BC]_{\text{O}}^* - [ANC_{\text{lim}}])Q + N_{\text{eco}} \quad (\text{D-4})$$

Equation (2) defines the maximum amount of acidifying deposition a watershed can handle to meet a prescribed ANC. Recognizing that N_{eco} only affects depositing nitrogen, the max S deposition when N deposition $\leq N_{\text{eco}}$ is defined as:

$$CL_{ANC_{\text{lim}}}(S) = ([BC]_{\text{O}}^* - [ANC_{\text{lim}}])Q \quad (\text{D-5})$$

The max N deposition when S deposition = 0

$$CL_{ANC_{lim}}(N) = ([BC]_o^* - [ANC_{lim}])Q + N_{eco} \quad (D-6)$$

Tradeoff Curves

Equations (D-5) and (D-6) establish the y and x intercepts, respectively, of a hypothetical Nitrogen/Sulfur tradeoff curve (Figure D-10). When all units are transformed to equivalent charge, there is a 1:1 slope in the region where nitrogen deposition exceeds Neco which illustrates the possibilities of combined nitrogen and sulfur deposition to meet a target ANC. Note that the concept of tradeoff between S and N is best realized where nitrogen deposition exceeds Neco. As long as nitrogen deposition is less than Neco, the amount of allowable sulfur deposition remains constant at Smax. Any deposition value above the horizontal and diagonal lines reflect levels greater than the targeted critical load. The terms Ndep and Sdep reflect deposition of total nitrogen and SOx, respectively.

The N/S tradeoff diagram is based on the following conditions:

1. $CL(S) = S_{max}$, when $N_{dep} < N_{eco}$;
2. For a given nitrogen deposition, N_{dep} ; the allowable sulfur deposition, $CL(S) = S_{max} - (N_{dep} - N_{eco})$, when $N_{max} > N_{dep} > N_{eco}$

The following conditions must be met in order to not exceed a CL;

$$S_{dep} \text{ is always } \leq ([BC]_o^* - [ANC_{lim}])Q,$$

and,

$$S_{dep} + N_{dep} \leq ([BC]_o^* - [ANC_{lim}])Q + N_{eco}$$

Note that $N_{max} - N_{eco} = S_{max}$

Delineating reduced nitrogen, NHx, deposition from total.

Because the standard addresses oxidized forms of nitrogen, it is useful to illustrate how reduced nitrogen deposition conceptually is incorporated in the deposition tradeoff diagram. Figure D-11 describes the tradeoff diagram in terms of reactive oxidized nitrogen (NOy) deposition and sulfur deposition. The NHx deposition displayed in Figure D-11 effectively is “neutralized” by

Neco, and therefore the remaining “pool” of Neco is available to neutralize NOy deposition. The impact of NHx deposition impacts the “allowable” NOy deposition to meet a target critical load. Since Nmax incorporates reduced and oxidized forms of nitrogen, the level of NHx directly impacts the amount of allowable NOy deposition where:

$$\text{Maximum NOy deposition} = N_{\max} - \text{NHx}$$

In equation form, the removal of NHx to develop oxidized nitrogen and SOx deposition tradeoff curves is represented as:

The max S deposition when N deposition < Neco

$$S_{\max} = CL_{ANC_{\lim}}(S_{\max}) = ([BC]_0^* - [ANC_{\lim}])Q \quad (\text{D-7})$$

The max NOy deposition when S deposition is zero

$$NOy_{\max} = CL_{ANC_{\lim}}(NOy_{\max}) = ([BC]_0^* - [ANC_{\lim}])Q + N_{eco} - \text{NHx} \quad (\text{D-8})$$

Or, $NOy_{\max} = N_{\max} - \text{NHx}$

Case where NHx > Neco

In cases where NHx is greater than Neco, the amount of maximum NOy deposition is decreased by a quantity equal to the difference between NHx dep and Neco as described by equation (D-8) (e.g., consider two cases of NHx = 1 and 4 with Neco a constant at 3). Equation (D-7) by definition remains satisfied in that Smax is defined as the allowable amount of sulfur deposition in the absence of any nitrogen deposition. However, because there always remains some residual atmospheric nitrogen burden in the form of NHx when all NOy is removed, the allowable sulfur deposition in concept also is reduced an amount equal to the difference between NHx dep and Neco, which is consistent with the condition that:

$$CL_{ANC_{\lim}}(S + NOy) \leq ([BC]_0^* - [ANC_{\lim}])Q + N_{eco} - \text{NHx}$$

$$S_{\max}^a \leq ([BC]_0^* - [ANC_{\lim}])Q + N_{eco} - \text{NHx}$$

$$NOy_{\max} \leq ([BC]_0^* - [ANC_{\lim}])Q + N_{eco} - \text{NHx}$$

Where S_{max}^{α} is the amount of allowable sulfur deposition in the presence of excess NH_x (Figure D-12).

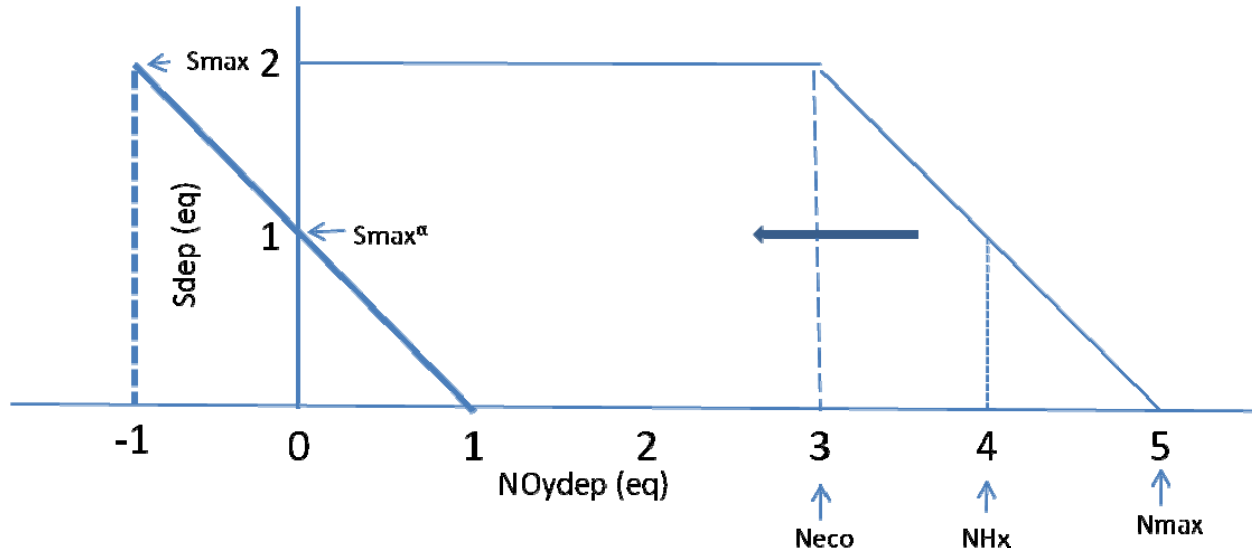


Figure D-12. NO_y and SO_x deposition tradeoff curve for hypothetical case where NH_x deposition exceeds $Neco$. The effect can be visualized as the system retaining a residual one equivalent unit of NH_x that can not be neutralized by $Neco$ with the consequent reduction on both allowable maximum amounts of SO_x and NO_y deposition.

Relating Concentrations of NO_y and SO_x to critical loads

Starting with:

1. $CL_{ANCLim}(N+S) = (BC^*_0 - ANCLim) \cdot Q + Neco$;
2. Substituting $CL_{ANCLim}(N+S) = Ndep + Sdep = NOydep + NHx + Sdep$ (conceived as any combinations NO_y , S , NH_x deposition that = $CL_{ANCLim}(N+S)$)
3. $NOydep + NHx + Sdep = (BC^*_0 - ANCLim) \cdot Q + Neco$;
4. $NOydep + Sdep = (BC^*_0 - ANCLim) \cdot Q + (Neco - NHx)$;
5. Converting deposition to concentration using $Sdep = [SO_x] \cdot T_{SO_x}$; $NOydep = [NO_y] \cdot T_{NO_y}$;
6. $[SO_x] \cdot T_{SO_x} + [NO_y] \cdot T_{NO_y} = (BC^*_0 - ANCLim) \cdot Q + Neco - NHx$;
7. $[NO_y]_{CL} = \frac{((BC^*_0 - ANCLim) \cdot Q + Neco - NHx) - Sdep}{T_{NO_y}} = \frac{CL_{ANCLim} - NHx - Sdep}{T_{NO_y}}$;

defining the maximum allowable NO_y concentration for any value of S_{dep} and a fixed value of NH_x.

$$8. [\text{SO}_x]_{\text{CL}} = [((\text{BC}_0^* - \text{ANC}_{\text{lim}}) \cdot Q + \text{Neco} - \text{NH}_x) - \text{NO}_y\text{dep}] / T_{\text{SO}_x} = \text{CL}_{\text{ANClim}} - \text{NH}_x - \text{Sdep} / T_{\text{SO}_x};$$

defining the maximum allowable SO_x concentration for any value of NO_ydep and a fixed value of NH_x.

With the condition that when N_{dep} < Neco;

$$9. [\text{SO}_x]_{\text{CL}} = [(\text{BC}_0^* - \text{ANC}_{\text{lim}}) \cdot Q] / T_{\text{SO}_x}, \text{ a constant value as all nitrogen deposition is neutralized}$$

Maximum allowable NO_y and SO_x concentrations defined as in the absence of the other component are defined as:

$$[\text{NO}_y]_{\text{max}} = (\text{Nmax} - \text{NH}_x) / T_{\text{NO}_y} = \text{NO}_y\text{max} / T_{\text{NO}_y} \text{ in the absence of any SO}_x \text{ deposition}$$

$$[\text{SO}_x]_{\text{max}} = \text{Smax} / T_{\text{SO}_x}; \text{ in the absence of any N deposition}$$

We also can define a maximum SO_x concentration in cases where NH_x exceeds Neco;

$$[\text{SO}_x]_{\text{max}}^a = [\text{Smax} - (\text{NH}_x - \text{Neco})] / T_{\text{SO}_x}; \text{ in the absence of NO}_y \text{ deposition and excess NH}_x \text{ beyond Neco.}$$

Appendix E

Derivation to use measured total nitrate as a surrogate for NO_y

Our recommended measurement approach is to use NO_y monitors to judge compliance with a NO_x/SO_x secondary standard. This derivation illustrates how the AAI equation would be modified to use total nitrate data from the CASTNET filter packs.

Two general approaches enable the use of measured total nitrate to estimate the level of NO_y consistent with the AAI formulation. The first approach introduces an aggregated dry oxidized nitrogen deposition transference ratio to separate total nitrate and NO_y and yield NO_y as a function of measured nitrate, based on CMAQ attributes consistent with the AAPI formulation. The second approach would be to adjust measured nitrate upward to represent NO_y. This adjustment would be performed by multiplying measured total nitrate by the CMAQ derived ratio of (ambient NO_y/ambient total nitrate) for the acid sensitive area of interest.

1. Rearranging AAPI expression to show NO_y as a function of measured total nitrate

$$AAI = \left[\frac{1}{Q} \cdot N_{eco} + [BC]_O^* \right]_{\%eco} - \frac{1}{Q} Dep_{\alpha NHx}^{Total} - \frac{1}{Q} [T_{\alpha NOy} \cdot C_{NOy}^{amb} + T_{\alpha SOx} \cdot C_{SOx}^{amb}]$$

$$T_{\alpha NOy} \cdot C_{NOy}^{amb} = NOy_{wetdep} + Tdry_{\alpha NOy} C_{NOy}^{amb} = NOy_{wetdep} + Tdry_{\alpha NOy} [C_{TNO3}^{amb} + C_{(NOy-TNO3)}^{amb}]$$

$$C_{NOy}^{amb} = Tdry_{\alpha NOy} [C_{TNO3}^{amb(measured)} + C_{(NOy-TNO3)}^{amb(CMAQ)}] / T_{\alpha NOy}$$

Where the new terms,

$Tdry_{\alpha NOy}$ is a CMAQ derived parameter that excludes wet deposited NO_y = [dry NO_y dep/ C_{NOy}^{amb}]

$C_{(NOy-TNO3)}^{amb(CMAQ)}$ is a CMAQ derived parameter calculated by subtracting nitric acid and p-NO₃ from NO_y

2. Adjust measured total nitrate upward to estimate ambient NO_y. This adjustment could be performed multiplying by the CMAQ NO_y/TNO₃ ratio, or by using the ratio of collocated NO_y and nitrate measurements.

Conclusions

Nitrate does not account for a significant portion of the ambient air oxidized nitrogen budget and can also miss a significant part of oxidized nitrogen deposition. These two concerns combined with the dynamic response of nitrate to changes in emissions, as discussed in chapter 2, outweigh any benefit to be derived from using an available, partial indicator like total nitrate.

Appendix F

Evaluation of Variability, Sensitivity and Uncertainty in the Acidification Index

F.1 INTRODUCTION AND PURPOSE

This appendix provides analyses and discussion of the relative uncertainty in the AAI equation. This includes analyses of the individual and combined components of the linked atmospheric-ecological effects system described in chapter 7, as well as important uncertainties in the scientific evidence that should be considered in developing options for the standard. This appendix is intended to integrate a variety of analyses related to the sensitivity of the models and model components to uncertainty and variability, and place the results of those analyses within the context of the conclusions that can be drawn regarding the components of the AAI. These components include ecosystem effects; dose-response relationships; underlying ecosystem sensitivity to acid deposition, biogeochemical, atmospheric and deposition processes; and characterization of ecosystem services. While several processes are imbedded in the AAI equation introduced in chapter 7, the level of the AAI, as in all NAAQS, is to include consideration of information on uncertainty and variability. Consequently, knowledge of the relative confidence and natural variability in the structural components of the AAI are considered in staff conclusions on options for ranges of the level of the standard. These analyses are not intended to be a comprehensive treatment of all uncertainties that exist relative to the overall review of the standards, instead, it focused on those that are most relevant in evaluating choices regarding the AAI form of the standard and options regarding the indicator, averaging time, and ranges of levels of the AAI-based NO_x and SO_x standard.

Uncertainty and sensitivity analyses are used to inform the relative confidence in the components and models that are used in defining the standard. Assessments of variability in the data used to determine parameters of the standard increases the level of understanding about the likelihood that alternative parameterizations of the standard will achieve targeted levels of protection when applied to sensitive ecosystems across the U.S. Assessments of the sensitivity of the overall AAI to the components of the equation proposed to calculate the AAI can help demonstrate how important uncertainty and variability in those components are in assessing the protection of ecosystems provided by an AAI standard. To evaluate the potential interactions

between uncertain and/or variable AAI components, a multifactor sensitivity analysis is also conducted. The ranges of component values evaluated in the multifactor sensitivity assessment are guided by individual variability and uncertainty analyses of specific components. In addition to informing considerations of the AAI level, an additional objective of these “confidence” related analyses and discussions is to help guide research and data collection efforts intended to reduce uncertainty for future NAAQS reviews and implementation efforts. Spatial and temporal variability analyses of AAI components are especially useful to inform monitoring network design, the spatial boundaries of acid sensitive regions, and averaging periods relevant to NAAQS implementation.

Significant emphasis is placed on evaluations of CMAQ due to the unique role that atmospheric models hold in the linked AAI system. The AAI as currently formulated relies on CMAQ for both the initial characterization of reduced nitrogen deposition, and the deposition transformation ratios (T_{NO_x} and T_{SO_x}) which characterize the relationships between atmospheric concentrations of NO_x and SO_x and deposition of N and S. Included are interpretations of model evaluation results from the REA (EPA, 2009) as well as more recent results related to wet deposition and the treatment of ammonia deposition. Comparison of model results to observations provides a general sense of the confidence we have that the models capture the spatial, temporal and compositional texture of the relevant atmospheric and deposition species that drive the linked atmospheric-ecosystem processes. Both model evaluation results and assessments of spatial and temporal variability guide implementation strategies for monitoring network design and emission inventory improvement. Sensitivity of CMAQ derived deposition transformation ratios to changes in emissions, and treatment of chemistry and variability over time provide insight into the stability of these parameters that are used in a relatively static manner in the AAI, and into how well proposed averaging times capture the overall spatial and temporal trends in the parameters.

We evaluate the sensitivity of critical load modeling components by comparing dynamic (MAGIC) and hybrid steady state model results, looking at terminal results of MAGIC. This approach was viewed as a test of the more reduced form approximations used in steady state modeling relative to more sophisticated treatment in MAGIC. The MAGIC critical load simulations also provide information on the temporal trajectory of ANC, including the expected time necessary to reach a desired ANC, which can help inform the level of the AAI, recognizing

that there may be additional consideration given to reaching a target ANC within a specific timeframe, e.g. by 2030 or 2040.

For the purposes of this discussion, we characterize *uncertainty* regarding models and their outputs as referring to the lack of knowledge regarding both the actual values of model input variables (parameter uncertainty) and the model characterization of physical systems or relationships (model uncertainty). In any application, uncertainty is, ideally, reduced to the maximum extent possible, but significant uncertainty often remains. It can be reduced by improved measurement and improved model formulation. Model evaluation results provide some insight into the relative uncertainty associated with the ability of models to capture key environmental state characteristics. Confidence regarding the fundamental science supporting causal determinations about the effects of acid deposition, and the translation of those effects into ecosystem services and values is less amenable to quantification. As a result, these uncertainties are more difficult to explicitly account for in development of the standards. In the case of the equation describing the AAI, a Monte Carlo style analysis (described in Appendix G) was used to assess the combined influences of parameter uncertainty. In addition, we evaluated the sensitivity of the AAI to its components using an elasticity analysis. The results of these assessments are addressed in section 7.6.

Sensitivity refers to the influence on modeled results due to perturbations in input variables or change of process formulations. Sensitivity analysis can provide a sense of how important different parameters and inputs might be to the outcomes of interest, e.g. the AAI level, but cannot by themselves indicate how important specific parameters actually are, because they do not incorporate information on the range of parameter values or the likelihood associated with any specific parameter value. Sensitivity results in this PAD are intended to provide insight into the relative stability of the AAI and associated NO_x and SO_x tradeoff curves and confidence in modeled parameterizations. Sensitivity analyses are especially useful in the absence of observed data to challenge models. For example, the NO_y and SO_x transference ratios are a model construct that is difficult, if not impossible, to compare to observations. The sensitivity of these ratios to changing meteorology, emissions and chemical mechanism treatments is evaluated in reference to the stability of these ratios under changing conditions. Low sensitivity here implies that the choice to use long-term averages of modeled ratios is justified. Sensitivity analyses also are used to discern the relative influence (on AAI results) of AAI parameters.

Toward that end, elasticity analyses were applied to determine the relative sensitivity of AAI results associated with individual and combined AAI parameters.

Variability refers to the heterogeneity in a population or variable of interest that is inherent and cannot be reduced through further data collection and research. In the context of the AAI and trade-off curves, variability is considered in guiding the design of monitoring and modeling analyses supporting implementation activities.

F.2 Uncertainty associated with ecosystem effects and dose – response relationships.

This section provides a brief summary of uncertainties based on the REA and is reproduced here to centralize all uncertainty discussions. There are different levels of uncertainty associated with relationships between deposition, ecological effects and ecological indicators. In Chapter 7 of the REA, the case study analyses associated with each targeted effect area were synthesized by identifying the strengths, limitations, and uncertainties associated with the available data, modeling approach, and relationship between the ANC and atmospheric deposition. The key uncertainties were characterized as follows to evaluate the strength of the scientific basis for setting a national standard to protect against a given effect (REA 7.0):

- **Data Availability: *high, medium or low quality*.** This criterion is based on the availability and robustness of data sets, monitoring networks, availability of data that allows for extrapolation to larger assessment areas, and input parameters for modeling and developing the ecological effect function. The scientific basis for the ecological indicator selected is also incorporated into this criterion.
- **Modeling Approach: *high, fairly high, intermediate, or low confidence*.** This value is based on the strengths and limitations of the models used in the analysis and how accepted they are by the scientific community for their application in this analysis.
- **Ecological Effect Function: *high, fairly high, intermediate, or low confidence*.** This ranking is based on how well the ecological effect function describes the relationship between atmospheric deposition and the ecological indicator of an effect.

The REA concludes that the available data are robust and considered *high quality*. There is high confidence about the use of these data and their value for extrapolating to a larger regional population of lakes. The EPA TIME/LTM network represents a source of long-term,

representative sampling. Data on sulfate concentrations, nitrate concentrations and ANC from 1990 to 2006 used for this analysis as well as EPA EMAP and REMAP surveys, provide considerable data on surface water trends.

There is *fairly high confidence* associated with modeling and input parameters. Uncertainty in water quality estimates (i.e., ANC) from MAGIC was derived from multiple site calibrations. The 95% confidence interval for pre-acidification of lakes was an average of 15 $\mu\text{eq/L}$ difference in ANC concentrations or 10% and 8 $\mu\text{eq/L}$ or 5% for streams (REA 7.1.2). The use of the critical load model used to estimate aquatic critical loads is limited by the uncertainties associated with runoff and surface water measurements and in estimating the catchment supply of base cations from the weathering of bedrock and soils (McNulty et al., 2007). To propagate uncertainty in the model parameters, Monte Carlo methods were employed to develop an inverse function of exceedances. There is *high confidence* associated with the ecological effect function developed for aquatic acidification. In calculating the ANC function, the depositional load for N or S is fixed by the deposition of the other, so deposition for either will never be zero (Figure F.1-6 REA).

Chapter 3 also reviews the basic evidence underlying effects on fish mortality, aquatic species diversity and more extended food web disruptions leading to adverse impacts on birds associated with aquatic acidification. There is high confidence associated with correlation between acidification and these ecological effects. Also, there is high confidence in the relationship between the ecological indicator, ANC, and the more direct chemical properties (lower pH and increased Al) associated with acidification.

F.3 Uncertainty in benefits estimates

Descriptions of the current provision of ecosystem services presented for each of the effect areas analyzed for this review followed by estimations of the damages incurred to selected services due to nitrogen and sulfur deposition. The current services are presented to give the reader a sense of the magnitude of the benefit the public receives from these ecosystems under current conditions. The data used in these descriptive passages is generally derived from government (either federal or state) sources we are reasonably certain to be of the highest quality. Where monetary values are placed on these services we have generally used widely cited studies, particularly meta analyses that provide an average value that smoothes the variation in WTP estimates. These estimates underestimate the total value of these services as they use

benefit estimates for a marginal increase in these services. It is likely that the total benefits of these services are greater because their marginal value likely is lower than the average value. While reductions in sulfur and nitrogen emissions would increase the size of the benefits from these services, for many of them it is unknown how significant the increase will be.

The analyses of damages incurred are more uncertain and are limited to those areas where data and tools were available. Only some services were analyzed which in some cases meant that the results were limited to one or two services and in the case of terrestrial nutrient enrichment no services had sufficient data available to attempt an estimate of damage. This means that the estimates presented are a very small part of the total damage incurred due to deposition.

Aquatic Acidification

Recreational Fishing Model

The analysis of recreational fishing damages presented in Chapter 4 is subject to the assumptions necessary to perform the analysis. The original analysis performed for the REA was based on projecting future benefits of increased recreational fishing based on a complete cessation of all nitrogen and sulfur emissions. These decisions under or over estimate the current damages to public welfare incurred from nitrogen and sulfur deposition. The magnitude of the bias in results is unknown in either direction however the majority of the assumptions influence the estimates downward. These include the use of emissions estimates that include projected decreases due to implementation of Title IV regulations in 2020. These emissions estimates are lower than current emissions and therefore lead to underestimation of damages. Because the models only value this improvement for New York residents (without accounting for out-of-state visitors) the damages are underestimates of the benefits of these improvements in the Adirondacks region.

The use of projected population in the REA analyses contributes to an overestimate of current damages since current population is smaller than future population. Further, these estimates are extrapolated from a 44 lake subset and applied to all Adirondack lakes. The representativeness of this sample is unknown. This analysis also does not account for any change in fishing demand (possible overestimate) and income (possible underestimate).

Benefits Transfer

The approach using the WTP estimates from the Banzhaf et al. (2006) study is subject to the same uncertainties described above and some additional considerations. Specifically there is some uncertainty regarding which types of ecosystem services are reflected in the study's estimates of the improvements in ecosystem services of reducing acidification, particularly provisioning and regulating services. The values likely include recreational fishing services, which mean *they cannot be added to the recreational fishing model results*, and other cultural services including other recreation and nonuse services. The inclusion in the survey of other ecosystem changes (birds, trees, etc.) leads to an overestimation of WTP for remediation of lake acidification alone. Finally, assumptions were required to align the Banzhaf survey scenarios to the likely results of complete removal of all nitrogen and sulfur emissions. These are reasonably close but not exact and may not be applicable to another baseline.

Conclusion. While these estimates are subject to uncertainty we are reasonably confident that they represent a good first-order approximation of the damages to recreational fishing due to nitrogen and sulfur deposition. Additionally it should be noted that the Banzhaf survey results represent a broader picture (though by no means complete) of the damages to ecosystem services in the Adirondacks. Finally, we would again like to emphasize that these estimates represent only a small sample of the damages incurred to a broad range of ecosystem services affected and the areas of the nation where acidic deposition is an ongoing issue.

F.4 Uncertainty in the AAI related to component parameters

Uncertainty within the AAI is divided into four components of analysis. First, an analysis of elasticity; second and third, analyses of uncertainty within individual components for atmospheric and ecosystem modeling, respectively; fourth, a Monte Carlo style analysis incorporating the uncertainty derived into the preceding section to assess the cumulative effect of the uncertainty of the input parameters. This appendix concludes with a summary discussion that includes more qualitative conclusions.

F.4.1 Elasticity Analyses

An elasticity analysis was applied to investigate sensitivity of the AAI to its components. The means, medians and quartiles of the AAI component variables were based on the range variable values across ecoregions that overlapped with the CMAQ domains. Elasticities measure

the percent change in the AAI for a 1% change in the AAI parameters: Q , N_{eco} , NH_x , BC_0^* , T_{NO_y} , T_{SO_x} , NO_y , and $(SO_2 + SO_4)$. We note that an earlier form of the expression is used where

$$Q \text{ is at the catchment level. } AAI = \frac{1}{Q} N_{eco} + BC_0^* - \frac{1}{Q} NH_x - \frac{1}{Q} [T_{NO_y} \cdot NO_y + T_{SO_x} \cdot (SO_4 + SO_2)]$$

In general, the formula for elasticity is:

$$E_{X_j}^{AAI} = \frac{\partial AAI}{\partial X_j} \cdot \frac{X_j}{AAI}$$

Where $E_{X_j}^{AAI}$ is the elasticity of AAI with respect to component X_j , and j is the number of components. So, for AAI defined as

$$AAI = \frac{1}{Q} N_{eco} + BC_0^* - \frac{1}{Q} NH_x - \frac{1}{Q} [T_{NO_y} \cdot NO_y + T_{SO_x} \cdot SO_x]$$

The set of relevant elasticities are:

For runoff, Q :

$$E_Q^{AAI} = -\frac{1}{Q^2} [N_{eco} - NH_x - T_{NO_y} NO_y - T_{SO_x} SO_x] \times \frac{Q}{AAI}, \text{ which can be rewritten as}$$

$$E_Q^{AAI} = -\frac{1}{Q} [AAI - BC_0^*] \times \frac{Q}{AAI}, \text{ or}$$

$$E_Q^{AAI} = -1 + \frac{BC_0^*}{AAI}$$

For BC_0^* ,

$$E_{BC_0^*}^{AAI} = \frac{BC_0^*}{AAI}$$

For N_{eco} ,

$$E_{N_{eco}}^{AAI} = \frac{1}{Q} \cdot \frac{N_{eco}}{AAI}$$

For NH_x ,

$$E_{NH_x}^{AAI} = -\frac{1}{Q} \cdot \frac{NH_x}{AAI}$$

For T_{NO_y} ,

$$E_{T_{NO_y}}^{AAI} = -\frac{1}{Q} \cdot NO_y \cdot \frac{T_{NO_y}}{AAI}$$

For T_{SO_x} ,

$$E_{T_{SOx}}^{AAPI} = -\frac{1}{Q} \cdot SOx \cdot \frac{T_{SOx}}{AAI}$$

For NOy,

$$E_{NOy}^{AAPI} = -\frac{1}{Q} \cdot T_{NOy} \cdot \frac{NOy}{AAI}$$

For SOx,

$$E_{SOx}^{AAI} = -\frac{1}{Q} \cdot T_{SOx} \cdot \frac{SOx}{AAI}$$

These elasticities can be evaluated at various points along the ranges of each component, as well as along ranges of the AAI. We evaluate the elasticities at the sample means, medians, first quartiles, and third quartiles. Elasticities are evaluated only for ecoregions that overlap the CMAQ modeling domain which provides values for reduced nitrogen and the transformation ratios (T_{NOx} and T_{SOx}). This will provide a reasonable assessment of the sensitivity of the AAI to input components. Table F-1 provides the estimated elasticities. Elasticities are summarized across ecoregions using means, medians, minimums, and maximums.

Note that elasticities can be either positive or negative. A negative elasticity means that the calculated AAI will decrease as a component increases. The magnitude of the elasticity depends on the values of the components and the starting value of AAI.

Based on the calculated elasticities, AAI is most responsive to changes in Q, BC0, and Neco with some responsiveness to reduced N. Note that for some components, such as Q, the elasticities switch signs depending on the values of the variables for which the elasticity is evaluated. This suggests potentially important interactions. AAI is not responsive to the transformation ratios, TNOx and TSOx at mean values of the AAI components. However, when the elasticities for TNOx and TSOx are evaluated at the first quartiles of the data, some locations in the Eastern U.S. show higher responsiveness to changes in TNOx and TSOx, with elasticities as high as 2.

Table F-1. Summary of Elasticity Results

| AAI Component | Metric for Which Elasticities are Evaluated | Mean Elasticity Across Ecoregions | Median Elasticity Across Ecoregions | Minimum Elasticity Across Ecoregions | Maximum Elasticity Across Ecoregions |
|--|---|-----------------------------------|-------------------------------------|--------------------------------------|--------------------------------------|
| Runoff (Q) | Mean | -0.1047 | 0.1221 | -20.4572 | 1.6005 |
| | Median | 0.2561 | 0.1426 | -6.2481 | 2.4578 |
| | 1 st Quartile | -0.9283 | 0.1303 | -135.2544 | 88.1063 |
| | 3 rd Quartile | 0.2988 | 0.1110 | -0.1810 | 7.5684 |
| Base Cation Weathering (BCO) | Mean | 0.8953 | 1.1221 | -19.4572 | 2.6005 |
| | Median | 1.2561 | 1.1426 | -5.2481 | 3.4578 |
| | 1 st Quartile | 0.0717 | 1.1303 | -134.2544 | 89.1063 |
| | 3 rd Quartile | 1.2988 | 1.1110 | 0.8190 | 8.5684 |
| Neco | Mean | 0.0179 | 0.1464 | -13.8545 | 1.6051 |
| | Median | 0.3376 | 0.2563 | -4.7203 | 2.5044 |
| | 1 st Quartile | 0.3543 | 0.2596 | -115.1112 | 137.0526 |
| | 3 rd Quartile | 0.3016 | 0.1440 | 0.0137 | 6.5565 |
| Reduced Nitrogen | Mean | -0.0409 | -0.0702 | -0.4708 | 3.9332 |
| | Median | -0.1407 | -0.1031 | -0.7957 | 1.0061 |
| | 1 st Quartile | -0.0308 | -0.1190 | -33.9063 | 35.3783 |
| | 3 rd Quartile | -0.1128 | -0.0615 | -1.9167 | -0.0050 |
| NOx Transformation Ratio (T _{NOx}) | Mean | 0.0089 | -0.0053 | -0.0597 | 1.0598 |
| | Median | -0.0061 | -0.0064 | -0.0506 | 0.2751 |
| | 1 st Quartile | -0.0191 | -0.0071 | -2.7061 | 1.7749 |
| | 3 rd Quartile | -0.0154 | -0.0044 | -0.5028 | -0.0002 |
| SOx Transformation Ratio (T _{SOx}) | Mean | 0.0019 | -0.0024 | -0.0185 | 0.3608 |
| | Median | -0.0045 | -0.0036 | -0.0413 | 0.1091 |
| | 1 st Quartile | 0.0040 | -0.0032 | -1.8023 | 1.9860 |
| | 3 rd Quartile | -0.0058 | -0.0021 | -0.1534 | -0.0002 |

* Elasticity is the percent change in AAI for a one percent change in the component variable. For example, when evaluated at the means of all component variables, the mean elasticity of AAI to the runoff variable Q is -0.1047, which means that for each 1 percent increase in Q, the AAI is reduced by 0.1047 percent.

Conclusions

Base cation weathering, BC_0^* , and hydraulic flow rate, Q , exerted strong influence on AAI, an expected result given the explicit dependency evident in the AAI expression. The transference ratios for NO_y (T_{NO_y}) and SO_x (T_{SO_x}) exhibited relatively less influence on AAI calculations than all other parameters when evaluated at means of the variables. However, in some locations, when evaluated at other values of the variables, AAI can be more sensitive to the deposition transformation ratios.

These results suggest focusing on the uncertainties in the non-atmospheric inputs, including base cation weathering and runoff rates, and the implications of those uncertainties in setting an AAI that will have a high likelihood of providing the targeted level of protection.

F.4.2 Individual Components of the AAI

F.4.2.1 Overview of CMAQ model application

The CMAQ model is a comprehensive, peer-reviewed (Aiyyer et al., 2007), three-dimensional grid-based Eulerian air quality model designed to simulate the formation and fate of gaseous and particle (i.e., particulate matter or PM) species, including ozone, oxidant precursors, and primary and secondary PM concentrations and deposition over urban, regional, and larger spatial scales (Dennis et al., 1996; U.S. EPA, 1999; Bryun and Schere, 2006). CMAQ is run for user-defined input sets of meteorological conditions and emissions. For this analysis, we are using predictions from several existing CMAQ runs. These runs include annual simulations for 2002 using CMAQv4.6 and annual simulations for each of the years 2002 through 2005 using CMAQv4.7 (Foley et al., 2010). CMAQv4.6 was released by the U.S. Environmental Protection Agency's (EPA's) Office of Research and Development (ORD) in October 2007. CMAQv4.7 along with an updated version of CMAQ's meteorological preprocessor (MCIPv3.4, Otte and Pleim, 2010)¹ were released in October 2008². The 2002 simulation with CMAQv4.6 was performed for both the Eastern and Western domains. The horizontal spatial resolution of the CMAQ grid cells in these domains is 12 x 12 km. The 2002 through 2005 simulations with CMAQv4.7 were performed for the eastern 12-km domain and for the continental United States

¹ The scientific updates in CMAQ v4.7 and MCIP v3.4 can be found at the following web links:
http://www.cmascenter.org/help/model_docs/cmaq/4.7/RELEASE_NOTES.txt
http://www.cmascenter.org/help/model_docs/mcip/3.4/ReleaseNotes

² The differences in nitrogen and sulfur deposition in the case study areas between CMAQ v4.6 and v4.7 for 2002 are small, as described in Chapter 3.

domain, which has a grid resolution of 36 x 36 km. The CMAQv4.6 and v4.7 annual simulations feature year-specific meteorology, as well as year-specific emissions inventories for key source sectors, such as utilities, on-road vehicles, nonroad vehicles, wild fires, and natural biogenic sources. Emissions for other sectors of the inventory for each of the years modeled rely on inventories for 2002. Details on the development of emissions, meteorology, and other inputs to the 2002 CMAQv4.6 runs can be found in a separate report (U.S. EPA, 2008). Inputs for the CMAQv4.7 runs for 2002 through 2005 were derived using procedures similar to those for the CMAQv4.6 2002 runs.

Additional details of the modeling domain, emissions and meteorological inputs are provided in EPA (2009; REA Appendices).

F.4.2.2 CMAQ Evaluation, Sensitivity and Variability Analyses

Past results. A variety of comparisons of modeled estimates to observations were included in the REA (EPA, 2009), and some of the highlights are summarized here in addition to new work on ammonia characterization and wet deposition. Readers are encouraged to review the earlier report. Ambient air concentrations and wet deposition observations are paired against modeled estimates. In contrast, dry deposition is always a modeled value, either derived from ambient or modeled ambient concentrations. Given the interest in relevant nitrogen and sulfur species, CASTNET observations were used extensively. Comparisons of modeled annual average total nitrate (sum of nitric acid and particulate nitrate), ammonium, sulfate, and sulfur dioxide to observations for the 2002 base year are provided in Figures F-1 through F-4. Normalized mean bias statistics for 2002-2005 base years are provided in Table F-2.

CMAQ overpredicts SO₂ and underpredicts SO₄. Although model performance is good for total SO_x, the inclusion of co-located SO₂ and sulfate measurements required for future secondary NO_x/SO_x NAAQS comparisons will help diagnose issues with the model's ability to partition these two species. CMAQ generally overpredicts total nitrate and slightly underpredicts ammonium and the model captures the monthly temporal patterns of sulfate, total nitrate and ammonium when all sites are aggregated (Figures F-5 to F-7). There are some basic incommensurabilities between model estimates and observations that complicate interpretation of model to observation comparisons, most notably the representation of space as a model represents a volume average of roughly 144 km², which depends on the time varying vertical

depth of the lowest modeled layer. Most surface based observations rely on point sampling and the extent to which a point is representative of broader volume space varies with meteorology, distribution of emissions and surface characteristics.

Table F-2. Normalized Mean Bias Statistics for Predicted and Observed Pollutant Concentration.

| Pollutant Concentrations | 2002 | 2003 | 2004 | 2005 |
|---------------------------------|-------------|-------------|-------------|-------------|
| SO ₂ | 45% | 39% | 47% | 41% |
| SO ₄ ²⁻ | -13% | -9% | -13% | -17% |
| TNO ₃ | 22% | 26% | 22% | 24% |
| NH ₄ ⁺ | 4% | 11% | 7% | 2% |

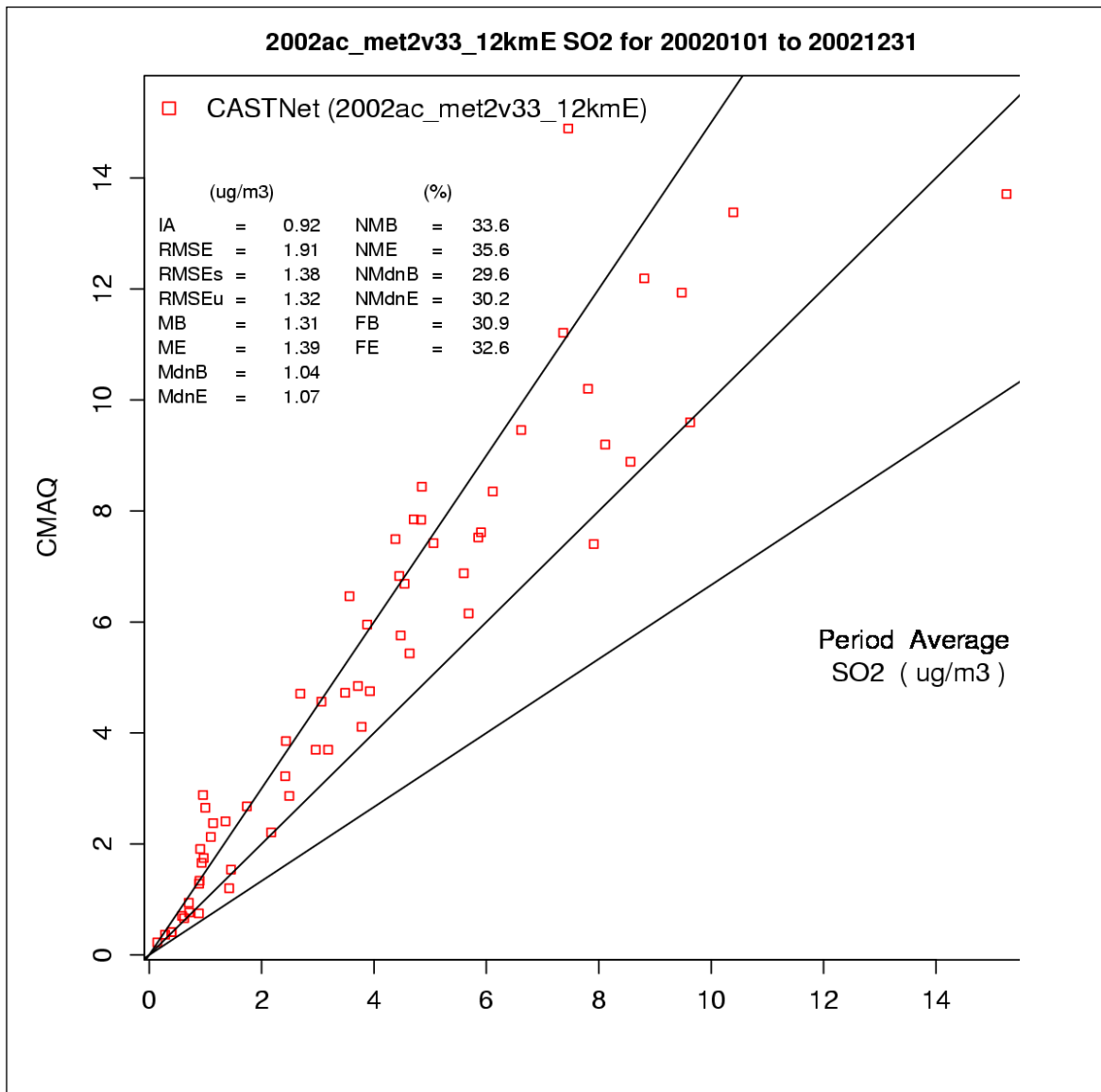


Figure F-1. 2002 CMAQv4.6 annual average SO₂ predicted concentrations versus observations at CASTNet sites in the eastern domain (note, units are in actual mass for SO₂, including oxygen).

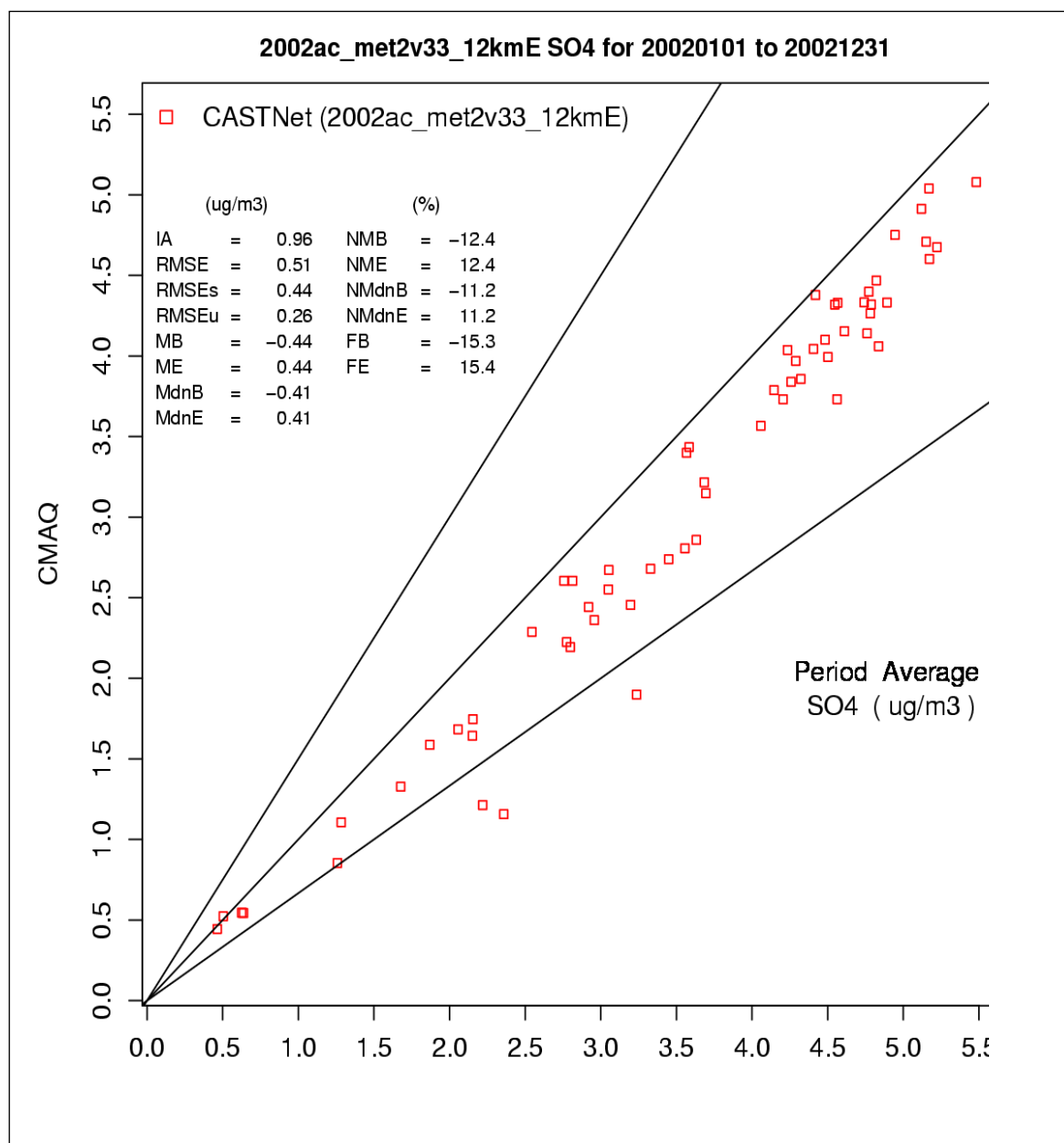


Figure F-2. 2002 CMAQv4.6 annual average SO_4^{2-} predicted concentrations versus observations at CASTNet sites in the eastern domain (note, units are in actual mass for SO_4 , including oxygen).

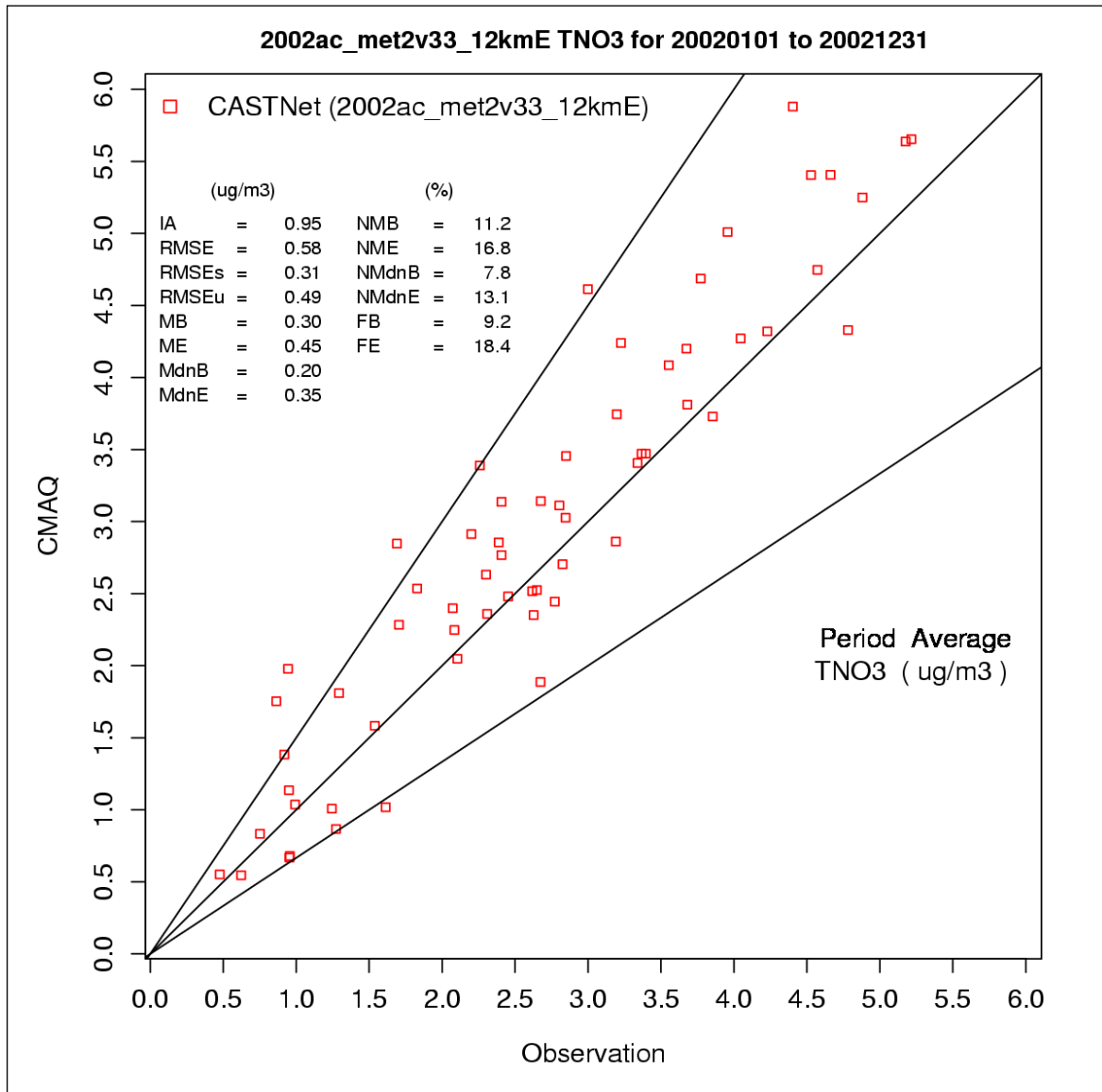


Figure F-3. 2002 CMAQv4.6 annual average TNO₃ predicted concentrations versus observations at CASTNet sites in the eastern domain (note, units are in actual mass for NO₃, including oxygen).

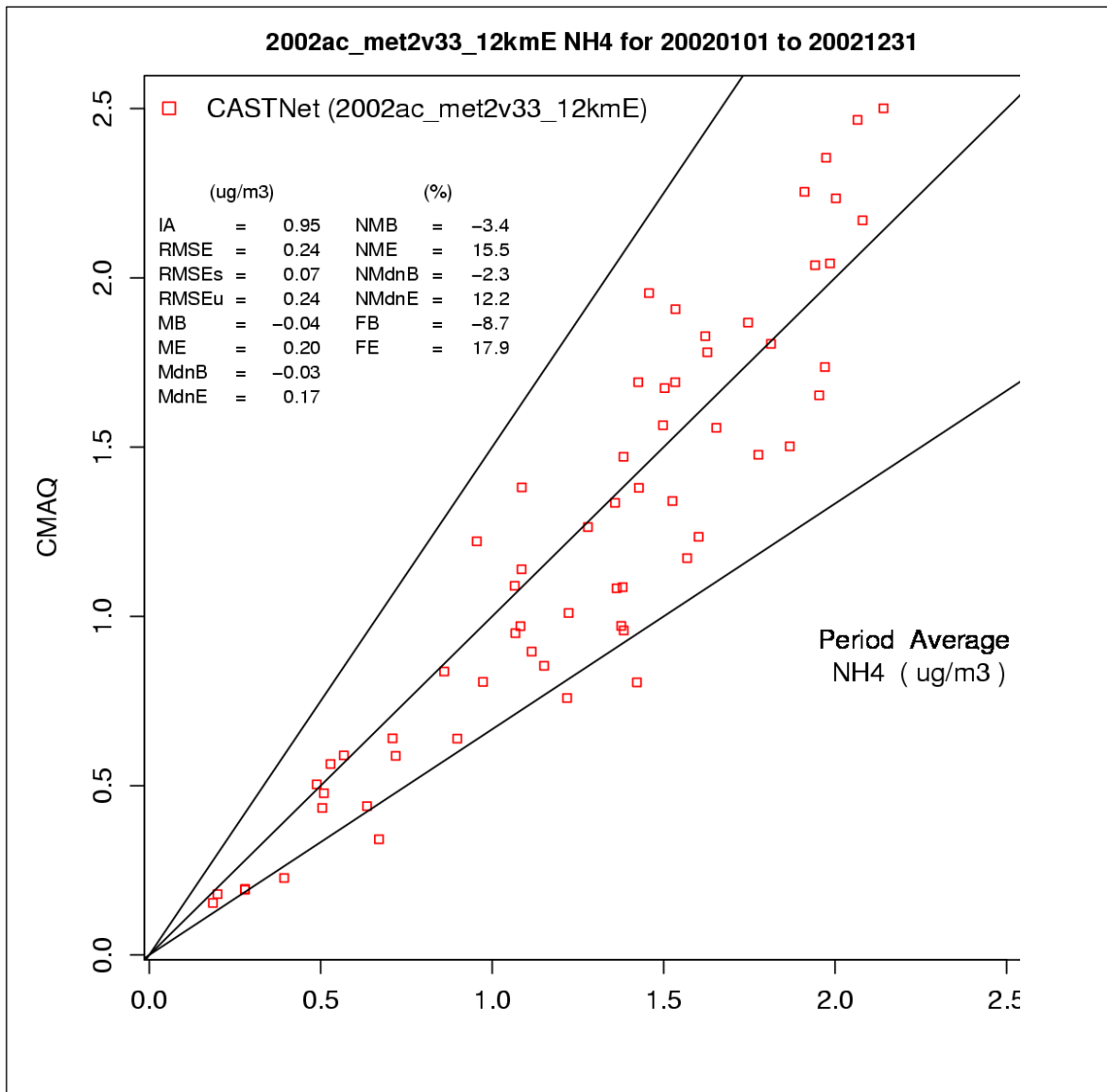


Figure F-4. 2002 CMAQv4.6 annual average NH_4^+ predicted concentrations versus observations at CASTNet sites in the eastern domain (note, units are in actual mass for NH_4 , including hydrogen).

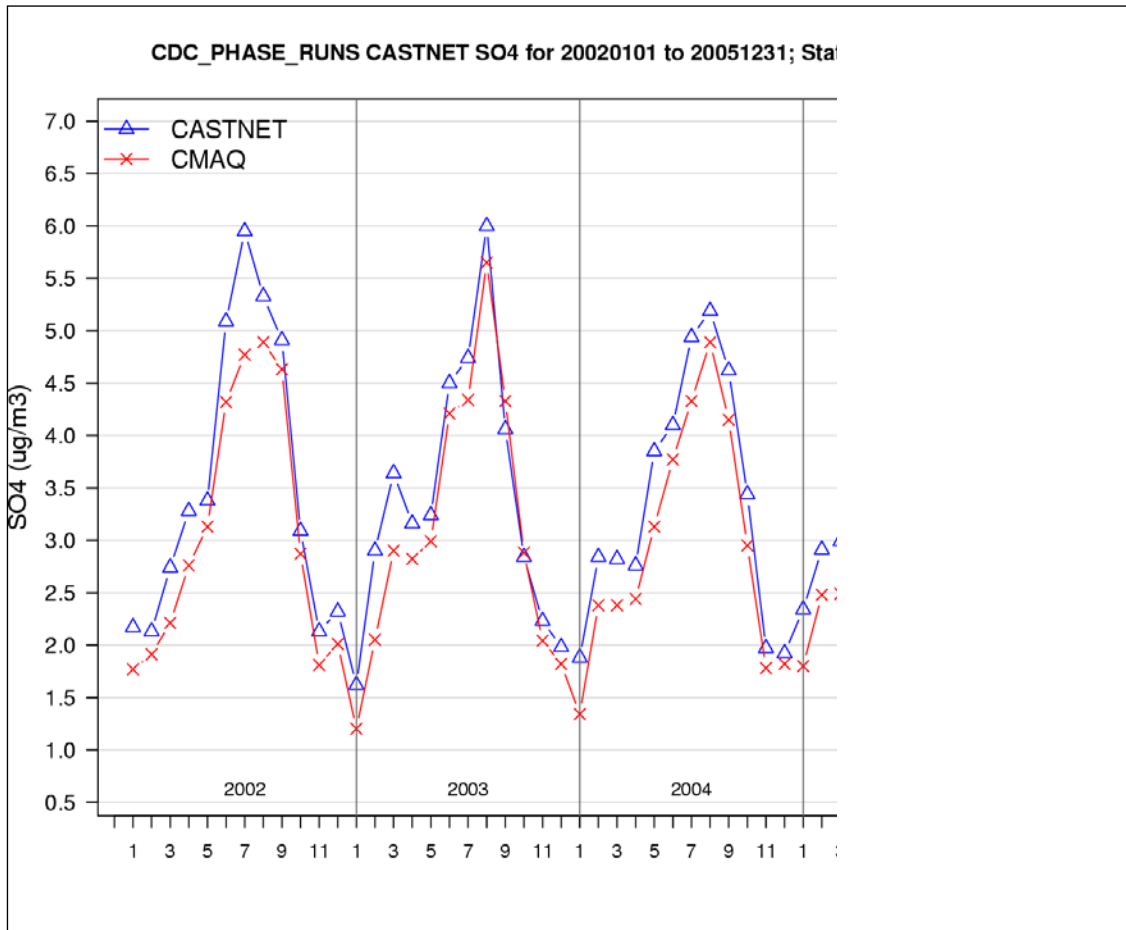


Figure F-5. 2002–2005 Domain-wide average SO_4^{2-} predicted concentrations and observations by month at CASTNet Sites in the eastern domain (note, units are in actual mass for SO_4 , including oxygen) .

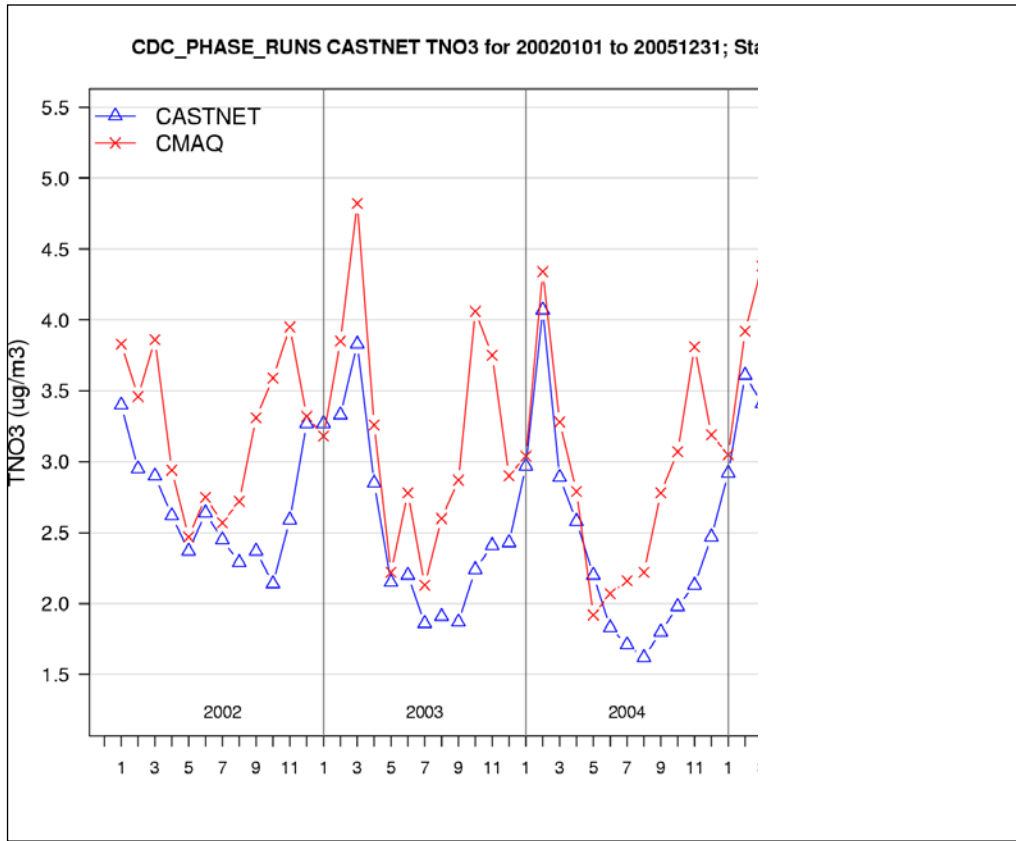


Figure F-6. 2002–2005 Domain-wide average TNO₃ predicted concentrations and observations by month at CASTNet sites in the eastern domain (note, units are in actual mass for NO₃, including oxygen).

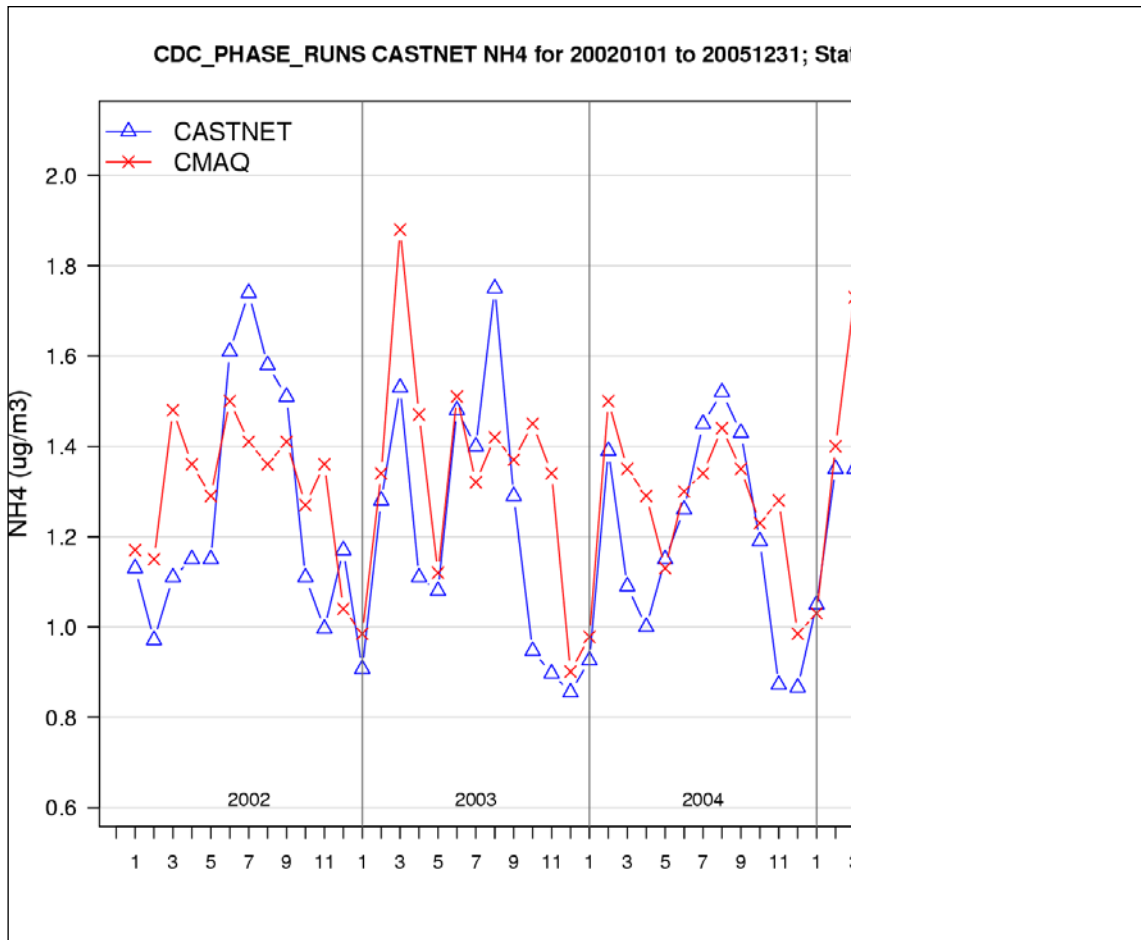


Figure F-7. 2002–2005 Domain-wide average NH₄⁺ predicted concentrations and observations by month at CASTNet sites in the eastern domain (note, units are in actual mass for NH₄, including hydrogen).

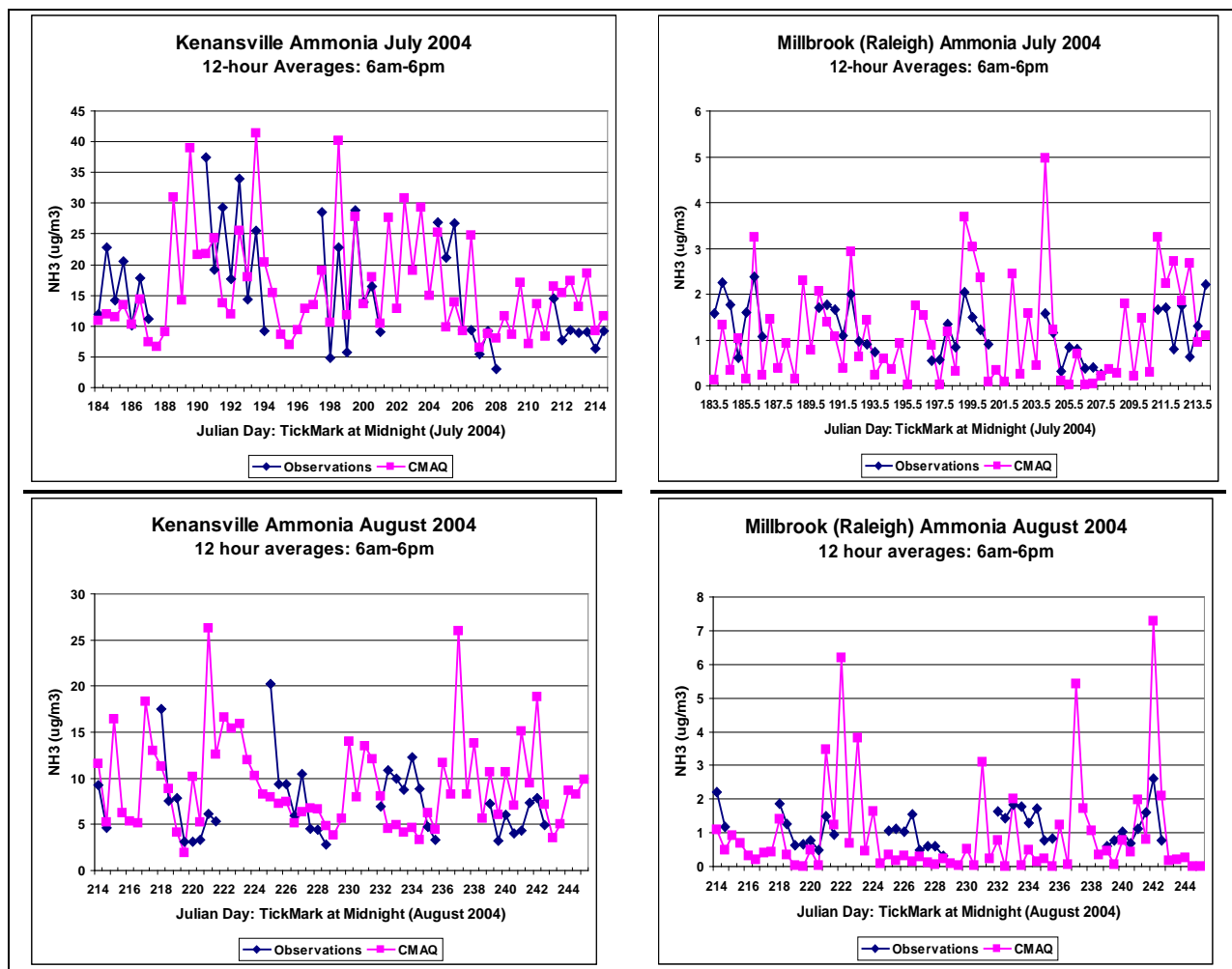


Figure F-8. Comparison of CMAQ predictions and measurements for 12-hour (6am-6pm) average NH₃ concentrations, with a monitoring cycle of 4 days on and 4 days off, at a high emission site (Kenansville) and a low emission urban site (Raleigh) in North Carolina compared to CMAQ for July 2004 (top) and August 2004 (bottom), from Dennis et al., 2010 (note, units are in actual mass for NH₃, including hydrogen).

Comparison with SEARCH Data

The SEARCH network (chapter 2) includes sites instrumented with continuously operating SO₂ monitors. Comparison of CMAQ estimated SO₂ and SEARCH data showed similar over-predictions to CASTNET data sets. The SEARCH data affords the ability to diagnose the diurnal aspects of SO₂ patterns, which is not possible with the weekly averaged CASTNET data. Example model to observation plots follow for the SEARCH sites reflecting regional air quality, located away from major sources.

OLF : Hourly SO2 (ppb), 2006

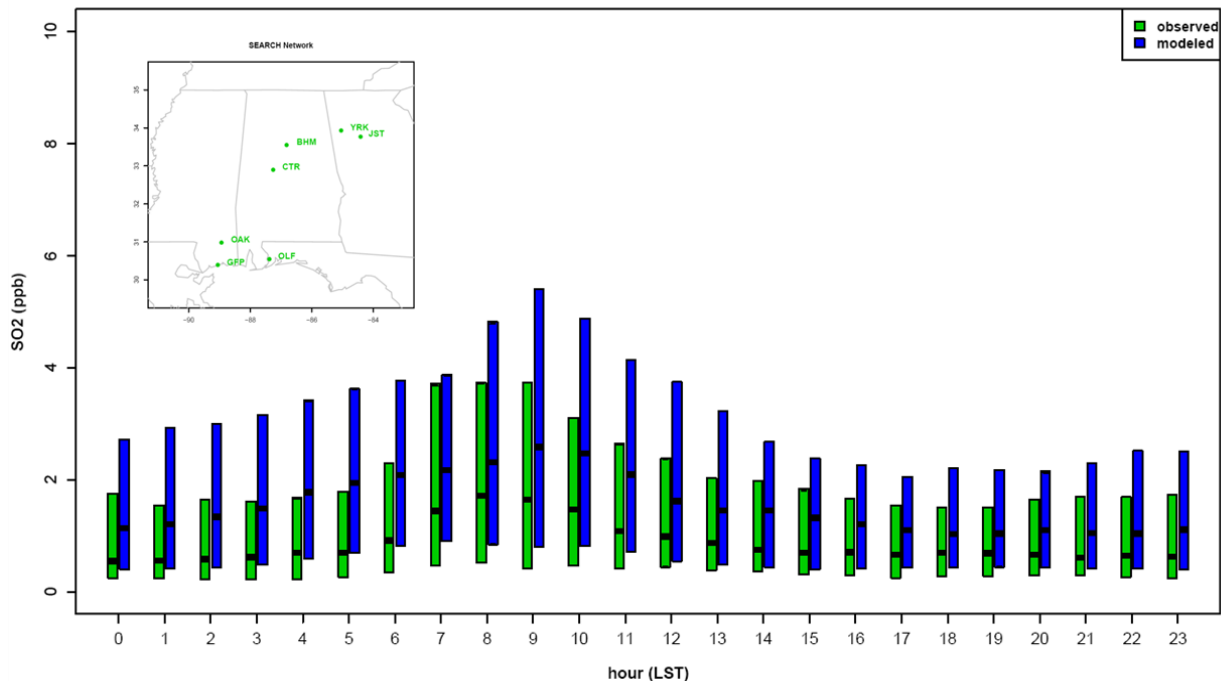


Figure F-9. 2006 hour by hour comparisons of CMAQ and SEARCH SO2 data at the Ook Grove, MS site (source, K. Foley, U.S. EPA-ORD)

CTR : Hourly SO2 (ppb), 2006

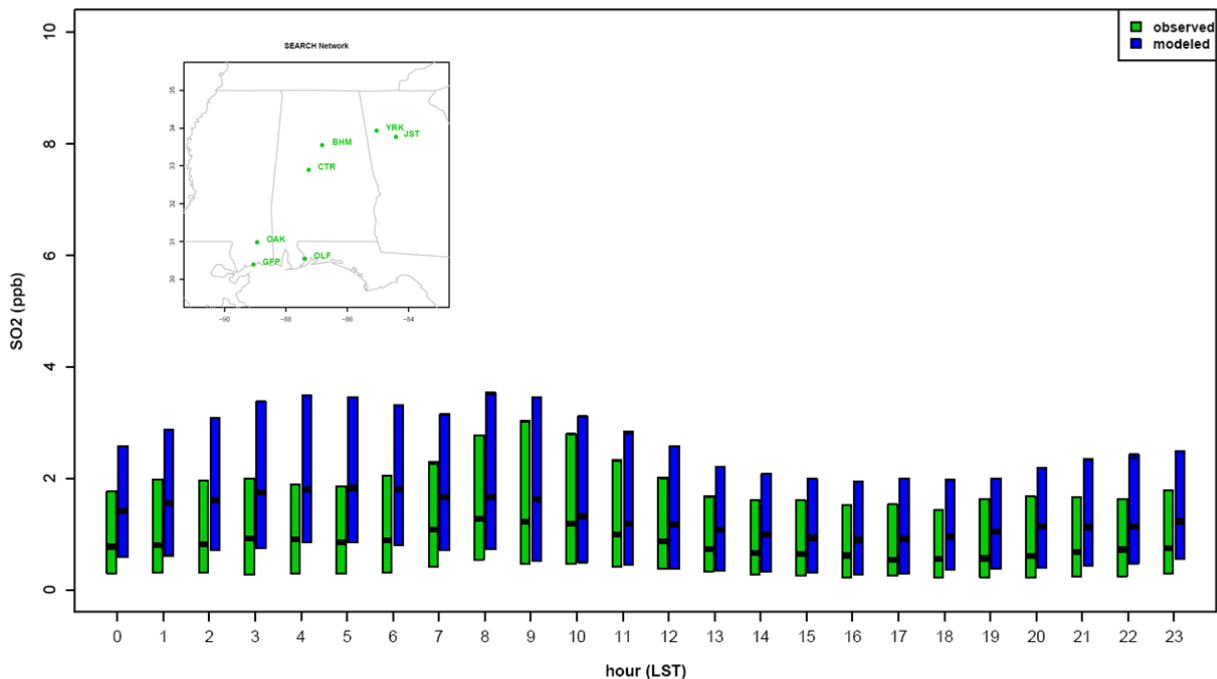


Figure F-10. 2006 hour by hour comparisons of CMAQ and CSEARCH SO2 data at the Centerville, AL site (source, K. Foley, U.S. EPA-ORD)

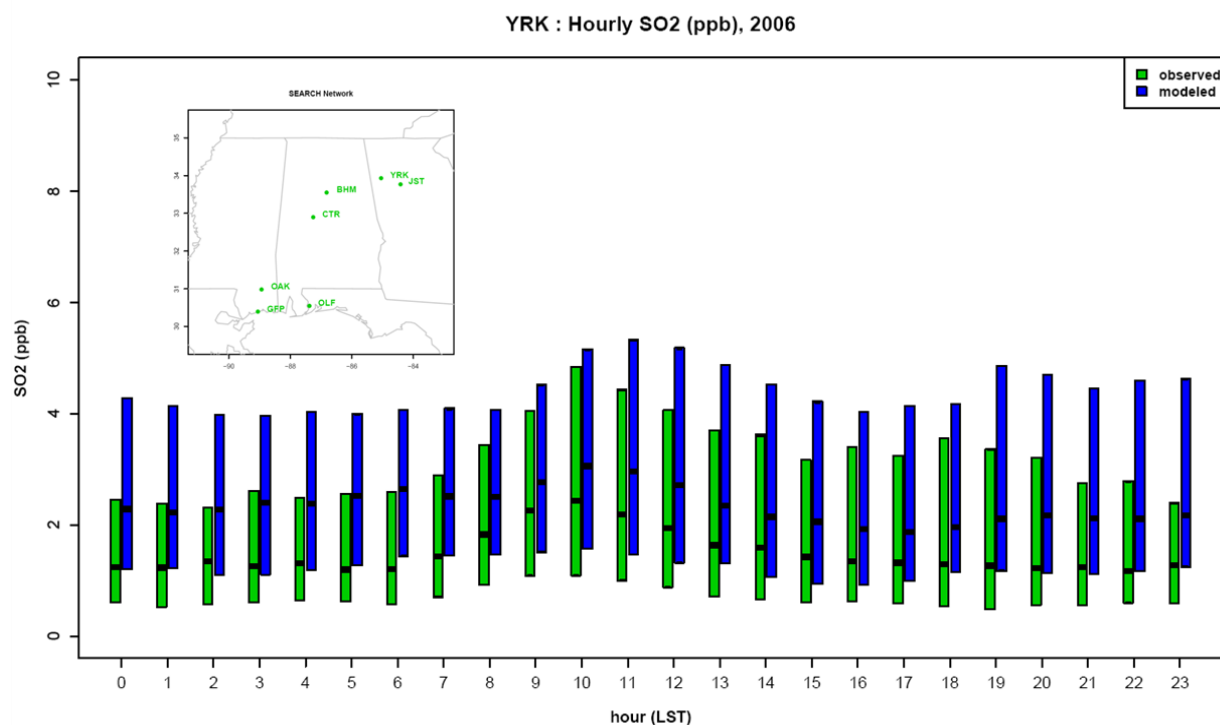


Figure F- 11. 2006 hour by hour comparisons of CMAQ and CSEARCH SO2 data at the Yorkville, GA site (source, K. Foley, U.S. EPA-ORD)

Wet deposition.

Modeled wet deposition in CMAQ is a function of the volume of predicted precipitation within a grid cell and the pollutant concentrations scavenged from the atmosphere during precipitation events. As a result, errors in modeled precipitation and in emission inputs can lead to significant bias and error in the wet deposition predictions compared to observed values. EPA (Dennis and Foley, 2010) has corrected CMAQ wet deposition predictions by scaling the model output based on observation-based gridded precipitation data generated by the Parameter-elevation Regressions on Independent Slopes Model (PRISM, 2004). The precipitation adjusted deposition fields are more highly correlated with observed values for all wet deposited nitrogen and sulfur species compared to the base model output (Figures F-12, F-13). In addition, the adjusted fields are better able to capture the spatial heterogeneity of accumulated wet deposition due to orographic effects on precipitation amounts.

Adjusting the wet deposition values to account for over-predictions in the model precipitation inputs revealed compensating errors for nitrate and ammonium. The negative bias seen in these species after the precipitation adjustment is believed to be due to missing emissions

sources. A second bias adjustment was performed for nitrate and ammonium based on observed levels at the NADP/NTN sites (Figure F-13). The final adjusted spatial fields of annual total wet deposition values are more consistent with observed wet deposition values. Ongoing studies suggest that much of this bias can be reduced in the Eastern half of the US by including nitrogen oxide produced by lightning and accounting for the bi-directional flux of ammonia. Once these model improvements are incorporated in CMAQ a second bias adjustment may not be needed in the East.

In 2011, the EPA will deploy a prototype flux measurement package over a grass field at the Duke Forest Blackwood Division. Dry deposition fluxes will include NO_y, NO₂, HNO₃, HONO, NO₃ aerosol, NH₃, NH₄ aerosol, SO₂, SO₄ aerosol and ozone. Concentrations of organic N in aerosol, but not fluxes, also will be measured. The availability of these flux measurements will enable a more direct assessment of CMAQ treatment of sulfur and nitrogen deposition processes.

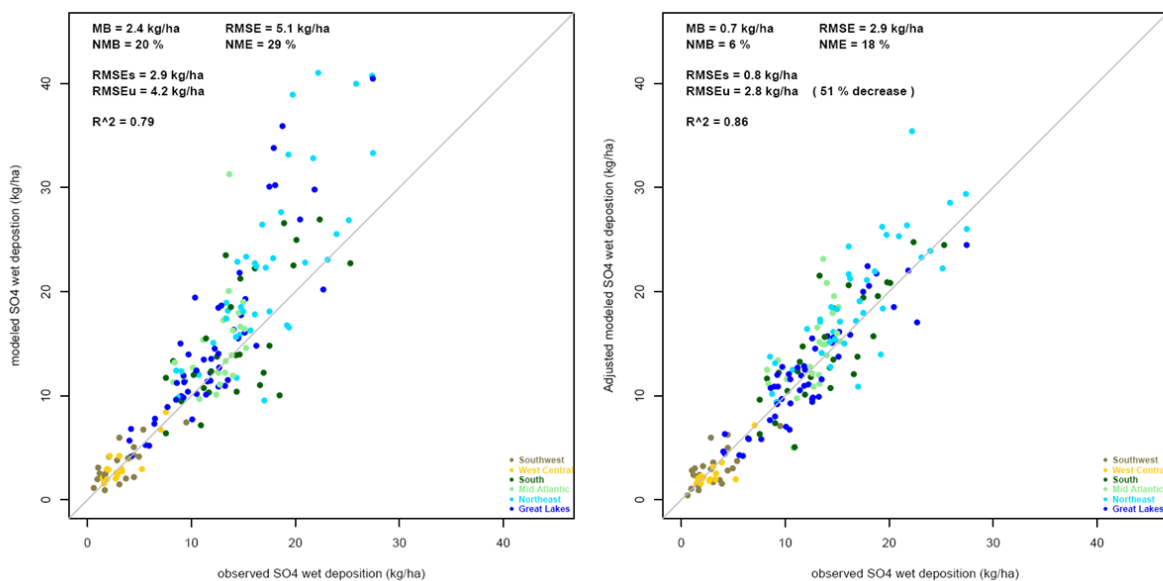


Figure F-12. Unadjusted (left) and PRISM (right) adjusted CMAQ annual wet deposited sulfate for 2002 (note, units are in actual mass for SO₄, including oxygen).

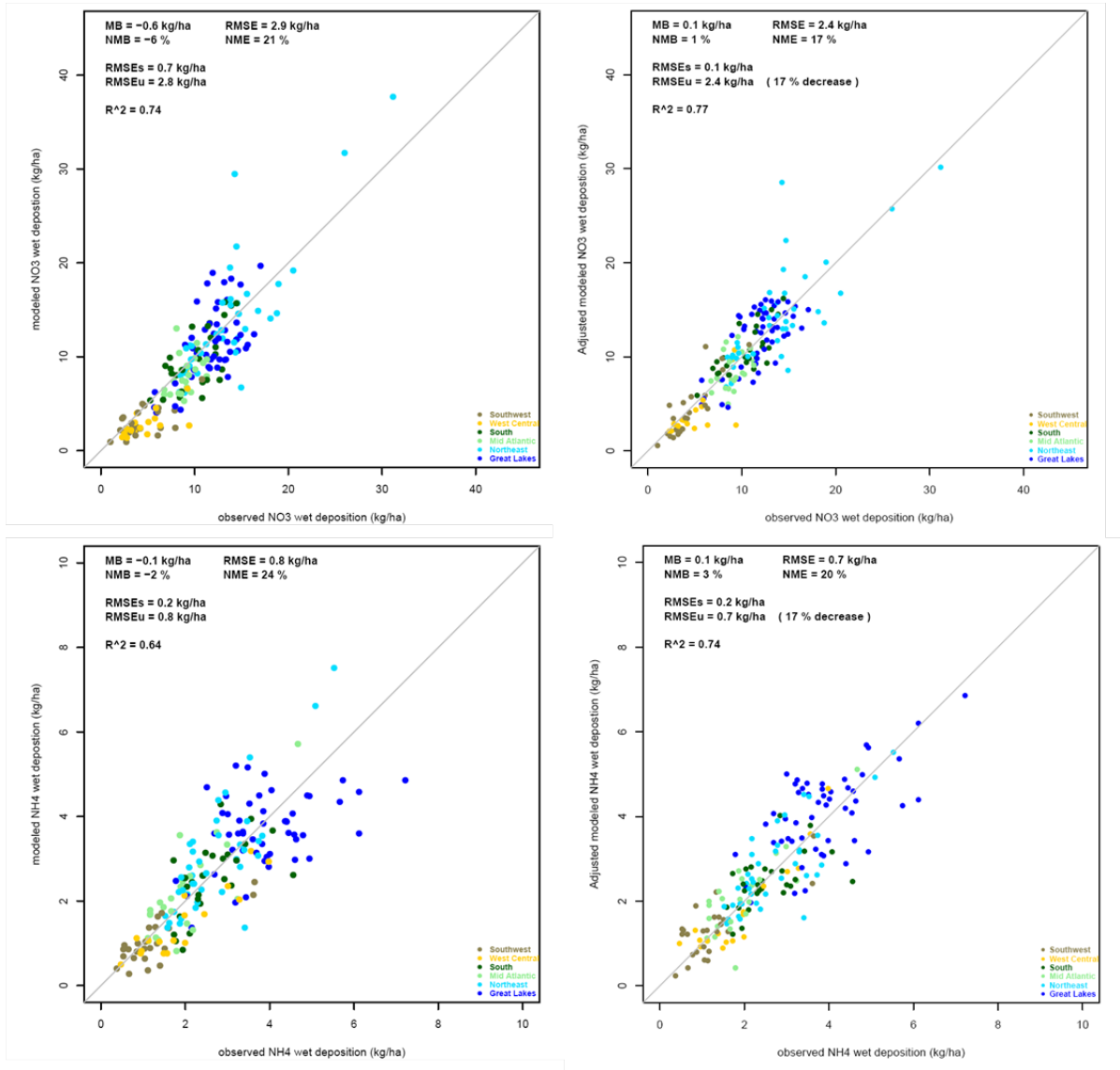


Figure F-13. Unadjusted (left) and PRISM and bias (right) adjusted CMAQ annual wet deposition of nitrate (top) and ammonium (bottom) (note, units are in actual mass for NH₄ and NH₃, including hydrogen).

Ammonia.

The role of NH_x deposition is incorporated in the AAPI expression as a parameter that influences the level of allowable concentrations of NO_y and SO_x , due to its role as part of the total reactive nitrogen budget which affects acidification. Characterizing ammonia deposition is challenging due to the variety of surface and vegetation types that influence ammonia dry deposition velocities as well the potential for bi-directional flux of ammonia. In addition, ammonia emission estimates remain relatively more uncertain than emissions of NO_x and SO_2 given the complexity of meteorology and agricultural practices that influence the spatial and temporal patterns of ammonia releases. An exploration of the sensitivity of ammonia to three different treatments of deposition processes in CMAQ was performed by EPA (Dennis et al., 2010) to test the inclusion of a bi-directional NH_3 flux algorithm and elucidate the relative importance associated with advection, deposition and chemical transformation on ammonia patterns. These treatments included a (1) base case of current CMAQ treatment using existing ammonia deposition velocity schemes and uni-directional deposition, (2) modified the base case by replacing ammonia deposition velocity calculations with SO_2 deposition velocities (SO_2 interacts with surfaces and vegetation similarly to NH_3 , but with reduced velocity) as a lower bound and (3) introducing a bi-directional flux algorithm to the base case (retaining NH_3 deposition velocities). Based on modeled process analysis that delineates the effects of deposition, chemical transformation and advection (horizontal and vertical) on emitted ammonia, the results (Figure F-14) suggest that ammonia patterns, especially when a bi-directional flux process is incorporated, are more indicative of a transported pollutant where emissions influence can span hundreds of kilometers, markedly different from some earlier perspectives where ammonia often was thought of as near source phenomenon due to high deposition velocities. The process analysis illustrates the importance of vertical advection which enables the movement of ammonia into traditional mesoscale flow patterns. The effect is enhanced by the reintroduction of deposited ammonia through bi-directional flux into the ambient environment.

From a monitoring perspective, a design that addresses the regional characterization of NO_y and SO_x would be consistent with characterizing NH_x . Not only would ammonia and ammonium measurements be useful for estimating dry deposition through deposition modeling approaches such as those used in CASTNET, but they would serve as important diagnostic data

to continually assess the effectiveness of NH_x deposition processes in models like CMAQ. This is especially important as we recognize a large uncertainty in the bi-directional formulation associated with the estimation of Γ , the emissions potential due to the existence of compensation points. Nonetheless, we can learn much about the NH_3 budget in spite of these uncertainties.

High priority research is ongoing to improve the bi-directional parameterization and the estimates of the leaf and soil gammas across different cropping regions and throughout the year. We are developing a software tool to estimate the soil Γ associated with fertilizer application. When we have a spatially and temporally varying Γ_g , we will investigate the emissions budgets for fertilized fields, as well as reexamine the animal operation emission budgets, as this will be of interest. Work to examine the seasonality of single cell budgets and their range of influence is continuing. Current and future CMAQ applications to ecosystem deposition will incorporate bi-directional flux treatment of ammonia.

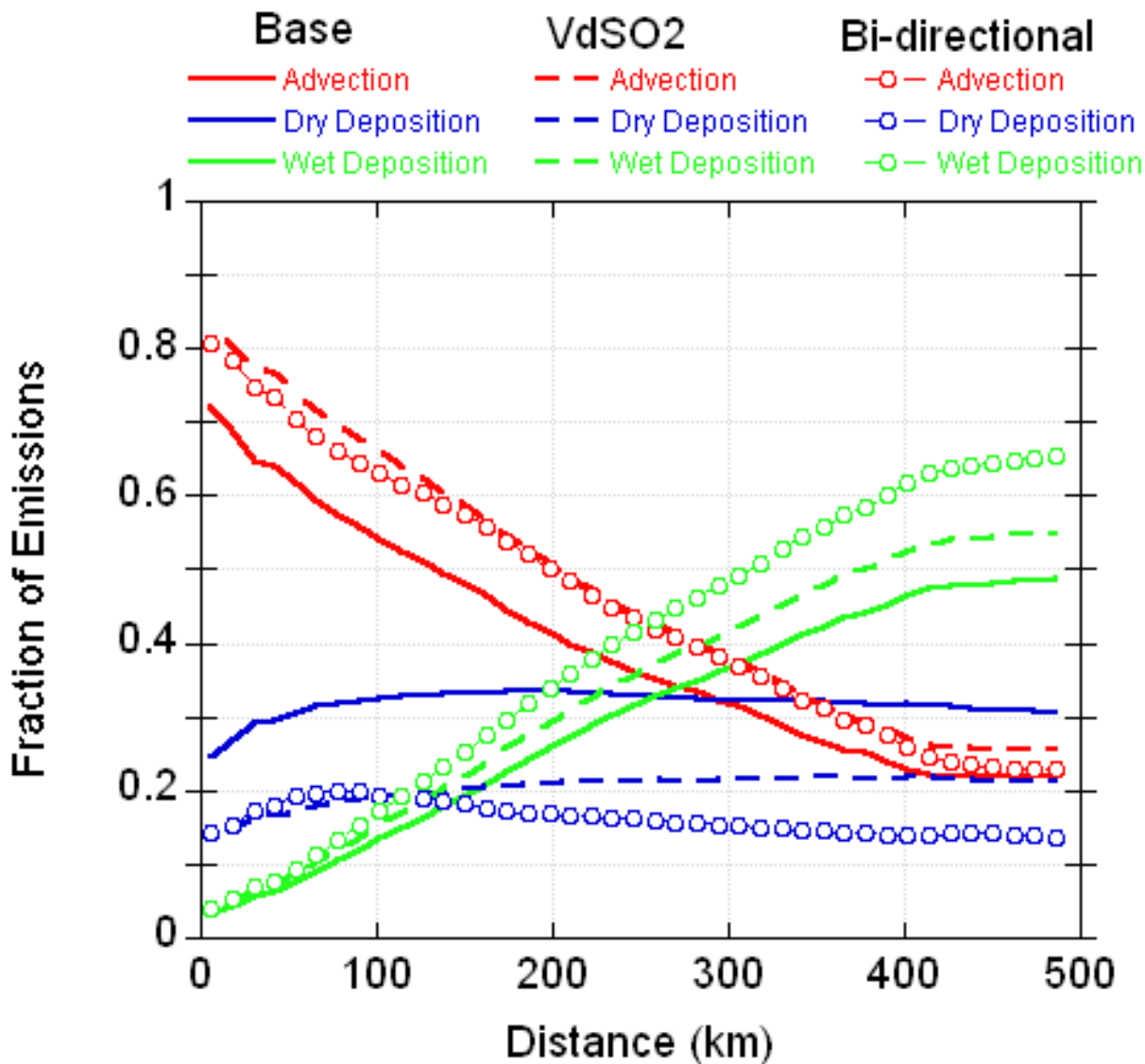


Figure F-14. Cumulative regional NH₃ budget of advection, wet- and dry deposition, calculated for an expanding box starting at the high-emitting Sampson County NC cell (from Dennis et al, 2010)

F.4.2.3 Variability and sensitivity of CMAQ generated components.

Ambient Concentration to Deposition Transformation ratios.

Derivation

Atmospheric pollutants deposit onto land and water surfaces through at least two major mechanisms: direct contact with the surface (dry deposition), and transfer into liquid

precipitation (wet deposition). The magnitude of each deposition process is related to the ambient concentration through the time-, location-, process- and species-specific *deposition velocity* (Seinfeld and Pandis, 1998):

$$Dep_i^{Dry} = v_i^{Dry} \cdot C_i^{Amb} \quad (1)$$

$$Dep_i^{Wet} = v_i^{Wet} \cdot C_i^{Wet} \quad (2)$$

where v_i^{Dry} and v_i^{Wet} are the dry and wet deposition velocities, Dep_i^{Dry} and Dep_i^{Wet} are the dry and wet deposition fluxes, C_i^{Amb} is the ambient concentration, and the i subscript indicates the pollutant species under study. The total deposition of each pollutant is

$$Dep_i^{Tot} = Dep_i^{Dry} + Dep_i^{Wet} \quad (3)$$

Substituting Equations 1 and 2 into Equation 3 yields

$$Dep_i^{Tot} = v_i^{Dry} \cdot C_i^{Amb} + v_i^{Wet} \cdot C_i^{Amb} \quad (4)$$

The total deposition of sulfur or nitrogen would therefore be:

$$Dep_{S|N}^{Tot} = \sum_i (v_i^{Dry} + v_i^{Wet}) \cdot m_i \cdot C_i^{Amb} \quad (5)$$

where m_i is the molar ratio of the atom (sulfur or nitrogen) of interest to the i th pollutant.

Ambient sulfur- and nitrogen-containing pollutants include gases such as sulfur dioxide (SO₂), ammonia (NH₃), various nitrogen oxides (NO, NO₂, HONO, N₂O₅), nitric acid (HNO₃), and organic nitrates such as peroxyacetyl nitrates (PAN); as well as particulate species such as sulfate (SO₄²⁻), nitrate (NO₃⁻), and ammonium (NH₄⁺). The species regulated by the SO_x/NO_x standard will include the sulfur-containing species above and the above oxidized forms of nitrogen (NO_y); ammonia and ammonium are not currently included as regulated pollutants.

Aggregation Issues

Equation 5 provides a relationship for converting a sulfur or nitrogen deposition to an “equivalent” airborne concentration. This is useful for setting the NAAQS, where we expect to convert deposition critical loads developed by the ecosystem models to ambient concentrations, which will then be the air quality standard. A major issue to consider during such conversion is the spatial, temporal and chemical resolutions of the deposition data and the resulting standards. Since the objective is to regulate total oxidized sulfur and nitrogen, and this is also the chemical

resolution provided by the ecosystem models, it is convenient to collect the deposition velocities and apply the m_i values to the C_i 's in Equation 5 and re-arrange it as

$$C_{S/N}^{Tot} = V_{S/N} \cdot Dep_{S/N}^{Amb} \quad (6)$$

where $V_{S/N}$ is a constant that relates total deposition of sulfur or nitrogen to the total ambient concentration. Since the deposition critical loads are annual total depositions, it is proposed that the standard be an annual average concentration. Data used to derive annual $V_{S/N}$ values will need to have the same spatial representativeness as the critical loads.

Air Quality Simulation Models

Ideally, $V_{S/N}$ values would be derived for each area of interest from concurrently collected sulfur and nitrogen deposition and concentration measurements. However, no monitoring network currently exists that can provide such information. We therefore propose using output of the Community Multi-scale Air Quality (CMAQ) model (EPA, 1999) for initial calculation of $V_{S/N}$ values.

CMAQ provides both concentrations and depositions of a large suite of pollutant species on an hourly basis for 12 km grids across the continental U.S. Its comprehensive structure is ideal for providing $V_{S/N}$ values that appropriately address the chemical and temporal aggregation issues discussed above, and weighted spatial averages of the gridded data can be used for areas that span multiple grid cells. The major potential drawback to using CMAQ output is that the data is simulated rather than measured, which calls its accuracy into question (discussed further below).

CMAQ does not directly calculate or use $V_{S/N}$ values; instead the following procedures are used in the code to model deposition:

1) v^{dry} values of gaseous pollutants are calculated in the CMAQ weather module called the Meteorology-Chemistry Interface Processor (MCIP) through a complex function of meteorological parameters (e.g. temperature, relative humidity) and properties of the geographic surface (e.g. leaf area index, surface wetness).

2) v^{dry} values for particulate pollutants are calculated in the aerosol module of CMAQ, which, in addition to the parameters needed for the gaseous calculations, also accounts for properties of the aerosol size distribution.

3) v^{wet} values are not explicitly calculated. Wet deposition is derived from the cloud processing module of CMAQ, which performs simulations of mass transfer into cloud droplets

and aqueous chemistry to incorporate pollutants into rainwater, all of which is conceptually contained in the v^{wet} parameter in Equation 2.

The deposition transference ratios³ introduced in Chapter 5 are referenced as T_{SO_x} and T_{NO_y} , to distinguish these parameters from an exact linkage to deposition velocity, which is uniquely associated with individual atmospheric species. Deposition transference ratios are defined as the annual wet and dry deposition of all oxidized species (NO_y for T_{NO_y} , SO_2 plus SO_4 for T_{SO_x}) divided by the average annual concentration of NO_y , for T_{NO_y} , or SO_4 plus SO_2 , for T_{SO_x} . The units for T_{NO_y} and T_{SO_x} are distance/time. Deposition transference ratios provide a mechanism to associate ambient concentrations to deposition loads and to determine if an area's air concentrations of NO_y and SO_x meet a NAAQS level using the AAI form. A deposition transformation ratio is an aggregate representation of the deposition process generated through modeling which does not lend itself to a traditional analysis relating observations and predictions. Furthermore, there is an implicit assumption that the response of deposition transformation ratios to changes in meteorology and emissions is relatively stiff, as these ratios are an attribute of the system that channels ambient air response associated with decreases in emissions of NO_x and SO_x to changes in deposition. The stiffness of the deposition transference ratios would suggest that the relationship between ambient concentrations and deposition is strictly a constant proportion, not impacted by the mixture and level of emissions or by changes in meteorology. To better understand the implications of this assumption, we investigated the relative variability of the modeled deposition transformation ratios across time and space, and the stability of the ratios relative to emissions and meteorological inputs was conducted to guide EPA in determining how uncertainties in this parameter may eventually impact AAI related calculations.

Spatial and Interannual Variation of T_S and T_N .

Generally small spatial and inter-annual variability exist in the deposition transformation ratios for the 2002 -2005 model years (Figure F-15). The inter-annual variability, calculated at the grid cell level, as measured by the median coefficient of variation is around 10% and the absolute values of the ratios remain stable, suggesting that year to year changes in meteorology

³ In the first draft of the Policy Assessment, the deposition transformation ratios were labeled V_{NO_x} and V_{SO_x} . For this draft, based on recommendations from CASAC, we have renamed these ratios T_{NO_x} and T_{SO_x} .

have minimal impact on the ratios. Spatial homogeneity of deposition transformation ratios within the two acid sensitive areas we evaluated in the REA (Adirondacks and Shenandoah) (Figure F-15) is consistent with a relatively homogeneous ambient concentration environment overlaid upon a landscape of similar vegetation and surface conditions. Such spatial homogeneity within case study areas provides confidence that an area wide application AAI will not be strongly dependent on the exact boundaries chosen to define an acid sensitive area.

T_{SOx} and T_{NOy} Sensitivity to emission changes.

The response of T_{SOx} and T_{NOy} to emission changes was explored by analyzing available base case 2005 and a CMAQ simulation emissions reduction scenario referred as the 2030 case. The 2030 case represents Eastern U.S. domain wide NOx and SOx emission reductions of 48% and 40%, respectively. Median changes in deposition transference ratios tended to be around zero (Figure F-16), with the Adirondack region exhibiting slightly higher response than the Shenandoah region and remainder of the Eastern U.S. domain.

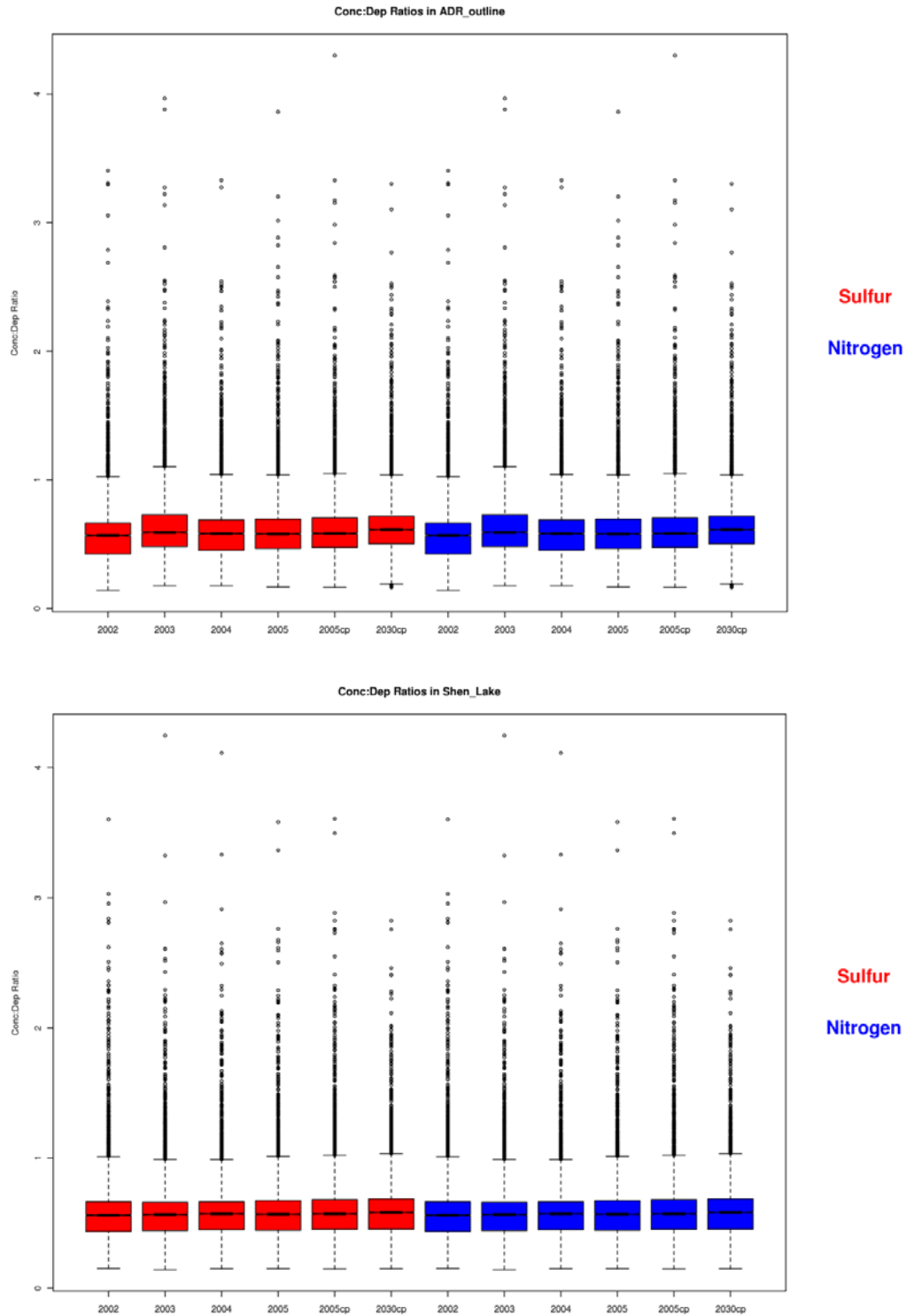


Figure F-15. Spatial and interannual variability of inverse deposition transference ratios, $1/T_{SO_x}$ and $1/T_{NO_y}$, for Adirondack (top) and Shenandoah case study areas.

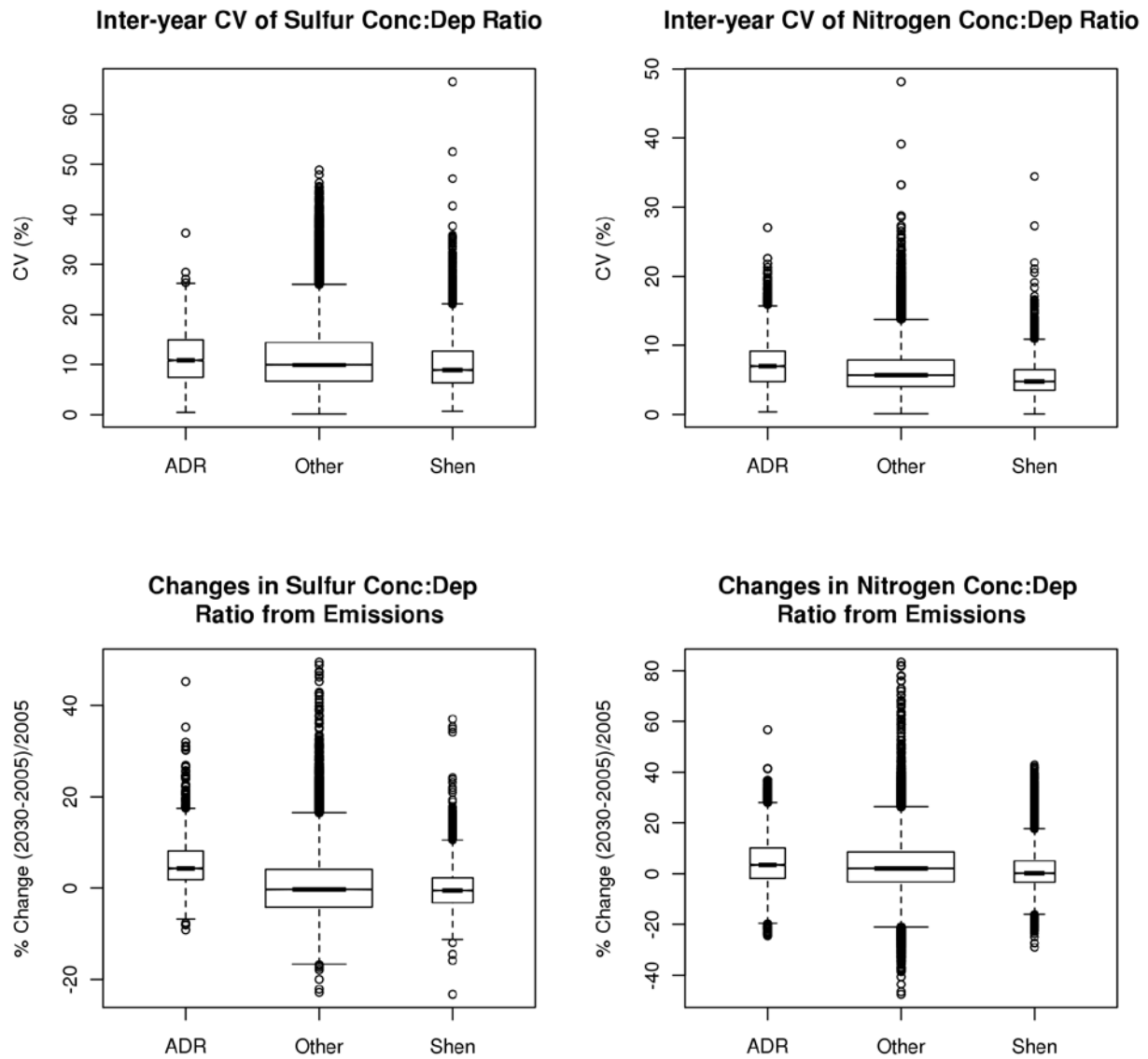


Figure F-16. Summary of inter-annual and emissions sensitivity variability of sulfur and nitrogen deposition transference ratios.

Comparisons of CMAQ and CASTNET and NADP generated T_{SO_x} and T_{NO_y}

Transference ratios based on CASTNET sulfur and nitrogen measurements, CASTNET derived dry deposition and NADP wet deposition were constructed to approximate ratios developed using measurements where possible. These ratios were developed to compare with CMAQ derived ratio. The limitations of the ratios constructed from observations include availability of only part of the NO_y species mix, total nitrate, as well as the use of a model to calculate dry deposition velocities. Nevertheless, any comparison to measurements not only can provide some assurance that CMAQ constructed ratios relate to observed data as well as serving as a potential diagnostic metric for modeled deposition processes. Modeled and observed ratios (Figure F-17) indicate closer agreement for T_{SO_x} relative to T_{NO_y} , an expected result given the missing nitrogen species in the CASTNET data set. It is difficult to diagnose the cause of differences as the dry deposition estimates from CASTNET are based on different modeling approach relative to that used in CMAQ. However, as observation data sets become more complete, these types of analyses can help elucidate what aspects of deposition characterization require improvement. The next logical steps in developing comparisons between observed and modeled ratios will be to replace CMAQ wet deposition with PRISM based wet deposition results to allow for a better spatial pairing of observed and modeled data sets. This would partially constrain the problem to differences in dry deposition calculation methods between CASTNET and CMAQ. EPA's ORD will be conducting sulfur and nitrogen dry deposition flux experiments in 2011. Those data will provide be extremely valuable diagnostic information to improve CMAQ deposition processes, which in turn will lead to improved confidence in CMAQ derived deposition ratios.

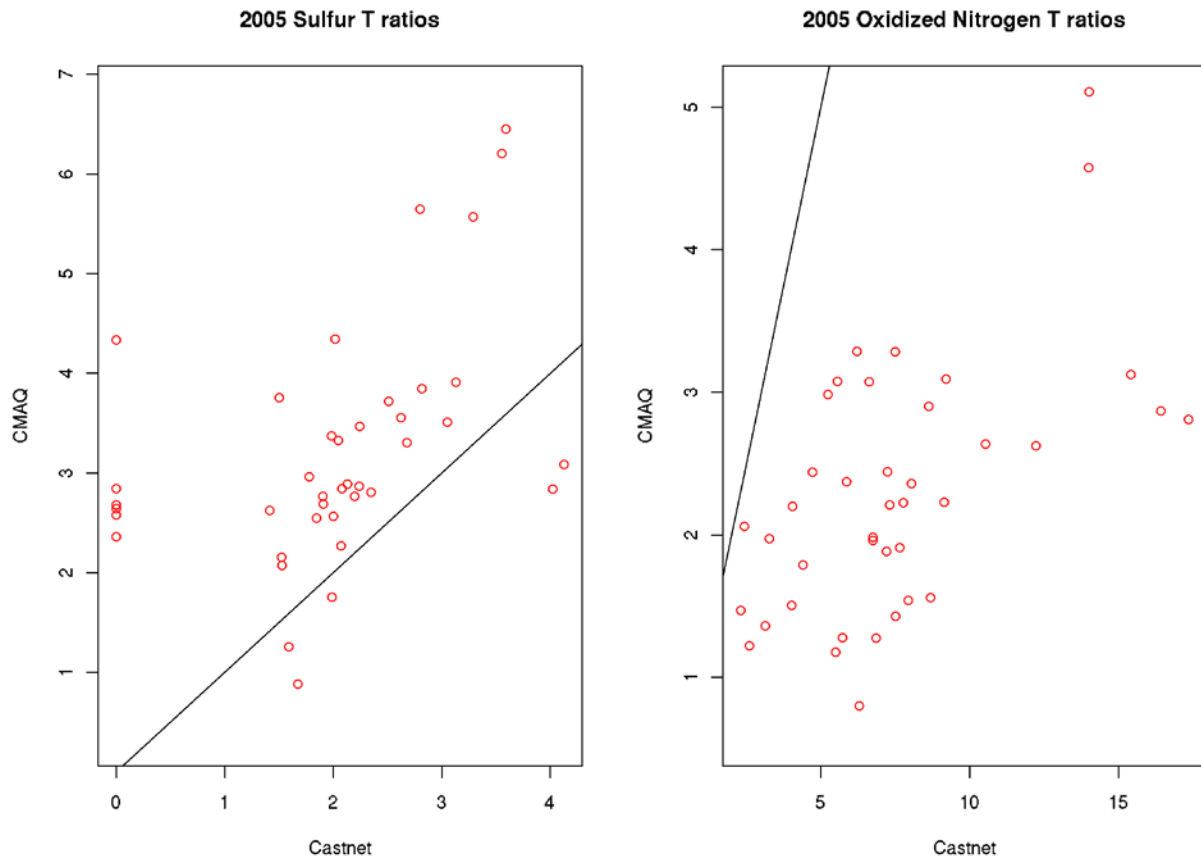


Figure F-17. Comparison of observation based and CMAQ derived transference ratios. Each point represents an annual average at the grid cell of the CASTNET station. The Observed values used NADP wet precipitation data, CASTNET air quality data and modeled dry deposition based on the CASTNET observations and the dry deposition model specific to CASTNET.

Comparisons between models

The variability in T ratios of SO_x and NO_x was explored by comparing their values from a number of different modeling scenarios. Model runs were procured for the purpose of analyzing variability from the following sources:

The variability in T ratios due to each of these sources is shown through boxplots specific to pollutants (i.e. SO_x and NO_x) and selected study areas (the Adirondacks, Shenandoahs) in Figures F-18 to F-21. The data in the boxplots are the T values of all grid cells whose center lies within the specified study area. The center line of each box are the population medians, the box edges are the 25th and 75th percentiles, the ends of the whiskers are the 10th and 90th percentiles, and the points are data that lie outside the 10th and 90th percentiles. The notches in the boxes indicate the significance differences in the medians: non-overlapping notches strongly suggest that the populations are significantly different. The model scenario that produced each box's data is indicated on the x-axis.

The boxplots show that, in general, there is not a large degree of inter-annual variability in T ratios. The notches of T ratios for nitrogen appear to overlap for all 4 years of CDC 12km and 36 km CMAQ runs in both study areas. The S values appear to be slightly high in the Shenandoahs in 2003 and lower in 2005 in the 12 km run. The 36 km result show what appears to be a decline in S values in both areas, especially when comparing the first 2 years to the latter 2 years. Results from the AURAMS 2005 runs appear to generally be similar to those of the 2005 CMAQ runs, which is surprising given the different mix of chemical species available for calculations and the much larger (45 km) grid size of the AURAMS model.

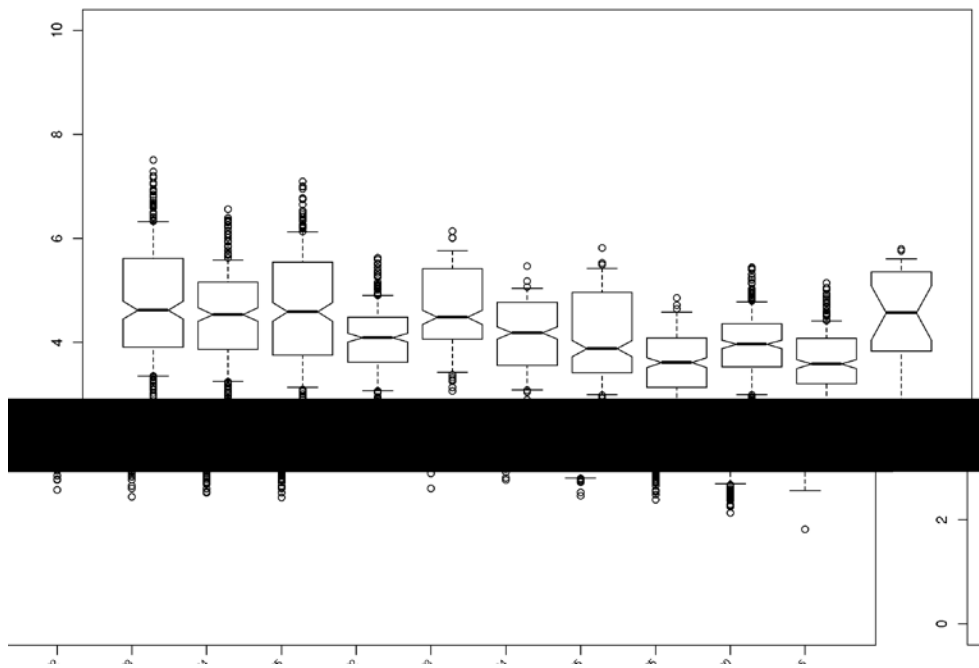


Figure F-18. Modeled generated T_{NOy} ratios in the Shenadoah area showing CMAQ 12 and 36 km values 2002 – 2005 and AURAMS 2005.

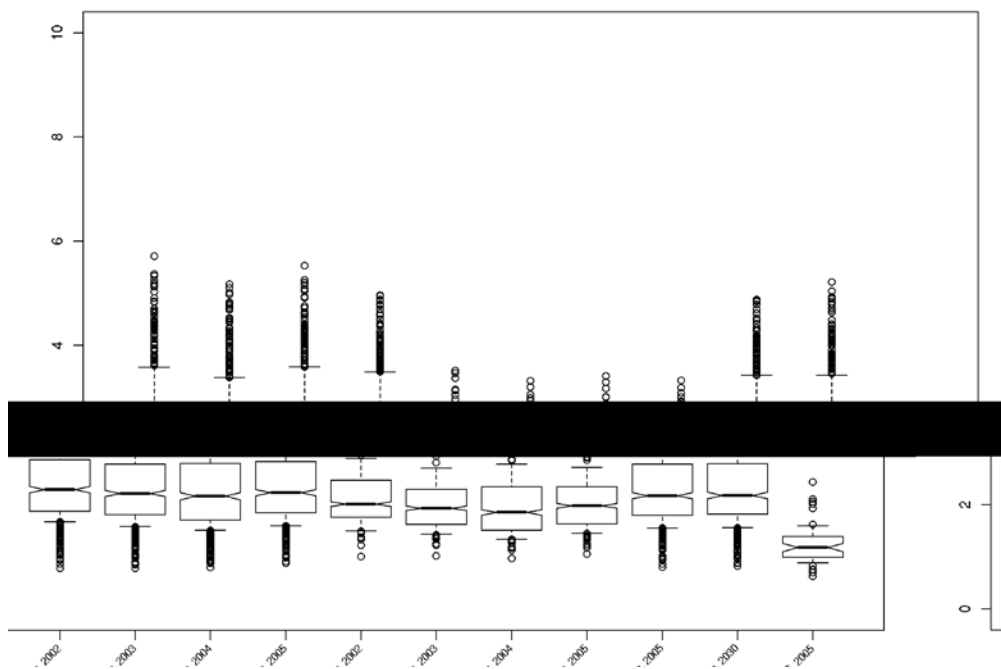


Figure F-19. Modeled generated T_{SOx} ratios in the Shenadoah area showing CMAQ 12 and 36 km values 2002 – 2005 and AURAMS 2005.

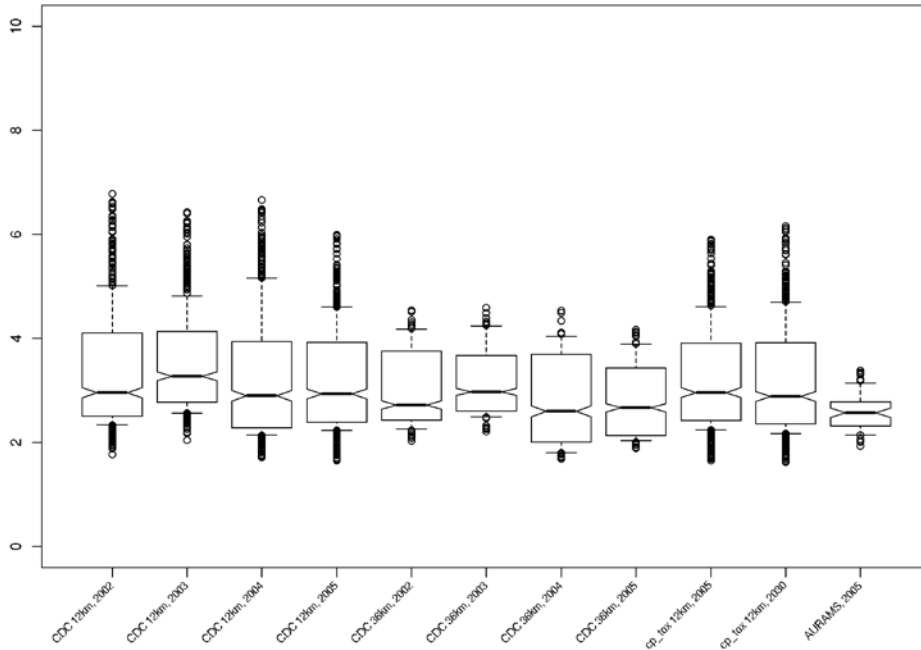


Figure F-20. Modeled generated T_{NOy} ratios in the Adirondacks area showing CMAQ 12 and 36 km values 2002 – 2005 and AURAMS 2005.

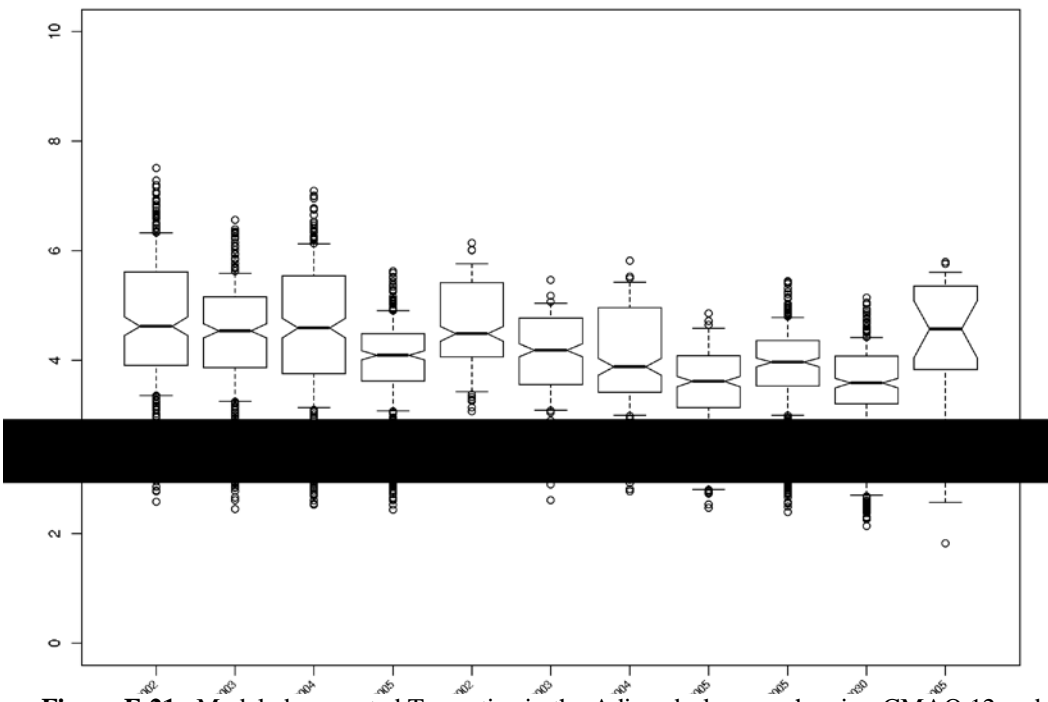


Figure F-21. Modeled generated T_{SOx} ratios in the Adirondacks area showing CMAQ 12 and 36 km values 2002 – 2005 and AURAMS 2005.

CMAQ uncertainties and the AAI

The AAI relies on CMAQ for the sulfur and nitrogen transference ratios and NH_x deposition. The model evaluation results, including the ammonia and wet precipitation treatments, reflect a continual process of model improvement designed to ingest the latest science within a framework links a myriad of atmospheric and surface processes across multiple pollutant species. While this document focuses in on the more direct processes affecting N and S deposition, these modifications are incorporated with the philosophy that the best science is being adopted and they in turn support the overall improvement of the models' treatment of all processes. The inclusion of better chemistry and physics of a particular process acts as an internal diagnostic tool for other processes that are linked throughout the model framework through basic conservation of mass principles. With respect to the AAI, the CMAQ model must be relied on to provide the spatial flexibility attendant with a national standard. As the model continually adopts the best science, confidence in relevant CMAQ generated AAI parameters is raised for both near term and future scenarios.

F.4.3 Ecosystem Modeling

F.4.3.1 MAGIC modeling

An extensive uncertainty analysis of the MAGIC model was conducted as part of the REA, and documented in Appendix 4 of the REF. This uncertainty analysis included comparison of MAGIC outputs with observed water chemistry and ANC values. The uncertainty analysis also included an approach for generating confidence intervals for predicted ANC, using ensembles of model results based on alternative model calibration methods.

The model performance comparisons documented in Appendix 4 of the REA show close correspondence between simulated and observed annual average surface water SO_4 , NO_3 , and ANC during the model calibration period for 44 lakes in the Adirondacks Case Study Area and 60 streams in the Shenandoah Case Study Area. These comparisons are reproduced in Figures F-22 and F-23. Comparisons in the ability of MAGIC to reproduce the temporal pattern of ANC for individual lakes was also assessed, and the model does reasonably well at matching the pattern of ANC, although the fit is not as good as during the model calibration period.

The estimated confidence bounds on predicted ANC suggest that the 95 percent upper confidence bound is on average 10 percent higher in lakes and 5 percent higher in streams. This suggests relatively low uncertainty introduced by the MAGIC modeling assumptions. MAGIC

modeling is used in developing the estimates of base cation weathering for comparison to the F-factor approach described in Chapter 5.

F.4.3.2 SSWC modeling

As stated in Appendix 4 of the REA, uncertainties in some elements of the SSWC modeling are not well understood. The version of the SSWC model used here uses the F-factor approach to estimate the preindustrial base cation supply for a given catchment. While this approach has been widely applied in Canada and Europe, it has only been used in a few cases within the United States and its assumptions and parameters have not been fully evaluated for aquatic systems. The natural or preindustrial catchment supply of base cations (i.e. weathering rates) has the most influence on the critical load calculation and also has the largest uncertainty (Li and McNulty, 2007). The uncertainty and ability to accurately estimate this parameter has not fully been evaluated and its uncertainty is unknown. It is important to note that for the United States, there is only one study for surface waters critical loads that compared steady-state and dynamic models and different steady-state approaches (MAGIC and F-factor) (Holdren et al. 1992) other than what is presented in Chapter 5. Holdren et al. (1992) compared critical loads calculated by the steady-state MAGIC and the SSWC F-factor model for lakes in the Northeast. In this study, steady-state MAGIC model yielded critical load values that show the same general trend and on average were 14 kg/(ha-yr) SO₄ higher than those from the SSWC F-factor approach, which is consistent with results, presented in Chapter 5. The two models converge at low critical, but diverge as the buffering potential for watersheds increase, as indicated by increasing critical loads.

The REA conducted an uncertainty assessment using Monte Carlo simulation methods to characterize the uncertainty in estimated critical loads using the SSWC, varying a number of important inputs including runoff rates, water chemistry variables, and acid deposition. The coefficients of variation (CV) for the estimated critical loads (standard deviation divided by the mean) were calculated for each lake in the study as a measure of relative uncertainty.

The results of this uncertainty analysis show that the coefficients of variation are on average very low for target ANC values within the range we are recommending (20 to 50 µeq/L). The CVs for critical loads are only 5% and 9% for critical load limits of 20 and 50 µeq/L, respectively. Although the average CV is relatively small for the population of sites modeled,

individual site CV can vary from 1% to 45%. This difference is due to the high degree of uncertainty in site specific parameters for particular sites.

These analyses suggest that uncertainties introduced in the AAI directly by the SSWC Factor model are likely to be moderate. Additional uncertainties are introduced by the generalization of the F-factor approach to estimate critical loads in locations where F-factors have not been developed.

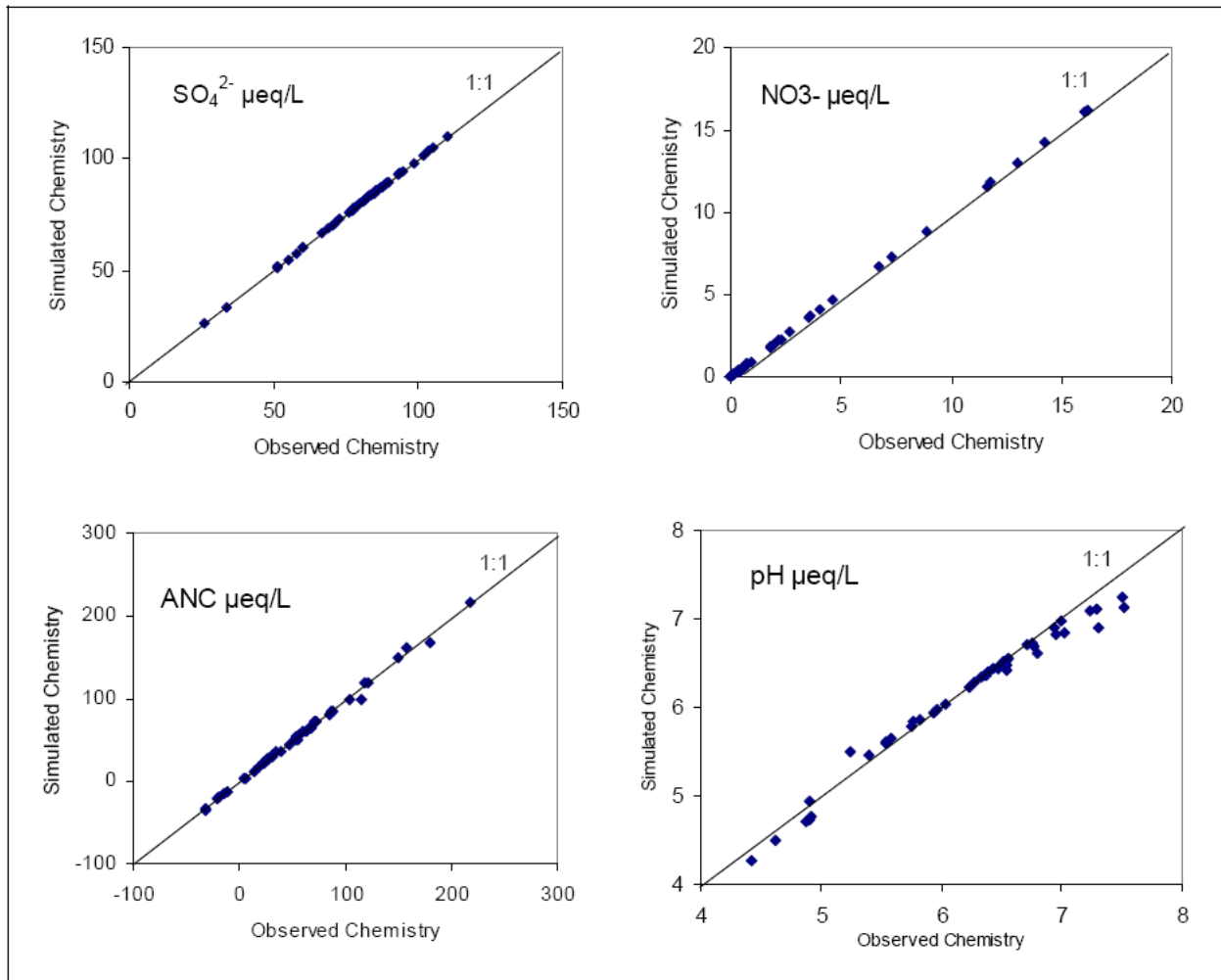


Figure F-22. Simulated versus observed annual average surface water SO_4^{2-} , NO_3^- , ANC, and pH during the model calibration period for each of the 44 lakes in the Adirondacks Case Study Area. The black line is the 1:1 line. (Source: reproduced from REA, Appendix 4, Figure 1.1-1).

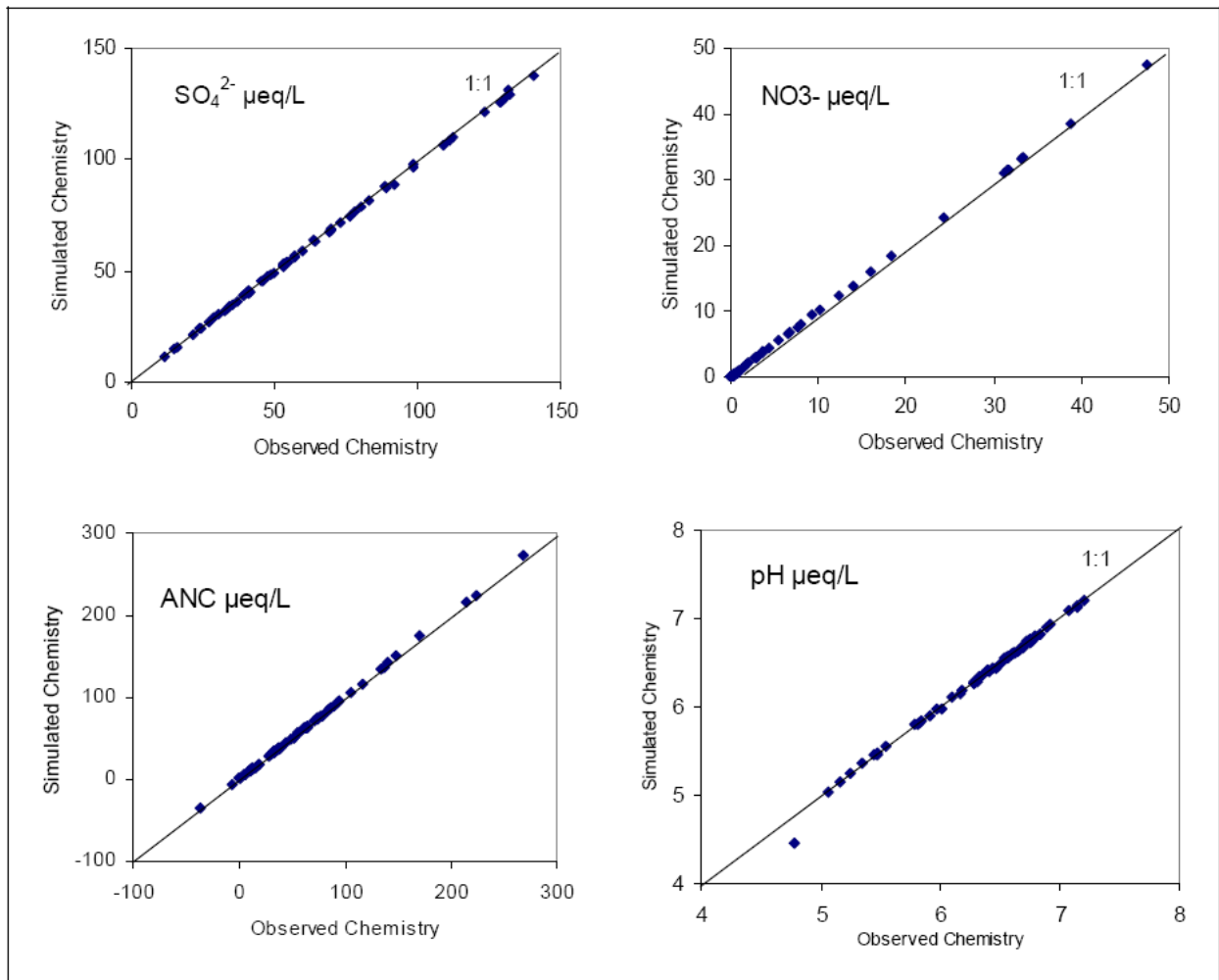


Figure F-23. Simulated versus observed annual average surface water SO₄²⁻, NO₃⁻, ANC, and pH during the model calibration period for each of the 60 streams in the Shenandoah Case Study Area. The black line is the 1:1 line. (Source: reproduced from REA, Appendix 4, Figure 1.1-2) .

F.4.4 Cumulative uncertainty analysis

An analysis of the cumulative effects of uncertainty on the AAI was conducted and is described in Appendix G. In summary, this included bootstrapping analyses of the parameters in the AAI equation to translate error in individual measurements to the regional values used in the equation. The parameters that are averages of grid-level CMAQ modeled values, *Ndep* and *NHx*, had bootstrapped uncertainty values of approximately $\pm 20\%$ (Figures G-1 and G-5). The transference ratios include two different grid-level CMAQ modeled values and had much higher uncertainty, exceeding 100% (Figures G-3 and G-4). The calculation of *Neco* also includes two different input values, the CMAQ derived *Ndep* values and lake specific nitrogen leaching values. The *Neco* results also had high uncertainty values, ranging from -65% to approximately 200% (Figure G-2). The critical load value for the region is affected by the *Q* and *BCo* values at the individual lakes within a region. Uncertainty in these parameters gave a regional uncertainty range for the critical load of $\pm 35\%$ (Figure G-6).

The results of the bootstrapping analyses were used to complete a cumulative analysis of uncertainty in a subsequent Monte Carlo style analysis. This analysis was illustrated in the form of the tradeoff curve for the concentrations of NO_y and SO_x (Figure G-7). The results in the two regions analyzed were similar. There was a range of uncertainty, with 50% of the distribution within $\pm 20\%$ of the observed value. Most importantly, the mean value of the results was very close to the observed value in both regions. This indicates that there is no systematic bias in the results despite what can be relatively high levels of uncertainty in the input parameters.

F.5 Modeling and Data Gaps

Deposition processes. Currently, there are efforts to improve a number of nitrogen and sulfur deposition processes in CMAQ. Active areas of model process improvement are in the treatment of lightning generated NO_x and the transference of nitrogen between atmospheric and terrestrial and aquatic media, often referred to as bi-directional flux. Lightning NO_x potentially provides a significant contribution to wet deposition as the resulting NO_x is rapidly entrained into aqueous cloud processes. Both the thermodynamics of soil processes and mass transfer of nitrogen species across the surface-atmosphere interface is governed by an assortment of temperature, moisture, advection and concentration patterns. These processes and mass transfer relationships are coupled within the emissions, meteorological, and chemical simulation processes and associated surface/vegetation and terrain information incorporated in or accessed by the CMAQ. In addition to research activities to improve the characterization of nitrogen-related processes in CMAQ, efforts are also underway to improve the general characterization of ammonia emissions which remains as an area of large uncertainty due to limited source data and the ubiquitous nature of these emissions. Another challenge for regional/national air quality modeling is properly representing the effects on pollutant concentrations, precipitation and therefore deposition of variable terrain features, particularly steep mountain-valley gradients and the interfaces to wide open basins encountered in the Western United States.

Two important enhancements regarding the treatment of wet precipitation and the bi-directional flux of ammonia were discussed in Chapter 2. In 2011, the EPA will deploy a prototype flux measurement package over a grass field at the Duke Forest Blackwood Division. Dry deposition fluxes will include NO_y , NO_2 , HNO_3 , HONO , NO_3 aerosol, NH_3 , NH_4 aerosol, SO_2 , SO_4 aerosol and ozone. Concentrations of organic N in aerosol, but not fluxes, also will be measured. The availability of these flux measurements will enable a more direct assessment of CMAQ treatment of sulfur and nitrogen deposition processes.

The interest in deposition of sulfur and nitrogen raises the potential importance of occult (cloud and fog related processes) deposition associated with mists and clouds, which may be particularly relevant for aquatic acidification of high elevation watersheds. Occult deposition currently is in the early stages of development within the CMAQ framework.

Lightning generated NO_x emissions have been an active area of research over the last decade and approaches that incorporate lightning count data and estimated NO_x generation based

on satellite measurements and aircraft campaigns have been tested in modern air quality models, including CMAQ. Lightning NO_x is hypothesized to increase upper tropospheric ozone levels and wet nitrogen precipitation, with relatively negligible impact on near surface ambient nitrogen patterns. It is anticipated that CMAQ will incorporate lightning NO_x for EPA assessments in the 2012 timeframe.

Interest in organic bound nitrogen has increased based on NADP measurements suggesting that organic nitrogen contributes as much as 30% of the total nitrogen in precipitation samples. Significant uncertainties regarding the origin and composition of organic nitrogen (Altieri et al., 2009) suggest research efforts to improve our understanding of organic nitrogen prior to developing parameterizations in air quality models. Concentrations of organic -N will be measured as part of EPA's flux studies in 2011. Questions regarding the relative contribution of anthropogenic or natural sources as well as the effects of re-entrainment from the surface require attention.

Atmospheric Observations. Chapter 2 addresses the current state of atmospheric observations relative to the NO_x/SO_x secondary standard and includes suggestions for enriching the observational data base used to evaluate models. This new standard poses measurement resource challenges as the current networks, with the exception of CASTNET and some National Park Service (NPS) efforts, there is sparse spatial coverage relevant to anticipated acid sensitive areas and the specific measurements related to NO_y, speciated NO_y and ammonia and ammonium. Temporally resolved data based on co-located measurements of continuously operating SO₂ and sulfate would help diagnose the partitioning of these species and support evaluation of SO_x deposition. As discussed above, deposition flux studies should be considered in a wide variety of ecoregions given the influence surface, vegetation type and meteorology imparts on deposition velocities.

Source emissions. Anthropogenic emissions of nitrogen oxides (NO and NO₂) and sulfur dioxide generally are believed to be well characterized as the major contributors of NO_x and SO₂ from energy generation and transportation sectors have a history of continuous improvements of emissions modeling as well as direct emission measurements for major power generating units. Greater uncertainty resides in natural emissions of NO_x from lightning processes (discussed above) and soil and agricultural related phenomena. Both NO_x and ammonia emissions are subject to re-emission after deposition as part of the complex cycling of

nitrogen in soils and biota. Characterizing the variety of agricultural practices that impact both ammonia and NO_x is complicated by the dispersed nature of agriculture processes as well as the influence of various meteorological factors on relevant biogeochemical processes controlling transformation and removal of nitrogen species.

Ecosystem processes and soil and surface water observations. The critical load modeling approaches underlying the standard require a variety of input data depending on the approach chosen. In general terms, the availability of watershed related deposition, soil and vegetation characteristics and surface water chemistry determine the approach taken. There is a relatively extensive source of data for critical load modeling using the steady state model for most of the contiguous U.S. However, several ecoregions included relatively small sample sizes of critical load estimates and an increased pool of data to increase the representativeness of water quality variables should be pursued at the national level.

Data to support dynamic modeling like MAGIC has focused on the Adirondack and Shenandoah regions. A more thorough characterization of nitrogen retention, dissolved organic carbon, soil chemistry in all acid sensitive areas would lead to reduced uncertainties in applying the AAI as well as future considerations for standards that incorporate terrestrial acidification and nutrient enrichment effects. In looking forward, it may not be practical to use dynamic modeling everywhere, but periodic application of dynamic models in different ecoregions gradually will result in an information system to revisit and evaluate many of the assumptions applied in national scale steady state modeling. This extension to previously undersampled areas is especially important in the mountainous West where there is evidence of aquatic acidification, yet many of the atmospheric attributes are markedly different than in Eastern systems, starting with a nitrogen dominated atmosphere, the strong influence of mountain-valley terrain on local meteorology and the closer proximity to transport of hemispheric pollution across the Pacific Ocean.

In addition to developing the data necessary to support existing models such as MAGIC, efforts should be made to continue develop dynamic models to simulate effects of acidic deposition on soil, drainage waters and biota, to test these models and to apply these as tools in determining critical loads. This research effort should address key uncertainties identified in this qualitative uncertainty analysis, including pre-industrial sulfate, nitrate, base cation, and ANC levels, as well as characterizing the relationships between naturally occurring organic acids and

acid deposition. In parallel, long term research plans and monitoring efforts should be designed to compare results from steady-state and dynamic models.

It is essential that surface water monitoring programs be maintained and soil and biological monitoring programs be strengthened, as they provide the information not only to support development of ecosystem models but also to enable broader application nationally in under sampled areas. A concerted effort to elevate and sustain water and soil observation programs is key to most foreseeable reviews and development of secondary standards relevant to the effects of atmospheric deposition. This is especially important as future reviews are likely to broaden the focus of ecological endpoints beyond aquatic acidification.

Linking modeling across atmospheric and terrestrial/aquatic media.

Research leading to improved linkages between atmospheric and watershed models would support assessments relating atmospheric deposition to ecosystem effects. The spatial scales of application typically are vastly different as watershed models target more spatially resolved catchment specific areas whereas air quality models such as CMAQ generally are applied at 12 km horizontal scale resolution. For example, consideration to nesting grid layers for finer scale resolution, similar to what is often performed to capture urban area gradients, could add insight into sub grid scale variability of deposition and the relative consequences on driving water quality models. However, the long time period averaging of water quality models tends to reduce the relative variation in spatial allocation of deposition. Research into bi-directional flux mechanisms is especially relevant to the model linkage between atmospheric and terrestrial models. The continued improvement and parallel adoption of soil process models is key to this linkage. Further efforts in characterizing the sources and processes related to reactive organic nitrogen most likely is best addressed through a linked modeling approach, given the likely dependence of organic nitrogen on a variety of ecosystem and atmospheric processes. Consideration of incorporating and modifying available processes to characterize cation deposition in air quality models is a potentially important step in linking atmospheric and terrestrial/aquatic media.

F.6 Summary and Conclusions

Uncertainty and natural variability exist in all of the components of the structure of the NO_x and SO_x standard introduced in this PA, and should be considered in establishing the level of the AAI. A summary of the relative uncertainties of these components is provided in Table F-3. On balance, the confidence level in the information and processes associated with the linkages from ecological effects to atmospheric conditions through deposition and ecosystem modeling is very high. The considerable body of evidence is conclusive with regard to causality between aquatic acidification and biological and ecological effects. Confidence in the linkage associating aquatic acidification and ANC is extremely high, as the aquatic chemistry describing this relationship, while nonlinear, is relatively simple with regard to chemical species and reactions. The relationships between deposition and ANC, while complicated by a variety of biogeochemical and hydrological processes and data requirements within watersheds, are well established and the critical load models have been thoroughly vetted through the scientific community with a demonstrated level of successful evaluation. The linkages between ambient concentrations of relevant species and deposition are best handled through air quality modeling systems like CMAQ. The relationship between concentrations and deposition loads is well characterized by these models, which are constrained by mass balance principles. While much of the physical and chemical processing that determine concentrations and consequent deposition is interwoven with numerous fundamental processes characterizing mass transport and atmospheric chemical oxidation, the science is relatively mature with years of applications and continued evolution of the models. The specific processes guiding nitrogen and sulfur chemistry and deposition are relatively simple. More challenging is the ability to parameterize processes at the air-surface interface which guide the estimation of deposition velocities and the re-emission of certain species, as well as many of the area wide natural processes and agricultural practices which influence emissions of oxidized and reduced forms of nitrogen.

The variety of uncertainty, variability and sensitivity analyses included in this chapter have been conducted under the assumption that the basic model construct is solid, as discussed immediately above, and are used to inform conclusions regarding the level of the AAI that incorporate consideration of uncertainty. These analyses are also useful in guiding implementation efforts related to future monitoring, emissions and model process improvements.

The influence of uncertainty on the level of the AAI can be thought of as reducing or increasing

relative stringency of the level to increase the likelihood that requisite protection of public welfare is provided. Throughout these discussions there is no apparent directional bias in the uncertainty regarding the biological, chemical and physical processes incorporated in the AAI. From the perspective of valuation of ecosystem services, the estimates generally are believed to be biased low, meaning the values of reaching a target level of protection are underestimated. However, quantification of these values is perhaps the most uncertain of all aspects considered. Consequently, the level of the AAI should be relatively high in a buffering context to account for the existence of uncertainties in several components. In addition to, but related to these uncertainties discussions, are considerations of time lag to reach a target level ANC due to ecosystem response dynamics, as well the uncertainties in the severity and prevalence of episodic events. Both of these considerations suggest support for an AAI that is somewhat higher than the target ANC supported by the specific evidence and risk information.

Table F-3. Summary of Qualitative Uncertainty Analysis of Key Elements Affecting the AAI form of the NO_x/SO_x Standards.

| Source | Description | Potential influence of uncertainty in element | | Knowledge-Base uncertainty | Comments |
|---|--|---|------------|----------------------------|---|
| | | Direction (negative implies less relative protection) | Magnitude | | |
| Major elements (and sub-models) of the ecological effects to ambient concentration framework | | | | | |
| Biological/ecosystem response to acidification | Clear associations between aquatic acidification (pH, elevated Al) and adverse ecosystem effects (fish mortality, decreased species diversity) | Both | Low | Low (regionally) | The ecosystem level responses are well studied at regional levels. The uncertainty increases at larger scales due to an increasing number of factors influencing the patterns (e.g. latitudinal species gradient, specie-area relationships, etc.). |
| Linkage between direct acidification species and ecological indicator (ANC) | The relationships across ANC, pH and dissolved Al are controlled by well defined aquatic equilibrium chemistry | Both | Low | Low | ANC is the preferred ecosystem indicator as it has a direct relationship with pH and the deposition species relevant to the NO _x /SO _x standard. |
| Linkage between ecological indicator and adverse ecological effects | Direct nonlinear associations between ANC and fish mortality and species diversity | Both | Low-medium | Low | Although the pH dependency on ANC is nonlinear, it is always directionally consistent. In extremely low and high ANC environments the relationship is of minimal value as catchments are in relatively “less sensitive” regimes due to natural conditions or extreme anthropogenic influence (i.e., acid mine drainage). In sensitive areas of concern the relationship essentially is similar to the relationships between direct acidification species and adverse effects. |
| Deposition to ANC linkage through Critical Load approach | Mass-balance Steady State critical load model is applied to determine critical load values. MAGIC | Both | Low | Low | The model formulation is well conceived and based on a substantial amount of research and applications available in the peer reviewed literature. There is greater uncertainty associated with the availability of data to |

| Source | Description | Potential influence of uncertainty in element | | Knowledge-Base uncertainty | Comments |
|--|--|---|-------------|----------------------------|---|
| | | Direction (negative implies less relative protection) | Magnitude | | |
| | model is used to validate steady State model. The Steady State critical load model formulation is used as the foundation for deriving the AAI equation. | | | | support certain model components. |
| Atmospheric concentrations to deposition | Deposition is a direct function of ambient concentration, influenced by several processes, and handled in the AAI through air quality modeling. | Both | Low | Low | The model design is appropriate given the spatial and temporal complexities that influence deposition velocity, as well as the variety of atmospheric species that generally are not measured. Greater uncertainty resides in the information (e.g., ammonia emissions) driving these calculations and availability of observations to evaluate model behavior. |
| Ecological indicator to changes in the value of ecosystem services | Definitions of public welfare may include economic considerations, based on the tradeoffs people would make to avoid the negative impacts of acidification, through effects on the values of ecosystem services. Empirical estimates of valuation for limited ecosystem service categories are used to | Negative | Medium-high | Low-medium | There are many studies that estimate the value of increasing services that may be affected by changes in acidification and eutrophication. However, few of these studies focus on the particular impact of acidification and eutrophication on the quality of these services and preferences for avoiding these impacts. Those studies that do are often limited to analyzing the impacts on a narrow population or particular change in environmental quality. The monetized benefits to fishers and to New York residents for ecosystem improvements in the Adirondacks associated with improvements to the ecological indicator are significant underestimates of the |

| Source | Description | Potential influence of uncertainty in element | | Knowledge-Base uncertainty | Comments |
|---|--|---|-----------|----------------------------|---|
| | | Direction (negative implies less relative protection) | Magnitude | | |
| | inform the discussions of adversity associated with alternative ANC levels. | | | | <p>total benefits in the U.S. This is because those living outside New York would value improvements to the Adirondacks and similar natural environments elsewhere.</p> <p>The methodologies used in the studies that underlie the estimates of the value of changes in ecosystem services in the Adirondacks region are sound and have been subject to peer review. The method of aligning the improvements valued in the Banzhaf et al. study with estimates of eliminating current damages leads to may lead to an over or underestimate of the benefits. The range of this difference is difficult to know a priori, but the total improvements in the share of lakes that improve above an ANC threshold of 20 µeq/L are consistent.</p> |
| Sub-components and data of individual models | | | | | |
| Atmospheric Components | | | | | |
| Dep _{SOx} | Annual deposition of sulfur mass from dry deposition of (SO ₂ and SO ₄) and wet SO ₄ derived from CMAQ 12km horizontal grid resolution averaged over 5 years | both | low | low | The treatment of SO _x deposition in EPA air quality models has evolved over the last two decades. There is general consensus that the overall mass balance of S is treated well with difficulties in spatial pairing of observations and modeled results of wet deposition. This spatial pairing has improved with the more recent PRISM adjustments. |
| Dep _{NOy} | Annual deposition of oxidized nitrogen mass from dry deposition of (all NO _y species) and wet NO ₃ | both | low | low-medium | The treatment of oxidized nitrogen deposition in EPA air quality models has evolved over the last two decades. There is general consensus that the overall mass balance of oxidized N is treated well. However, the broad range of |

| Source | Description | Potential influence of uncertainty in element | | Knowledge-Base uncertainty | Comments |
|--|--|---|-----------|----------------------------|---|
| | | Direction (negative implies less relative protection) | Magnitude | | |
| | derived from CMAQ 12 km horizontal grid resolution averaged over 5 years | | | | deposition velocities across NO _y species, and especially uncertainties regarding the deposition of significant species such as NO ₂ pose ongoing challenges. Similarly, a shortage of NO _y species measurements as well a lack of techniques to directly measure dry deposition impede progress on improving parameterization of N dry deposition. |
| Dep _{NH_x} | Annual deposition of reduced nitrogen mass from dry deposition of (NH ₃ and SO ₄) and wet NH ₄ derived from CMAQ 12km horizontal grid resolution averaged over 5 years | both | low | medium | NH _x deposition also is quantified through CMAQ applications. The well dispersed nature of agricultural based emissions that are influenced strongly by meteorological and surface /soil characteristics continues to challenge characterization of ammonia emissions. Recent incorporation of a bi-directional flux process in CMAQ improves consistency with available scientific understanding and yields improved time and space pairing of limited observations with model results. A lack of both ammonia and ammonium ambient observations continues to compromise our ability to characterize uncertainty in our treatment of NH _x . As with all dry deposition estimates, technologies for direct measurements are not available routinely. Both NH _x deposition and NO _x deposition are assigned low values of magnitude based on a general dominating role of sulfur deposition. |
| Wet deposition (generically – N and S species) | Wet component of total deposition as described in the Dep terms, above | both | low | low | Wet deposition remains an attribute of relatively high confidence based on the ability to directly measure chemical components in precipitation samples. However, given the stochastic nature of precipitation, |

| Source | Description | Potential influence of uncertainty in element | | Knowledge-Base uncertainty | Comments |
|--|---|---|-----------|----------------------------|--|
| | | Direction (negative implies less relative protection) | Magnitude | | |
| | | | | | models have a difficult time in matching observations. The use of 5 year averages and post-processing PRISM adjustments have reduced uncertainty in spatial pairing of observations and modeled estimates. |
| Dry deposition (generically – N and S species) | Dry component of total deposition as described in the Dep terms, above | both | medium | Medium-high | The absence of direct dry deposition measurements combined with the significant variability in the parameters that influence dry deposition velocity reduces the confidence level in dry deposition relative to wet deposition. |
| Deposition Transference Ratios | CMAQ derived ratio of total oxidized deposition to concentration averaged over one year | both | low | unknown | Transference ratios enable the connection between deposition and the policy relevant ambient air indicators, NO _y and (SO ₂ + SO ₄). They are strictly a model construct and cannot be evaluated in a traditional model to observation context. The low sensitivity of these ratios to emission changes and inter annual meteorology combined with low spatial variability indicate that these ratios are necessarily stable. |
| C _{NO_y} | Ambient concentrations of NO _y through observations. | negative | low | Low-medium | Adequate spatial coverage of NO _y observations does not exist, but will be addressed in the proposed rule. The monitoring technology only over the last 5 years has been perceived as “routine” based on incorporation in the NCore network. However FRM status for NO _y instruments currently is not available. The negative bias direction is a standard caveat to any instrument relying on internal air stream conversion of atmospheric species prior to detection. |
| C _{SO_x} | Ambient concentrations of | both | low | Low | A lack of adequate spatial coverage is the primary concern |

| Source | Description | Potential influence of uncertainty in element | | Knowledge-Base uncertainty | Comments |
|------------------------------|---|---|-------------|----------------------------|--|
| | | Direction (negative implies less relative protection) | Magnitude | | |
| | NOy through observations. | | | | for SO2 + SO4 observations. FRM status is not available for SO4; although the long track record of accurate and precise CASTNET FP measurements indicates that achieving FRM status is a low hurdle. |
| Ecosystem Components | | | | | |
| BC ₀ [*] | Pre-industrial base cation concentrations | negative | Medium-high | high | Both the F-factor approach and process based MAGIC modeling were used to generate BC ₀ [*] . Excellent agreement between both approaches was established in the Shenandoah streams. The more comprehensive data requirements of MAGIC limit its widespread use to the Adirondacks, although for consistency the F-factor approach was applied nationwide. The analyses also illustrated greater divergence at higher critical loads, or areas with greater acid buffering capacity and high bas cation levels. These conditions often are screened out of our population distribution analyses, and when included do not affect the location within the distribution of the more sensitive water bodies. Since MAGIC (the preferred approach) tends to overestimate BC ₀ [*] relative to the F factor approach, and the F-factor is more widely applied nationally, the BC ₀ [*] estimates are viewed as conservative leading to a slight positive bias in estimating critical loads. Although we have many modeled estimates of BC ₀ [*] , there is a lack of direct measurements of BC weathering rates. |
| Neco | | positive | low | medium | The term Neco, as defined, has a relatively medium confidence level and is a direct function of the uncertainty |

| Source | Description | Potential influence of uncertainty in element | | Knowledge-Base uncertainty | Comments |
|--------|--|---|-----------|----------------------------|---|
| | | Direction (negative implies less relative protection) | Magnitude | | |
| | | | | | inherent in the deposition estimates from CMAQ and surface measurements of NO ₃ . However, this “measurement” difference approach reflects the average of all influencing processes (dinitrification, uptake, immobilization) over the time period of measurements. Consequently, there is an inherent assumption of a relatively static system (Neco is applied in a steady state model) that generally is not tested. In concept, a true steady state vision of Neco would be based on a mature forested ecosystem. The relative bias of Neco is related, largely, to the relative productivity of the forest. The challenge in determining any potential bias in Neco is to determine the relative “maturation age” of an ecosystem which requires knowledge of future land use activities. In areas of high land use restrictions of a recovering forest, Neco would be assumed to be overestimated. The relative magnitude of Neco often is mitigated by the dominance of SO _x in controlling acidification processes in many systems. Furthermore, it is unclear to what extent any stored N will be released back into the system, which is assumed to not occur in the linked system model. |
| Q | Annual runoff rate (distance/time) for a catchement. | both | low | high | Data used to calculate Q was compiled in 1985. Streamflow data were collected at over 12,000 gauging stations during 1951-80; 5,951 stations were selected for the analysis. See Gebert and others (1987) for a complete description of how the runoff was determined from the streamflow data. Appropriate maps of the data can show |

| Source | Description | Potential influence of uncertainty in element | | Knowledge-Base uncertainty | Comments |
|--------|--|---|-----------|----------------------------|--|
| | | Direction (negative implies less relative protection) | Magnitude | | |
| | | | | | <p>the geographical distribution of runoff in tributary streams for the years 1951-80 and can describe the magnitudes and variations of runoff nationwide. The data was prepared to reflect the runoff of tributary streams rather than in major rivers in order to represent more accurately the local or small scale variation in runoff with precipitation and other geographical characteristics.</p> <p>W.F., Graczyk, D.J., and Krug, W.R., 1987, Average annual runoff in the United States, 1951-80: U.S. Geological Survey Hydrologic Investigations Atlas HA-710, scale 1:7,500,000.</p> |
| DOC | Surface water dissolved organic carbon | negative | low | medium | <p>Water bodies with high DOC levels (> 10mg/l) were screened out of the critical load calculations in order to avoid naturally acidic systems. However, the inherent assumption of $ANC = \sum \text{strong CA} - \sum \text{strong AN}$ does not explicitly account for contributions of weak organic acids. Consequently, a small positive bias pervades the critical load calculations (i.e., the CL estimates are high). The knowledge base value of M reflects a general shortage of DOC data.</p> |

REFERENCES:

- Aiyyer, A, Cohan, D., Russell, F., Stockwell, W., Tanrikulu, S., Vizuete, W., and Wilczak, J. 2007. *Final Report: Third Peer Review of the CMAQ Model*.
- Altieri, K.E., B.J. Turpin and S.B. Seitzinger, 2009, Composition of dissolved organic nitrogen in continental precipitation investigated by ultra-high resolution FT-ICR mass spectrometry, *Environmental Science and Technology*, 43, 18, 6950 – 6955.
- Byun, D.W., and Schere, K.L. 2006. Review of the Governing Equations, Computational Algorithms, and Other Components of the Models-3 Community Multiscale Air Quality (CMAQ) Modeling System. *J. Applied Mechanics Reviews*, 59 (2), 51–77.
- Dennis, R. and K. Foley, 2009, Adapting CMAQ deposition fields for critical loads analyses, presented at 2009 NADP Conference; manuscript in preparation.
- Dennis, R., R. Mathur, J.E. Pleim and J.T. Walker, 2010, Fate of Ammonia Emissions at the Local to Regional Scale as Simulated by the Community Multiscale Air Quality Model, *Atmospheric Pollution Research*.
- Foley, K.M., Roselle, S.J, Appel, K.W., Phave, P.V., Pleim, J.E., Otte, T.L., Mathur, R., Sarwar, G., Young, J.O., Gilliam, R.C., Nolte, C.G., Kelly, J.T., Gilliland, F.B., Bash, J.O. (2010) Incremental testing of the Community Multiscale Air Quality (CMAQ) modeling system version 4.7, *Geosci. Model Dev.*, 3, 205-226.
- Holdren, G.R., T.C. Strickland, P.W. Shaffer, P.F. Ryan, P.L. Ringold and R.S. Turner. 1992. Sensitivity of Critical Load Estimates for Surface Waters to Model Selection and Regionalization Schemes, *J. Environ. Qual.* 22:279-289.
- Otte, T.L. and Pleim, J.E. (2010) The Meteorology-Chemistry Interface Processor (MCIP) for the CMAQ modeling system, *Geosci. Model Dev.*, 3, 243-256.
- PRISM Climate Group, Oregon State University, <http://www.prismclimate.org>, created 4 Feb 2004 U.S. EPA (Environmental Protection Agency) 2009.
- Risk and Exposure Assessment for Review of the Secondary National Ambient Air Quality Standards for Oxides of Nitrogen and Oxides of Sulfur-Main Content - Final Report. U.S. Environmental Protection Agency, Research Triangle Park, NC, EPA-452/R-09-008a.

Appendix G

Cumulative Uncertainty Analysis

This appendix provides analyses of the relative uncertainty in the AAI equation. The analysis involves a Monte Carlo style approach that incorporates the relative uncertainties of the input parameters. Cumulative results are illustrated in the form of the trade-off curve of the allowable atmospheric concentrations of the oxides of N and S.

From the general form of the standard:

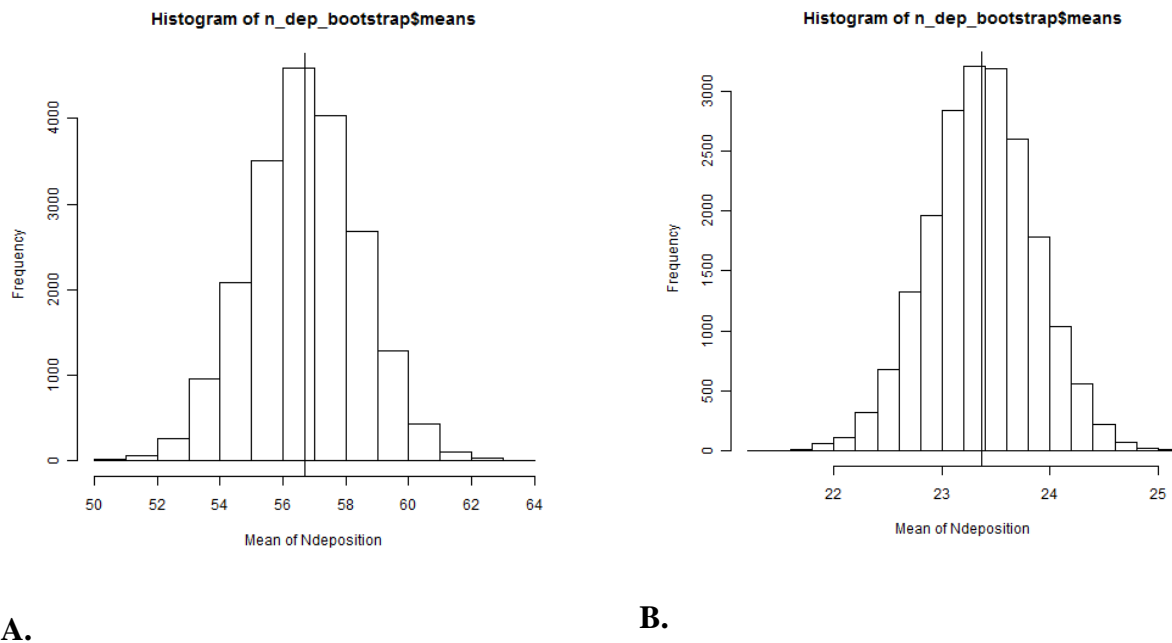
$$AAI = \{AN_{clim} + CL_r/Q_r\} - NH_x/Q_r - T_{NO_y} [NO_y]/Q_r - T_{SO_x}[SO_x]/Q_r$$

There are six sources of uncertainty in calculating an AAI value for measured atmospheric concentrations of the oxides of N and S; however these individual uncertainties are not applied in the same manner. Four of these, *Neco*, *NH_x*, *T_{noy}* and *T_{sox}* rely on data from CMAQ modeling. The uncertainty in CMAQ values can be high (see appendix F for detailed discussion of CMAQ modeling). These values as they are used in the AAI equation are averaged either across individual water bodies in the ecoregion or across CMAQ 12 km grids within the ecoregion. In order to translate the uncertainty to the AAI equation, these averaged values were bootstrapped using uncertainty in CMAQ modeling to obtain an estimated uncertainty in the average values. Uncertainty in the parameters *BC_o* and *Q* affect the selection of a representative Critical Load (*CL*) value for the region. To analyze this, the *CL* value was bootstrapped to generate a distribution of *CL* values reflecting the underlying uncertainty in *BC_o* and *Q*. In all cases the error was modeled as a normal Gaussian distribution and the bootstrapping was repeated 20,000 times to generate the distributions.

Two ecoregions were chosen to assess the uncertainty, the Northern Highlands (region 5.3.1) and the Northern Great Plains (region 9.3.3). Region 5.3.1 was chosen because it had the largest number of critical load data points to work with (819). Region 9.3.3 was chosen because it is a relatively less acid sensitive region that had a large enough number of Critical Load data points (164) to use for analyses. For all of these analyses an ANC level of 50 and a percentile of 75% were selected.

Nitrogen Deposition (Ndep)

Modeled nitrogen deposition (*Ndep*) is used in two different components of the AAI, the *Neco* value and in *Tnoy*. Figure G-1 shows the results of bootstrapping analyses. These analyses allowed for 100% uncertainty in the deposition at the grid level. Averaged over the entire regions the bootstrapped distribution has uncertainty that is $\pm 15\%$ in Region 5.3.1 and $\pm 10\%$ in Region 9.3.3.



A. **B.**
Figure G-1. Bootstrap distribution of mean nitrogen deposition for Regions 5.3.1 (A) and 9.3.3 (B)

Nitrogen Uptake (Neco)

The *Neco* term directly uses the mean deposition. The *Neco* is calculated as the Average $Neco = Ndep - Nitrogen\ Leaching\ (Nleach)$, where *Ndep* is the regional average and *Nleach* is a lake specific value. *Neco* is calculated at each lake individually, and the mean *Neco* for the region is used in the AAI equation. *Ndep* was selected randomly from the distribution generated above (Figure G-1). *Nleach* was allowed to have 30% uncertainty. Figure G-2 shows the results of the *Neco* bootstrapping analysis of the mean values for the two regions. The results indicate that the

mean *Neco* term varies widely with a range of <20 to >120 in Region 5.3.1 and <10 to 60 in Region 9.3.3. This equates to a range of uncertainty that is from approximately -75% to 135% in Region 5.3.1 and -65% to 218% in Region 9.3.3.

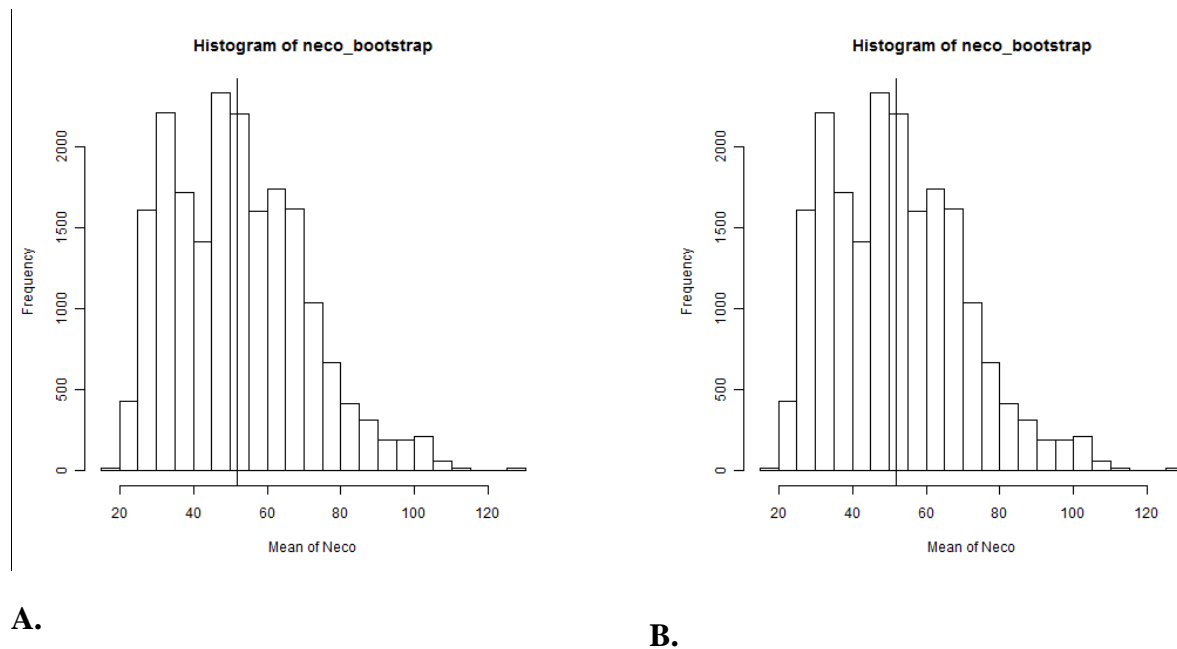


Figure G-2. Bootstrap distribution of mean Nitrogen uptake (*Neco*) for Regions 5.3.1 (A) and 9.3.3 (B)

Transference Ratios (*Tnoy*, *Tsox*)

The Nitrogen transference ratio (*Tnoy*) also uses CMAQ derived values for Nitrogen deposition, but *Tnoy*, and the transference ratio for S, *Tsox*) are calculated at the grid level. The transference ratio analyses included uncertainty at the grid level in N and S deposition and in the ambient concentrations of NO_y and Sox (*Nconc* and *Sconc*), also modeled by CMAQ. The transference ratios were calculated as $Tnoy = Ndep/Nconc$ and $Tsox = Sdep/Sconc$. Uncertainty in the CMAQ values was included randomly before the ratio was calculated, with uncertainty in deposition (*Ndep* and *Sdep*) up to 75%, and uncertainty in concentration (*Nconc* and *Sconc*) up to 25%. The uncertainty in the deposition terms is lower than used above because this value incorporates the concentration terms in CMAQ, so a portion of the uncertainty in these two terms will covary and would be directly offset in the calculation of the transference ratios. The mean value for the region was then calculated. The results of these analyses are shown in figures G-3

and G-4. In both analyses there were a small number of extreme outliers and the axes in the figures have been truncated to allow better visualization of the results. These outliers were included in the final analyses. The results were similar for T_{noy} and T_{sox} . The range of values, excluding outliers, was larger for both ratios in Region 5.3.1, but in both regions the uncertainty ranged from -75% to > 100%, excluding the extreme outliers.

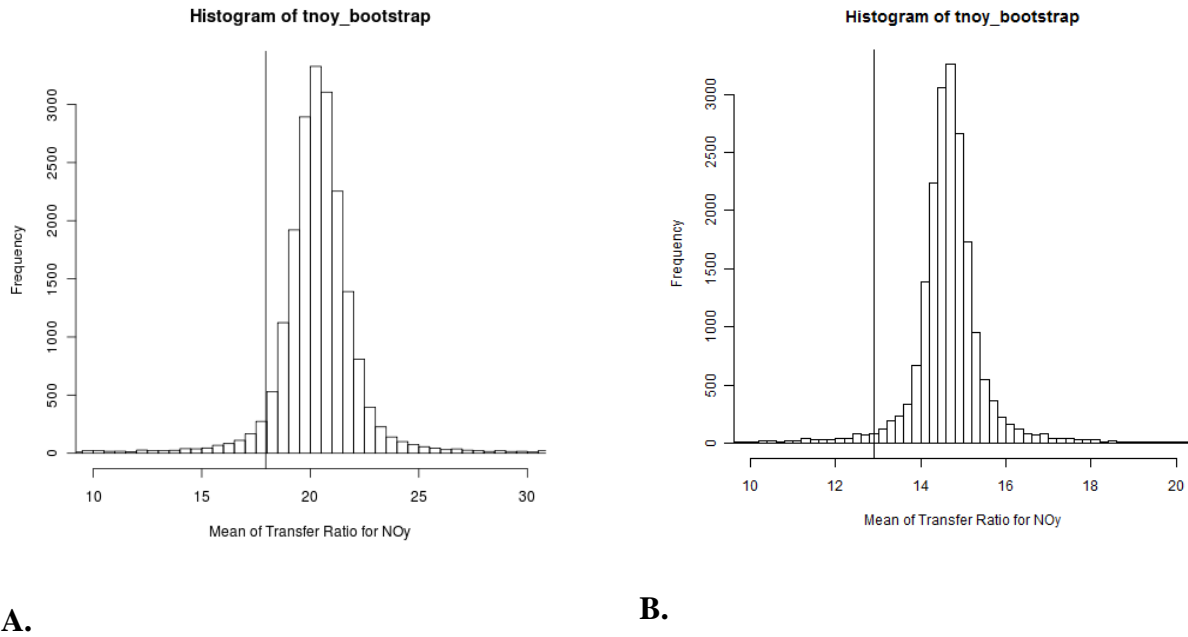
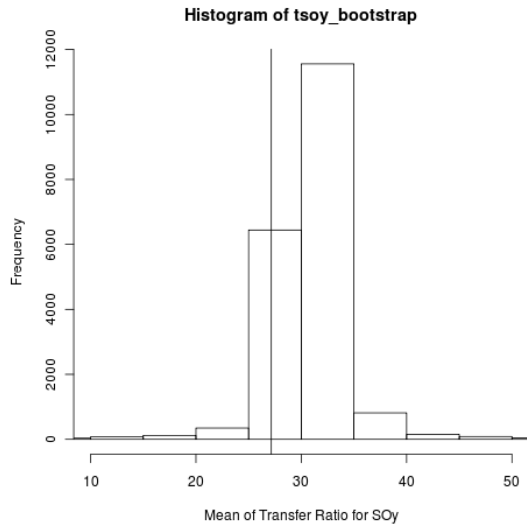
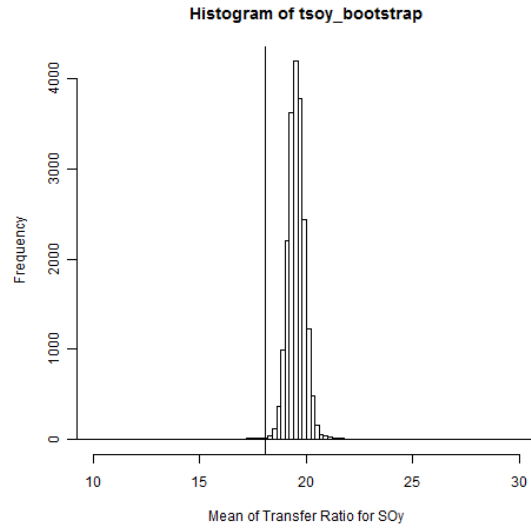


Figure G-3. Bootstrap distribution of mean nitrogen transference ratios (T_{noy}) for Regions 5.3.1 (A) and 9.3.3 (B)



A.

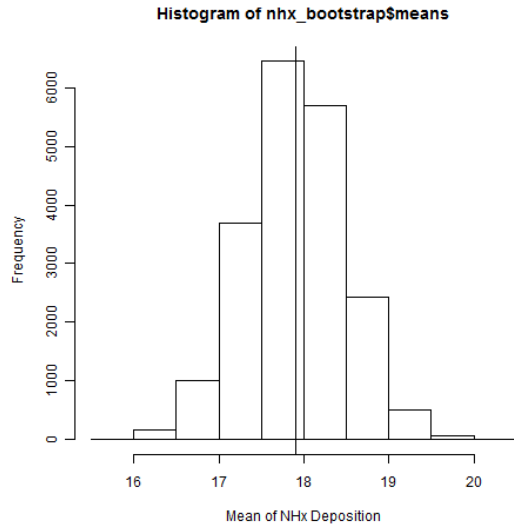


B.

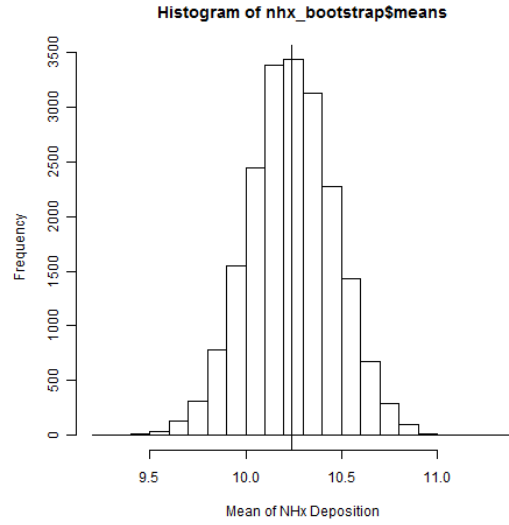
Figure G-4. Bootstrap distribution of mean sulfur transference ratios (Tsox) for Regions 5.3.1 (A) and 9.3.3 (B)

Reduced Nitrogen

Reduced nitrogen deposition (NH_x) was analyzed in the same way as $Ndep$ with the same uncertainty of 100%. The results are show in figure G-5. The average NH_x deposition is higher in Region 5.3.1, but in both regions the range or uncertainty is approximately $\pm 20\%$.



A.

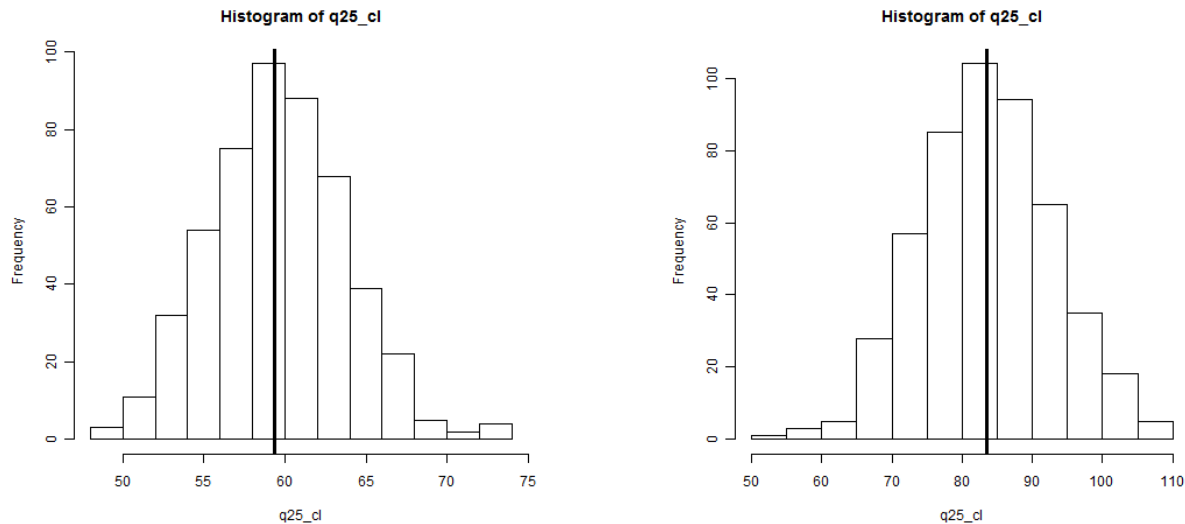


B.

Figure G-5. Bootstrap distribution of mean reduced nitrogen deposition (NHx) for Regions 5.3.1 (A) and 9.3.3 (B)

Critical Load

The critical load (*CL*) that is selected to represent the ecoregion is dependent on the Target Percentile and level set as part of the standard. This value is represented in the AAI equation as the Base Cation weathering (*BCo*) and the hydrologic term, *Q*. Uncertainty in these two terms will affect the value of the *CL*. As represented in the AAI equation, *BCo* and *Q* are constants that, together with the selected ANC level, are equal to the representative *CL*. To model this uncertainty the *CL* values were bootstrapped including 70% uncertainty in the *BCo* term and 5% uncertainty in the *Q* term. These results are shown in Figure G-6. The *CL* has an uncertainty range of approximately $\pm 30\%$ in Region 5.3.1 and -25% to 35% in Region 9.3.3.



A.

B.

Figure G-6. Bootstrap distribution of representative critical load values for Regions 5.3.1 (A) and 9.3.3 (B)

Combined Uncertainty in the AAI

To illustrate the combined effect of the uncertainty developed above a trade-off curve representing the allowable combined concentrations of S and N was developed. The trade-off curve was derived using the raw data for these ecoregions (Figure F-7, dashed lines). The curve was then derived again using values from the derived distributions of *Neco*, *NHx*, *Tnoy*, *Tsox*, and the *CL*. This was repeated 20,000 times with the resulting curves plotted in light gray in Figure G-7. The solid black lines represent 95% confidence intervals, the inner quartiles (25th and 75th percentiles) and the mean. For this analysis the *Neco* term was treated separately from the CL selection to allow plotting of the tradeoff curves.

In Region 5.3.1 the mean value derived from the modeling is the same as the value derived from the raw data and the curves are directly on top of each other. The 95% confidence intervals represent a range of approximately $\pm 15\%$ and the inner quartile approximately $\pm 5\%$ relative to the maximum allowable concentration of S oxides. The uncertainty associated with the maximum allowable concentration of NOx is larger when looking at the 95% confidence

interval, approximately $\pm 45\%$, and at the inner quartiles, $\pm 20\%$ uncertainty. The larger uncertainty on the NO_x axis is due to the Neco and NH_x terms.

In Region 9.3.3 the mean value derived from the modeling is the same as the curve derived from the raw data. The 95% confidence intervals represent a range of uncertainty that is approximately $\pm 25\%$ and $\pm 10\%$ for the inner quartiles relative to the maximum allowable concentration of S oxides. The uncertainty associated with the maximum allowable concentration of NO_x is in the same range for this region.

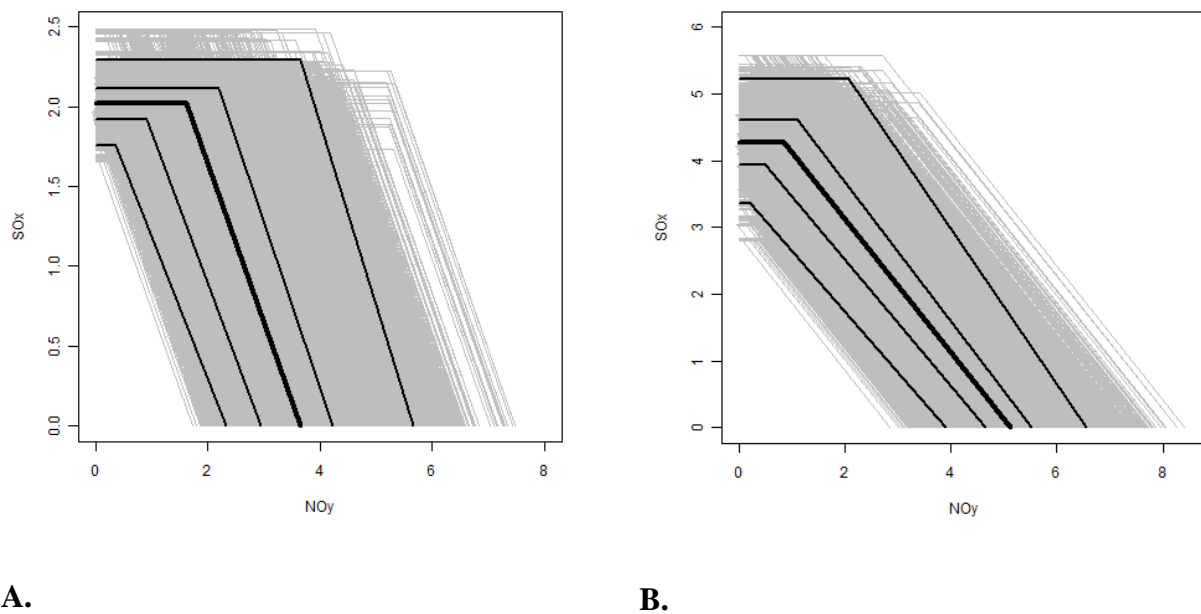


Figure G-7. NO_y/SO_x tradeoff curve with results of cumulative uncertainty analysis for Regions 5.3.1 (A) and 9.3.3 (B)

United States
Environmental Protection
Agency

Office of Air Quality Planning and Standards
Health and Environmental Impacts Division
Research Triangle Park, NC

Publication No. EPA-452/R-11-005b
February 2011
